Neuronal death mechanisms in cerebellar Purkinje cells

Inauguraldissertation

Zur
Erlangung der Würde eines Doktors der Philosophie
vorgelegt der
Philosophisch-Naturwissenschaftlichen Fakultät
der Universität Basel

von

Stephane HEITZ

Aus Strasbourg (France)

BASEL / 2008

Genehmigt von der Philosophisch-Naturwissenschaftlichen Fakultät

Auf antrag von

- Pr. Dr. Markus Ruegg
- Pr. Dr. Peter Scheiffele
- Pr. Dr. Pierrick Poisbeau
- Pr. Dr. Josef Kapfhammer
- Dr. Yannick Bailly
- Dr. Bernard Poulain
- Dr. Fekrije Selimi
- Dr. Patrice Codogno

Basel, den 16. September 2008

Prof. Dr. Eberhard Parlow
(Dekan)

Thesis presented for the degree of
DOCTOR OF PHILOSOPHY EN CO-TUTELLE of

UNIVERSITE LOUIS PASTEUR
FRANCE
Discipline: Neurosciences
Ecole Doctorale Vie et Santé

&

UNIVERSITÄT BASEL
SWITZERLAND
Discipline : Neurosciences
Philosophisch-Naturwissenschaftliche Fakultät

Neuronal death mechanisms in cerebellar Purkinje cells

by

Stéphane HEITZ

Defended September 22nd 2008 in front of:

Dr. Patrice Codogno	External reporter
Pr. Peter Scheiffele	External reporter
Pr. Pierrick Poisbeau	ULP internal reporter
Pr. Markus Ruegg	UniBasel internal reporter
Dr. Fekrije Selimi	External examiner
Dr. Yannick Bailly	PhD co-supervisor
Pr. Josef Kapfhammer	PhD co-supervisor
Dr. Bernard Poulain	PhD co-supervisor

Contribution of others

Stipend support:
- Neurex Network to S. Heitz
- Roche Research Foundation to S. Heitz
- Fondation Novartis pour la Recherche en Sciences Biomédicales to S. Heitz

Supervision: Dr Y. Bailly and Prof J. Kapfhammer

Statistical support: Dr J-L Rodeau

Western Blotting support: Dr N. Grant

Genotyping support: Vanessa Gautheron, Drs Yves Lutz and Jean-Paul Fuchs

Project costs: 30000€

Project funds:
- G.I.S. Infections à prions to Dr Y. Bailly
- Travel Grant Région Alsace to S. Heitz
- Travel Grant Société des Neurosciences to S. Heitz
- Centre National de la Recherche Scientifique funds to Dr Y. Bailly
- University funds, Université Louis Pasteur to S. Heitz
- University funds, Universität Basel to Prof J. Kapfhammer and S. Heitz

Infrastructures:
- Institut des Neurosciences Cellulaires et Intégratives, Département Neurotransmission et Sécrétion Neuroendocrine, UMR 7168/LC2, CNRS and Université Louis Pasteur
- Anatomisches Institut der Universität Basel
- Plateforme d'Imagerie *in vitro*, IFR 37 des Neurosciences
- Animal facility at the Anatomisches Institut der Universität Basel
- Plateforme d'Exploration Fonctionnelle, IFR 37 des Neurosciences

Acknowledgments

The work presented in this thesis was carried out in cotutelle between the Anatomisches Institut der Universität Basel and the Départment Neurosécrétion et Sécrétion Neuroendocrine of INCI in Strasbourg managed by Dr Marie-France Bader. I thank her for warm welcome during my DEA and my thesis.

I thank Pr Josef Kapfhammer for his engagement and his participation in the co-direction of my thesis and the enriching discussions for both scientific and technical aspects.

I thank Dr Yannick Bailly for encouraging me from the first day of my DEA and the fascinating scientific adventure of the last 4 years and Dr Bernard Poulain for accepting to be my co-supervisor.

I wish to thank my jury members Drs Fekrije Selimi and Patrice Codogno, Prs Peter Scheiffele, Pierrick Poisbeau and Markus Ruegg for their interest in my work and for judging. A special thank to Dr Jean Mariani for his implication in my work.

Many scientific thanks for advice to Dr Hadi Zanjani for the quantification method of Purkinje cells, to Dr Nancy Grant for the intricacies of a Western blot and how to write a an comprehensible English, Dr Laure Rondi-Reigg for the secrets of footprint tests and Dr Jean-Luc Rodeau for statistical analysis.

I wish to thank Brenda Bonnici and Vesna Radojevic for sharing their benches when the female mice delivered at an unexpected moment and Markus Saxer for technical help. A special happy thought to Brenda for those fascinating debates concerning the European Union.

Many thanks to Vanessa Gautheron who constantly made genotypes for me and revealed the mystery of the SSCP and to Drs Yves Lutz and Jean-Paul Fuchs for their expertise in Dpl genotyping.

Many thanks to Fabrice Richard and Raphael Leschiera who helped me during their training courses in cutting some mouse brains and counting autophagic profiles in ultrastructural sections, respectively.

I also wish to thank Dr Sophie Reibel-Foisset, Dr Dominique Ciocca and Nicolas Lethenet for their technical help in the animal facility.

Je tiens à remercier mon petit rossignol alsacien, Anne-Marie, qui a supporté mes blagues pendant 5 longues années. Blagues qui n'étaient qu'une réplique à ses trémolos et concerts improvisés de Poulenc ou de chant lyrique scandinaves. Sache que tes essais culinaires me manqueront grandement.

Un grand merci à Guy, dont j'ai supporté les blagues pendant 5 ans, pour son immense savoir et pour toute son aide technique. Je n'oublierai pas tes interventions enflammées sur l'allongement du temps de travail. Puisses-tu profiter pleinement et heureusement de ta retraite le jour venu.

Egalement mille mercis à Monique et surtout Valérie à qui j'ai décommandé sans relâche des séances de microscopie et qui, avec une constance inébranlable, a fait semblant de croire à mes excuses douteuses. Les pauses café-bredele me laissent un souvenir impérissable.

Je remercie grandement tous les membres de NSN et plus particulièrement Jean-Luc Dupont pour nos traits d'humour concernant le « Joe Bar Team », Renaud pour nos discussions doctorales, Fanny, Aurore, Aurélie, Petra, Valérie, Frédéric (x2), Cédric, Alexandre, Yann, Etienne, Stéphane (x2), Nicolas pour nos discussions tout court.

Merci au Dr Michael Gutnic pour m'avoir donné l'opportunité d'enseigner les statistiques aux étudiants de cycle de Licence.

Merci également à tous ceux avec qui j'ai collaboré au sein de l'Addal et surtout Jennifer pour son indéfectible amitié.

Merci surtout à ma maman et à Eleonore, mon épouse, pour m'avoir encouragé durant cette période. Merci à ma petite Camille de m'avoir laissé dormir la nuit, lorsque je rédigeais le présent manuscrit.

Je ne saurais finir ces remerciements sans mentionner le grand Albert Einstein dont la théorie de la relativité restreinte à grandement contribué à sauver mes années de lycée ainsi qu'Olivier Combeau, enseignant de biologie au Séminaire de Jeunes de Walbourg, pour avoir cru en moi dès le début et m'avoir poussé dans cette voie alors que je n'étais qu'un petit adolescent insolent.

Table of contents

Abbreviations

3-MA	3-Methyladenine
ABC	Avidine Biotin Complex
Apaf1	Apoptosis protease activating factor-1
ATG	Autophagy gene
BH	Bcl homology
BSE	Bovine spongiform encephalopathy
CARD	Caspase recruitment domain
CJD	Creutzfeld Jacob disease
DED	Death effector domain
DFF45	DNA fragmentation factor 45kDa
DISC	Death-inducing signal complex
DIV	Days *in vitro*
DNA	Desoxyribonucleic acid
Dpl	Doppel
E13.5	Embryonic day 13.5
EGL	External germinal layer
ER	Endoplasmic reticulum
ERAD	Endoplasmic reticulum associated degradation
FADD	Fas-associated death domain
Fas	Fibroblast-associated
FLIP	FADD-like-ICE-inhibitory protein
GABA	γ amino butyric acid
GluR	Glutamate receptor
ho	*hotfoot*
IP_3R	Inositol triphosphate receptor
IR	Immunoreactivity
JNK	c-jun N-terminal protein kinase
LTD	Long term depression
LTP	Long term potentiation
Lc	*Lurcher*
LYATT	Lysosomal amino acid transporter
MAPK	Mitogen-activated protein kinase
MEM	Minimum essential medium
MOMP	Mitochondrial outer membrane permeabilisation
NASP	1-Naphtyl-acetyl-spermine
NDUFS	Subunit of the mitochondrial respiratory complex I
Neo	Neomycine
NGS	Normal goat serum
NHS	Normal horse serum
ORF	Open reading frame

P2	Postnatal day 2
PB	Phosphate buffer
PBS	Phosphate buffer saline
PCD	Programmed cell death
PCR	Polymerase chain reaction
PI3-K	Phosphoinositide 3-kinase
PKC	Proteine kinase C
PrP^{C}	Cellular prion protein
PrP^{res}	Prion protein resistant to proteinase K
PSD	Post-synaptic density
PTP	Protein tyrosine phosphatase
RML	Rocky mountain laboratory
ROS	Reactive oxygen species
rpm	Rotations per minute
Scrg1	Scrapie responsive gene 1
SOD	Superoxide dismutase
SQSTM	Sequestosome
SSCP	Single-strand conformation polymorphism
TNF-R1	Tumor necrosis factor receptor 1
TOR	Target of rapamycin
TRADD	TNF-R-associated death domain
TRAIL-R	TNF-related apoptosis-inducing ligand receptor
TSE	Transmissible spongiform encephalopathy
UPR	Unfolded protein response

Introduction

During the course of my thesis, I investigated the participation of apoptotic and autophagic cell death programs in neuropathologies. Neuronal cell death mechanisms are known to play a major role in neurodegenerative diseases and the physiopathological significance of the interplay between apoptotic and autophagic cascades is still not understood. Insights into the complex patterns of neuronal cell death observed in nervous system diseases are critically needed to take up the challenge of designing novel neurodegenerative disease therapies, specifically targeting cell death pathways.

A million people worldwide are affected by neurodegenerative diseases, a heterogeneous group of degenerative conditions affecting specific areas of the central nervous system. The majority of neurodegenerative pathologies are age-related disorders, and these diseases are becoming an increasing health and socio-economical problem in industrialized countries (Mayeux, 2003). Neurodegenerative diseases such as amyotrophic lateral sclerosis, Alzheimer, Parkinson, Huntington and prion diseases induce progressive cognitive or movement impairment depending on the type of neuronal cells undergoing selective degeneration (Troncoso et al., 1996; Cleveland, 1999; Nunomura et al., 2007). Although these diseases are phenotypically well described, the molecular mechanisms leading ultimately to neuronal death remain unclear, and despite vigorous research efforts, therapy options have not been found.

In Alzheimer (Nakagawa et al., 2000; Nixon et al., 2005), Parkinson (Webb et al., 2003; Hayley et al., 2004), Huntington (Hickey and Chesselet, 2003) and prion (Lucassen et al., 1995; Liberski et al., 2008) diseases, autophagy and apoptosis have been shown to be activated in parallel. If apoptosis is an absolute programmed cell death mechanism, in most cases, autophagy constitutes cell defense mechanisms towards cellular dysfunction or stress. Thus, both apoptosis and autophagy may be triggered by common upstream

signals resulting in either combined autophagy and apoptosis or a switch between the two mechanisms in a mutually exclusive manner (Chu, 2006; Maiuri et al., 2007).

I focused my investigations on the cerebellar Purkinje cell in mouse models with mutations which specifically affect these neurons using a combination of biochemical, histological and cytological methods *in situ* as well as in organotypic cerebellar cultures. This approach has provided new insights into the complex molecular and cellular events underlying neuronal stress and degeneration.

The cerebellum presents several advantages for the anatomical study of neurodegeneration: *i*) it consists of the repetition of a single neuronal circuit made up of a few types of neurons and afferences centered on the Purkinje cell which emits the only output of the cerebellar cortex, *ii*) cerebellar abnormalities are usually straightforward to recognize because cerebellar damage manifests itself as abnormalities in gait and posture (ataxia), *iii*) many spontaneous mutations that affect cerebellar development and function have been recognized and lead to Purkinje cell degeneration (Appendix N°1). Purkinje cell death was investigated in *Lurcher* and *hotfoot* mice with mutations of the *Grid2* gene coding for the glutamatergic receptor GluRδ2 on one hand and, in the Nagasaki $Prnp^{0/0}$ mutant mouse deficient for the prion protein and overexpressing its neurotoxic paralogue Doppel on the other hand.

The aims of this project were

1) **To determine the mechanisms of *Lurcher* Purkinje cell death.** The *Lurcher* mutation transforms the GluRδ2 receptor into a constitutively opened channel. In *Lurcher* heterozygous mice, cerebellar Purkinje cells are permanently depolarized, a characteristic that has been thought to be the primary cause of their postnatal apoptotic death, although autophagy has been suggested to contribute to GluRδ2-induced death (Yue et al., 2002). The more dramatic phenotype of *Lurcher* homozygotes is probably due to a simple gene dosage effect of the mutant allele. We have analyzed the phenotype of *Lurcher*/*hotfoot* heteroallelic mutants bearing only one copy of the *Lurcher* allele and no wild-type *Grid2* to determine the effects of the absence of wild-type GluRδ2 receptors on Purkinje cell survival in these mutants. Using a pharmacological approach in organotypic cerebellar cultures, I further analyzed the respective contributions of autophagy

and excitotoxicity-induced apoptosis in the GluRδ2-*Lurcher* Purkinje cell survival and growth.

2) **To analyze the involvement of autophagy in the dendritic development and synaptogenesis of Purkinje cells.** The Purkinje cells of the *hotfoot* mutant mice are lacking GluRδ2 and display impaired climbing fiber (Kashiwabuchi et al., 1995) and parallel fiber (Kurihara et al., 1997) innervations indicating that GluRδ2 is involved in Purkinje cell excitatory synaptogenesis. During normal development, the postsynaptic spines deafferented by supernumerary climbing fiber elimination may involve GluRδ2-dependent autophagy. In the *hotfoot* adult cerebellum, Purkinje cells display many postsynaptic spines devoid of presynaptic innervation (Kashiwabuchi et al., 1995). The persistence of these spines may be due to the lack of GluRδ2-dependent autophagic mechanism. I analyzed Purkinje cell development in the *hotfoot* cerebellum to estimate the contribution of GluRδ2-dependent mechanisms (autophagy?) to the excitatory synaptogenesis of Purkinje cells. Firstly, the survival and dendritic development of Purkinje cells were compared between *hotfoot* and wild-type organotypic cerebellar cultures, and then climbing fiber development was examined during the postnatal period in the *hotfoot* cerebellum.
3) **To assess which neuronal death mechanisms are activated by Doppel during Purkinje cell degeneration in prion protein-deficient Nagasaki mutant mice.** In the Nagasaki mutant mouse, Purkinje cells prematurely die from toxicity induced by Doppel, a prion protein-like protein overexpressed in the absence of the cellular prion protein (PrP^C) (Moore et al., 2001; Wong et al., 2001; Cui et al., 2003; Sakudo et al., 2005b). To provide insight into the neuroprotective properties of PrP^C, as well as into the cell death programs triggered by Doppel, transgenic models were examined by biochemical and anatomical analysis.

The literature review of my thesis is divided into four parts which include an overview of apoptosis and autophagy – **the molecular basis of programmed cell death** - an overview of anatomy, development and physiological functions of the brain region under the focus of my research - **the mouse cerebellum** - and an overview of the mutant mice models of Purkinje cell degeneration analyzed in my thesis – **the *hotfoot* and the *Lurcher* Grid2 mutant mice** – and – **the Nagasaki prion protein-deficient mice**. The

results obtained in the *Grid2* mutant mice studies are presented in the format of unpublished data and a publication, and the data obtained in the Nagasaki mutant mice studies are presented in the format of publications. Afterwards, I shall integrate the results obtained from these models, and discuss the results in the light of other neuropathologies and highlight the importance of interplay between apoptosis and autophagy in neuronal response to pathological insults.

1. Molecular basis of programmed neuronal cell death

Cell death is a fundamental process involved in the regulation of tissue homeostasis and necessary for the elimination of supernumerary and diseased cells. This is achieved by two major active self-destruction mechanisms: the regulated and the unregulated pathways (Fig. 1). The unregulated cell death mechanism is a non-programmed cell death pathway often called necrosis and is caused by overwhelming stress. Characteristic features of necrosis include organelle swelling, mitochondrial dysfunction, massive oxidative stress and plasma membrane permeabilization. Necrosis irreversibly leads to the release of intracellular organelles and inflammation (Zong et al., 2004; Ditsworth et al., 2007). The regulated cell death mechanisms essentially comprise two programmed cell death (PCD) pathways: apoptosis (or type I PCD), the first characterized form of PCD, and autophagy (or type II PCD) which has been proposed to be an alternative cell death pathway, but is still controversial (Tsujimoto and Shimizu, 2005; Chu, 2006). Both are essential for discrete removal of supernumerary cells such as neurons during normal development. Under pathological conditions, apoptosis and autophagy may be activated in addition to necrosis.

1.1 ***Apoptosis: the type I programmed cell death***

Apoptosis is a highly conserved and complex cellular mechanism (Kerr et al., 1972). In mammals, external signals trigger two major pathways leading to the activation of caspases: the mitochondrial pathway (intrinsic pathway) and the death receptor pathway (extrinsic pathway).

1.1.1 Caspases, the main effectors of apoptosis

Caspases are a family of 14 cysteine-dependent aspartate-specific acid proteases that mediate and execute the apoptotic cell death program (Yuan et al., 1993; Salvesen and Dixit, 1997). All caspases exist as a latent pro-form of a single polypeptide chain, and are activated by specific cleavage at aspartic acid residues which leads to the formation of active tetramers and initiate apoptosis (Shi, 2002).

Caspases can be divided into 3 groups with respect to their structure and function (reviewed in Degterev et al., 2003):

- Group I or inflammatory caspases (Caspases 1, 4, 5, and 11) are not involved in apoptosis but play a role in the maturation of cytokines during inflammatory processes.
- Group II or initiator caspases (Caspases 2, 8, 9, 10, and 12) are long prodomain-containing caspases including DEDs-containing caspases (8 and 10) and CARD-containing caspases (2 and 9).
- Group III or effector caspases (Caspases 3, 6 and 7) are executioner caspases. These short prodomain-containing caspases are activated by upstream initiator caspases and cleave multiple cellular substrates.

Caspases 13 and 14 are still not characterized and are structurally close to inflammatory caspases.

1.1.2 The intrinsic pathway

The intrinsic apoptotic pathway is initiated in the mitochondria and the endoplasmic reticulum. The major event is the mitochondrial outer membrane permeabilization (MOMP). MOMP is mainly regulated by a specific class of proteins belonging to the B-cell/Lymphoma-2 family (Bcl-2 family), which play a pivotal role in the activation of the caspase cascade.

1.1.2.1 The Bcl-2 family

The Bcl-2 family of proteins can be divided into 2 groups:

- The anti-apoptotic proteins BCL-2, BCL-$_{XL}$, BCL-w, MCL-1.
- The pro-apoptotic proteins BAX, BAK, BOK, BID, BIM, BAD.

All Bcl-2 family members have at least one of the 4 known Bcl-homology domains (BH1 to 4) which correspond to α-helical segments (Adams and Cory, 1998). Some pro-apoptotic proteins called “BH3-only” proteins (BID, BIM, BAD) contain only a BH3 domain (Puthalakath and Strasser, 2002), and others such as “BH123”-containing proteins (BAX, BAK, BOK) share BH1 to 3 with BCL-2 (Adams and Cory, 1998). In this context, the BH3 domain is presumed to be an essential death domain and both BH3-only and BH123 domain proteins are required for the induction of apoptosis (Cheng et al., 2001).

1.1.2.2 The apoptotic mitochondrial cascade

In normal conditions, the pro-apoptotic proteins are cytosolic and anti-apoptotic proteins (Krajewski et al., 1993) are membrane-bound proteins of the ER and the mitochondria (Zhu et al., 1996). In the mitochondria, anti-apoptotic proteins sequester the pro-apoptotic ones in stable mitochondrial complexes, thereby preventing the activation of BH123 proteins such as BAX and BAK (Cheng et al., 2001). Apoptotic signals are able to activate BID by inducing homodimerization and translocation of BAX and BAK to the mitochondria (Fig. 2) (Wolter et al., 1997; Gross et al., 1998; 1999). BAX can be activated by another pathway which also involves activation of the transcription factor p53 when DNA is damaged (Lane, 1992; Miyashita and Reed, 1995). Homodimerization of BAX allows an efflux of cytochrome c due to the constitution of a pore in the mitochondrial outer membrane (Fig. 2) (Liu et al., 1996; Newmeyer and Ferguson-Miller, 2003). The binding of cytochrome c to the apoptosis protease activating factor-1, Apaf1 (Zou et al., 1997) causes the formation of a complex called the apoptosome in the presence of ATP. The subsequent recruitment of procaspase-9 will lead to the activation of the effector caspases 3, 6 and 7 (Fig. 2) (Li et al., 1997; Cecconi et al., 1998).

1.1.2.3 The ER stress apoptotic cascade

Oxidative stress can induce the unfolded protein response (UPR) in the endoplasmic reticulum (ER) which permits the elimination of misfolded protein aggregates. The UPR can be unable to counteract the stress which leads to the triggering of apoptosis (Fig. 3) (Breckenridge et al., 2003; Rao et al., 2004a). This mechanism requires the release of calcium from the ER through the binding of a small amount of cytochrome c released from the mitochondria. This positive feedback will result in the activation of the caspase cascade (Rao et al., 2004b). The Bcl-2 family members BCL-2, BAX and BAK themselves can also act at the ER level (Zong et al., 2003). BCL-2 is able to interrupt the described above crosstalk between ER and mitochondria, while BAX and BAK regulate the Ca^{2+} release from the ER (Scorrano et al., 2003) and promote caspase-12 activation. Activated caspase-12 will then translocate from the ER to the cytosol, directly cleave procaspase-9 to activate the effector caspase-3 (Szegezdi et al., 2003) and finally cause apoptotic cell death.

1.1.3 The extrinsic pathway

The extrinsic pathway is activated by ligand binding to death receptors such as tumor necrosis factor receptor 1 TNF-R1 (Tartaglia et al., 1993), fibroblast-associated Fas (Suda et al., 1993) and TNF-related apoptosis-inducing ligand receptor TRAIL-R (Griffith et al., 1998) which are transmembrane proteins (Fig. 4) with an extracellular cysteine-rich domain and an intracellular death domain. The ligand-bound TNF-R1, Fas and TRAIL-R transmit apoptotic signals through the binding of their death domain with the death domain of the TNF-R-associated death domain protein TRADD (Hussein et al., 2003) or the Fas-associated death domain protein FADD (Chinnaiyan et al., 1995; 1996) (Fig. 4). The N-terminal death effector domain DED (Lee et al., 2000) and caspase recruitment domain CARD (Hofmann et al., 1997) of FADD will be activated leading to the activation of caspases 8 and 10 (Fig. 4) (Weber and Vincenz, 2001) and the formation of the death-inducing signal complex DISC (Lee et al., 2000; Wang, 2001; Lavrik et al., 2003). This complex will finally activate effector caspase-3 (Fig. 4) (Stennicke et al., 1998). The caspase signaling initiated by the death receptors is regulated by the FADD-like-ICE-inhibitory protein FLIP which competitively inhibits the recruitment of procaspase-8 by FADD (Irmler et al., 1997; Scaffidi et al., 1999).

The c-jun N-terminal protein kinase JNK, a member of the mitogen-activated protein kinase (MAPK) is involved in TNF-induced apoptosis and may play a pro-apoptotic role in neurons. JNK can phosphorylate and thereby inactivate BCL-2 and BCL-$_{XL}$ (Fig. 4) (Basu and Haldar, 2003) and can activate the proapoptotic BH3-only protein BIM (Becker et al., 2004).

An intrinsic, mitochondrial-dependent apoptotic pathway has been shown to be activated by TNF-R1 and Fas (McKenzie et al., 2008) through the cleavage of the Bcl-2 family member BID by caspase-8 (Li et al., 1998; Scaffidi et al., 1998). The resulting truncated form tBID has been shown to induce the release of cytochrome c (Luo et al., 1998) and apoptosis. On the basis of the recruitment of the mitochondrial pathway by death receptors, two types of responses have described. Type I cells respond by activation of caspase-8 in the DISC inducing apoptosis. However, type II cells respond by only a small amount of FADD and caspase-8 recruitment to the DISC requiring the intrinsic pathway to induce apoptosis. Along this line, in *Bid*$^{-/-}$ mice, hepatocytes behave like type II cells after Fas-L treatment, whereas thymocytes respond to Fas-L in a type I manner (Zheng and Flavell, 2000).

1.1.4 The targets of caspases

The cleavage and subsequent activation of effector caspases (3, 6 and 7) by the initiator caspases 2, 8, 9, 10 and 12 is called the caspase cascade (Degterev et al., 2003). In addition, caspase-8 is able to activate the BH3-only BID protein.

Caspase-3, the predominant effector caspase, activates the signal components that affect the morphological changes associated with apoptosis. These components include the DNA fragmentation factor 45kDa (DFF45) (Liu et al., 1997) involved in DNA degradation (Enari et al., 1998; Mukae et al., 1998) and the subunit of the mitochondrial respiratory complex I (NDUFS) which causes the overproduction of reactive oxygen species (ROS) and the disruption of electron transport (Ricci et al., 2004). The disruption of actin filaments (Kothakota et al., 1997) and cell-to-cell interactions (Ku et al., 1997; Schmeiser et al., 1998) also induced by the effector caspases contribute to the dismantling of the cellular architecture.

The caspases are responsible for the activation of pro-apoptotic protein kinases such as ROCK1 in response to TNF-R activation (Coleman et al., 2001) and MEKK1 through Jun-kinase pathway during Fas-induced apoptosis (Deak et al., 1998). The caspases also cleave anti-apoptotic protein kinases including AKT (Bachelder et al., 2001) and FAK in response to TRAIL signaling leading to a loss of survival signals (Wen et al., 1997).

Caspases have been shown to cleave anti-apoptotic Bcl-2 family members such as BCL-2, BCL-$_{XL}$ suggesting that a positive feedback mechanism is set off by apoptosis (Degterev et al., 2003).

1.1.5 Neuronal apoptosis

Since the pioneering work of Levi-Montalcini on the survival of developing neurons (Hamburger and Levi-Montalcini, 1949), the essential role of apoptosis in the control of neuronal numbers during development of the nervous system has been supported by an increasing number of data (Becker et al., 2004). Neuronal apoptosis not only has a major role in sculpting relationships between neuronal populations in the developing brain, but is also the cardinal cell death process in many neurodegenerative diseases (Yuan and Yankner, 2000).

1.1.5.1 Apoptosis during neuronal development

Transgenic mouse lines over-expressing or knocked-out for the major factors involved in the mitochondrial pathway have been generated, and these models have revealed the importance of intrinsic mitochondrial apoptosis during brain development. For example, knocking-out the pro-apoptotic factor *Bax* gene has been shown to result in the increase of specific neuronal populations, such as peripheral ganglia, motor pools in the spinal cord and trigeminal brainstem nuclear complex (White et al., 1998) and Purkinje cells in the cerebellum (Fan et al., 2001) suggesting that these neurons undergo a period of naturally occurring, BAX-mediated cell death during brain development. This is also in line with the increase of Purkinje cell population observed when BCL-2, the main BAX antagonist is overexpressed (Zanjani et al., 1996).

An interesting study by Krajewska et al (2002) has described the onset of BAX, BAK, BCL-2, BID and BCL-$_{XL}$ expression in the developing central nervous system and outlined the antagonistic functions of these pro and anti-apoptotic factors in the formation of the neuronal tube and in the differentiation of proliferative zones in the developing brain.

1.1.5.2 Apoptosis in neurodegenerative diseases

In ischemic brain tissue, neuronal cell death has been shown to occur by Fas-dependent, (Northington et al., 2001) caspase-3-mediated apoptosis (Namura et al., 1998).

Neuronal death mechanisms have been extensively investigated in a number of neurodegenerative diseases including amyloid neuropathologies. In Alzheimer disease, the β–amyloid peptide is known to induce oxidative stress (Behl et al., 1994) which activates caspase-12-mediated apoptosis (Nakagawa et al., 2000). In prion diseases, apoptosis is detected in the prion-infected brain tissue (Fairbairn et al., 1994; Lucassen et al., 1995). This neuronal loss has been shown to result from the neurotoxicity of the abnormal proteinase-resistant forms PrP^{res} of the prion protein PrP^{C} (Forloni et al., 1996). More recently, *Bax* inactivation has been shown to antagonize apoptosis of infected cerebellar granule cells *in vitro* (Chiesa et al., 2005). However, the neurodegenerative events induced by the cerebellotropic 22L scrapie strain were changed neither in the *Bax*$^{-/-}$ nor in the *Hu-bcl-2* overexpressing mice (Bailly, unpublished). Similar results were obtained with the 6PB1 bovine spongiform encephalopathy (BSE) strain in *Bax*$^{-/-}$ mice

(Coulpier et al., 2006) and with RML scrapie strain in *Bax*$^{-/-}$ and *Hu-bcl-2* overexpressing mice (Steele et al., 2007). In expanded polyglutamine repeats diseases such as Huntington disease, abnormal protein aggregates have been shown to activate caspase-8-mediated apoptosis (Ona et al., 1999; Sanchez et al., 1999).

In Parkinson disease, an augmentation of IFN-γ (Teismann et al., 2003) has been shown to upregulate Fas activating the extrinsic apoptotic pathway (Hayley et al., 2004).

The mutant superoxide dismutase (SOD) responsible for amyotrophic lateral sclerosis forms intra-neuronal aggregates and induces oxidative stress resulting in neuropathological features including apoptosis similar to those observed in Alzheimer and Huntington diseases (Cleveland, 1999).

1.2 ***Autophagy***

Normal cellular development and cellular response to changes in the extra- and intra-cellular media require a balance between synthesis and degradation of protein. Autophagy is a lysosomal pathway involved in the degradation of long-lived cytosolic proteins (De Duve et al., 1955). In the focus of my thesis, autophagy involving the sequestration and subsequent lysosomal degradation of bulk cytosol is macro-autophagy. An alternative cellular-to-vacuole targeting pathway is a specific autophagic process which permits selective degradation without bulk cytosol (Harding et al., 1996). It will not be detailed here although it has led to a better understanding of autophagic mechanisms (Wang and Klionsky, 2003).

1.2.1 Induction and regulation of autophagy

The discovery of TOR (Kunz et al., 1993), a target of the autophagy-inducer rapamycin (Blommaart et al., 1997a), initiated the study of mechanisms regulating autophagy. TOR inhibits autophagy and is activated by amino acids (Luiken et al., 1994), class I phosphoinositide 3-kinase (PI3-K) (Codogno and Meijer, 2005), eIF2a and Ras (Meijer and Codogno, 2004) and is inhibited by class III PI3-K (Blommaart et al., 1997b). The autophagic cascade is mediated by 31 autophagy genes (ATGs) in mammalian cells. Eighteen of these ATGs are involved in the formation of the autophagosome (Kabeya et al., 2007). In the initial phase of the autophagic cascade, ATG13 normally phosphorylated by TOR, is dephosphorylated, thereby allowing it to complex with ATG1 (Fig. 5).

Beclin1 (ATG6) belongs to the class III PI3-K complex (Kihara et al., 2001) and is able to inhibit TOR and trigger the autophagic cascade. Beclin1 and BCL-2 have been shown to interact via their common BH3 domain (Liang et al., 1998). Beclin1 is expressed by cortical, hippocampal and cerebellar neurons (Liang et al., 1998; Yue et al., 2002; Diskin et al., 2005) and its activation is a hallmark of autophagy during neurodegeneration (Shibata et al., 2006).

1.2.2 The autophagic sequence

Our current knowledge about the molecular basis of the autophagic cascade is summarized in the Figure 5.

1.2.2.1 Role of ATGs in the autophagosome formation

The dephosphorylation of ATG13 allows its binding to ATG1. The ATG1-13 complex then recruits ATGs 11-17-20-24 (Kamada et al., 2000) leading to the formation of the autophagosome. The construction of the autophagosome from the pre-autophagosomal membrane depends on 2 conjugation systems (Ohsumi and Mizushima, 2004). The first associates ATG16 to ATGs 5-7-10-12 to form the isolation membrane as a pre-autophagosome (Mizushima et al., 2003) from cytosolic organelles. The second is the ATG8/LC3 system (Mizushima et al., 1998). ATG8/LC3 was first identified as microtubule associated protein1-light chain 3 (Mann and Hammarback, 1994). In the autophagic process, pro-LC3 is processed into a cytosolic form LC3-I (Kabeya et al., 2000). LC3-I is activated by ATG7 (Tanida et al., 2001) and cleaved into a LC3-II membrane-bound form by ATG4 and conjugated with a phosphatidylethanolamine (PE) by ATG3 (Kabeya et al., 2000) (Tanida et al., 2002). Pre-autophagosome membrane-bound LC3-II-PE seems to be required for completion of the autophagosome (Kabeya et al., 2000). Finally, LC3-II delipidation by ATG4 will let it leave the autophagosome (Kirisako et al., 2000).

1.2.2.2 The autophagolysosome

After completion, the autophagosome fuses with lysosomes, a step involving the autophagosome-specific GTPase Rab7 (Gutierrez et al., 2004) and the lysosome-specific proteins Lamp1 and Lamp2 (Eskelinen et al., 2002). After fusion, the autophagosome inner single-membrane vesicle is released inside the vacuole lumen and termed

autophagic body and this autophagic body is then degraded by lysosomal enzymes such as cathepsins B, D and L (Punnonen et al., 1992; Uchiyama, 2001). Cathepsin B is a cysteine protease which belongs to the papain superfamily (Takio et al., 1980), cathepsin D is an aspartine protease which belongs to the pepsin superfamily of proteinases (Ferguson et al., 1973) and cathepsin L is a thiol protease (Kirschke et al., 1977).

Once degradation has been completed, monomeric units are exported to the cytosol for reuse. ATG22 has been identified as a putative amino acid effluxer (Yang et al., 2006) that cooperates with other vacuolar permeases such as the lysosomal amino acid transporters LYAAT 1 and 2 (Sagne et al., 2001)

1.2.3 Physiological autophagy

1.2.3.1 Autophagic degradation of cellular components

Autophagy is an essential mechanism of cell survival. In response to starvation, cells degrade their own cytoplasmic material by an autophagic-dependent mechanism. Autophagy is a survival mechanism of mammalian HeLa cells to serum and amino acids deprivation. Indeed, blockade of autophagy in this case induces apoptotic cell death (Boya et al., 2005). Cultured bone marrow cells deficient for BAX and BAK undergo autophagy if the interleukin 3 growth factor is suppressed, allowing extended survival. RNAi blocking ATG5 or ATG7 rapidly induces cell death (Lum et al., 2005). *In-vivo*, ATG7 deficiency in the central nervous system provokes apoptosis of cortical, hippocampal and cerebellar neurons (Komatsu et al., 2006).

In the developing brain, constitutive activation of autophagy is implicated in neuroprotection and cellular remodeling of neurites and growth cones during neurite extension (Hollenbeck, 1993). Autophagy can also selectively degrade cell-surface receptors. At neuromuscular junction of *Caenorhabditis elegans*, presynaptic terminals can induce clustering of GABA-A receptors leading to their degradation by a LC3 homolog-mediated autophagy (Rowland et al., 2006).

1.2.3.2 Autophagy: the type II programmed cell death

A role for autophagy in regulating cell populations during development of living organisms is increasingly considered as a phylogenetically old process. For example, in *Drosophila*, embryonic salivary glands (Lee and Baehrecke, 2001) and the fat body at the end of larval stage are eliminated by autophagic programmed cell death (Rusten et al.,

2004). During moth development, autophagy may be involved in the elimination of larval intersegmental muscles (Schwartz et al., 1993).

This type II programmed cell death is called autophagic cell death (Cao et al., 2006) and is characterized by a marked proliferation of autophagic vacuoles and the progressive disappearance of cellular organelles (Schweichel and Merker, 1973). In autophagic cell death, cells, such as neurons, destined for elimination internalize cytoplasmic components into autophagic compartments for self-degradation, and death subsequently occurs by hyperactive autophagy (Nixon, 2006).

1.2.4 Autophagy in neuropathologies

Autophagy has been linked to a number of pathologies including neuropathologies (Nishino et al., 2000; Nixon, 2006). Axotomy rapidly induces autophagic activity in mouse central neurons, well before the beginning of axonal remodeling (Matthews, 1973).

In neurodegenerative diseases including Alzheimer, Parkinson, Huntington and prion diseases, mis-aggregated proteins accumulate in spite of autophagic activity and this has lead to the concept of autophagic failure or autophagic stress. The specific recognition of ubiquitin-positive aggregated proteins has been shown to be mediated by p62/SQSTM1 (Rideout et al., 2004; Bjorkoy et al., 2005) an adaptor protein between ubiquitinated proteins and LC3-expressing autophagosomes (Filimonenko et al., 2007; Pankiv et al., 2007). Accumulation of autophagic profiles are features of degenerative neurons in Alzheimer- and prion-diseased brains (Nixon et al., 2005; Liberski et al., 2008). In Alzheimer disease, autophagy at the synaptic level parallels decreased synaptic activity (Sikorska et al., 2004). In Huntington disease too, the abnormal accumulation of autophagic vacuoles containing mutated huntingtin (Ravikumar et al., 2005) is believed to induce neuronal apoptosis (Hickey and Chesselet, 2003). In Parkinson disease, the cell death pattern is complex with features of apoptosis in addition to the accumulation of autophagosome-like structures (Stefanis, 2005). Alpha-synuclein mutations that have been identified in certain cases of Parkinson disease can induce cell death in association with accumulation of autophagic vacuoles that are not completely acidified or missing cathepsin D (Stefanis et al., 2001).

1.3 ***Interplay between autophagic and apoptotic pathways***

1.3.1 Apoptosis blockade induces autophagy

Experiments on *Bax*$^{-/-}$; *Bak*$^{-/-}$ double knock-out MEF and bone marrow cell lines exposed to either DNA damage or stress signals indicate overactivation of autophagy. In MEF cells, massive autophagy delays cell death and can be abrogated by knocking-down Beclin1 or ATG5 gene (Shimizu et al., 2004). Conversely, in bone marrow cells, increased autophagy favors cell survival whereas knock-down of ATG5 or ATG7 genes restores cell death (Lum et al., 2005).

Blockade of lipopolysaccharide-induced apoptosis by inhibition of caspases triggers autophagic cell death of L929 macrophages. This can be abrogated by knocking-down the Beclin1 gene (Yu et al., 2004; Xu et al., 2006). This indicates that deficiency or blockade of apoptosis can switch the cell response from stress to autophagy.

1.3.2 Blockade of autophagy induces apoptosis

Cells with deficient autophagic machinery can undergo apoptosis. Along this line, Lamp2-deficient HeLa cells can not complete autophagic process, and this results in a strong activation of apoptotic cell death (Boya et al., 2005; Gonzalez-Polo et al., 2005). These data support the concept of a dual autophagic and apoptotic cell death mechanism in the above mentioned neurodegenerative diseases (Chu, 2006; Nixon, 2006).

1.3.3 Crosstalk between apoptosis and autophagy

1.3.3.1 Regulation of apoptosis by ATGs

Surprisingly, overexpression of the autophagy gene ATG5 leads to increased apoptosis, but not autophagy. Yousefi et al (2006) demonstrated that calpain can cleave ATG5 into its truncated form, tATG5. This tATG5 induces apoptosis and the release of mitochondrial cytochrome c. Moreover, tATG5 has been shown to directly bind BCL-$_{XL}$. Thus, ATG5 plays an important role in the regulation of apoptosis because tATG5 is able to sequester Bcl-2 anti-apoptotic proteins, thereby allowing the pro-apoptotic homodimerization of BAX (Fig. 6) (Yousefi et al., 2006).

1.3.3.2 Regulation of autophagy by Bcl-2 family members and caspases

Beclin1, a major ATG (see §1.2.1) was initially shown to bind BCL-2 (Liang et al., 1998). This interaction inhibits autophagy induced by starvation. For a presently

unexplained reason, only the ER-bound, but not mitochondria-bound BCL-2 can inhibit autophagy (Pattingre et al., 2005).

Interestingly, caspases are not only used during apoptosis, but also function in the regulation of autophagic cell death as in the case of the *Drosophila* salivary gland (Martin and Baehrecke, 2004). Beclin1 and ATG7-dependent autophagic death has also been shown to be induced by caspase-8 inhibition (Yu et al., 2004).

1.3.3.3 Regulation of autophagy by the apoptotic extrinsic pathway

A functional relationship between autophagy and the extrinsic apoptotic pathway (Jia et al., 1997) is further supported by the absence of autophagic vacuoles in cultured mammary epithelial cells where TRAIL-mediated apoptosis is inhibited (Mills et al., 2004) and by the induction of autophagy by TNFα activation in T-lymphoblastic cells (Jia et al., 1997). In addition, some proteins involved in the extrinsic signaling pathway have recently been implicated in autophagy. For example, down-regulation of ATG5 expression in HeLa cells suppresses cell death and vacuole formation induced by IFNγ and FADD (Pyo et al., 2005).

These data demonstrate that common upstream signals may trigger autophagy and apoptosis, meaning that apoptotic and autophagic machinery share common pathways that either link or polarize the cellular response.

2. The mouse cerebellum

The cerebellum is a highly folded hindbrain structure that lies dorsal to the pons and medulla. Three pairs of cerebellar peduncles, the inferior, middle and superior peduncles connect the cerebellum to the brainstem.

*2.1 **The cerebellar anatomy***

2.1.1 General organization

The cerebellum is bilaterally symmetrical: two lateral hemispheres are separated medially by the central longitudinal vermis (Larsell, 1952). It is divided into anterior and posterior lobes by a transverse primary fissure and a ventral flocullonodular lobe. The cerebellum has a folded appearance with fissures separating its antero-posterior extent into 10 lobules (Fig. 7A). Two major structures can be discerned: a uniformly structured cortex surrounding 3 right and left deep cerebellar nuclei within the central white matter: the fastigial (median), the interposed (intermediate) and the dentate (lateral) nuclei (Fig. 7B) (Larsell, 1952).

2.1.2 The cerebellar cortex

Each single folium is composed of a cortex or superficial grey matter over a central white matter. The cerebellar cortex is histologically homogenous with a uniform microstructure throughout the entire cerebellum and has 4 main neurons: the granule, the Purkinje (Purkinyé, 1877), the Golgi and the basket/stellate cells. Three layers make up the cerebellar cortex (Fig. 7B). The outer molecular layer contains basket/stellate cells (Ramón y Cajal, 1911), the Purkinje cell dendritic tree and parallel fibers emanating from the granule cells. The Purkinje cell somata form a dense monolayer between the internal granular layer and the molecular layer (Palay and Chan-Palay, 1974). The internal granular layer contains the granule cells and the Golgi cells (Ramón y Cajal, 1911). The deep cerebellar nuclei contain deep cerebellar neurons and interneurons.

2.1.2.1 The Purkinje cell

Purkinje cells are the principal neurons of the cerebellar cortex (Fig. 7B) and serve as the sole output from the cerebellar cortex to the deep cerebellar nuclei (Palay and Chan-Palay, 1974; Ito, 1984). Within the Purkinje cell layer, Purkinje cells express

biochemical heterogeneity of certain proteins (such as zebrin I and II) that segregate Purkinje cells into sagitally organized bands (Hawkes et al., 1985; Sotelo and Wassef, 1991; Bailly et al., 1995; Sarna and Hawkes, 2003). The Purkinje cell dendritic tree has a planar shape oriented in the sagittal plane (Fig. 7B) (perpendicular to the long axis of the folium) and is formed from one to two primary branches that further subdivide into secondary and tertiary branches (Palay and Chan-Palay, 1974; Ito, 1984). Two types of spines are located along the dendritic tree: *i*) spines that are restricted to the major dendritic trunks and bear primarily climbing fiber synapses and *i*) spines that stem from distal tertiary branchlets and make synapses with parallel fibers (Ramón y Cajal, 1911; Ito, 1984).

The axon of the Purkinje cell emerges from the basal pole of the soma, descends through the internal granular layer and makes GABAergic synapses mainly on the deep cerebellar neurons (Palay and Chan-Palay, 1974). Some Purkinje cell axons from specific lobules (lobule X and the floculus) make synapses on the neurons of the vestibular nuclei to mediate balance (Ito, 1984). Collaterals are also emitted along the descending Purkinje cell axon and re-enter the Purkinje cell layer in the same sagittal plane as the Purkinje cell dendrites. These collaterals contribute to supra- and infraganglionic plexuses, which form above and below the Purkinje cell layer, thereby inhibiting adjacent Purkinje, Golgi, basket and stellate cells (Palay and Chan-Palay, 1974).

2.1.2.2 The granule cells

The granule cells are found in the internal granular layer (Fig. 7B) and relay inputs from mossy fibers to the Purkinje cells. Granule cell somata are 5 to 8 µm in diameter and their dendrites, which are generally short, receive mossy fiber terminals (rosettes) to form complex synapses (glomeruli) with inhibitory Golgi axon terminals (Palay and Chan-Palay, 1974; Ito, 1984; Voogd and Glickstein, 1998). Granule cell axons ascend through the molecular layer, bifurcate and run parallel to the longitudinal axis of the folium as parallel fibers (Palay and Chan-Palay, 1974; Voogd and Glickstein, 1998) forming *en passant* synapses on the spines of the Purkinje cell tertiary dendrites and on the inhibitory interneurons.

2.1.2.3 The interneurons

There are at least five types of interneurons in the cerebellar cortex (Fig. 7B): the basket, the stellate, the Golgi, the Lugaro and the unipolar brush cells (Palay and Chan-Palay, 1974). All of these interneurons, with the exception of the unipolar brush cells, have been shown to be inhibitory (Eccles et al., 1966c; Aoki et al., 1986). The basket and stellate axons provide lateral inhibition in the parasagittal plane to adjacent Purkinje cell somata and dendrites, respectively (Palay and Chan-Palay, 1974). The Golgi cell dendrites receive input from granule cells as well as from mossy fibers and, provide feed-back inhibition to granule cells (Palay and Chan-Palay, 1974) thereby forming a closed inhibitory circuit in the cerebellar cortex.

2.1.3 The cerebellar afferents

The olivocerebellar fibers (i.e. climbing fibers) and the mossy fiber system constitute the two major cerebellar afferent systems. Both systems carry sensorimotor information directly to the deep cerebellar nuclei and also to the cerebellar cortex to regulate the extent to which the climbing and the mossy fibers activate the deep cerebellar nuclei. The differences that emerge in the synaptic strength within the cerebellar cortex are thought to form the basis of cerebellar plasticity during learning (De Zeeuw and Yeo, 2005).

2.1.3.1 The olivocerebellar system

Climbing fibers are one of the main operational inputs into the cerebellar cortex. Electrophysiological (Eccles et al., 1966b), autoradiographic (Courville and Faraco-Cantin, 1978) and degeneration (Desclin, 1974) techniques have shown that climbing fibers originate exclusively from neurons in the inferior olive of the medulla. The inferior olive sends olivocerebellar axons to the cerebellum, where the final segment of the axon takes the form of a climbing fiber in the cerebellar cortex. The olivocerebellar projection predominantly crosses the medullary midline, terminating in the contralateral hemicerebellum with the addition of very small uncrossed component innervating the ipsilateral cerebellum (Chan-Palay et al., 1977; Sugihara et al., 1999). From the inferior cerebellar peduncle, axons extend into the white matter and branch into the cortex in the parasagittal plane (Azizi and Woodward, 1987) to synapse onto 5 to 7 Purkinje cells (Sugihara et al., 2001).

In the rat, the olivocerebellar projection has an organized topography that is arranged into a pattern of parallel longitudinal zones in the cerebellar cortex (Azizi and Woodward, 1987; Sugihara et al., 2001). In general, each subnucleus of the inferior olive projects contralateral climbing fibers that closely adhere to one or more parasagittal Purkinje cell zones which then projects to a specific part of the deep cerebellar nuclei (Campbell and Armstrong, 1983; Wassef et al., 1992; Sugihara et al., 2001). Furthermore, each olivary subnucleus gives off collaterals to the deep cerebellar nuclei, which receives Purkinje cell input from the same parasagittal zone(s) (Andersson and Armstrong, 1987) and in turn, the deep cerebellar neurons project to the same olivary subnuclei from which they receive collaterals (Ruigrok and Voogd, 2000). In summary, the Purkinje cells in each longitudinal zone receive climbing fibers from a discrete zone within the inferior olive and these Purkinje cells send axons to a specific region in the deep cerebellar nuclei. A salient feature of the adult murine cerebellum is that each Purkinje cell receives input from only one climbing fiber, but every climbing fiber can innervate 5 to 7 Purkinje cells.

In the white matter, the olivocerebellar axons are thick (2 to 3 µm in diameter) and myelinated (Palay and Chan-Palay, 1974; Sugihara et al., 1999). However, as they ascend towards the internal granular layer, the axons become unmyelinated in the Purkinje cell layer and synapse onto the thick dendritic trunks of the Purkinje cells (Palay and Chan-Palay, 1974; Sugihara et al., 1999). In the Purkinje cell dendritic tree, climbing fiber arborisations emit fine beaded tendrils (including varicosities approximately 2 µm thick) that run along the Purkinje cell dendrites and synapse onto spines. These climbing fiber-Purkinje cell synapses are entirely covered by sheets of Bergmann glia (Palay and Chan-Palay, 1974). In addition to climbing fibers projecting onto Purkinje cells, climbing fibers also send collateral branches to the deep cerebellar nuclei (Palay and Chan-Palay, 1974; Sugihara et al., 1999; Ruigrok and Voogd, 2000; Sugihara et al., 2001).

2.1.3.2 The mossy fiber relay system

Mossy fibers are the second main cerebellar afferent and have different morphological and anatomical characteristics than the climbing fibers. They are derived from multiple sensory sources in the brainstem and the spinal cord (e.g. spino-cerebellar, vestibulo-cerebellar and lateral reticular, pontine reticulo-tegmental and external cuneate nuclei) (Palay and Chan-Palay, 1974; Voogd and Glickstein, 1998). Those mossy fibers

that arise from the brainstem or pons enter the cerebellum via the contralateral middle cerebellar peduncle (Mihailoff et al., 1981), while spinal mossy fibers enter the cerebellum through the inferior and superior peduncles (Chan-Palay et al., 1977). Similar to climbing fibers, mossy fibers run a myelinated axon into the white matter and emit collaterals to the deep cerebellar nuclei (Arsenio Nunes et al., 1988). From the white matter, mossy fibers ascend into the internal granular layer to synapse onto granule cell soma and dendrites (Palay and Chan-Palay, 1974). Their synaptic terminals form tapering enlargements called rosettes (Arsenio Nunes et al., 1988) that are enveloped by granule cell dendrites and Golgi cell axons.

Mossy fiber terminals were previously thought to have a very different spatial distribution in the cerebellar cortex compared to climbing fibers. Yet, new anatomical analysis shows the convergence of both afferent systems (Pijpers et al., 2006) such that non-adjacent cerebellar zones that receive the same climbing fiber input also share the same mossy fiber input. Unlike their distribution, the action of mossy fibers on Purkinje cells is different from that of climbing fibers. Firstly, excitatory activation of mossy fibers is exerted onto Purkinje cells indirectly by parallel fibers, the granule cell axons. Secondly, each parallel fiber contacts many Purkinje cells in the translobular plane and has a few synapses with each single Purkinje cell.

2.1.4 The cerebellar efferents

The major input to the deep cerebellar nuclei is made by the Purkinje cell axons (Voogd and Ruigrok, 2004) and the organization of the cortico-nuclear projection gives rise to the three functional zones of the cerebellum. Purkinje cells whose axons terminate onto the fastigial nucleus are located predominantly in the vermis, ventral paraflocculus and flocculus while Purkinje cell axons which terminate in the interposed and dentate nuclei primarily compose the paravermis and hemispheres, respectively. In turn, these three functional zones differ in the type of afferents received and are assumed to be implicated in different aspects of motor activity. For example, the vermis is considered to control balance both in stance and locomotion (Thach and Bastian, 2004) whereas goal-directed and visually-guided movements, in addition to the modulation of rhythmic-synchronized movements are controlled by the paravermis and hemispheres (Cooper et al., 2000).

Furthermore, individual deep cerebellar nuclei have characteristic efferent targets. The fastigial nuclei send both crossed and uncrossed efferent projections to the vestibular nuclei, the inferior olive, the pontine and lateral reticular nuclei. The interposed nuclei project primarily to the contralateral red nucleus. The dentate nuclei project principally to the contralateral thalamus, the prefrontal cortex and the red nucleus.

2.1.5 The cerebellar circuitry

The key neuron of the cerebellar circuit is the Purkinje cell, as it integrates a variety of inputs and is the sole efferent of the cortex. Purkinje cells receive 2 main excitatory inputs (Fig. 8): climbing fibers making synapses directly onto Purkinje cells in a 1 climbing fiber:1 Purkinje cell ratio and mossy fibers, indirectly via granule cells, in an approximately 100, 000 parallel fibers:1 Purkinje cell ratio (Eccles et al., 1966a; Ito, 1984). Climbing fibers stimulate sagitally oriented bands of Purkinje cells, whilst parallel fibers activate a transverse beam. It is presumed that cerebellar function takes place at the intersection of these two afferents. Simultaneously, Purkinje cell activity is modulated by the basket and stellate axons (Fig. 8) (running in a plan perpendicular to parallel fibers) which sharpen the Purkinje cell output by inhibiting sagitally adjacent Purkinje cells. The Golgi cells provide feedback inhibition to the mossy fiber-granule cell synapse and inhibit the transversally activated Purkinje cell beam (Fig. 8) (Palay and Chan-Palay, 1974). Then, the Purkinje cell axons exit the cortex and inhibit the deep cerebellar nuclei. In turn, the axons of the deep cerebellar neurons exit the cerebellum via the superior and inferior peduncles and transmit information to other motor centers (for example, the red nucleus and the thalamus).

2.1.6 Development of the cerebellar neurons and afferents

The first neurons to form are the inferior olivary neurons, followed by the deep cerebellar neurons and the Purkinje cells, which leave the ventricular neuroepithelium and settle in the developing cortical plate before birth (Altman and Bayer, 1997). The inhibitory interneurons also originate from the neuroepithelium of the 4th ventricle, migrate like the Purkinje cells but continue to proliferate during their transit through the deep cerebellar mass (Schilling, 2000). Similarly, a secondary neuroepithelium, the external germinal layer (EGL), is generated prenatally, the precursor cells migrating onto

the surface of the cerebellar plate by birth. This latter epithelium produces the granule cells (Altman and Bayer, 1997).

2.1.6.1 Development of the Purkinje cells

The Purkinje cells originate in the neuroepithelium of the 4th ventricle from embryonic day 13 (E13) (Altman, 1975). They ascend through the zone of the deep cerebellar nuclei to the cortical plate on the surface of the cerebellar primordium anlage by E15 (Altman and Bayer, 1978) leaving their axons behind and establishing synaptic contacts with deep cerebellar neurons as early as E20 (Eisenman et al., 1991). From E20, climbing fibers are present in the Purkinje cell plate (Chedotal and Sotelo, 1992) and make transient contacts with Purkinje cells (Morara et al., 2001), suggesting very early influence of climbing fibers on Purkinje cells. At birth, the morphological features of Purkinje cells are clearly apparent at the inner boundary of the EGL and are arranged in a 6-12 cell-deep plate (Altman and Bayer, 1997). Their somata contain a large clear nucleus and minimal cytoplasm that emit short thin processes across the EGL (Altman and Bayer, 1997).

From birth to postnatal day 2 (P2), transient synapses exist between climbing fiber axon terminals and transient emerging dendrites of the Purkinje cells (Armengol and Sotelo, 1991; Chedotal and Sotelo, 1993). From P3 to P4, Purkinje cells begin to align in a monolayer (Altman and Bayer, 1997) which is thought to be influenced by parallel fiber growth from above and granule cell migration to Purkinje cells from below (Goldowitz and Hamre, 1998). They display fine somatic processes that receive immature climbing fiber arbors (Mason et al., 1990; Armengol and Sotelo, 1991). From P5 to P7, a large apical cone develops increasing the Purkinje cell somatic cytoplasm, and extends into the molecular layer (Altman and Bayer, 1997). At P7, Purkinje cells begin to develop primary dendrites which receive parallel fiber synapses (Scelfo and Strata, 2005) while their perisomatic processes receive climbing fiber synapses (Altman and Bayer, 1997). The morphology of the Purkinje cells has transformed by P10, with somatic processes reabsorbed into the soma and basket cell axons contacting Purkinje cell somata (Berry and Bradley, 1976). By P12, the apical dendrites enlarge forming numerous secondary and tertiary branches (Altman and Bayer, 1997). From P12 to P15, the Purkinje cell dendritic arbor increases in complexity, first laterally and then growing in height in parallel with the molecular layer (Berry and Bradley, 1976) and generation of parallel

fiber synapses (Altman and Bayer, 1997). By P14, the distal branches of the Purkinje cell dendrites and spines located in the lower half of the molecular layer receive parallel fibers (Altman and Bayer, 1997). At P15, the Purkinje cell dendritic tree has formed its full width and the Purkinje cell soma is synaptically mature (Berry and Bradley, 1976). By P21, parallel fibers establish synapses with the distal spines on the dendritic tree in the upper half of the molecular layer (Altman and Bayer, 1997). The growth of the Purkinje cell dendritic tree continues through the upper molecular layer until P30 as the parallel fibers do (Berry and Bradley, 1976).

2.1.6.2 Development of the granule cells

At birth, the EGL has formed 6 to 8 rows of differentiating granule cell precursors. These cells undergo rapid proliferation until P9 and the EGL increases in depth with 8 to 12 rows of cells (Altman and Bayer, 1997). The EGL displays two distinct zones of cells: an outer proliferative zone and an inner premigratory zone of bipolar cells (Altman and Bayer, 1997). The bipolar cells of the premigratory zone grow processes that elongate laterally and run parallel to the developing pial surface to become parallel fibers whilst the bipolar cell somata remain on this plane (Altman and Bayer, 1997). Once the parallel fibers have grown their optimal length, the soma migrates vertically to its position in the internal granular layer while the parallel fiber remains in the upper region of the molecular layer (Altman and Bayer, 1997). By P6, functional synapses exist between parallel fibers and Purkinje cells (Scelfo and Strata, 2005). From P7 to P12, the generation of granule cell numbers increase reaching a peak from P10 to P11 and maximal migration occurs between P9 and P17 (Altman and Bayer, 1997). From P15, the granule cells in the internal granular layer develop short claw-like dendrites that envelope the immature mossy fiber rosettes (Altman and Bayer, 1997).

2.1.6.3 Development of the climbing fibers

The development of the climbing fiber is concurrent with the development of the cerebellar cortex. The inferior olive neurons are generated in the dorsal neuroepithelium of the caudal hindbrain between E12 and E13 (Bourrat and Sotelo, 1991) and their axons extend and invade the cerebellar cortical plate by E17 where they are arranged in broad sagittal zones resembling the adult climbing fiber distribution and contact Purkinje cells (Arsenio Nunes and Sotelo, 1985; Chedotal and Sotelo, 1993). The onset of transient

(non-synaptic) contacts between climbing fiber axon terminals and transient Purkinje cell somatic processes first occur embryonically (Chedotal and Sotelo, 1993; Morara et al., 2001). Postnatally, climbing fibers undergo 4 major developmental stages:

- The "creeper stage" (Fig. 9). By P2 climbing fibers begin to "creep" as mini arbors to associate with immature Purkinje cell somata and their transient somatic processes via attachment plates within the Purkinje cell plate. Although this contact regresses by P3, a large portion of climbing fibers maintain contacts onto several adjacent Purkinje cells (Chedotal and Sotelo, 1993). These early postnatal contacts are functional (Crepel et al., 1976) despite their perisomatic location.
- The "pericellular nest stage" (Fig. 9). By P5, climbing fibers make pericellular nests onto the Purkinje cell somata aligned in a monolayer (Chedotal and Sotelo, 1993). Each Purkinje cell receives inputs from several climbing fibers, with a maximum mean number of 3.5 climbing fibers synapsing onto perisomatic processes of each Purkinje cell (Ramón y Cajal, 1911; Crepel et al., 1976; Mariani and Changeux, 1981; Lohof et al., 1996).
- The "capuchon stage" (Fig. 9). Between P8 and P9 a somatodendritic translocation occurs and climbing fibers terminate onto the main trunk of the developing Purkinje cell dendritic tree (Ramón y Cajal, 1911; Mason et al., 1990). The regression of multi-innervation that reduces the percentage of Purkinje cell innervation by 50% is contemporaneous with the climbing fiber translocation (Crepel et al., 1976; Chedotal and Sotelo, 1992).
- The "young climbing fiber stage" (Fig. 9). From P10 to P15, reorganization of climbing fiber terminals occurs (Chedotal and Sotelo, 1992) so the adult 1:1 relation between climbing fibers and Purkinje cells is reached (Crepel et al., 1981; Mariani and Changeux, 1981).

One salient feature of the developing climbing fiber-Purkinje cell synapse is the elimination of transient climbing fiber multi-innervation. This mechanism is highly dependent on the presence of granule cells and the formation of normal parallel fiber-Purkinje cell synapses (Mariani and Changeux, 1980; Sugihara et al., 2000). Multiple innervations of climbing fibers persists when granule cell numbers are decreased in mutant rodents such as *weaver* and *reeler* (Appendix N°1) (Mariani et al., 1977; Puro and Woodward, 1977). Multiple climbing fiber innervation is also maintained abnormally

when parallel fibers are unable to form normal synapses with Purkinje cells in the *staggerer* (Mariani and Changeux, 1980) and the *hotfoot* mutant mice (§3.5.2).

2.1.6.4 Development of the mossy fibers

Mossy fibers derived from the brainstem nuclei also develop during embryogenesis and emerge into the cerebellar white matter by P3 (Arsenio Nunes and Sotelo, 1985). From P3 to P5, they invade the internal granular layer where they make synapses onto granule cell dendrites and by P7, mossy fibers are organized in topographical arrangement matching that of the adult mossy fiber input (Arsenio Nunes and Sotelo, 1985). By P15, the mossy fibers forming rosettes with granule cell dendritic branches are biochemically mature (Altman and Bayer, 1997). However, the presence of only minimal number of glomeruli prevents mossy fiber-granule cell synapses maturity until P21 (Altman, 1972), even though parallel fiber-Purkinje cell synapses are active at P7 (Scelfo and Strata, 2005).

2.2 ***Functions of the cerebellum***

The anatomical organization of the cerebellum and its afferents and efferents are particularly important when considering the role of the cerebellum in different modes of information processing. However, the relative contributions of each structure as well as the functional changes that occur between these structures and other motor and non-motor centers of the brain during learning and memory are unclear. Overall, in terms of cerebellar efferent flow, there appears to be two close efferent "loops" (Fig. 10): one with the red nucleus and the other with the premotor/motor cortex. In the first case, the deep cerebellar nuclei project axons to the red nucleus which in turn projects to the precerebellar nuclei of the spinal cord, medulla (e.g. external cuneate nucleus and inferior olive) and pons (e.g. pontine gray and vestibular nuclei) that also receive peripheral input. The precerebellar nuclei innervate the cerebellar cortex and a subset of deep cerebellar neurons to form one closed circuit (Altman and Bayer, 1997). As the precerebellar nuclei receive peripheral input (by way of the spinal cord) and cerebellar input (by way of the deep cerebellar nuclei and red nucleus), they may form part of a regulatory or readjustment system between both external and internal input (Palay and Chan-Palay, 1974; Altman and Bayer, 1997).

In the second case, the deep cerebellar nuclei project directly to the thalamus (Fig. 10) that receives input from the motor cortex, and the premotor, parietal and prefrontal cortices. Also, the thalamus and the motor cortex project to the pontine nuclei, which in turn project to the deep cerebellar nuclei forming another closed circuit. This massive descending path from the cerebral cortex to the pontine nuclei is thought to carry information about an extended action (Altman and Bayer, 1997). The structural link between the cerebellar cortex-deep cerebellar nuclei and cerebellar function provides a site where the process of motor learning and non-motor activities may occur, although the mechanisms involved are not fully elucidated.

2.2.1 Motor functions

The importance of the cerebellum and its components in motor functions are demonstrated by studies using cerebellar lesions and mutant mice. The removal of the whole cerebellum causes a lack of sensorimotor coordination and impaired equilibrium in both neonatal and adult rats (Zion et al., 1990; Caston et al., 1995). Comparatively, the removal of half of the cerebellum has a differential effect on adult and neonatal rats (Molinari et al., 1990). In adult rats, the effects include asymmetrical gait, deficits in dynamic postural adjustments and coordination and a side preference contralateral to the lesion (Molinari et al., 1990). However, neonatal hemicerebellectomised rats exhibit a normal gait, but a delay in acquiring dynamic postural adjustment and a permanent impairment of motor skills (Petrosini et al., 1990). The transition from normal motor development to defective motor behavior following neonatal hemicerebellectomy, referred to as “growing into a deficit”, is evidenced by the progressive reduction of hind limb grasping and a directional bias in posture correction (Petrosini et al., 1990). It has been suggested that these motor abnormalities are independent of cerebellar control in early development, but as the rat matures, the retention of these motor skills requires a cerebellar circuit (Petrosini et al., 1990).

Further investigations using mutant mice have provided evidence for the relative roles of the deep cerebellar nuclei and the cortex in cerebellar function. The mutant mice models include *Lurcher* mice which display cerebellar cortical and inferior olive degeneration and *Hu-bcl-2*-overexpressing mice which exhibit an excess of neurons. *Lurcher* mutant mice are ataxic and limited in equilibrium, motor coordination and postural sensorimotor skills in complex motor tasks (Hilber et al., 1998; Hilber and

Caston, 2001). As deep cerebellar neuron output is the only part of the cerebellar circuit remaining in this mutant, the deep cerebellar neuron activity is apparently adequate for simple sensorimotor tasks, but not for more complex tasks. Similarly, transgenic *Hu-bcl-2* mice that possess supernumerary Purkinje, granule and inferior olivary neurons display impairment of complex motor abilities, such as synchronized walking movement, but not in basic motor tasks (Rondi-Reig et al., 1999). This indicates that one function of the deep cerebellar nuclei is to learn and maintain simple sensorimotor behavior, while a correct cerebellar cortical circuit is necessary for complex learning.

2.2.2 Cognitive functions

A role of the cerebellum in cognitive functions is supported by a variety of studies based on neuroanatomical, functional imaging, clinical and experimental approaches (Schmahmann and Sherman, 1997). The extensive interconnexions between the neocortex and lateral cerebellar hemispheres have led to the interpretation that these two structures are functionally related hence implying a cerebellar role in cognition (Middleton and Strick, 2000). Although these studies demonstrate cerebellar processing in non-motor tasks, the specific regions of the vermis and the lateral zone involved in these functions remain poorly defined. Generally, lesions to the lateral zone of the rat cerebellum induce selective deficits in spatial orientation tasks, but not in visuomotor abilities, while lesions to the vermis only impair visuomotor abilities (Joyal et al., 1996). Furthermore, vermal lesions induce autistic-like symptoms, such as limited attention capacity and decreased anxiety (Bobee et al., 2000).

The cerebellum is also involved in associative learning as shown by results of avoidance-condition tasks. In these tasks, cerebellectomised rats learn as fast as intact rats to avoid an electrical shock when given an auditory stimulus. However, retention of the acquired conditioned response does not occur, indicating that the cerebellum is required to maintain learned avoidance behavior (Dahhaoui et al., 1990).

2.2.3 Spatial functions

Spatial functions have been reported to be affected by cerebellar pathologies (Petrosini et al., 1996; Molinari et al., 1997). Indeed, cerebellar connections with structures known to mediate visuospatial abilities such as frontal and parietal regions, limbic system and superior colliculus are consistent with this hypothesis (Schmahmann

and Pandya, 1989; 1997). Patients with Friedreich's ataxia perform spatial tasks deficiently (Fehrenbach et al., 1984) and patients with focal cerebellar lesions develop spatial deficits (Wallesch and Horn, 1990).

Mutant mice such as *Lurcher*, *Pcd*, *nervous* and *staggerer* mice develop different spatial impairments, such as exploratory deficits in mazes and defective spatial memory (Lalonde and Botez, 1990). *Lurcher* mice display deficits in habituation (Lalonde et al., 1986b) and in controlling the direction of swimming (Lalonde et al., 1988a) in aquatic mazes. Selective Purkinje cell degeneration in *Pcd* mice apparently interferes with the acquisition of spatial tasks (Goodlett et al., 1992). *Staggerer* mutant mice that loose Purkinje cells and granule cells, exhibit prolonged exploration of new environments and deficits in maze learning (Lalonde et al., 1987; 1988b). In complex environment, n*ervous* mutant mice which have damaged Purkinje cells and deep cerebellar neurons lack ability to retain the learned behavior compared to controls (Lalonde and Botez, 1985; Lalonde et al., 1986a). This suggests that an intact cerebellar cortical circuit and afferents are needed for learning and retention of spatially demanding tasks.

3. The *hotfoot* and *Lurcher* Grid2 mutant mice

Ionotropic glutamate receptors mediate most of the excitatory synaptic transmission in the central nervous system and are essential for synaptic plasticity (Brockie and Maricq, 2006). These include AMPA receptor subunits (GluR1-GluR4, GluRA-D), Kainate receptor subunits (GluR5-GluR7, KA1 and KA2) and NMDA receptor subunits (NR1, NR2A-NR2D and NR3A-NR3B). Two additional members of this superfamily, termed δ1 and δ2 have been identified in both mouse and rat brain.

3.1 ***The Grid2 gene***

The δ2 glutamate receptor (GluRδ2) has been identified in both mouse and rats by homology screening of mouse cDNA libraries. It is positioned at equal distances in the phylogenic tree from NMDA, AMPA and Kainate receptors (Araki et al., 1993; Lomeli et al., 1993) and is coded by the *Grid2* gene which contains 16 exons over a region of 1.4Mb located on chromosome 6 in mice (see review in Yuzaki, 2003). This may be a reason for the numerous of spontaneous mutations of this locus. Sixteen of these mutations provoke ataxia. The high frequency of *Grid2* mutations reflects its hypermutability as underlined by the occurrence of two independent translocations recently reported in a relatively small colony (Robinson et al., 2005).

Two natural *Grid2* mutant mice have been extensively studied since their discovery in the 60's, *Lurcher* (Phillips, 1960) and *hotfoot* (Dickie, 1966). Indeed, investigating these two mutant mice has brought important insights into the roles of GluRδ2 in Purkinje cell synaptogenesis and programmed cell death (Gounko et al., 2007).

3.2 ***Structure and localization of GluRδ2***

3.2.1 GluRδ2 is an orphan glutamate receptor

The topology of GluRδ2 is predicted to be similar to other ionotropic GluRs with an extracellular N-terminal region containing LIVBP-like and LAOBP-like domains, three transmembrane domains (TM1, TM3 and TM4), an ion channel-forming segment (TM2) and a cytoplasmic C-terminal region (Fig. 11A) (Araki et al., 1993; Lomeli et al., 1993).

GluRδ2 is an ionotropic glutamate receptor because:

- it possesses four hydrophobic segments (Araki et al., 1993),
- it shares amino acid sequence with other GluR channel subunits,

- it is localized at the parallel fiber-Purkinje cell synapses (Araki et al., 1993; Mayat et al., 1995; Takayama et al., 1995) where it is a receptor of the postsynaptic density beard by the Purkinje cell spine (Takayama et al., 1995; Landsend et al., 1997),
- it is co-expressed with AMPA GluR2/3 receptors in the postsynaptic membrane of the Purkinje cell synapses (Takayama et al., 1995; Landsend et al., 1997)
- it has the characteristic ion channel pore of glutamate receptors (Kohda et al., 2000).

However, it does not form functional glutamate-gated ion channels when expressed in transfected cells and does not bind glutamate analogs (Araki et al., 1993; Lomeli et al., 1993). In addition it does not complex with other glutamate receptor subtypes (Mayat et al., 1995). For these reasons it is considered to be an *orphan* glutamate receptor.

3.2.2 The GluRδ2 of Purkinje cells

Similarly to other glutamate receptors (Ajima et al., 1991), the distribution of GluRδ2 differs at the two main types of excitatory synapses of the Purkinje cell dendritic tree, the climbing fiber-Purkinje cell and parallel fiber-Purkinje cell synapses. In the adult cerebellum, GluRδ2 is expressed at the postsynaptic side of the parallel fiber-Purkinje cell synapse, but is absent from the climbing fiber-Purkinje cell synapse (Takayama et al., 1996; Landsend et al., 1997). Nevertheless, in the postnatal rat cerebellum, GluRδ2 is expressed at both climbing fiber-Purkinje cell and parallel fiber-Purkinje cell synapses although it disappears from climbing fiber-Purkinje cell synapse as early as P15 (Zhao et al., 1997). At this time, the multiple innervations of Purkinje cells by climbing fibers have completely regressed while parallel fiber-Purkinje cell synaptogenesis peaks. This specific developmental change in synaptic localization of GluRδ2 suggests that it is involved in parallel and climbing fiber synaptogenesis with Purkinje cell (Mayat et al., 1995).

*3.3 **Molecular partners of GluRδ2***

As illustrated in Figure 11B, a number of proteins involved in the docking and trafficking, as well as in the functional regulation of GluRδ2 have been identified.

The cytoplasmic C-terminal tail of all ionotropic GluRs intervenes in synaptic clustering (Malinow and Malenka, 2002). The post-synaptic anchoring PDZ proteins specifically recognize the C-terminus of their associated receptor (Hung and Sheng, 2002). Along this

line, the sequence of the 4 last amino acids of the GluRδ2 C-terminus has been shown to specifically bind the post-synaptic density (PSD)-93 protein, a member of the PSD-95 family of PDZ proteins, at the parallel fiber-Purkinje cell synapse (Roche et al., 1999). Finally, yeast two hybrid screening revealed that several PDZ-containing proteins interact with GluRδ2 C-terminus. These proteins include:

- the protein-tyrosine phosphatase PTP-MEG (Hironaka et al., 2000) which might play a role in the regulation of the activity of GluRs through tyrosine dephosphorylation
- delphilin which is selectively localized at the post-synaptic side of the parallel fiber-Purkinje cell synapse (Miyagi et al., 2002) and may link GluRδ2 with the actin cytoskeleton
- n-PIST an activator of the autophagy inducer Beclin-1 (Yue et al., 2002)
- scaffold proteins Shank 1 and 2 (Uemura et al., 2004) which allow GluRδ2 interaction with the main post-synaptic actors of long-term depression: the metabotropic glutamate receptor mGluR1, the AMPA-type glutamate receptors and the inositol 1,4,5-triphosphate receptor (IP_3R)
- PICK1, a protein interacting with C kinase 1 (Yawata et al., 2006). PICK1 has been shown to be involved in long term depression (LTD) and interacts with the C-terminus of GluRδ2. This demonstrates the importance of the GluRδ2 C-terminus in cerebellar LTD (Kohda et al., 2007)
- S-SCAM/MAGI-2, a PDZ domain-containing protein localized at post-synaptic site of Purkinje cell synapses. Binding of S-SCAM/MAGI-2 with GluRδ2 is regulated by protein kinase C (PKC)-mediated phosphorylation of the receptor and this may be necessary for the trafficking and clustering of GluRδ2 (Yap et al., 2003a)
- Spectrin, a member of the actin-binding family of proteins. Thus, spectrin may directly act on immobilization and clustering of GluRδ2 at the parallel fiber-Purkinje cell synapse (Hirai and Matsuda, 1999)
- EMAP, a microtubule-associated protein which binds selectively GluRδ2 and spectrin (Ly et al., 2002) indicating the involvement of cytoskeleton in GluRδ2 trafficking.

Finally, new insights into the intracellular movement, anchoring and clustering of GluRδ2 at the post-synaptic membrane have been provided by the discovery of Region A, a region adjacent to the TM4 of GluRδ2 (Fig. 11B) (Matsuda and Mishina, 2000; Matsuda et al.,

2004), and of the Adaptor protein complex-4 AP-4 (Yap et al., 2003b). Indeed, the former has been shown to target GluRδ2 from the endoplasmic reticulum to the plasma membrane and the latter has been shown to be involved in the intracellular trafficking of GluRδ2.

3.4 ***GluRδ2 in LTD***

Data from treatment of Purkinje cells with either antisense oligonucleotides (Hirano et al., 1994) or antibody against GluRδ2 (Hirai et al., 2003) also implicate GluRδ2 as a critical element in AMPA receptor trafficking and the induction of LTD at the parallel fiber-Purkinje cell synapse. Indeed, the C-terminus of GluRδ2 has been shown to be phosphorylated by the PKC *in vitro* and a LTD-inducing signal *in vivo* (Kondo et al., 2005). GluRδ2 devoid of C-terminal PDZ-ligand domains cannot restore the abrogated LTD in *Grid2*$^{-/-}$ mice (Kohda et al., 2007; Kakegawa et al., 2008). Transgenic *Grid2*$^{-/-}$ mice carrying mutant GluRδ2 with specific PDZ-ligand domain deletions have been generated (Uemura et al., 2007; Yasumura et al., 2008). Deletion of the C-terminal PDZ-ligand domain, the T site (Fig. 11B), revealed an impairment of LTD induction at the parallel fiber-Purkinje cell synapse and a distal expansion of climbing fiber territory. However, elimination of surplus climbing fiber innervation at proximal dendrites appeared to proceed normally (Uemura et al., 2007). Nevertheless, when S segment (Fig. 11B), the second PDZ-binding domain of the C-terminus, was deleted, the amount of GluRδ2 in cerebellar PSD fractions was reduced. In addition, mismatched parallel fiber and naked spines emerged and the climbing fiber territory expanded to distal regions of Purkinje cell dendritic tree (Yasumura et al., 2008). This implies a differential involvement of these PDZ-binding domains in diverse GluRδ2 functions.

3.5 **Hotfoot*, a natural Grid2 knock-out mouse***

The *hotfoot* mutation was first described in mouse by Dickie (1966) but has only recently been related to GluRδ2 (Lalouette et al., 1998). The *hotfoot* mutation causes a natural GluRδ2 deficiency due to a deletion in the *Grid2* gene. At least, 18 independent *hotfoot* mutations of the *Grid2* gene have been documented causing ataxia in the *hotfoot* mouse (Mouse Genome Informatics, 2000). The recessive loss-of-function mutations carried by the *hotfoot* alleles of *Grid2* result in ataxia without Purkinje cell death. Two specific *hotfoot* mutations *hotfoot*-4J (*ho-4J*) (Lalouette et al., 1998) and *hotfoot*-Nancy (*ho*^{Nancy}) (Lalouette et al., 2001) are of particular interest. The *ho-4J* mutation results in the loss of 170 amino acids from the extracellular N-terminal LIVBP-like domain of GluRδ2 (Lalouette et al., 1998). This deletion

induces the retention of GluRδ2 in the ER (Matsuda and Yuzaki, 2002; Wang et al., 2003). The *ho*^{Nancy} mouse expresses a truncated transcript lacking TM1, 2 and 3. No protein could be detected by Western Blot (Lalouette et al., 2001) indicating that this *hotfoot* mutant is a complete *Grid2* knock-out mutant that does not express any GluRδ2 protein.

3.5.1 The hotfoot behavioral phenotype

Motor coordination is impaired in all *hotfoot* mice as early as P12 (Kashiwabuchi et al., 1995) due to a dysfunction of deficient Purkinje cells. In addition, the GluRδ2$^{ho/ho}$ mouse displays a characteristic involuntary spontaneous eyeblink that can be suppressed by ablation of cerebellar floculi. This suggests an abnormal signal output by the cerebellar cortex (Yoshida et al., 2004). These motor impairments are likely to result from Purkinje cell dysfunction due to the lack of GluRδ2 at parallel fiber synapses.

3.5.2 Development and synaptogenesis of the Purkinje cells in the hotfoot GluRδ2$^{ho/ho}$ *mice*

In the adult cerebellar cortex, GluRδ2 is exclusively expressed in parallel fiber-Purkinje cell synapses (Fig. 12A) (Landsend et al., 1997), although it is transiently expressed in developing climbing fiber-Purkinje cell synapses (Zhao et al., 1997).

GluRδ2$^{ho/ho}$ Purkinje cell dendrites display naked postsynaptic spines which are surrounded by Bergmann glia and are equipped with PSD but are lacking contact with presynaptic parallel fiber boutons (Fig. 12B) (Kashiwabuchi et al., 1995). Quantification of parallel fiber-Purkinje cell synapses in GluRδ2$^{ho/ho}$ cerebellar molecular layer indicated a loss of parallel fiber synapses (Kurihara et al., 1997). In addition, *Grid2* knock-out mice (GluRδ2$^{-/-}$) selectively devoid of GluRδ2 proteins in cerebellar Purkinje cells, also had naked spines (Fig. 12B) (Takeuchi et al., 2005) and mismatching of parallel fiber boutons and Purkinje cell postsynaptic densities on tertiary spines, as previously described in natural *hotfoot* mutant mice (Lalouette et al., 2001). Furthermore, the multiple climbing fiber innervation of Purkinje cells persists abnormally in the *hotfoot* adult (Kashiwabuchi et al., 1995) whereas the normal projection domain of climbing fibers (i.e. the primary and secondary Purkinje cell dendrites) extends distally to tertiary spiny branchlets (Fig. 12B). Here, climbing fibers make aberrant ectopic synapses on the spiny branchlets of the neighboring Purkinje cells (Ichikawa et al., 2002). The blockade of electrical activity in wild-type cerebellum induces the formation of parallel fiber synapses on primary and secondary dendrites which are normally specific for

climbing fiber synapses (Fig. 12C). In this case, the expression of GluRδ2 occurs in both climbing fiber- and parallel fiber-Purkinje cell synapses (Morando et al., 2001) suggesting that climbing fiber activity normally prevents GluRδ2 targeting to proximal dendrites in the mature Purkinje cells. In support of this hypothesis, the blockade of the electrical activity of climbing fibers induced the expression of GluRδ2 at the proximal spines which are reinnervated by parallel fibers in the absence of climbing fiber innervation (Fig. 12C) (Cesa et al., 2003). The reinnervation of these spines by climbing fibers after restoring electrical activity was accompanied by the disappearance of GluRδ2. These data demonstrate that GluRδ2 is downregulated by mature climbing fiber activity.

3.6 The Lurcher *mutation kills Purkinje cells*

The *Lurcher* mutation was first described as a spontaneous mutation in mouse by Phillips (1960) and is attributed to a semi-dominant gain-of-function mutation in the SYTANLAAF motif of the TM3 domain of the *Grid2* gene (Zuo et al., 1997). The perinatal death of the homozygous GluRδ2$^{Lc/Lc}$ mutant mice can be explained by the loss of large trigeminal motor neurons involved in suckling (Cheng and Heintz, 1997).

The heterozygous GluRδ2$^{Lc/+}$ mutant mice display specific ataxia due to postnatal Purkinje cell degeneration which results in an almost total loss of the Purkinje cell population and target death-related loss of granule cells (Swisher and Wilson, 1977; Wetts and Herrup, 1982).

3.6.1 The Lurcher *mutation and glutamate receptors*

The implication of the mutated SYTANLAAF motif in the constitutive activation of GluRδ2^{Lc} has been validated by inducing this mutation in AMPA and kainate receptors which then display similar activity without ligand binding, slower deactivation and desensitization in the presence of an agonist (Kohda et al., 2000; Schwarz et al., 2001). This indicates that the *Lurcher* mutation affects receptor affinity and that this conserved SYTANLAAF motif plays a major role in the ionic channel properties of ionotropic glutamate receptors. This motif seems to play an important role in the gating properties of AMPA and NMDA GluR channels too, because these properties are also altered when the *Lurcher* mutation is introduced in these receptors (Ikeno et al., 2001). The introduction of the *Lurcher* mutation in GluR1 increased the affinity of GluR1^{Lc} for glutamate and reduced the desensitization of GluR1^{Lc} channel at low receptor occupancy. This explains the small and sustained current observed in these

GluR1^{Lc} channels (Klein and Howe, 2004). GluR1^{Lc} and GluR6^{Lc} mutant receptors expressed in HEK cells can form functional heteromeric channels with GluRδ2^{Lc}, which permit glutamate-induced currents. In contrast, the formation of heteromeric wild-type GluRδ2/iGluR channels modifies glutamate signaling by forming non-functional channels, leading to the reduction of glutamate-induced currents (Kohda et al., 2003). The pore of GluRδ2^{Lc} shows functional similarities to Ca^{2+}-permeable AMPA/kainate receptors and is able to form ion channels that are potentiated by extracellular Ca^{2+} at physiological concentrations (Wollmuth et al., 2000). This Ca^{2+} influx or Ca^{2+}-dependent potentiation may contribute to the role of GluRδ2 in cerebellar LTD.

3.6.2 The molecular basis of Purkinje cell death in the Lurcher *mouse*

The massive neurodegeneration observed in the cerebellar cortex of the GluRδ2$^{Lc/+}$ mouse has been shown to involve apoptosis (Phillips, 1960; Norman et al., 1995; Wullner et al., 1995; Selimi et al., 2000c). Purkinje cell death is believed to result from excitotoxic effects of the *Lurcher* mutation in the GluRδ2 receptor (Zuo et al., 1997) even in the absence of any ligand binding (Kohda et al., 2000).

Investigation of the apoptotic mechanisms leading to Purkinje cell death in the *Lurcher* mouse revealed increased BAX and BCL-$_{XL}$ expression by Purkinje cells (Wullner et al., 1998). Nevertheless, overexpressing *Bcl-2* (Zanjani et al., 1998a) and knocking-out *Bax* only delayed Purkinje cell death (Doughty et al., 2000; Selimi et al., 2000c). Overexpressing *Bcl-2* prevented target-related cell death of inferior olivary neurons (Zanjani et al., 1998b), whereas inactivation of *Bax* rescued granule cells from target-related apoptotic cell death (Selimi et al., 2000c). The involvement of mitochondrial apoptotic factors in *Lurcher*-induced cell death is supported by the translocation of cytochrome c from mitochondria to the Apaf1 complex during the period of maximal neuronal death in the cerebellum of the GluRδ2$^{Lc/+}$ mouse (Frischmuth et al., 2006). The effector protein caspase-3, but not the apoptotic factor p53, was shown to be involved in apoptosis of GluRδ2$^{Lc/+}$ Purkinje cells and granule cells (Doughty et al., 2000; Selimi et al., 2000a; 2000b). As both *Bax* inactivation and *Bcl-2* overexpression only delayed GluRδ2$^{Lc/+}$ Purkinje cell death, Bcl-2 family members seem to contribute to Purkinje cell apoptosis, but additional extracellular apoptotic signaling cannot be ruled out. Indeed, the elimination of tissue plasminogen activator, a serine protease known to activate caspase-8 also delayed GluRδ2$^{Lc/+}$ Purkinje cell and granule cell apoptosis (Lu and Tsirka, 2002). Caspase-3 was not detected in many cerebellar neurons stained with fluoro-Jade B, a

specific marker for dying neurons (Baurle et al., 2006). These data suggest that more than one neuronal death mechanism operates in the GluRδ2$^{Lc/+}$ Purkinje cells. Further investigations should help to elucidate complex neuronal responses elicited by excitotoxicity in the *Lurcher* Purkinje cells.

4. The Nagasaki prion protein-deficient mice

Prion diseases or transmissible spongiform encephalopathies (TSEs) are infectious, fatal neurodegenerative diseases that affect humans and various animals. These include Creutzfeld Jacob disease, scrapie and BSE (appendix N°2). In humans, prion diseases manifest as rapid progressive dementias with clinical visual or cerebellar signs and akinetic mutism.

The agents that cause TSEs are known as prions (Prusiner, 1982). One hypothesis postulates that prions are PrP^{res} (prion protein resistant to proteinase K) (Bolton et al., 1982; Prusiner et al., 1984) a conformational isoform of the host cellular prion protein, PrP^{C} (Caughey and Raymond, 1991). Although many different functions have been attributed to PrP^{C}, its physiological function remains unclear.

4.1 ***The prion protein family***

The prion gene family consists in three known members: the prion protein gene *Prnp*, the Doppel gene *Prnd* and the Shadoo gene *Sprn*.

4.1.1 The prion protein gene Prnp

The prion protein gene *Prnp* is located on chromosome 2 in mice (Horiuchi et al., 1998) and encodes PrP^{C} (Oesch et al., 1985; Basler et al., 1986). PrP^{C} is the cardinal protein involved in prion diseases (Bueler et al., 1993) including the genetic forms of TSEs caused by mutations in *Prnp*. These are hereditary Creutzfeld-Jacob disease, fatal familial insomnia and Gertsmann-Straüssler-Scheinker syndrome.

4.1.2 The Doppel gene Prnd

The Doppel gene *Prnd* is located 16kB downstream of the murine *Prnp* locus and encodes a 179 amino acid-long prion protein-like Doppel (Dpl) (Moore et al., 1999; Li et al., 2000a) which shares 25% identity with PrP^{C}. Detailed analysis of the toxicity of abnormal overexpression of Dpl in central neurons in some $Prnp^{0/0}$ mouse lines is one of the research axis of my thesis (see below).

4.1.3 The Shadoo gene Sprn

Shadoo, a short protein homologous for the central hydrophobic region of PrP^{C} was discovered while looking for nucleotide sequences homologous to the *Prnp* sequence. The

Shadoo coding gene *Sprn* is located on chromosome 7 in mouse and its expression is restricted to the brain (Premzl et al., 2003).

4.1.4 The prion proteins

4.1.4.1 The cellular prion protein

The cellular prion protein is a glycosyl phosphatidyl inositol (GPI)-anchored glycoprotein that contains a long, flexible N-terminal tail, three α-helices, and a two-stranded antiparallel β-sheet that flanks the first α-helix. PrP^{C} displays a single disulfide bond which links helices 2 and 3 thereby stabilizing the C-terminus (Fig. 13). The N-terminus contains two specific regions, a copper-binding N-terminal octapeptide regions and a hydrophobic core (Fig. 13) (Locht et al., 1986; Riek et al., 1997). Mutations within this hydrophobic region favor the formation of C- and N-terminal ^{ctm}PrP and ^{Ntm}PrP transmembrane topological variants of PrP^{C}. The ^{Ctm}PrP causes neurodegeneration (Hegde et al., 1998). Although it does not appear to be infectious when inoculated in reporter mice, transgenic mice expressing ^{Ctm}PrP develop neurological illness and neuronal death that resembles certain prion diseases (Stewart et al., 2005).

4.1.4.2 Doppel

Dpl, like PrP^{C}, is an α-helical protein with a C-terminal GPI anchor (Fig. 13) (Silverman et al., 2000). Nevertheless Dpl resembles a truncated form of PrP^{C} with approximately 25% sequence identity and an additional outer disulfide bond (Lu et al., 2000). Disruption of the helix B separates it into B and B′ regions, and the two β-strands have opposing orientations (Fig. 13). Interestingly, no evidence of disease association with Dpl could be disclosed (Mead et al., 2000) and Dpl does not have any scrapie isoform (Settanni et al., 2002; Peoc'h et al., 2003).

4.1.4.3 Shadoo

Murine Shadoo is a protein with N- and C-terminal signal sequences similar to PrP^{C} and Doppel (Fig. 13) (Premzl et al., 2003). Shadoo shares homology to the PrP^{C} N-terminal domain with a series of N-terminal charged tetrarepeats. As mentioned, the bulk of the homology between Shadoo and PrP^{C} is found within the hydrophobic tract. Additionally, Shadoo is devoid of cysteine residues, preventing the formation of stabilizing disulfide bonds.

Shadoo has recently been shown to counteract neurotoxic activity of Dpl in a PrP^C-like neuroprotective activity (Watts et al., 2007)

4.2 ***The cellular prion protein PrP^C***

4.2.1 Expression of PrP^C in the central nervous system

Prion protein gene expression is detected as early as E13.5 in the developing mouse brain (Manson et al., 1992). It further increases in a region-specific manner during the postnatal period (Mobley et al., 1988). In addition, glial cells express prion protein mRNAs throughout postnatal development in rodent brain (Moser et al., 1995). In the adult, high levels of PrP^C are found in brain and spinal cord neurons (Manson et al., 1992; Harris et al., 1993), as well as in neurons and Schwann cells of the peripheral nervous system (Ford et al., 2002). In the brain, PrP^C has been detected in neurons of the olfactory bulb, the neocortex, the amygdala, the putamen, the hippocampus, the brainstem and the cerebellum (Fournier et al., 1995; Sales et al., 1998; Haeberle et al., 2000; Laine et al., 2001; Mironov et al., 2003; Bailly et al., 2004; Galvan et al., 2005). PrP^C is a neuronal cell surface protein (Caughey and Raymond, 1991) distributed in patches on the surface of the cerebellar Purkinje cells, granule cells and deep cerebellar neurons (Bailly et al., 2004). The preferential synaptic distribution of PrP^C has been described at pre- and post-synaptic elements of excitatory synapses on Purkinje cells (Haeberle et al., 2000; Bailly et al., 2004), as in other central synapses (Fournier et al., 1995; Bailly et al., 2004). Taking into account the synaptic localization of PrP^C and electrophysiological studies on hippocampal slices devoid of PrP^C strongly suggest that PrP^C has important synaptic functions (Collinge et al., 1994; Fournier et al., 1995; Herms et al., 1999). Indeed, in these hippocampal slices, long term potentiation is impaired (Collinge et al., 1994) and the expression level of PrP^C is correlated with glutamatergic synaptic transmission (Carleton et al., 2001). Moreover, Ca^{2+}-activated K^+ currents are decreased in Purkinje cells from *Prnp*-ablated mice (Herms et al., 2001) and the whole cell current of granule cells incubated with a recombinant PrP is reduced (Korte et al., 2003). This and the fact that hippocampal neurons depleted in cholesterol have an abnormal cell membrane expression of PrP^C (Galvan et al., 2005) suggest an important role for PrP^C in the regulation of synaptic transmission.

In cultured fetal hippocampal neurons, expression of a recombinant form of PrP results in the elaboration of axons and dendrites and increases the number of synaptic contacts (Kanaani et al., 2005). Neuritogenesis decreases when neurons or astrocytes do not express PrP^C in

neuron-astrocyte cocultures (Lima et al., 2007) and it has been demonstrated *in vivo* that PrP^C also plays an important role in cellular differentiation during neural development (Steele et al., 2006). Taken together, these data indicate that PrP^C can function as a growth factor involved in neurogenesis and the development of neuronal polarity.

4.2.2 Cell trafficking of PrP^C

PrP^C biosynthesis is achieved by translocation to the ER due to the presence of an N-terminal signal peptide. This signal peptide is then cleaved in the ER lumen and the C-terminal GPI anchor is added (Caughey et al., 1989). The secreted PrP^C form is then transported to the cell surface where it is expressed for 1 hour before undergoing endocytosis in early endosomes (Fig. 14). The important intracellular amount of PrP^C (35 to 50%) indicates that integral PrP^C is continuously cycled between the cell surface and the endosomes (Fig. 14) (Shyng et al., 1993). In this way, endocytosis of raft-associated PrP^C is likely to involve a clathrin-dependent mechanism. The copper-binding N-terminal region of PrP^C is implicated in this mechanism since deletions within the N-terminal region of PrP^C reduces internalization of the protein (Shyng et al., 1994; 1995). Furthermore, when copper ions bind to the N-terminal octapeptide repeats, PrP^C is liberated from lipid rafts prior to its internalization by clathrin-mediated endocytosis (Fig. 14) (Taylor et al., 2005). In addition, this mechanism of endocytosis depends on the intervention of the low-density-lipid receptor 1 (Taylor and Hooper, 2007).

Inhibition of the proteasome induces a cytosolic accumulation of PrP^C indicating that PrP^C can be catabolized through the ER-associated degradation (ERAD) pathway (Fig. 14) (Yedidia et al., 2001).

4.2.3 Neuronal effects of PrP^C deficiency

Less than a decade after the discovery of PrP^C, mice homozygous for disrupted *Prnp* were generated in order to characterize its physiological functions. Two *Prnp* knock-out ($Prnp^{0/0}$) mutant mouse lines Zurich I (Bueler et al., 1992) and Edinburgh (Manson et al., 1994) were generated and developed normally. Only subtle deficiencies related to neuronal functions were detected. Alteration of sleep rhythms characterized by enhanced sleep fragmentation including short waking episodes was observed in these *Prnp*-deficient mice (Tobler et al., 1996; 1997). In addition, several alterations were observed including impairment of long-term potentiation, weakened GABA receptor-mediated inhibition (Collinge et al., 1994) and

disruption of K+ currents (Colling et al., 1996) in hippocampal slices of these *Prnp*-deficient mice. Interestingly, these neurophysiological phenotypes were rescued by the introduction of a high number of transgenic copies of *Prnp* confirming that this phenotype is a consequence of the loss of PrP^C (Whittington et al., 1995). Moreover, loss of PrP^C alters both the intracellular calcium homeostasis of cultured cerebellar granule cells (Herms et al., 2000) and the maximal increase of intracellular calcium concentration provoked by depolarization in Purkinje cells. These data provide strong evidence that Ca2+-activated K+ currents in mice are reduced due to an altered intracellular calcium homeostasis. Furthermore, a profound but transient impairment of synaptic excitation and plasticity has been evidenced in granule cells of 3 week-old $Prnp^{0/0}$ mice suggesting that PrP^C plays an important role in granule cell development (Prestori et al., 2008).

In addition, PrP^C deficiency also impairs the anti-apoptotic PI3-kinase/Akt pathway, leading to apoptotic caspase-3 activation (Weise et al., 2006) (see below).

4.2.4 Molecular partners of PrP^C

Identification of molecular partners of PrP^C is one way to elucidate its potential physiological functions. The trafficking of PrP^C implies that it is exposed to a large number of molecular partners in various cell compartments, including the extracellular matrix, plasma membrane and vesicular compartments. The N-terminal domain of PrP^C has been shown to be critical for the internalization of the protein (Gauczynski et al., 2001) and several molecules bind PrP^C *in vitro* although the physiological relevance of these interactions remains to be determined.

High concentrations of PrP^C have been purified with caveolae-like domains (Vey et al., 1996) supporting an interaction with caveolin, a transmembrane adaptor of caveolae-like domains (Harmey et al., 1995). Such a direct interaction might explain the functional coupling of PrP^C that has been demonstrated with Fyn (Mouillet-Richard et al., 2000; Toni et al., 2006), a tyrosine kinase involved in mediating semaphorin function (reviewed in Ahmed and Eickholt, 2007). A number of intracellular proteins involved in neuronal signaling processes are able to bind PrP^C. They include synapsin Ib, Grb2, and prion interactor protein Pint-1 (Spielhaupter and Schatzl, 2001) although the significance of their interaction with PrP^C remains obscure.

At the cell surface, N-CAM (Schmitt-Ulms et al., 2001), glycosaminoglycans (Pan et al., 2002) and clathrin (Shyng et al., 1994; 1995) are plasmalemma-bound molecular partners of

PrP^C. Glycosaminoglycans could intervene in the pathogenic conversion of PrP^C (Pan et al., 2002) and clathrin is involved in the endocytosis of PrP^C (see above) (Shyng et al., 1994; 1995). Interaction of N-CAM with PrP^C permits the recruitment of N-CAM to lipid rafts and activation of Fyn (Santuccione et al., 2005).

Prior to its endocytosis, PrP^C can also bind the 37/67 kDa laminin receptor (Rieger et al., 1997; Gauczynski et al., 2001; Hundt et al., 2001). A binding site in both PrP^C and laminin receptor may provide direct interaction, and a second one depends on heparan sulfate proteoglycan (HSPG)-mediated interaction (Rieger et al., 1997; Gauczynski et al., 2001; Hundt et al., 2001). In turn, laminin receptor binds both PrP^C and laminin (Rieger et al., 1999)

and PrP^C binds laminin itself (Graner et al., 2000; Coitinho et al., 2006). These interactions may have important consequences during neuritogenesis (Graner et al., 2000) and memory processing (Coitinho et al., 2006).

The stress inducible protein 1 (STI1) was discovered as an additional PrP^C-associated membrane protein (Zanata et al., 2002). STI1 is a co-chaperone protein organizing Heat Shock proteins 70 and 90 complexes. STI1 binds to the hydrophobic core of PrP^C to induce neuroprotection by preventing protein kinase A-dependent cell death (Lopes et al., 2005). Binding of ST1 to PrP^C is also able to induce neuritogenesis (Lopes et al., 2005). This mechanism requires endocytosis of STI1-bound PrP^C (Caetano et al., 2008). In addition, interaction between STI1 and PrP^C also affects short- and long-term memory (Coitinho et al., 2007).

Na^+/K^+ ATPase, β-actin, α-spectrin and creatine kinase-β have been identified as potential molecular partners of PrP^C in PrP/affinity chromatography fractions (Petrakis and Sklaviadis, 2006). PrP^C, in association with Na^+/K^+-ATPase and cytoskeletal proteins may cluster and stabilize receptors in the cell membrane, while creatine kinase-β might regulate vesicle transport and neurotransmitter release.

4.2.5 Copper-binding and anti-oxidative properties of PrP^C

The well-established copper-binding and anti-oxidant properties of PrP^C are thought to be important in the regulation of synaptic copper concentration and its anti-apoptotic functions.

Copper is an essential cofactor of many cellular redox reactions and it is now widely accepted that PrP^C is a copper-binding protein (Brown et al., 1997a). Binding of a copper ion to PrP^C is achieved by two of the N-terminus octapeptide repeats (Fig. 13) (Stockel et al., 1998; Garnett and Viles, 2003) and by two histidines close to the hydrophobic core (Jones et

al., 2004). The octapeptide repeats specifically bind up to 4 Cu^{2+} ions copper in a pH-dependent and negatively cooperative manner (Walter et al., 2006). Indeed, at physiological pH, Cu^{2+} initially binds to PrP^{C} at the two histidines with a high affinity. Subsequently Cu^{2+} ions bind to single histidine residues within the octarepeat region with a lower affinity (Wells et al., 2006a; Wells et al., 2006b; Klewpatinond et al., 2008). In addition, there is evidence that Cu^{2+} can facilitate PrP^{C} self association (Wells et al., 2006a; Wells et al., 2006b) and that zinc significantly alters the distribution of copper among the available binding modes (Walter et al., 2007).

Copper binding alters PrP^{C} biochemical and biological properties by switching the α-helical tertiary structure into a β-sheet configuration that is different from the β-sheet-rich pathological PrP^{res} (Qin et al., 2000; Quaglio et al., 2001; Leclerc et al., 2006). Copper-bound PrP^{C} has increased protease resistance (Quaglio et al., 2001). PrP-deficient mice are hyper sensitive to copper toxicity and oxidative stress (Brown et al., 1998) which can be explained by the reduction in the activity of Cu/Zn superoxide dismutase (Brown et al., 1997b; Brown et al., 2002) and glutathione reductase (White et al., 1999) in neurons. Thus, PrP^{C} is proposed to have a proper superoxide dismutase activity (Brown et al., 1999) which directly detoxifies reactive oxygen species (ROS), responsible for oxidative stress-induced apoptosis (Brown et al., 2002). Alternatively, but not exclusively, PrP^{C} may indirectly up-regulate distinct Cu/Zn superoxide dismutases depending on the level of its copper charge (Fig. 15) (Brown et al., 2001; Sakudo et al., 2005a).

4.2.6 Anti-apoptotic activity of PrP^{C}

Neuronal apoptosis occurs in the brain infected by scrapie (Lucassen et al., 1995) and in fatal familial insomnia (Dorandeu et al., 1998) suggesting that either prions are pro-apoptotic agents or PrP^{C} has an anti-apoptotic cytoprotective function that is absent in prion-infected brains due to its conversion in pathological PrP^{res}. This important question remains to be answered.

Using a yeast two-hybrid system, Kurschner and Morgan (1995; 1996) demonstrated that PrP^{C} binds Bcl-2 family members through a common BH domain. This suggests that PrP^{C} could have BCL-2-like properties. In PrP-deficient neurons, serum-free culture conditions induced apoptosis that was abrogated by either PrP^{C} or BCL-2 (Kuwahara et al., 1999). This suggests that PrP^{C} is an anti-apoptotic BCL-2-like protein. This is supported by the suppression of BAX-dependent apoptosis in human neurons by PrP^{C}. This anti-BAX effect

has been shown to be specific for the octapeptide repeat domain of PrP^C (Bounhar et al., 2001). Furthermore, BAX-mediated neuronal death is counteracted by overproduction of cytosolic PrP^C induced by ERAD reverse translocation (Roucou et al., 2003). The anti-apoptotic properties of PrP^C have been challenged because induction of PrP^C expression in HEK cells provokes p53-mediated caspase-3 activation (Paitel et al., 2002; 2003; 2004). However, this was subsequently shown to be a cell line-specific effect since PrP^C upregulation has no neurotoxic effect on N2A cells. Moreover, antibody-induced down-regulation of PrP^C increased BAX expression, caspase-3 induction and apoptosis (Zhang et al., 2006). Also, PrP-deficient neuronal cell lines underwent down-regulation of BAX, caspase-3 and cytochrome c after PrP^C expression was restored (Kim et al., 2004). Recently, PrP^C anti-apoptotic activity was shown to be independent of BCL-2 in yeast (Bounhar et al., 2006). In addition, the anti-BAX properties of PrP^C have been confirmed *in vivo* as PrP^C rescued neurons from ethanol-induced BAX-mediated apoptosis (Gains et al., 2006). On the other hand, PrP^C does not prevent BAK- , BID- and staurosporine-induced apoptosis indicating that anti-apoptotic properties of PrP^C are BAX-specific. Indeed, PrP^C prevents the initial conformational change of BAX necessary for its pro-apoptotic activation (Roucou et al., 2005).

4.3 ***The prion protein paralogue Doppel***

Research efforts to determine the functions of PrP^C in knock-out mutant mice (Fig. 16) have revealed that large deletions in *Prnp* result in the ectopic neuronal expression of Dpl. Such disruptions of *Prnp* extend into the upstream region of intron 2 resulting in cis-activation of *Prnd*. This allows an abnormal intergenic splicing between the *Prnp* promoter and the *Prnd* ORF (Moore et al., 1999) and prevents cleavage of *Prnp* pre-mRNA which is elongated up to the last exon of *Prnd*. The production of chimerical mRNAs made up of *Prnp* exons 1 and 2 and *Prnd* coding exons results in abnormal regulation of *Prnd* under the control of the *Prnp* promoter (Fig.17) (Moore et al., 1999; Li et al., 2000a; 2000b; Yoshikawa et al., 2007). The resulting ectopic Dpl neuronal expression in $Prnp^{0/0}$ mouse lines (Fig. 16) such as Ngsk (Sakaguchi et al., 1995; 1996), Rcm0 (Moore et al., 1999), ZrchII (Rossi et al., 2001) and Rikn (Kuwahara et al., 1999) leads to late onset Purkinje cell degeneration and ataxia.

4.3.1 Somatic and germinal expression of Dpl

Dpl is highly expressed in Sertoli cells and spermatozoa of the testis (Peoc'h et al., 2002) (Tranulis et al., 2001) during adulthood. During embryogenesis, Dpl is transiently expressed under the control of Brn-3a and Brn-3b transcription factors in dorsal root ganglia and spinal cord neurons as early as E13.5 (Calissano et al., 2004). Lower levels of Dpl mRNA are detected in spleen, heart, bone marrow, skeletal muscles and neocortex of the neonatal hamster, but not in kidney, liver and lung (Li et al., 2008). Significant levels of Dpl expression have never been detected in the brain of any adult mammalian species.

4.3.2 Physiological functions of Dpl

The only obvious phenotypic feature of Dpl-deficient *Prnd*$^{0/0}$ mice is male, but not female sterility. *Prnd*$^{0/0}$ spermatid numbers are strongly reduced and spermatozoid heads are misoriented (Behrens et al., 2002). This deficit impairs the capacity of the spermatozoid to cross the *zona pellucida* of the egg (Behrens et al., 2002). The important oxidative DNA damages resulting from Dpl deficiency in male gametes suggests that Dpl is involved in spermatogenesis through its anti-oxidant protective functions (Paisley et al., 2004). In addition, the subcellular localization of Dpl appears to evolve with the different stages of male gametogenesis with a strong early nuclear localization before concentrating in the cytoplasm (Kocer et al., 2007).

The structural homology between PrP^{C} and Dpl (Fig. 13) suggests a subcellular colocalization. Indeed, the immunohistochemical distribution of Dpl in the brain of *NP*$^{0/0}$ mouse and of PrP^{C} in the brain of wild-type mouse are similar (Al Bersaoui et al., 2005). In neuroblastoma cell cultures, Dpl and PrP^{C} get internalized together from patches on the plasma membrane (Massimino et al., 2004). In addition, like PrP^{C} (Zidar et al., 2008), Dpl is a copper-binding protein (Qin et al., 2003). Since copper-binding is a prerequisite for PrP^{C} through interaction with the precursor of laminin receptor, the binding of Dpl to this precursor suggests that PrP^{C} and Dpl are internalized together (Yin et al., 2004). Nevertheless, Dpl does not interact with all the molecular partners of PrP^{C}. It does not interact with Grb2 (Azzalin et al., 2005), but interacts with RACK1 (Azzalin et al., 2006), an intracellular adaptor protein involved in the regulation of intracellular calcium (Sklan et al., 2006). Whereas PrP^{C} increases the concentration of subplasmalemmal calcium pools in CHO cells, Dpl has a depleting effect which can be abolished by PrP^{C}. This is consistent with a functional interplay

and an antagonistic role of the two proteins, whereby PrP^C protects and Doppel sensitizes cells toward stress conditions (Brini et al., 2005).

4.3.3 The neurodegenerative phenotype of the Nagasaki mouse

When the first $NP^{0/0}$ mouse line overexpressing Dpl was observed to display premature Purkinje cell loss (Sakaguchi et al., 1996), it was postulated that PrP^C was needed to ensure Purkinje cell survival during aging (Nishida et al., 1999). In other words, the resistance to prion disease conferred by PrP^C deficiency should result in late onset ataxia. Several neuropathological signs have been reported in the brain of the Dpl-overexpressing mice, including necrosis of pyramidal cells in the hippocampus (Moore et al., 2001), torpedo-like varicosities of Purkinje cell axons projecting into the granular layer, abnormal myelinisation in the spinal cord and peripheral nervous system (Nishida et al., 1999), and abnormal astrocytic and microglial activation in the forebrain and cerebellum (Atarashi et al., 2001).

Subsequently, Dpl was shown to be expressed in $NP^{0/0}$ Purkinje cells and hippocampal pyramidal cells and to be responsible for Purkinje cell neurodegeneration (Li et al., 2000a; 2000b). Furthermore, overexpression of Dpl in the non-ataxic ZrchI $Prnp^{0/0}$ mice induced severe granule and Purkinje cell loss in the cerebellum (Moore et al., 2001). Conversely, Purkinje cell neurodegeneration did not occur when Dpl overexpression was suppressed by knocking-out *Prnd* in ZrchII $Prnp^{0/0}$ mutant mice. These data confirm that Dpl is responsible for Purkinje cell death in the Dpl-overexpressing $Prnp^{0/0}$ mutant mouse lines (Genoud et al., 2004). Furthermore, decreased Dpl expression in ZrchI $Prnp^{0/0}$; $NP^{0/0}$ and ZrchI $Prnp^{0/0}$; ZrchII $Prnp^{0/0}$ double mutant mice displayed a delayed neurological effect of Dpl in proportions suggesting that the onset of ataxia and Purkinje cell loss is Dpl gene dose-dependent (Moore et al., 2001; Rossi et al., 2001; Valenti et al., 2001).

4.3.4 Neurotoxicity of Doppel

4.3.4.1 Doppel can be considered as a N–terminal truncated PrP (ΔPrP)

To identify regions of the PrP^C sequence involved in prion disease, ZrchI mice expressing N-terminal truncated PrP^C have been generated. Among these transgenic mouse lines, the ΔPrP (lacking aa32-134) transgenic mouse display severe granule cell loss and severe ataxia that is rescued by re-expression of a full-length PrP (Shmerling et al., 1998). When targeted to Purkinje cells, the ΔPrP transgene induces Purkinje cell loss and ataxia, as observed in Dpl-overexpressing mouse lines, suggesting that Dpl and ΔPrP cause Purkinje cell death by the

same mechanism (Flechsig et al., 2003). Indeed, Dpl fused with the N-terminal segment lacking in ΔPrP has anti-apoptotic activity *in vitro* (Lee et al., 2006).

4.3.4.2 Pro-apoptotic properties of Doppel

Pro-apoptotic properties of Dpl were suggested by TUNEL-identification of apoptotic granule cells in the cerebellar cortex of ZrchI mice transgenically expressing Dpl (Moore et al., 2001). Indeed, oxidative stress was observed in Dpl overexpressing central neurons of *Rcm0* mice with increased activity of heme oxygenase 1, as well as neuronal and inducible nitric oxide synthase (Wong et al., 2001). Furthermore, abnormal activation of nitric oxide synthase by exogenous Dpl peptide was antagonized by exogenous PrP^C in cultured cerebellar cells (Cui et al., 2003). Removing serum from culture medium of Dpl-overexpressing Rikn hippocampal neurons (Kuwahara et al., 1999) induced apoptosis which could be abolished by reexpression of PrP^C, suggesting that PrP^C-Dpl interaction can regulate cell survival (Sakudo et al., 2005b). Dpl-induced apoptosis involves a caspase-dependent apoptotic pathway since N2A cells transfected with a plasmid coding for Dpl display activation of the apoptotic effector caspase-3, DNA fragmentation and apoptosis (Qin et al., 2006). In addition, overexpression of BCL-2 in ΔPrP mice reduced caspase-3 activation (Nicolas et al., 2007).

4.3.4.3 Doppel and PrP^C antagonism

Two hypothetical mechanisms have been proposed to explain the interaction between PrP^C and Dpl: the competition mechanism and the sensitization mechanism (Fig. 18).

1.1.1.1.1 The competition model

In the competition model (Fig. 18A), PrP^C and a still unknown low affinity molecule called π compete to bind an unidentified ligand L_{PrP} to elicit an anti-apoptotic activity (Shmerling et al., 1998; Kuwahara et al., 1999). Dpl as well as ΔPrP are able to bind L_{PrP} in the absence of PrP^C and, this would hijack its cell survival-promoting properties into apoptosis (Shmerling et al., 1998; Flechsig et al., 2003; Lee et al., 2006). Along this line, the laminin receptor precursor protein has been proposed to be a potential L_{PrP} because it binds both PrP^C and Dpl (Gauczynski et al., 2001; Hundt et al., 2001; Yin et al., 2004).

1.1.1.1.2 The sensitization model

Serum withdrawal increases apoptosis of *Prnp*-deficient neurons (Kuwahara et al., 1999), suggesting that PrP^C has a neuroprotective role itself (Fig. 18B). Indeed, PrP^C SOD activity

(Brown et al., 1999) can antagonize Dpl-induced oxidative stress (Wong et al., 2001; Cui et al., 2003) and N-terminal truncated PrP^C abrogates its capacity to rescue neurons from Dpl toxicity (Atarashi et al., 2003). In the sensitization hypothesis, the apoptogenic oxidative damage caused by Dpl would not be detoxified in neurons because lacking PrP^C.

Results

1. Purkinje cell death mechanisms induced by mutations of the glutamatergic GluRδ2 receptor in mouse

1.1 *Publication 1.* **Lurcher GRID2-induced death and depolarization can be dissociated in cerebellar Purkinje cells. Selimi F, Lohof AM, Heitz S, Lalouette A, Jarvis CI, Bailly Y, Mariani J. Neuron (2003) 37:813-9.**

Based on data showing that the C-terminus region of GluRδ2^{Lc} activates the autophagic promoter Beclin1 (Liang et al., 1998) via nPIST (Yue et al., 2002), the first research theme of my thesis was focused on the mechanisms controlling the onset of Purkinje cell death induced by GluRδ2^{Lc}. I contributed to a first study in which heteroallelic mutant mice expressing only one copy of the *Lurcher* allele and no copy of the wild-type allele were generated. In these mice, Purkinje cell death occurred already at P5, when the cerebellum is not yet obviously affected and preceded chronic depolarization in GluRδ2$^{Lc/+}$ mutant mice. In the GluRδ2$^{ho/Lc}$ Purkinje cells, autophagic profiles occurred in correlation with massive Purkinje cell death, when GluRδ2^{Lc} could not induce depolarization of Purkinje cells. These results suggest that GluRδ2^{Lc} receptors activate a neuronal death pathway independent of depolarization.

1.2 GluRδ2^{Lc}-induced excitotoxicity kills Purkinje cells

Although the *Lurcher* mutation has been known to be responsible for excitotoxic apoptotic Purkinje cell death for a long time, clear evidence for autophagy has only been recently obtained showing autophagosomes accumulation in axonal swellings as well as in somato-dendritic compartments of the *Lurcher* Purkinje cells (Wang et al., 2006). The increased density of mitochondria and oxidative stress in the GluRδ2$^{Lc/+}$ Purkinje cells suggests that an apoptotic pathway is activated in these neurons (McFarland et al., 2007). Nevertheless, autophagic profiles appear in GluRδ2$^{Lc/+}$ Purkinje cells before ion flux-mediated excitotoxicity induces neuronal death suggesting the early activation of a non-ionotropic cell death mechanism. The putative dissociation between non-ionotropic (reflected by autophagy) and ionotropic neurotoxic cascade may be achieved by experimentally blocking GluRδ2^{Lc}-mediated ion flux. For this reason, I treated GluRδ2$^{Lc/+}$ organotypic cerebellar cultures with 1-Naphtyl-acetyl-spermine (NASP), an open channel blocker known to considerably reduce Ca^{2+} entry (Koike et al., 1997) and GluRδ2$^{Lc/+}$-mediated currents (Kohda et al., 2000). If autophagy is independent from GluRδ2$^{Lc/+}$-induced excitotoxicity, NASP-blockade of excitotoxic ion flux is predicted to not affect autophagy in the treated GluRδ2$^{Lc/+}$ Purkinje cells.

1.2.1 Blockade of ion flux excitotoxicity rescues GluRδ2$^{Lc/+}$ Purkinje cells

Organotypic cerebellar cultures obtained from P0 GluRδ2$^{Lc/+}$ and wild-type cerebellum were maintained for 6 and 12 days *in vitro* (DIV) (Fig. 19A). NASP treatment during the 12 day-long culture period restored GluRδ2$^{Lc/+}$ Purkinje cell numbers to wild-type levels (P = 0.97) while this treatment had no effect on wild-type Purkinje cells (P = 0.97) (Fig. 19B). When the culture period was restricted to 6 days, equivalent Purkinje cell populations survive in GluRδ2$^{Lc/+}$ and wild-type cultures whereas 6 day-long NASP treatment had no effect on either culture (P = 0.95) (Fig. 19B). In addition, GluRδ2$^{Lc/+}$ Purkinje cells did not survive when NASP treatment was applied during the 6 first days of the 12 DIV period (P = 1.00). On the contrary, when these 12 DIV GluRδ2$^{Lc/+}$ cerebellar organotypic cultures were treated with NASP for either the 4 or the 2 last days, there was an increased Purkinje cell survival (P < 0.05 and P < 0001) (Fig. 19B). GluRδ2$^{Lc/+}$ Purkinje cell numbers were restored to wild-type level when NASP treatment was applied for the last 6 days of the 12 DIV period (P = 0.29) (Fig. 19B). This indicates that Purkinje cells of 12 DIV cerebellar organotypic cultures from P0 GluRδ2$^{Lc/+}$ mice have a differential sensitivity to GluRδ2^{Lc} toxicity after 6 DIV.

1.2.2 Blockade of ionotropic excitotoxicity suppresses autophagy and rescues dendritic development of GluRδ2$^{Lc/+}$ Purkinje cells.

Immunofluorescent staining for the autophagic marker LC3B disclosed autophagic corpuscles in the soma of CaBP-positive GluRδ2$^{Lc/+}$ Purkinje cells which display severe dendritic atrophy after 12 DIV in organotypic cultures (Fig. 20 A-C). Blocking the excitotoxicity of GluRδ2$^{Lc/+}$ by NASP treatment for 12 DIV suppressed LC3B immunoreactivity (Fig. 20 E, F)of GluRδ2$^{Lc/+}$ Purkinje cells (Fig. 20 D, F) and rescued wild-type-like morphology of the dendritic arborisation (Fig. 20 G-I).

NASP treatment during the 12 day-long culture period (Fig. 21A) restored GluRδ2$^{Lc/+}$ Purkinje cell dendritic area and maximum dendritic length to the same extent as wild-type (P = 0.87 and P = 0.91) while this treatment had no effect on wild-type Purkinje cells (P = 0.91 and P = 1.00) (Fig. 21B). The dendritic area and maximum dendritic length of GluRδ2$^{Lc/+}$ Purkinje cells were not restored by a NASP treatment applied during the 6 first days of the 12 DIV period (P = 0.57 and P = 0.76) (Fig. 21B). On the contrary, in these 12 DIV GluRδ2$^{Lc/+}$ cerebellar organotypic cultures, NASP treatment during the last 4 days induced a significant increase in the maximum dendritic length of Purkinje cells (P < 0.05) (Fig. 21B). GluRδ2$^{Lc/+}$ Purkinje cell dendritic area and maximum dendritic length were restored to the same extent as wild-type Purkinje cells when NASP treatment was applied for the last 6 days of the 12 DIV period (P = 1.00 and P = 0.77) (Fig. 21B). As observed for Purkinje cell survival, this indicates that growth of Purkinje cells in cerebellar organotypic cultures during 12 DIV from P0 GluRδ2$^{Lc/+}$ mice is only sensitive to GluRδ2^{Lc} toxicity after 6 DIV.

*1.3 **Impaired survival and dendritic development of* **hotfoot** *Purkinje cells ex vivo.***

The effect of a GluRδ2-deficiency on Purkinje cell survival and growth was investigated in cerebellar organotypic slice cultures derived from natural *Grid2* knock-out *hotfoot* mice (Table 1). The GluRδ2$^{ho/ho}$ Purkinje cell population was significantly decreased compared to the wild-type Purkinje cell population (T = 2.89, P < 0.05) (Fig. 22A). No significant differences between the two genotypes were evident by a quantitative measurement of dendritic tree area (W = 16.0, P = 1.00) and maximum dendritic length (W = 10.0, P = 0.058). Nevertheless, estimation of branching points disclosed a significant difference between GluRδ2$^{ho/ho}$ and wild-type secondary (P < 0.01) and tertiary (P < 0.0001) dendritic

ramifications whereas the GluRδ2$^{ho/ho}$ and wild-type proximal dendrites did not differ (P = 0.97) (Fig. 22B, C).

1.4 ***Delayed climbing fiber translocation in the developing*** **hotfoot** ***cerebellar cortex***

During the normal postnatal period, pruning of multiple climbing fiber innervation of Purkinje cells establishes the mono-innervation of each Purkinje cell by a single climbing fiber (Lohof et al., 1996). This regressive phenomenon is contemporaneous of climbing fiber somato-dendritic translocation (Chedotal and Sotelo, 1992). Whereas in the adult GluRδ2$^{ho/ho}$ cerebellar cortex, immature multiple climbing fiber innervation of Purkinje cells is abnormally maintained and the climbing projection domain on Purkinje cells is aberrantly extended (Ichikawa et al., 2002), little is known about the developmental sequence of climbing fiber-Purkinje cell relationships during the postnatal period. Using specific immunolabelling of climbing fibers by VGlut2, the somato-dendritic translocation of the climbing fibers was found to be delayed in the GluRδ2$^{ho/ho}$ cerebellar cortex as soon as the end of the pericellular nest stage at P10 (Fig. 23).

2. Doppel-induced cell death mechanism(s) in prion protein-deficient Purkinje cells of the Nagasaki mutant mouse

In PrP-deficient mice of the Nagasaki strain ($NP^{0/0}$), ectopic expression of PrP-like protein Doppel (Dpl) in central neurons induces significant Purkinje cell death resulting in late-onset ataxia. In an initial set of experiments, I have found that $NP^{0/0}$ Purkinje cell death can be partly prevented by either knocking-out the apoptotic factor BAX or overexpressing the anti-apoptotic factor BCL-2 suggesting that apoptosis may be involved in Dpl-induced death of Purkinje cells. In the next set of experiments using Western blotting and immunohistofluorescence, I showed that before (3-4 months) and during significant PC loss (6-8 months), the $NP^{0/0}$ Purkinje cells displayed increased expression of the scrapie responsive gene 1 (Scrg1) potentially associated with autophagy and of the autophagic markers LC3B and p62. At the ultrastructural level, autophagic-like profiles accumulated in somato-dendritic and axonal compartments of the $NP^{0/0}$, but not in those of the wild-type Purkinje cells. Interestingly, the most robust autophagy was observed in $NP^{0/0}$ Purkinje cell axon compartments in the deep cerebellar nuclei suggesting that autophagy is initiated in the axons. Taken together, these results indicate that Dpl may trigger both autophagic and apoptotic

processes in $NP^{0/0}$ Purkinje cells. The increased autophagic features observed in the Purkinje cells of the $NP^{0/0}$ mice may result from either an upregulation of autophagy or an extensive accumulation of autophagosomes due to progressive dysfunctioning of autophagy as observed in amyloid neurodegenerative diseases. In this latter case, impaired autophagic proteolysis may trigger apoptotic cascades.

2.1 ***Publication 2.*** **Bax contributes to Doppel-induced apoptosis of prion protein-deficient Purkinje cells. Heitz S, Zanjani H, Lutz Y, Gautheron V, Bombarde G, Richard F, Fuchs JP, Vogel M, Mariani J, Bailly Y. Dev Neurobiol, (2007) 67:670-686.**

2.2 ***Publication 3.*** **BCL-2 counteracts Dpl-induced apoptosis of prion protein-deficient Purkinje cells in the Ngsk Prnp$^{0/0}$ mouse. Heitz S, Gautheron V, Lutz Y, Rodeau J-L, Zanjani HS, Sugihara I, Bombarde G, Richard F, Fuchs J-P, Vogel MW, Mariani J, Bailly Y. Dev Neurobiol, (2008) 68:332-348**

2.3 ***Publication 4.*** **Autophagy and cell death of Purkinje cells overexpressing Doppel in Ngsk Prnp-deficient mice. Heitz S, Leschiera R, Haeberlé A-M, Demais V, Grant N, Bombarde G, Bailly Y. Brain Pathol, in review.**

Discussion

I will briefly summarize the main results of my thesis and discuss them in the specific context of the *Lurcher* and the Nagasaki mutant mice and other murine models of neurodegeneration. The importance of apoptotic and autophagic processes in the degeneration of Purkinje cells in *Lurcher* and Nagasaki mice will be then compared in light of the mechanisms provoking neuronal death in the two models. Finally, future experimental research axes will be described that could further improve our knowledge of neuronal death mechanisms in the central nervous system.

1. Excitotoxicity and autophagy are related during *Lurcher* Purkinje cell death

Young postnatal GluRδ2$^{Lc/+}$ Purkinje cells have been reported to display autophagy before they undergo excitotoxic apoptotic cell death (Yue et al., 2002). This autophagy has been suggested to occur independently from GluRδ2^{Lc}-induced ionotropic excitotoxicity since I contributed to show that Purkinje cell death and autophagy occur in the heteroallelic GluRδ2$^{Lc/ho}$ double mutant mouse well before ionotropic excitotoxic cell death could operate in GluRδ2$^{Lc/+}$ Purkinje cells (Selimi et al., 2003: publication 1). In most cases, autophagy is believed to constitute a major neuroprotective response to cellular stress and metabolic deficiencies, but autophagy may also be a response to an early, GluRδ2^{Lc}-mediated injury distinct from ionotropic excitotoxicity.

A clue for the mechanism underlying Purkinje cell death in this model comes from my recent experiments on organotypic cerebellar cultures of GluRδ2$^{Lc/+}$ mice. The massive death of GluRδ2$^{Lc/+}$ Purkinje cells which occurs in this model was rescued by treatment with NASP, a cationic open channel blocker. This indicates that excitotoxicity is the main cause of GluRδ2^{Lc}-induced Purkinje cell death. Furthermore, NASP treatment downregulated the

expression of the autophagic marker LC3B-II in the GluRδ2$^{Lc/+}$ Purkinje cells as shown by immunocytofluorescence of organotypic cerebellar cultures. This suggested that autophagy depends on the excitotoxic mechanism induced by the aberrant functioning of mutated GluRδ2^{Lc}. One open question is whether this excitotoxicity-related autophagy is a neuroprotective response or a true cell death pathway activated by excitotoxic stress in parallel with apoptosis. The possible rescue of some GluRδ2$^{Lc/+}$ Purkinje cells when autophagy is inhibited with 3-methyl-adenine (3-MA) in *Lurcher* organotypic cerebellar cultures may support the latter hypothesis.

In addition, NASP treatment alone was sufficient to completely restore arborisation of the GluRδ2$^{Lc/+}$ Purkinje cell dendritic tree to the same extent as the wild-type suggesting that GluRδ2^{Lc} also mediates dendritic atrophy of the GluRδ2$^{Lc/+}$ Purkinje cells. Indeed, dendritic growth seems to proceed normally until 6 DIV in organotypic culture and until P6 *in vivo* (Bailly et al., 1996). The remaining question is whether GluRδ2^{Lc}-mediated autophagy is involved in Purkinje cell dendritic atrophy. Insight into this question will come from determining the effect of the autophagy inhibitor 3-MA on the dendritic growth of the GluRδ2$^{Lc/+}$ Purkinje cells in organotypic cerebellar cultures.

My investigations indicate that Purkinje cell death also occurs in the absence of GluRδ2 in the deficient *hotfoot* mutant mice, even though Purkinje cell loss could not be evidenced *in vivo* (Kurihara et al., 1997), suggesting that firstly, GluRδ2$^{ho/ho}$ Purkinje cells are more sensitive to cell death conditions and secondly, that these conditions may be counteracted *in situ*, but exacerbated in organotypic cerebellar cultures. In addition, the Purkinje cell dendritic tree of GluRδ2$^{ho/ho}$ mutant mice is not as developed as the wild-type mice in organotypic culture indicating that GluRδ2$^{ho/ho}$ Purkinje cell growth is impaired in organotypic cultures. On the other hand, the extent of the Purkinje cell dendritic tree is similar in wild-type and GluRδ2$^{ho/ho}$ mice *in situ* (Ichikawa et al., 2002). My data in organotypic cerebellar cultures confirm that GluRδ2 plays an essential role in the survival and dendritic development of Purkinje cells in this model. Restoring GluRδ2 expression in GluRδ2$^{ho/ho}$ and GluRδ2$^{-/-}$ mutant mice re-establishes the normal synaptic configuration of parallel fiber- and climbing fiber-Purkinje cell innervation (Kohda et al., 2007). The numerous naked spines on GluRδ2$^{ho/ho}$ Purkinje cell dendrites are reinnervated by homologous afferences. This is unlikely to occur in organotypic cultures of GluRδ2$^{ho/ho}$ Purkinje cells since both sources of homologous afferents are lacking. In such conditions, restoring GluRδ2 expression in these

neurons in the presence or absence of 3-MA might provide insight into the potential role of this receptor in the autophagic recycling of naked spines lacking afferent inputs. Furthermore, treating GluRδ2$^{ho/ho}$ Purkinje cells in organotypic cerebellar cultures with the autophagic activator rapamycin should indicate whether the naked spines of the GluRδ2$^{ho/ho}$ Purkinje cells can be recycled by autophagy.

Since Purkinje cell dendritic growth has not yet been investigated in the postnatal cerebellum of the *hotfoot* mouse, retardation in postnatal dendritic development as a potential factor of synaptogenesis impairment cannot be ruled out. This is in line with the deficiency in climbing fiber translocation observed in the cerebellar cortex of the 10 to 15 day-old postnatal GluRδ2$^{ho/ho}$ mutant mice. At this age, GluRδ2 is expressed at the climbing fiber-Purkinje cell synapses in the wild-type cerebellum (Zhao et al., 1997). Thus, the receptor is likely to promote climbing fiber translocation since this process is delayed when GluRδ2 is lacking in the GluRδ2$^{ho/ho}$ Purkinje cells. An important role in Purkinje cell excitatory synaptogenesis has been assigned to GluRδ2 based on its expression in climbing fiber-Purkinje cell synapses during translocation and pruning periods, impaired synaptogenesis in GluRδ2-lacking Purkinje cells, and the observed shift in the partition of Purkinje cell projection domain between parallel and climbing fibers. Whether expression of GluRδ2 is altered in the abnormal development of parallel and climbing fiber synapses in other experimental and mutant models of impaired Purkinje cell excitatory synaptogenesis is an interesting, but still unanswered question. In addition, the involvement of autophagy in the climbing fiber synaptogenesis needs to be examined during the main elimination period of climbing fiber synapse using immunocytochemistry for autophagic markers at the electron microscopy scale.

More than one single mechanism probably accounts for the death of Purkinje cells in GluRδ2$^{Lc/+}$ mutants. The deletion of *Bax* expression alters the pattern of caspase-3 activation, but only delays GluRδ2$^{Lc/+}$ Purkinje cell death (Selimi et al., 2000c) implying that BAX is involved in the caspase-3-dependent death mechanism (Selimi et al., 2000b). Also delayed death of Purkinje cells in GluRδ2$^{Lc/+}$ mutant mice overexpressing *Bcl-2* supports the involvement of pro-apoptotic members of the Bcl-2 family in GluRδ2$^{Lc/+}$ Purkinje cell apoptosis (Zanjani et al., 1998a; 1998b). On the other hand, autophagy has been demonstrated in GluRδ2$^{Lc/+}$ Purkinje cells by LC3 immuncytochemistry and by ultrastructural analysis suggesting that autophagy also plays a central role in GluRδ2^{Lc}-induced Purkinje cell death. In addition, GluRδ2^{Lc} promotes activation of the major autophagic factor Beclin1 in

GluRδ2$^{Lc/+}$ Purkinje cells (Yue et al., 2002). The participation of multiple cell death pathways is further evidenced in GluRδ2$^{Lc/+}$ Purkinje cells by caspase-3 immunohistochemistry and FluoroJade-B labelling which indicates that the cellular overload produced by the initial *Grid2* defect in *Lurcher* mutants apparently activates a variety of apoptotic and non-apoptotic pathways in the Purkinje cell population (Baurle et al., 2006). In addition, nitric oxide-induced oxidative stress occurs in dying GluRδ2$^{Lc/+}$ Purkinje cells (McFarland et al., 2007) and the resulting production of ROS is known to induce autophagy (Djavaheri-Mergny et al., 2006) as well as apoptosis (reviewed in Orrenius, 2007). Nevertheless, treating GluRδ2$^{Lc/+}$ organotypic cerebellar Purkinje cells with NASP, believed to block excitotoxicity, not only significantly reduces Purkinje cell death and dendritic atrophy, but also abrogates the induction of autophagy. This supposes that the induction of autophagy in GluRδ2$^{Lc/+}$ Purkinje cells is not uniquely mediated by the property of GluRδ2^{Lc} channels to promote Beclin1 activity, but is also a cellular response to metabolic stress. Taking into account the downregulation of autophagy and the rescue of GluRδ2$^{Lc/+}$ Purkinje cells by NASP, GluRδ2^{Lc} is likely to induce autophagy in Purkinje cells by a ROS-mediated pathway rather than through its nPIST-mediated interaction with Beclin1. Altogether, these data suggest that the functional significance of autophagy in GluRδ2$^{Lc/+}$ Purkinje cells is likely to be related to a neuroprotective mechanism in response to excitotoxic insult.

2. Multiple death mechanisms induced by Dpl in Nagasaki Purkinje cells

Activation of the neurotoxic mechanism triggered by Dpl in prion-protein deficient *NP*$^{0/0}$ Purkinje cells had previously been shown to provoke the premature death of these neurons (Li et al., 2000b). Our analysis of the impact of *Bax* knock-out as well as of overexpression of *Bcl-2* on Dpl-induced Purkinje cell death revealed a contribution of Bcl-2 family members to Dpl-mediated apoptosis. Although the Purkinje cell population is partially rescued in the *NP*$^{0/0}$*:Bax*$^{-/-}$ and *NP*$^{0/0}$*-Hu-bcl-2* double mutant mice indicating that BAX is involved in Dpl-induced apoptosis, numerous Purkinje cells died by a BAX-independent mechanism in the double mutants (Heitz et al., 2007; 2008: publications 2 and 3). Such a mechanism may be either apoptotic or non-apoptotic. This question has led my further investigations to determine a possible role of autophagy in Dpl-induced Purkinje cell death (Dron et al., 2005; Heitz et al.,

in review: publication 4). Robust autophagy was observed in *NP*$^{0/0}$ Purkinje cells well before significant neuronal loss. Ultrastructural examination showed an abnormal accumulation of autophagic vacuoles and autophagolysosomes in *NP*$^{0/0}$ Purkinje cells which, in addition to the upregulation of the autophagic markers LC3B-II and p62 in these neurons, suggested that autophagic flux was either upregulated or impaired. At the current state of my research, the most plausible hypothesis is that abnormal upregulation of autophagy occurs in Purkinje cells at a maximal rate that reaches a plateau as early as 3 months and continues until 8 months as indicated by the persistence of p62 and LC3B-II upregulation. In this case, autophagy is likely to be a neuroprotective response to Dpl-induced stress, but ultimately is insufficient to prevent neuronal death. Another possibility could be that autophagy precedes and is causally linked to the subsequent onset of programmed Purkinje cell death (Canu et al., 2005; Djavaheri-Mergny et al., 2006; 2007). Alternatively, robust accumulation of autophagic organelles and p62 upregulation could reflect an impairment of the autophagic flux in Dpl-diseased Purkinje cells as it has been proposed in Alzheimer-diseased neurons. Indeed, the accumulation of autophagosomes, late autophagic vacuoles, lysosomes and autophagolysosomes in dystrophic neurites has also been reported in Alzheimer-diseased brain (Nixon et al., 2005; Yu et al., 2005) and other neurodegenerative pathologies such as prion diseases (Liberski et al., 2008). A deficiency in the autophagic process has also been proposed to occur in Huntington disease to explain the abnormal accumulation of p62-positive aggregates (Filimonenko et al., 2007) that are normally degraded through autophagy (Ravikumar et al., 2004). In this case, autophagic stress would be induced by the incapacity of the diseased neurons to clear p62-bound misfolded protein aggregates (Chu, 2006). The robust accumulation of autophagic organelles and the upregulation of p62 argue in favor of the impairment of autophagy in *NP*$^{0/0}$ Purkinje cells.

The contribution of autophagy to Dpl-induced Purkinje cell death needs to be further analyzed *in vitro* using autophagy antagonist 3-MA and agonist rapamycin in *NP*$^{0/0}$ organotypic cerebellar cultures. If autophagy contributes directly to Dpl-induced Purkinje cell death, neuronal death should be increased by rapamycin and decreased by 3-MA. On the other hand, if autophagy is a neuroprotective reaction to Dpl toxicity, rapamycin should rescue Purkinje cells and 3-MA should increase Purkinje cell death. Furthermore, investigating autophagy in the *NP*$^{0/0}$*:Bax*$^{-/-}$ and *NP*$^{0/0}$*-Hu-bcl-2* double mutant mice will provide novel insights into the relationships between intrinsic pathway of apoptosis and autophagy in the mechanism of Dpl-induced Purkinje cell death. Indeed, it is important to determine the

mechanism by which *NP$^{0/0}$:Bax$^{-/-}$* and *NP$^{0/0}$-Hu-bcl-2* Purkinje cells die. This mechanism could be autophagic independently of Bcl-2 family-related apoptosis or non-autophagic by an extrinsic apoptotic pathway (Fig. 24).

3. Differential combination of apoptosis and autophagy in Nagasaki and *Lurcher* cerebellar Purkinje cells

In light of previous reports in the literature, my results support the concept that both apoptosis and autophagy occur in Nagasaki and *Lurcher* cerebellar Purkinje cells (Table 2) (Selimi et al., 2003: publication 1; Heitz et al., 2007, 2008, in review: publications 2, 3 and 4). Although several apoptotic pathways including intrinsic and extrinsic pathways are likely to contribute to *Lurcher* Purkinje cell death (Selimi et al., 2000a; Lu and Tsirka, 2002; Selimi et al., 2003: publication 1), much less is known about the apoptotic mechanism triggered by Dpl in *NP$^{0/0}$* Purkinje cells. Certainly, the BAX-dependent intrinsic pathway is responsible for part of the *NP$^{0/0}$* Purkinje cell loss (Heitz et al., 2007, 2008: publications 2 and 3) but the results reported above argue for a second still unknown and likely extrinsic pathway. On the other hand, autophagy has recently been reported to mediate GluRδ2^{Lc}–induced Purkinje cell degeneration (Yue et al., 2002; Selimi et al., 2003: publication 1). These data show that LC3-positive autophagy occurs abundantly before Purkinje cell death without any signs of autophagic flux impairment such as autophagosome accumulation and p62 upregulation (Wang et al., 2006). The axonal origin of autophagosomes in GluRδ2$^{Lc/+}$ Purkinje cells was clearly evidenced and the incidence of autophagosomes is much less within the cell bodies and dendrites of GluRδ2$^{Lc/+}$ Purkinje cells (Wang et al., 2006). Such a limited autophagy probably cannot rescue GluRδ2$^{Lc/+}$ Purkinje cells from death, but might activate or enhance apoptotic pathways triggered by the massive Ca^{2+} entry through the constitutively activated GluRδ2^{Lc} channels (McFarland et al., 2007). Very interestingly, the autophagic features displayed by the *NP$^{0/0}$* Purkinje cells are strikingly different. Most of the autophagic organelles accumulate within Purkinje cell axon terminals and dystrophic swellings suggesting the axonal initiation of autophagy, but also autophagic flux impairment. This deficiency is supported by the upregulation of p62 in the *NP$^{0/0}$* Purkinje cells (Heitz et al., in review: publication 4). These differences indicate that Dpl and *Grid2* trigger specific cascades of programmed cell death in the same type of central neuron, the cerebellar Purkinje cell.

Autophagic deficiency has been reported in several neurodegenerative diseases including Alzheimer and prion diseases (Nixon, 2006; Liberski et al., 2008) where it is believed to contribute to neurodegeneration. Thus, the $NP^{0/0}$ Purkinje cell provides an attractive model to the cellular and molecular mechanisms of neuronal death in these pathologies in perspective of designing new therapeutic approaches.

Material and Methods

1. Animals and genotyping

1.1 ***Animals***

1.1.1 The Grid2$^{Lc/+}$(Lurcher) and the Grid2$^{ho/ho}$ (hotfoot) mice

Grid2$^{Lc/+}$ mice (gift from J. Mariani) were intercrossed to obtain *Grid2*$^{Lc/Lc}$, *Grid*$^{+/+}$, *Grid2*$^{Lc/+}$ mice in the same litter. *Grid2*$^{ho/ho}$ mice (gift from J. Mariani) were crossed with *Grid2*$^{+/+}$ mice to get *Grid2*$^{ho/+}$ mice. Littermates were intercrossed to obtain *Grid2*$^{ho/ho}$, *Grid2*$^{ho/+}$ and *Grid2*$^{+/+}$ mice in the same litter. The generation of *Grid2*$^{ho/Lc}$ mice is described in Selimi et al., 2003 (Publication 1).

Grid2^{Lc}, *Grid2*$^{+}$ and *Grid2*^{ho} alleles were identified using the further mentioned probes and primer sets.

1.1.2 The NP$^{0/0}$, the NP$^{0/0}$:Bax$^{-/-}$ and the NP$^{0/0}$-Hu-bcl-2 mice

Bax$^{-/-}$ mice were generated by deleting exons 2 to 5 (Knudson et al., 1995) and *Hu-bcl-2* mice from the NSE73a strain were generated by injecting embryos with the EB-2 construct in the cloning vector pSK+ containing the human BCL-2 coding region (Tsujimoto and Croce, 1986; Martinou et al., 1994). Further breeding strategies were designed taking into account that *Bax*$^{-/-}$ males and *Hu-bcl-2* females are sterile. *NP*$^{0/0}$ mice were generated by deleting the entire open reading frame (ORF) of the *Prnp* gene, located in exon 3, as well as 5' and 3' non-coding flanking regions (Sakaguchi et al., 1995) and the deleted sequence was replaced by a Neo cassette. For this study, founding mice have been first backcrossed with C57BL/6 mice for at least 10 generations.

For the generation of the *NP*$^{0/0}$:*Bax*$^{-/-}$ double mutant mouse line, *NP*$^{0/0}$ males and females (gift from S. Katamine) were then crossed with *Bax*$^{+/-}$ males and females (gift from S. Korsmeyer) and offspring were identified by PCR genotyping using the further mentioned

primer sets. $NP^{+/0}$:$Bax^{+/-}$ mice were further intercrossed, generating $NP^{0/0}$:$Bax^{-/-}$, $NP^{0/0}$:$Bax^{+/-}$, $NP^{0/0}$:$Bax^{+/+}$, $NP^{+/0}$:$Bax^{-/-}$, $NP^{+/0}$:$Bax^{+/-}$, $NP^{+/0}$:$Bax^{+/+}$, $NP^{+/+}$:$Bax^{+/+}$, $NP^{+/+}$:$Bax^{+/-}$ and $NP^{+/+}$:$Bax^{-/-}$ genotypes. The $NP^{0/0}$:$Bax^{-/-}$ double mutants were obtained by crossing $NP^{0/0}$:$Bax^{+/-}$ males with $NP^{0/0}$:$Bax^{-/-}$ or $NP^{0/0}$:$Bax^{+/-}$ females.

$NP^{0/0}$ females were crossed with *Hu-bcl-2* males in order to generate the $NP^{0/0}$-*Hu-bcl-2* double mutant mouse line, and offspring were identified using the further mentioned probes and primer sets. $NP^{+/0}$-*Hu-bcl-2* males were further crossed with $NP^{0/0}$ females to generate $NP^{0/0}$-*Hu-bcl-2* offspring. Strict littermates of the different genotypes have been used throughout the study.

Mice were bred at the animal facilities of Anatomisches Institut in Basel and of Neurosciences IFR37 in Strasbourg. They were maintained and submitted to experiments according to the NIH guidelines (NIH Publication 80-23, revised 1996), the European Communities Council Directive of November 24, 1986 (86/609/EEC) and approved by the Swiss authorities. A minimal number of animals was used and handled with maximum care to minimize their suffering.

1.2 ***Genotyping***

1.2.1 DNA extraction

Tail samples from weanling pups were used to extract DNA. Tails were transferred in a mix of 615µl Tris-SDS-EDTA buffer (TSE, Tris 25mM pH8, SDS 1%, EDTA 25mM pH8, NaCl 75mM) and 15µl Proteinase K diluted 10mg/ml (Sigma Aldrich) for 4 hours at 55°C before centrifugation at 13000 rotations per minute (rpm) for 4 min. Supernatant was collected in 500µl isopropanol and centrifuged as previously described. The pellet was washed in 500µl ethanol 100% and centrifuged. Ethanol was removed and 100µl water was added to the pellet.

1.2.2 Genotyping

Genotyping for $Grid2^{Lc}$ and $Grid2^{ho}$ alleles was performed by PCR followed by single-strand conformation polymorphism (SSCP) using the *Grid2* forward 5'TAAAAGCATATTGATGTTGTTG3' and reverse 5'CAGCATTTGTCAGGTTTGGTGAC3' primers. Cycling parameters for PCR were 5 min at 94°C for one cycle, and 1 min at 94°C , 1 min at 60°C and 1 min at 72°C for a total of 35 cycles before 7 min at 72°C for one last cycle. A solution of 10µl of blue bromophenol

(0.05%), xylene cyanol (0.05%) and 20mM EDTA pH8 in formamide was added to 10µl of each sample before electrophoresis on a 15% acrylamide gel (Biorad) over-night at 4°C using a DCode Universal Mutation Detection System (Biorad). The gel was further stained with the Silver Staining kit (Amersham) and the *Lurcher* and wild-type alleles were detected by 2 different bands and the *hotfoot* allele by the absence of any band.

Genotyping for *Bax* was performed by PCR by using a set of three primers: *Bax* exon 5 forward primer (5'GAGCTGATCAGAACCATCATG3'), *Bax* intron 5 reverse primer 5'GTTGACCAGAGTGGCGTAGG3') and Neo reverse primer (5'CCGCTTCCATTGCT-CAGCGG3'). Cycling parameters were 2 min at 94°C for one cycle, and 45 sec at 94°C , 45 sec at 55°C and 1.5 min at 72°C for a total of 40 cycles before 7 min at 72°C for one last cycle. Four µl of DNA loading buffer (Sigma-Aldrich) was added to 8µl of each sample before an electrophoresis on a 2% agarose gel (Sigma-Aldrich) at 130V for 10 min. Bands were revealed using the UV Appligene equipment (Oncor). The Bax^{-} allele was determined by a band of 507 base pairs (Bp) and the Bax^{+} allele by a band of 304 Bp.

Genotyping for *Hu-bcl-2* was performed by PCR by using a set of two primers: *Hu-bcl-2* transgenic forward 5'GAA-GAC-TCT-GCT-CAG-TTT-GG3' and reverse 5'ATG-AGC-CTT-GGG-ACT-GTG-AA3'. Cycling, electrophoresis and identification of bands parameters were the same as for *Bax* genotyping. The presence of the *Hu-bcl-2* transgene was determined by a band of 496 Bp.

Genotyping for Dpl was performed by PCR. The *Prnp* ORF was identified using the following primers: forward 5'CCGCTACCCTAACCAAGTGT3' and reverse 5'CCTAGACCACGAGAATGCGA3', both located within the *Prnp* ORF; $NP^{0/0}$ mutants were identified using the following primers: forward 5'TGCCGCACTTCTTTGTGAAT3' and reverse 5'CGGTGGATGTGGAATGTGT3' (within Neo cassette). Cycling parameters were 5 min at 94 °C for one cycle, and 45 sec at 94 °C, 30 sec at 53 °C and 1.5 min at 72 °C for a total of 30 cycles before 10 min at 72 °C for one last cycle. Electrophoresis and identification of bands parameters were the same as for *Bax* genotyping. The $Prnp^{+}$ allele was determined by a band of 347 Bp and the $Prnp^{0}$ allele by a band of 228 Bp.

2. Methods

2.1 ***Organotypic cerebellar culture***

Organotypic cerebellar cultures were realized using the static culture method. This method, first described by Yamamoto et al (1989) and further developed by Stoppini et al (1991), allows maintaining postnatal 350µm-thick cerebellar slices in culture. Due to the sagittal orientation of the Purkinje cell in the cerebellar folia, it is possible to preserve almost the complete Purkinje cell within a slice. New-born (P0) *Grid*$^{+/+}$, *Grid2*$^{Lc/+}$ mice and P8 *Grid2*$^{ho/ho}$, *Grid2*$^{ho/+}$ and *Grid2*$^{+/+}$ mice were decapitated and their brain aseptically removed and placed into ice-cold preparation medium made of minimal essential medium (MEM, Gibco) and 2mM glutamax I (Gibco) pH 7.3. The cerebellum was dissected, the meninges removed and 350 µm-thick sagittal sections were cut using a McIllwain tissue cutter under aseptic conditions. Tissue slices were separated and transferred onto permeable membranes (Millicell, Millipore) and incubated on a layer of serum-containing culture medium (25% Basal Eagle's medium, 25% horse serum, 2mM glutamax I, 3.6mM glucose in MEM, Gibco) in a humidified atmosphere with 5% CO_2 at 37°C. The medium was changed every 2-3 days for a total of 12 days. 1-Naphtyl-acetyl-spermine NASP (Sigma-Aldrich) was added at a concentration of 50µM at medium changes.

2.2 ***Histology***

Mice were anaesthetized with sodium pentobarbital (0.15 mL per 100g i.p.; Sanofi) after which brain was dissected and immersed overnight in Carnoy's fixative (60% ethanol, 30% chloroform, 10% acetic acid). After washes in iso-butanol (Carlo Erba), the brain was embedded in paraffin and sectioned 10 µm-thick in the sagittal plane. Sections were deparaffinised and rehydrated in decreasing concentrations of ethanol. They were then immersed in a solution of cresyl violet-thionine (25mg each in 100 ml of water) for 7 minutes, submitted to differentiation in 95% acidic ethanol and mounted in Eukitt before examination with a light microscope (Axioskop-II, Zeiss, Jena, Germany).

2.3 ***Immunohistochemitry***

2.3.1 Tissue sections

Mice were anaesthetized with a mixture of 5% ketamine and 5% xylazine (0.1 mL of the mix per 30g i.p.) and transcardiacally perfused with 4% paraformaldehyde in 0.1M phosphate

buffer (PB) pH 7.3. Brains were then immersed for 4 hours in the same fixative at 4°C before either cryoprotection in 0.44M sucrose in PB at 4°C over-night and freezing in liquid nitrogen (wild-type, *NP$^{0/0}$*, *NP$^{0/0}$:Bax$^{-/-}$* and *NP$^{0/0}$-Hu-bcl-2* mice) or immersion in iso-butanol for 4 days before embedding in paraffin (wild-type, *NP$^{0/0}$*, *NP$^{0/0}$:Bax$^{-/-}$* and *NP$^{0/0}$-Hu-bcl-2* mice). Frozen sections were cut (10µm-thick) in the cerebellum with a cryostat (Leica) and paraffin sections were cut (10µm-thick) with a microtome (Leica). Paraformaldehyde-fixed brains of wild-type and *Grid2$^{ho/ho}$* mice was dissected and sagittal and transversal cerebellar sections (50µm-thick) were obtained with a vibratome (Leica).

2.3.2 Immunohistochemistry

Frozen sections and vibratome floating sections were rinsed in 0.1M phosphate buffer saline (PBS) pH 7.3. Paraffin sections were deparaffinised in toluene and rehydrated in decreasing concentrations of alcohol. All sections were pre-incubation for 45 min in a blocking solution at room temperature. This was made of PBS containing 3% normal goat serum (NGS) and 0.5% Triton X-100 for immunohistofluorescence on frozen and paraffin sections, 2% normal horse serum (NHS) and 0.05% Triton X-100 for immunoperoxidase on paraffin sections and, 0.02% gelatin (D^{r} Oetker), 0.25% Triton-X 100 and 0.1M lysine for immunohistofluorescence on vibratome sections. The sections were then incubated overnight at 4°C in the blocking solution containing specific primary antibodies (Table 3).

Then, sections were rinsed in PBS (2x10 min) and incubated with secondary antibodies (Table 3) in blocking solution. Immunoperoxidase detection was achieved using the avidin biotin complex (ABC) method with 3,3'-diamino-benzidine tetra-hydrochloride (Fast-DAB, Sigma Aldrich). After rinsing in PBS, the fluorescent sections were mounted in Mowiol and the immunoperoxidase sections were mounted in Eukitt. The frozen and the paraffin sections were examined with a light microscope equipped with fluorescence and differential interference contrast illumination (Axioskop-II, Zeiss, Jena, Germany). The vibratome fluorescent sections were analyzed with a Zeiss confocal microscope LSM 510.

2.3.3 Immunohistofluorescence in organotypic cerebellar cultures

Cultures were fixed in a 4% paraformaldehyde in PB overnight at 4°C before rinsing in PB. The cultures were pre-incubated for 45 min in blocking solution made of 3% NGS and 0.1% Triton X-100 in PB (PBT). The sections were then incubated overnight at 4°C with either rabbit polyclonal antibodies against CaBP (Swant and gift from Dr Thomasset) diluted

1/1000 and mouse monoclonal antibody against LC3B (Nanotools) diluted 1/20 in PBT containing 0.3% NGS.

Sections were then rinsed in PB (2x10 min) and incubated with fluorescent secondary antibodies (table 3). After rinsing in PB, the cultures were mounted in Mowiol before examination with a fluorescence microscope (Axioskop-II, Zeiss, Jena, Germany).

2.4 ***Transmission electron microscopy***

Mice were anaesthetized as described above (§2.2) and transcardially perfused with fixative in PB (Table 4). Vibratome sections (60µm-thick) were submitted to Scrg1- and GABA-immunocytochemistry using respectively pre-embedding and post-embedding immunogold as previously described (Heitz et al., in review: publication 4). The samples from cerebellar sections destined to ultrastructural analysis were prepared according to a classical protocol for transmission electron microscopy (Selimi et al., 2003: publication 1). The ultrathin sections were examined with a Hitachi 7500 transmission electron microscope equipped with an AMT Hamamatsu digital camera.

2.5 ***Western blotting***

Western blotting was performed to evaluate the expression of LC3B-I and –II, p62 and Lamp1 in wild-type and $NP^{0/0}$ cerebella according to the protocol described in Heitz et al., in review (publication 4).

2.6 ***Quantitative analysis***

In all Purkinje cell quantitative analysis performed in these studies, Purkinje cell counts were performed by me with the genetic identity of the animal masked.

2.6.1 Morphometric analysis of Purkinje cell dendritic tree in organotypic cerebellar cultures

The size and the ramification degree of the Purkinje cell dendritic tree were evaluated by measuring the following morphometric features: the dendritic area, the distance between the tip of the longest dendrite and the center of the soma (maximum dendritic length) and the number of dendrite branching points per Purkinje cell.

At least 15 Purkinje cells were selected in each mouse studied. These neurons displayed well visible axon and dendrites because isolated from the surroundings. These cells were

photographed with a CoolSnap Pro digital camera (Photometrics) and Image Pro plus software (Media Cybernetics) was used to measure the dendritic area and the maximum dendritic length. The dendrite branching points were counted visually. All morphometric data were submitted to statistical analysis. The non-parametric test of Mann-Witnney was used to compare wild-type and *hotfoot* Purkinje cell dendritic extent and the non-parametric test of Kruskall-Wallis followed, when justified, by *post-hoc* tests for multiple comparisons was used to compare the effects of NASP treatments on wild-type and *Lurcher* Purkinje cell dendritic extent. The significance threshold was set at $P = 0.05$.

2.6.2 Quantitative analysis of Purkinje cells in organotypic cerebellar cultures

Only CaBP-immunopositive Purkinje cells with neurites were counted in 4 organoypic cultures obtained from each mouse in these studies.

Comparison of Purkinje cell numbers between untreated and NASP-treated wild-type and *Lurcher* organotypic cerebellar cultures was submitted to two-way analysis of variance (factor genotype, factor treatment) followed, when justified, by *post hoc* Tukey test for multiple comparisons.

Student test was performed to compare wild-type and *hotfoot* Purkinje cell numbers in organotypic cerebellar cultures. The significance threshold was set at $P = 0.05$.

2.6.3 Size of the cerebellar vermis

The size of the cerebellar vermis was estimated by measuring the mean area of seven sagittal cresyl-violet-stained sections (Image J) separated from each other by 400µm.

2.6.4 Quantitative analysis of Purkinje cells in tissue sections

The Purkinje cell population was quantified and statistically evaluated as previously described (Heitz et al., 2007; 2008: publications 2 and 3) by a profile-based sampling method (Guillery and Herrup, 1997) using the Hendry correction factor (Hendry, 1976).

Appendix

1. Models of Purkinje cell degeneration

Purkinje cell death manifests itself by ataxia and tremor. In addition to the *Grid2* mutant mice and Nagasaki mutant mice, several other mutant mice are featured by Purkinje cell death.

1.1 ***Purkinje cell death and murine mutations***

1.1.1 The nervous mutant mouse

In the cerebellum of *nervous* mutant mice, some Purkinje cells initially develop an alteration of their mitochondria at P9 and further degenerate by P19 when most of their cytoplasmic organelles lyses and the cytoplasmic matrix abruptly condenses followed by cell death (Landis, 1973). The observation of dying Purkinje cells in 12 month-old *nervous* mice suggests a continuous progression of Purkinje cell death process (Sotelo and Triller, 1979) throughout lifespan. Interestingly, Purkinje cell death is not random with 60% of Purkinje cells dying in the vermis and 90% in the hemispheres (Wassef et al., 1987). Purkinje cell death was more important in the anterior lobe than in the posterior one, with zebrin-positive cells exhibiting an enhanced sensitivity to the *nervous* mutation. Although the molecular target of this mutation remains unknown, the selective alteration of the mitochondria seems to indicate that oxidative stress may be at the origin of the Purkinje cell death in this mutant. The late cell death process is probably necrosis since ultrastructural features characterizing apoptosis have not been described (Landis, 1973).

1.1.2 The toppler mutant mouse

This autosomal mutation is characterized by a specific gait alteration (Duchala et al., 2004) and a severe loss of Purkinje cells between P14 and P30. The degenerating Purkinje cells have nuclear DNA double-strand breaks and are TUNEL-positive, suggesting that they die by apoptosis.

1.1.3 The Purkinje cell degeneration (pcd) mutant mouse

Mice homozygous for this mutation lose their Purkinje cells during the third and fourth postnatal weeks. In 4 month-old *pcd/pcd* cerebellum, some Purkinje cells survive, only in the lobule X (Wassef et al., 1986). Degenerating Purkinje cells show nuclear condensation and shrinkage of the cytoplasm suggesting apoptotic cell death (Landis and Mullen, 1978). Characterization of the *pcd* mutant alleles revealed mutations in the Nna1 gene. Nna1 encodes a putative nuclear protein containing a zinc carboxypeptidase domain initially identified by its induction in spinal motor neurons during axonal regeneration (Fernandez-Gonzalez et al., 2002). As degenerating Purkinje cells are TUNEL-positive and have a decreased expression of BCL-2, Purkinje cell death in this mutant occurs essentially by apoptosis (Gillardon et al., 1995a; 1995b).

1.1.4 The woozy mutant mouse

The *woozy* mutation affects Sil1 a protein of the HSP70 family which is present in the lumen of the ER. It is characterized by a late Purkinje cell death which starts after 10 weeks of age and continues until 18 months (Zhao et al., 2005). This progressive death process affects essentially the anterior lobe. Dying Purkinje cells are TUNEL- and caspase-3-positive suggesting that apoptosis is the death mechanism involved. Nevertheless, electron microscope analysis has also disclosed the occurrence of autophagy (Zhao et al., 2005). The abnormal accumulation of proteins resulting from the inactivation of Sil1 may provoke ER stress with subsequent alteration of calcium homeostasis and thus may also contribute to the death of Purkinje cells (Zhao et al., 2005).

1.1.5 The Niemann Pick disease type C

Niemann-Pick disease type C (NPC) is an early onset autosomal recessive disorder characterized by accumulation of cholesterol and other lipids in late endosomes/lysosomes (Loftus et al., 1997). About 95% of the cases are caused by mutations in the *NPC1* gene, whereas the remaining 5% are due to mutations in the *NPC2* gene. The Purkinje cells are preferentially affected with less than 10% neurons remaining in 2 month-old *npc1* mutant mice, but surprisingly glia in the corpus callosum is affected earlier (German et al., 2001). Investigations of the basis of neurodegeneration in these mice have shown that dying Purkinje cells have features of autophagic cell death (Ko et al., 2005) with increased levels of LC3-II

(Bi and Liao, 2007). Furthermore, increases in autophagic activity are closely associated with alterations in lysosomal function and protein ubiquitination (Bi and Liao, 2007).

1.1.6 The leaner mutant mouse

The *leaner* mutant (tg^{la}) mouse is severely ataxic due to cerebellar atrophy, resulting from gradual degeneration of granule, Purkinje, and Golgi cells (Herrup and Wilczynski, 1982; Frank et al., 2003). Pycnotic granule cells are numerous in the internal granular layer as early as P10 but significant Purkinje cell loss is not observed until the end of the first postnatal month and continues at a low rate throughout the life of the animal (Herrup and Wilczynski, 1982). Molecular analysis has shown a mutation in the gene coding for the $Ca_v2.1$ voltage-gated calcium channel which is highly expressed in the cerebellum (Volsen et al., 1995) and hippocampus (Day et al., 1996). The tg^{la} mutation results in alteration of calcium homeostasis of cerebellar Purkinje cells which can be attributed to reduced uptake by the ER (Dove et al., 2000). In addition, an apoptotic process kills cerebellar granule cells with a peak at P20 (Lau et al., 2004). This is accompanied by decreased expression of nNOS (Frank-Cannon et al., 2007). Altogether, these data suggest that a major dysfunction of calcium homeostasis is responsible for granule and Purkinje cell death in this mutant.

1.1.7 The hyperspiny mouse

The *hyperspiny* Purkinje cell mutant mice show cerebellar symptoms from P10. The cerebellum is slightly hypoplastic and histological examination reveals that Purkinje cells have reduced dendritic arbors. As the name of the mutant implies, the proximal dendrites and soma of the Purkinje cells are studded with spines (Guenet et al., 1983). Focal axonal swellings are also found in nearly all axons (Sotelo, 1990b). Axonal pathology leads to a retrograde degeneration resulting in a 15% Purkinje cell loss (Guenet et al., 1983; Sotelo, 1990b; 1990a).

1.1.8 The tambaleante mouse

The *tambaleante* spontaneous mutation particularly affects Purkinje cells, because these neurons suffer from a late, slow and progressive degenerative process starting at about 2 months of age (Wassef et al., 1987). In one year-old mice, the degeneration is almost complete with less that 1% surviving neurons (Wassef et al., 1987; Rossi et al., 1995). Pathological signs are characterized by moderate thickening of the main axonal stems. The

recurrent axon collaterals and varicose axonal enlargements or torpedoes commonly accompany these alterations (Rossi et al., 1995). Dense somatic material, autophagic vacuoles and autophagolysosomes are observed in the soma and dendrites of these Purkinje cells (Dusart et al., 2006) suggesting that Purkinje cells undergo autophagic degeneration. Nevertheless, some Purkinje cells exhibit apoptotic-like condensation of the nucleus, and dendritic debris of the dying Purkinje cells can be seen in the molecular layer of 6 to 12 month old *tambaleante* cerebella. Therefore, it is likely that after an initial intense autophagic phase, the affected Purkinje cells follow a different death pathway, probably involving apoptosis (Dusart et al., 2006).

1.1.9 The weaver mutant mouse

The autosomal recessive *weaver* mutation is a single amino acid exchange in a G-protein coupled, inwardly rectifying K^+ channel (GIRK2) (Patil et al., 1995) and generates chronic depolarization of the affected neurons (Patil et al., 1995; Liss et al., 1999). This leads to massive death of granule cells (80%) during the 2 first postnatal weeks (Smeyne and Goldowitz, 1989). Dying granule cells display typical apoptotic morphology, DNA fragmentation (Smeyne and Goldowitz, 1989; Gillardon et al., 1995a), increased Bax expression (Wullner et al., 1995) and successive activation of caspase-9 and caspase-3 (Peng et al., 2002). In addition, about 40% of Purkinje cells and 25% of the deep cerebellar neurons also die postnatally (Maricich et al., 1997).

1.1.10 The staggerer mutant mouse

The autosomal recessive *staggerer* (*Rora*^{sg}) mutation causes a deletion of the *Rora* gene (Hamilton et al., 1996) which encodes a retinoid-like nuclear receptor involved in neuronal differentiation and maturation, with high expression in Purkinje cells (Hamilton et al., 1996; Ino, 2004). In homozygotes, Purkinje cells declined in number before P5 and, at the end of the first postnatal month, only 25% of them remained (Herrup and Mullen, 1979). The remaining *Rora*^{sg} Purkinje cells are reduced in size, lack tertiary dendritic spines receiving synaptic contacts from parallel fibers (Sotelo, 1975) and are multiply innervated by climbing fibers, a sign of developmental arrest (Mariani, 1982).

1.1.11 The reeler mutant mouse

The autosomal recessive *reeler* mutation disrupts the *Reln* gene (D'Arcangelo et al., 1995) which encodes reelin, an extracellular matrix protein involved in neural adhesion and migration at critical stages of development (D'Arcangelo et al., 1995; Hack et al., 2002). *Reeler* mutants display essentially architectonic disorganization in the cerebellum (Mariani et al., 1977) and the inferior olive (Goffinet, 1983). In the *reeler* cerebellum 90% of granule cells (Caviness and Rakic, 1978), 50% loss of Purkinje cells (Heckroth et al., 1989) and 20% of inferior olivary neurons (Blatt and Eisenman, 1985) are loss. In addition, adult *reeler* Purkinje cells are innervated by more than one climbing fiber (Mariani et al., 1977; Mariani, 1982).

1.2 ***Purkinje cell death in neurological disorders***

1.2.1 Brain ischemia

Brain ischemia induces increases in glutamate, intracellular calcium, and release of free radicals leading to neuronal death (Lipton, 1999; Welsh et al., 2002). A massive excitotoxic loss of Purkinje cells is correlated with ataxia in patients recovering from global ischemic stroke (Sarna and Hawkes, 2003). The origin of this excitotoxic neuronal death is complex, probably, resulting from the intensive innervation of Purkinje cells by glutamatergic climbing/parallel fibers (Sarna and Hawkes, 2003), deficiency of glutamate reuptake (Welsh et al., 2002; Yamashita et al., 2006) and persistent activation of AMPA receptors (Hamann et al., 2005).

1.2.2 Alzheimer disease

Purkinje cell loss was originally demonstrated in brains of patients deceased from familial and sporadic Alzheimer diseases (Fukutani et al., 1996). Significant cerebellar atrophy was related to a 35% loss of Purkinje cells (Wegiel et al., 1999). This loss was accompanied by a loss of inferior olivary neurons and a massive cerebellar gliosis (Sjobeck and Englund, 2001). This is manifested by some of the symptoms and signs observed in Alzheimer disease such as spatial disorientation.

1.2.3 Huntington disease

In the Huntington disease, Purkinje cell loss has been reported (Rodda, 1981), but the death mechanisms causing neuronal death is unknown. Dying Purkinje cells characteristically

exhibit neuronal intranuclear inclusions, condensation of both cytoplasm and nucleus, and ruffling of the plasma membrane while maintaining ultrastructure of cellular organelles (Turmaine et al., 2000). These cells do not develop any sign of nuclear or cytoplasmic blebbing, apoptotic bodies, or DNA fragmentation (Turmaine et al., 2000) and this suggests that Purkinje cell death mechanism is neither apoptosis nor necrosis.

1.2.4 Prion diseases

Creutzfeld-Jacob disease induces a virtually complete disappearance of parallel fibers (Berciano et al., 1990) caused by massive loss of granule cells which is total in the cerebellar vermis (Hauw et al., 1981; Tiller-Borcich and Urich, 1986; Berciano et al., 1990; Kovacs et al., 2001). This is accompanied by hypertrophy of primary and secondary Purkinje cell dendrites (Tiller-Borcich and Urich, 1986) which express PrP^C (Lemaire-Vieille et al., 2000). Interestingly, Fas, Fas-L, and Bax expression are increased and caspase-3 immunoreactivity is enhanced in the cytoplasm of surviving Purkinje cells in CJD (Puig and Ferrer, 2001) suggesting either impairment of apoptosis or non-apoptotic roles for these proteins. In addition, the heat shock protein Hsp72 accumulates in TUNEL-negative Purkinje cells and is absent from TUNEL-positive granule cells suggesting that this protein helps to rescue Purkinje cells from the TSE (Kovacs et al., 2001). This suggests that accumulation of the inducible Hsp-72 in Purkinje cells may be part of a cytoprotective mechanism in prion-diseased cerebellum.

2. Prion diseases

Prion diseases are infectious, genetic, or sporadic TSEs, characterized by prion protein aggregation and neurodegeneration. These diseases include kuru and CJD in humans, scrapie in sheep and BSE in animals. These diseases are incurable, with a variety of motor or cognitive symptoms and fatal issue (Knight and Will, 2004).

Current understanding of TSEs have evolved from the concept of the "prion" that is a proteinaceous, nucleic acid-free, infectious particle (Prusiner, 1998). The pathogenesis of prion diseases is attributed to major changes in the metabolism of PrP^C (Aguzzi et al., 2008).

2.1 The Prion Concept: a protein-only hypothesis of infection

The infectious agent responsible for the transmission of the disease is probably not constituted of nucleic acids since this agent is resistant to doses of radiation that inactivate viruses and bacteria (Alper, 1985). Also, its sensitivity profile to various chemicals differs from viruses and viroids (Behrens and Aguzzi, 2002).

A protein unusually resistant to proteolysis has been evidenced and is required for infectivity without the intervention of any other component (Prusiner et al., 1984). Therefore, a single protease-resistant protein (PrP^{res}), component of the infectious agent (Prusiner, 1998), may be responsible for the transmission of TSEs. The infectious particle shares an identical amino acid sequence with PrP^{C} (Oesch et al., 1985; Basler et al., 1986) suggesting that PrP^{res} is an abnomal conformer of PrP^{C} with distinctive properties (Prusiner et al., 1984).

Several hypotheses postulate the nature of the infectious particle. In the virino hypothesis, (Kimberlin and Wilesmith, 1994) the infectious agent consists of an essential scrapie-specific nucleic acid associated with PrP^{C}. Nevertheless, no evidence for TSE-specific nucleic acids has yet been obtained (Safar et al., 2005). The protein-only hypothesis (Griffith, 1967; Weissmann, 1991; Prusiner, 1998) is currently the most widely accepted. In this hypothesis, posttranslational modifications of the α-helical structure of PrP^{C} into a β-sheet structure results in the production of PrP^{res} from host PrP^{C} (Baldwin et al., 1994). This explains the capacity of PrP^{res} to form protease-resistant aggregates which in turn accumulate within the brain (Ross and Poirier, 2004). *Prnp* knockout mice, devoid of prion protein, are resistant (Sailer et al., 1994) to infection with pathogenic PrP^{res} and reintroduction of *Prnp* restores infectibility and prion pathogenesis in these mice (Aguzzi and Polymenidou, 2004). This suggests that the presence of endogenous PrP^{C} is essential for the development of the disease.

The mechanism of infection and propagation might involve a catalytic cascade where infection with PrP^{res} or conversion of PrP^{C} into PrP^{res} leads to further conversion of PrP^{C} into PrP^{res}. The newly formed PrP^{res} will in turn convert a new PrP^{C} molecule into a proteinase K-resistant entity.

2.2 Molecular and cellular basis of neurodegeneration in prion diseases

2.2.1 Apoptosis

Hypothalamic cell lines infected by scrapie prions develop features of apoptosis such as DNA fragmentation and activation of caspases (Schatzl et al., 1997; Unterberger et al., 2005). In addition, activation of the JNK pathway has been demonstrated (Carimalo et al., 2005),

suggesting that this pathway may be involved in prion-induced neuronal death. In addition, the expression of Fas-L, Bcl-2, BAX, and active caspase-3 are modified in Purkinje cells of human CJD cerebellum (Puig and Ferrer, 2001). An immunohistochemical study shows overexpression of BAX, but not caspase-3 in scrapie-infected sheep (Lyahyai et al., 2006). This suggests that although apoptosis is a relevant cell death pathway in prion disease, it is probably not the exclusive pathway.

2.2.2 Autophagy

The accumulation autophagic vacuoles in TSEs has been described (Liberski et al., 2004; 2008) and may result from intraneuronal accumulation of PrP^{res}. This suggests that accumulation of PrP^{res} may lead to localized sequestration and phagocytosis of neuronal cytoplasm and ultimately to neuronal loss (Jeffrey et al., 1992).

2.2.3 Synaptic and dendritic pathology

A progressive loss of dendritic spines has been reported in addition to dendritic atrophy in CJD brains (Fraser, 2002). Notch-1, an inhibitor of dendritic growth and maturation, is increased and correlates with regressive dendritic changes, suggesting that Notch-1 could be a mediator of this process (Ishikura et al., 2005). The resulting loss of synapses and dendritic spines may isolate neurons from electrical stimuli and trophic factors, which could trigger self-destructive mechanisms (Fraser, 2002; Unterberger et al., 2005) and is probably BAX-independent (Chiesa et al., 2005). This loss of dendritic spines starts with the emergence of dendritic varicosities at sites where spines protrude from the dendrite (Fuhrmann et al., 2007).

References

1. Adams JM, Cory S. 1998. The Bcl-2 protein family: arbiters of cell survival. Science 281(5381):1322-1326.

2. Aguzzi A, Polymenidou M. 2004. Mammalian prion biology: one century of evolving concepts. Cell 116(2):313-327.

3. Aguzzi A, Sigurdson C, Heikenwaelder M. 2008. Molecular mechanisms of prion pathogenesis. Annu Rev Pathol 3:11-40.

4. Ahmed A, Eickholt BJ. 2007. Intracellular kinases in semaphorin signaling. Adv Exp Med Biol 600:24-37.

5. Ajima A, Hensch T, Kado RT, Ito M. 1991. Differential blocking action of Joro spider toxin analog on parallel fiber and climbing fiber synapses in cerebellar Purkinje cells. Neurosci Res 12(1):281-286.

6. Al Bersaoui R, Robert I, Lutz Y, Blanc F, Sommermeyer-Leroux G, Shibaguchi H, Aunis D, Fuchs JP. 2005. Purkinje-cell degeneration in prion protein-deficient mice is associated with a cerebellum-specific Doppel protein species signature. FEBS Letters 579(12):2715-2721.

7. Alper T. 1985. Scrapie agent unlike viruses in size and susceptibility to inactivation by ionizing or ultraviolet radiation. Nature 317(6039):750.

8. Altman J. 1972. Postnatal development of the cerebellar cortex in the rat. 3. Maturation of the components of the granular layer. J Comp Neurol 145(4):465-513.

9. Altman J. 1975. Postnatal development of the cerebellar cortex in the rat. IV. Spatial organization of bipolar cells, parallel fibers and glial palisades. J Comp Neurol 163(4):427-447.

10. Altman J, Bayer SA. 1978. Prenatal development of the cerebellar system in the rat. I. Cytogenesis and histogenesis of the deep nuclei and the cortex of the cerebellum. J Comp Neurol 179(1):23-48.

11. Altman J, Bayer SA. 1997. Development of the cerebellar system in relation to its evolution, structure, and function New york(CRC Press):783.

12. Andersson G, Armstrong DM. 1987. Complex spikes in Purkinje cells in the lateral vermis (b zone) of the cat cerebellum during locomotion. J Physiol 385:107-134.

13. Aoki E, Semba R, Kashiwamata S. 1986. New candidates for GABAergic neurons in the rat cerebellum: an immunocytochemical study with anti-GABA antibody. Neurosci Lett 68(3):267-271.

14. Araki K, Meguro H, Kushiya E, Takayama C, Inoue Y, Mishina M. 1993. Selective expression of the glutamate receptor channel delta 2 subunit in cerebellar Purkinje cells. Biochem Biophys Res Commun 197(3):1267-1276.

15. Armengol JA, Sotelo C. 1991. Early dendritic development of Purkinje cells in the rat cerebellum. A light and electron microscopic study using axonal tracing in 'in vitro' slices. Brain Res Dev Brain Res 64(1-2):95-114.

16. Arsenio Nunes ML, Sotelo C. 1985. Development of the spinocerebellar system in the postnatal rat. J Comp Neurol 237(3):291-306.

17. Arsenio Nunes ML, Sotelo C, Wehrle R. 1988. Organization of spinocerebellar projection map in three types of agranular cerebellum: Purkinje cells vs. granule cells as organizer element. J Comp Neurol 273(1):120-136.

18. Atarashi R, Sakaguchi S, Shigematsu K, Arima K, Okimura N, Yamaguchi N, Li A, Kopacek J, Katamine S. 2001. Abnormal activation of glial cells in the brains of prion protein-deficient mice ectopically expressing prion protein-like protein, PrPLP/Dpl. Mol Med 7(12):803-809.

19. Atarashi R, Nishida N, Shigematsu K, Goto S, Kondo T, Sakaguchi S, Katamine S. 2003. Deletion of N-terminal residues 23-88 from prion protein (PrP) abrogates the potential to rescue PrP-deficient mice from PrP-like protein/doppel-induced Neurodegeneration. J Biol Chem 278(31):28944-28949.

20. Azizi SA, Woodward DJ. 1987. Inferior olivary nuclear complex of the rat: morphology and comments on the principles of organization within the olivocerebellar system. J Comp Neurol 263(4):467-484.

21. Azzalin A, Del Vecchio I, Chiarelli LR, Valentini G, Comincini S, Ferretti L. 2005. Absence of interaction between doppel and GFAP, Grb2, PrPc proteins in human tumor astrocytic cells. Anticancer Research 25(6B):4369-4374.

22. Azzalin A, Del Vecchio I, Ferretti L, Comincini S. 2006. The prion-like protein Doppel (Dpl) interacts with the human receptor for activated C-kinase 1 (RACK1) protein. Anticancer Research 26(6B):4539-4547.

23. Bachelder RE, Wendt MA, Fujita N, Tsuruo T, Mercurio AM. 2001. The cleavage of Akt/protein kinase B by death receptor signaling is an important event in detachment-induced apoptosis. J Biol Chem 276(37):34702-34707.

24. Bailly Y, Schoen SW, Delhaye-Bouchaud N, Kreutzberg GW, Mariani J. 1995. 5'-nucleotidase activity as a synaptic marker of parasagittal compartmentation in the mouse cerebellum. J Neurocytol 24(11):879-890.

25. Bailly Y, Kyriakopoulou K, Delhaye-Bouchaud N, Mariani J, Karagogeos D. 1996. Cerebellar granule cell differentiation in mutant and X-irradiated rodents revealed by the neural adhesion molecule TAG-1. J Comp Neurol 369(1):150-161.

26. Bailly Y, Haeberle AM, Blanquet-Grossard F, Chasserot-Golaz S, Grant N, Schulze T, Bombarde G, Grassi J, Cesbron JY, Lemaire-Vieille C. 2004. Prion protein (PrPc) immunocytochemistry and expression of the green fluorescent protein reporter gene under control of the bovine PrP gene promoter in the mouse brain. J Comp Neurol 473(2):244-269.

27. Baldwin MA, Pan KM, Nguyen J, Huang Z, Groth D, Serban A, Gasset M, Mehlhorn I, Fletterick RJ, Cohen FE, et al. 1994. Spectroscopic characterization of conformational differences

between PrPC and PrPSc: an alpha-helix to beta-sheet transition. Philos Trans R Soc Lond B Biol Sci 343(1306):435-441.

28. Basler K, Oesch B, Scott M, Westaway D, Walchli M, Groth DF, McKinley MP, Prusiner SB, Weissmann C. 1986. Scrapie and cellular PrP isoforms are encoded by the same chromosomal gene. Cell 46(3):417-428.

29. Basu A, Haldar S. 2003. Identification of a novel Bcl-xL phosphorylation site regulating the sensitivity of taxol- or 2-methoxyestradiol-induced apoptosis. FEBS Lett 538(1-3):41-47.

30. Baurle J, Kranda K, Frischmuth S. 2006. On the variety of cell death pathways in the Lurcher mutant mouse. Acta Neuropathol 112(6):691-702.

31. Becker EB, Howell J, Kodama Y, Barker PA, Bonni A. 2004. Characterization of the c-Jun N-terminal kinase-BimEL signaling pathway in neuronal apoptosis. J Neurosci 24(40):8762-8770.

32. Behl C, Davis JB, Lesley R, Schubert D. 1994. Hydrogen peroxide mediates amyloid beta protein toxicity. Cell 77(6):817-827.

33. Behrens A, Aguzzi A. 2002. Small is not beautiful: antagonizing functions for the prion protein PrP(C) and its homologue Dpl. Trends Neurosci 25(3):150-154.

34. Behrens A, Genoud N, Naumann H, Rulicke T, Janett F, Heppner FL, Ledermann B, Aguzzi A. 2002. Absence of the prion protein homologue Doppel causes male sterility. Embo J 21(14):3652-3658.

35. Berciano J, Berciano MT, Polo JM, Figols J, Ciudad J, Lafarga M. 1990. Creutzfeldt-Jakob disease with severe involvement of cerebral white matter and cerebellum. Virchows Arch A Pathol Anat Histopathol 417(6):533-538.

36. Berry M, Bradley P. 1976. The growth of the dendritic trees of Purkinje cells in the cerebellum of the rat. Brain Res 112(1):1-35.

37. Bi X, Liao G. 2007. Autophagic-lysosomal dysfunction and neurodegeneration in Niemann-Pick Type C mice: lipid starvation or indigestion? Autophagy 3(6):646-648.

38. Bjorkoy G, Lamark T, Brech A, Outzen H, Perander M, Overvatn A, Stenmark H, Johansen T. 2005. p62/SQSTM1 forms protein aggregates degraded by autophagy and has a protective effect on huntingtin-induced cell death. J Cell Biol 171(4):603-614.

39. Blatt GJ, Eisenman LM. 1985. A qualitative and quantitative light microscopic study of the inferior olivary complex of normal, reeler, and weaver mutant mice. J Comp Neurol 232(1):117-128.

40. Blommaart EF, Luiken JJ, Meijer AJ. 1997a. Autophagic proteolysis: control and specificity. Histochemical Journal 29(5):365-385.

41. Blommaart EF, Krause U, Schellens JP, Vreeling-Sindelarova H, Meijer AJ. 1997b. The phosphatidylinositol 3-kinase inhibitors wortmannin and LY294002 inhibit autophagy in isolated rat hepatocytes. European Journal of Biochemistry 243(1-2):240-246.

42. Bobee S, Mariette E, Tremblay-Leveau H, Caston J. 2000. Effects of early midline cerebellar lesion on cognitive and emotional functions in the rat. Behav Brain Res 112(1-2):107-117.

43. Bolton DC, McKinley MP, Prusiner SB. 1982. Identification of a protein that purifies with the scrapie prion. Science 218(4579):1309-1311.

44. Bounhar Y, Zhang Y, Goodyer CG, LeBlanc A. 2001. Prion protein protects human neurons against Bax-mediated apoptosis. J Biol Chem 276(42):39145-39149.

45. Bounhar Y, Mann KK, Roucou X, LeBlanc AC. 2006. Prion protein prevents Bax-mediated cell death in the absence of other Bcl-2 family members in Saccharomyces cerevisiae. FEMS Yeast Res 6(8):1204-1212.

46. Bourrat F, Sotelo C. 1991. Relationships between neuronal birthdates and cytoarchitecture in the rat inferior olivary complex. J Comp Neurol 313(3):509-521.

47. Boya P, Gonzalez-Polo RA, Casares N, Perfettini JL, Dessen P, Larochette N, Metivier D, Meley D, Souquere S, Yoshimori T, Pierron G, Codogno P, Kroemer G. 2005. Inhibition of macroautophagy triggers apoptosis. Mol Cell Biol 25(3):1025-1040.

48. Breckenridge DG, Germain M, Mathai JP, Nguyen M, Shore GC. 2003. Regulation of apoptosis by endoplasmic reticulum pathways. Oncogene 22(53):8608-8618.

49. Brini M, Miuzzo M, Pierobon N, Negro A, Sorgato MC. 2005. The prion protein and its paralogue Doppel affect calcium signaling in Chinese hamster ovary cells. Molecular Biology of the Cell 16(6):2799-2808.

50. Brockie PJ, Maricq AV. 2006. Ionotropic glutamate receptors: genetics, behavior and electrophysiology. WormBook:1-16.

51. Brown DR, Qin K, Herms JW, Madlung A, Manson J, Strome R, Fraser PE, Kruck T, von Bohlen A, Schulz-Schaeffer W, Giese A, Westaway D, Kretzschmar H. 1997a. The cellular prion protein binds copper in vivo. Nature 390(6661):684-687.

52. Brown DR, Schulz-Schaeffer WJ, Schmidt B, Kretzschmar HA. 1997b. Prion protein-deficient cells show altered response to oxidative stress due to decreased SOD-1 activity. Exp Neurol 146(1):104-112.

53. Brown DR, Schmidt B, Kretzschmar HA. 1998. Effects of copper on survival of prion protein knockout neurons and glia. J Neurochem 70(4):1686-1693.

54. Brown DR, Wong BS, Hafiz F, Clive C, Haswell SJ, Jones IM. 1999. Normal prion protein has an activity like that of superoxide dismutase. Biochem J 344 Pt 1:1-5.

55. Brown DR, Clive C, Haswell SJ. 2001. Antioxidant activity related to copper binding of native prion protein. J Neurochem 76(1):69-76.

56. Brown DR, Nicholas RS, Canevari L. 2002. Lack of prion protein expression results in a neuronal phenotype sensitive to stress. J Neurosci Res 67(2):211-224.

57. Bueler H, Fischer M, Lang Y, Bluethmann H, Lipp HP, DeArmond SJ, Prusiner SB, Aguet M, Weissmann C. 1992. Normal development and behaviour of mice lacking the neuronal cell-surface PrP protein. Nature 356(6370):577-582.

58. Bueler H, Aguzzi A, Sailer A, Greiner RA, Autenried P, Aguet M, Weissmann C. 1993. Mice devoid of PrP are resistant to scrapie. Cell 73(7):1339-1347.

59. Caetano FA, Lopes MH, Hajj GN, Machado CF, Pinto Arantes C, Magalhaes AC, Vieira Mde P, Americo TA, Massensini AR, Priola SA, Vorberg I, Gomez MV, Linden R, Prado VF, Martins VR, Prado MA. 2008. Endocytosis of prion protein is required for ERK1/2 signaling induced by stress-inducible protein 1. J Neurosci 28(26):6691-6702.

60. Calissano M, Ensor E, Brown DR, Latchman DS. 2004. Doppel expression is regulated by the Brn-3a and Brn-3b transcription factors. Neuroreport 15(3):483-486.

61. Campbell NC, Armstrong DM. 1983. Topographical localization in the olivocerebellar projection in the rat: an autoradiographic study. Brain Res 275(2):235-249.

62. Canu N, Tufi R, Serafino AL, Amadoro G, Ciotti MT, Calissano P. 2005. Role of the autophagic-lysosomal system on low potassium-induced apoptosis in cultured cerebellar granule cells. J Neurochem 92(5):1228-1242.

63. Cao Y, Espinola JA, Fossale E, Massey AC, Cuervo AM, MacDonald ME, Cotman SL. 2006. Autophagy is disrupted in a knock-in mouse model of juvenile neuronal ceroid lipofuscinosis. J Biol Chem 281(29):20483-20493.

64. Carimalo J, Cronier S, Petit G, Peyrin JM, Boukhtouche F, Arbez N, Lemaigre-Dubreuil Y, Brugg B, Miquel MC. 2005. Activation of the JNK-c-Jun pathway during the early phase of neuronal apoptosis induced by PrP106-126 and prion infection. Eur J Neurosci 21(9):2311-2319.

65. Carleton A, Tremblay P, Vincent JD, Lledo PM. 2001. Dose-dependent, prion protein (PrP)-mediated facilitation of excitatory synaptic transmission in the mouse hippocampus. Pflugers Arch 442(2):223-229.

66. Caston J, Vasseur F, Stelz T, Chianale C, Delhaye-Bouchaud N, Mariani J. 1995. Differential roles of cerebellar cortex and deep cerebellar nuclei in the learning of the equilibrium behavior: studies in intact and cerebellectomized lurcher mutant mice. Brain Res Dev Brain Res 86(1-2):311-316.

67. Caughey B, Race RE, Ernst D, Buchmeier MJ, Chesebro B. 1989. Prion protein biosynthesis in scrapie-infected and uninfected neuroblastoma cells. J Virol 63(1):175-181.

68. Caughey B, Raymond GJ. 1991. The scrapie-associated form of PrP is made from a cell surface precursor that is both protease- and phospholipase-sensitive. J Biol Chem 266(27):18217-18223.

69. Caviness VS, Jr., Rakic P. 1978. Mechanisms of cortical development: a view from mutations in mice. Annu Rev Neurosci 1:297-326.

70. Cecconi F, Alvarez-Bolado G, Meyer BI, Roth KA, Gruss P. 1998. Apaf1 (CED-4 homolog) regulates programmed cell death in mammalian development. Cell 94(6):727-737.

71. Cesa R, Morando L, Strata P. 2003. Glutamate receptor delta2 subunit in activity-dependent heterologous synaptic competition. J Neurosci 23(6):2363-2370.

72. Chan-Palay V, Palay SL, Brown JT, Van Itallie C. 1977. Sagittal organization of olivocerebellar and reticulocerebellar projections: autoradiographic studies with 35S-methionine. Exp Brain Res 30(4):561-576.

73. Chedotal A, Sotelo C. 1992. Early Development of Olivocerebellar Projections in the Fetal Rat Using CGRP Immunocytochemistry. Eur J Neurosci 4(11):1159-1179.

74. Chedotal A, Sotelo C. 1993. The 'creeper stage' in cerebellar climbing fiber synaptogenesis precedes the 'pericellular nest'--ultrastructural evidence with parvalbumin immunocytochemistry. Brain Res Dev Brain Res 76(2):207-220.

75. Cheng EH, Wei MC, Weiler S, Flavell RA, Mak TW, Lindsten T, Korsmeyer SJ. 2001. BCL-2, BCL-X(L) sequester BH3 domain-only molecules preventing BAX- and BAK-mediated mitochondrial apoptosis. Molecular Cell 8(3):705-711.

76. Cheng SS, Heintz N. 1997. Massive loss of mid- and hindbrain neurons during embryonic development of homozygous lurcher mice. J Neurosci 17(7):2400-2407.

77. Chiesa R, Piccardo P, Dossena S, Nowoslawski L, Roth KA, Ghetti B, Harris DA. 2005. Bax deletion prevents neuronal loss but not neurological symptoms in a transgenic model of inherited prion disease. Proc Natl Acad Sci U S A 102(1):238-243.

78. Chinnaiyan AM, O'Rourke K, Tewari M, Dixit VM. 1995. FADD, a novel death domain-containing protein, interacts with the death domain of Fas and initiates apoptosis. Cell 81(4):505-512.

79. Chinnaiyan AM, Tepper CG, Seldin MF, O'Rourke K, Kischkel FC, Hellbardt S, Krammer PH, Peter ME, Dixit VM. 1996. FADD/MORT1 is a common mediator of CD95 (Fas/APO-1) and tumor necrosis factor receptor-induced apoptosis. J Biol Chem 271(9):4961-4965.

80. Chowdhury I, Tharakan B, Bhat GK. 2006. Current concepts in apoptosis: the physiological suicide program revisited. Cell Mol Biol Lett 11(4):506-525.

81. Chu CT. 2006. Autophagic stress in neuronal injury and disease. J Neuropathol Exp Neurol 65(5):423-432.

82. Cleveland DW. 1999. From Charcot to SOD1: mechanisms of selective motor neuron death in ALS. Neuron 24(3):515-520.

83. Codogno P, Meijer AJ. 2005. Autophagy and signaling: their role in cell survival and cell death. Cell Death Differ 12 Suppl 2:1509-1518.

84. Coitinho AS, Freitas AR, Lopes MH, Hajj GN, Roesler R, Walz R, Rossato JI, Cammarota M, Izquierdo I, Martins VR, Brentani RR. 2006. The interaction between prion protein and laminin modulates memory consolidation. Eur J Neurosci 24(11):3255-3264.

85. Coitinho AS, Lopes MH, Hajj GN, Rossato JI, Freitas AR, Castro CC, Cammarota M, Brentani RR, Izquierdo I, Martins VR. 2007. Short-term memory formation and long-term memory consolidation are enhanced by cellular prion association to stress-inducible protein 1. Neurobiol Dis 26(1):282-290.

86. Coleman ML, Sahai EA, Yeo M, Bosch M, Dewar A, Olson MF. 2001. Membrane blebbing during apoptosis results from caspase-mediated activation of ROCK I. Nat Cell Biol 3(4):339-345.

87. Colling SB, Collinge J, Jefferys JG. 1996. Hippocampal slices from prion protein null mice: disrupted Ca(2+)-activated K+ currents. Neurosci Lett 209(1):49-52.

88. Collinge J, Whittington MA, Sidle KC, Smith CJ, Palmer MS, Clarke AR, Jefferys JG. 1994. Prion protein is necessary for normal synaptic function. Nature 370(6487):295-297.

89. Cooper SE, Martin JH, Ghez C. 2000. Effects of inactivation of the anterior interpositus nucleus on the kinematic and dynamic control of multijoint movement. J Neurophysiol 84(4):1988-2000.

90. Coulpier M, Messiaen S, Hamel R, Fernandez de Marco M, Lilin T, Eloit M. 2006. Bax deletion does not protect neurons from BSE-induced death. Neurobiol Dis 23(3):603-611.

91. Courville J, Faraco-Cantin F. 1978. On the origin of the climbing fibers of the cerebellum. An experimental study in the cat with an autoradiographic tracing method. Neuroscience 3(9):797-809.

92. Crepel F, Mariani J, Delhaye-Bouchaud N. 1976. Evidence for a multiple innervation of Purkinje cells by climbing fibers in the immature rat cerebellum. J Neurobiol 7(6):567-578.

93. Crepel F, Delhaye-Bouchaud N, Dupont JL. 1981. Fate of the multiple innervation of cerebellar Purkinje cells by climbing fibers in immature control, x-irradiated and hypothyroid rats. Brain Res 227(1):59-71.

94. Cui T, Holme A, Sassoon J, Brown DR. 2003. Analysis of doppel protein toxicity. Mol Cell Neurosci 23(1):144-155.

95. D'Arcangelo G, Miao GG, Chen SC, Soares HD, Morgan JI, Curran T. 1995. A protein related to extracellular matrix proteins deleted in the mouse mutant reeler. Nature 374(6524):719-723.

96. Dahhaoui M, Caston J, Auvray N, Reber A. 1990. Role of the cerebellum in an avoidance conditioning task in the rat. Physiol Behav 47(6):1175-1180.

97. Day NC, Shaw PJ, McCormack AL, Craig PJ, Smith W, Beattie R, Williams TL, Ellis SB, Ince PG, Harpold MM, Lodge D, Volsen SG. 1996. Distribution of alpha 1A, alpha 1B and alpha 1E voltage-dependent calcium channel subunits in the human hippocampus and parahippocampal gyrus. Neuroscience 71(4):1013-1024.

98. De Duve C, Pressman BC, Gianetto R, Wattiaux R, Appelmans F. 1955. Tissue fractionation studies. 6. Intracellular distribution patterns of enzymes in rat-liver tissue. Biochem J 60(4):604-617.

99. De Zeeuw CI, Yeo CH. 2005. Time and tide in cerebellar memory formation. Curr Opin Neurobiol 15(6):667-674.

100. Deak JC, Cross JV, Lewis M, Qian Y, Parrott LA, Distelhorst CW, Templeton DJ. 1998. Fas-induced proteolytic activation and intracellular redistribution of the stress-signaling kinase MEKK1. Proc Natl Acad Sci U S A 95(10):5595-5600.

101. Degterev A, Boyce M, Yuan J. 2003. A decade of caspases. Oncogene 22(53):8543-8567.

102. Desclin JC. 1974. Histological evidence supporting the inferior olive as the major source of cerebellar climbing fibers in the rat. Brain Res 77(3):365-384.

103. Dickie M. 1966. New mutations Mouse news lett (34):30.

104. Diskin T, Tal-Or P, Erlich S, Mizrachy L, Alexandrovich A, Shohami E, Pinkas-Kramarski R. 2005. Closed head injury induces upregulation of Beclin 1 at the cortical site of injury. J Neurotrauma 22(7):750-762.

105. Ditsworth D, Zong WX, Thompson CB. 2007. Activation of poly(ADP)-ribose polymerase (PARP-1) induces release of the pro-inflammatory mediator HMGB1 from the nucleus. J Biol Chem 282(24):17845-17854.

106. Djavaheri-Mergny M, Amelotti M, Mathieu J, Besancon F, Bauvy C, Souquere S, Pierron G, Codogno P. 2006. NF-kappaB activation represses tumor necrosis factor-alpha-induced autophagy. J Biol Chem 281(41):30373-30382.

107. Djavaheri-Mergny M, Amelotti M, Mathieu J, Besancon F, Bauvy C, Codogno P. 2007. Regulation of autophagy by NFkappaB transcription factor and reactives oxygen species. Autophagy 3(4):390-392.

108. Dorandeu A, Wingertsmann L, Chretien F, Delisle MB, Vital C, Parchi P, Montagna P, Lugaresi E, Ironside JW, Budka H, Gambetti P, Gray F. 1998. Neuronal apoptosis in fatal familial insomnia. Brain Pathol 8(3):531-537.

109. Doughty ML, De Jager PL, Korsmeyer SJ, Heintz N. 2000. Neurodegeneration in Lurcher mice occurs via multiple cell death pathways. J Neurosci 20(10):3687-3694.

110. Dove LS, Nahm SS, Murchison D, Abbott LC, Griffith WH. 2000. Altered calcium homeostasis in cerebellar Purkinje cells of leaner mutant mice. J Neurophysiol 84(1):513-524.

111. Dron M, Bailly Y, Beringue V, Haeberle AM, Griffond B, Risold PY, Tovey MG, Laude H, Dandoy-Dron F. 2005. Scrg1 is induced in TSE and brain injuries, and associated with autophagy. Eur J Neurosci 22(1):133-146.

112. Duchala CS, Shick HE, Garcia J, Deweese DM, Sun X, Stewart VJ, Macklin WB. 2004. The toppler mouse: a novel mutant exhibiting loss of Purkinje cells. J Comp Neurol 476(2):113-129.

113. Dusart I, Guenet JL, Sotelo C. 2006. Purkinje cell death: differences between developmental cell death and neurodegenerative death in mutant mice. Cerebellum 5(2):163-173.

114. Eccles JC, Llinas R, Sasaki K. 1966a. The mossy fibre-granule cell relay of the cerebellum and its inhibitory control by Golgi cells. Exp Brain Res 1(1):82-101.

115. Eccles JC, Llinas R, Sasaki K. 1966b. The excitatory synaptic action of climbing fibres on the purinje cells of the cerebellum. J Physiol 182(2):268-296.

116. Eccles JC, Llinas R, Sasaki K. 1966c. The inhibitory interneurones within the cerebellar cortex. Exp Brain Res 1(1):1-16.

117. Eisenman LM, Schalekamp MP, Voogd J. 1991. Development of the cerebellar cortical efferent projection: an in-vitro anterograde tracing study in rat brain slices. Brain Res Dev Brain Res 60(2):261-266.

118. Enari M, Sakahira H, Yokoyama H, Okawa K, Iwamatsu A, Nagata S. 1998. A caspase-activated DNase that degrades DNA during apoptosis, and its inhibitor ICAD. Nature 391(6662):43-50.

119. Eskelinen EL, Illert AL, Tanaka Y, Schwarzmann G, Blanz J, Von Figura K, Saftig P. 2002. Role of LAMP-2 in lysosome biogenesis and autophagy. Mol Biol Cell 13(9):3355-3368.

120. Fairbairn DW, Carnahan KG, Thwaits RN, Grigsby RV, Holyoak GR, O'Neill KL. 1994. Detection of apoptosis induced DNA cleavage in scrapie-infected sheep brain. FEMS Microbiol Lett 115(2-3):341-346.

121. Fan H, Favero M, Vogel MW. 2001. Elimination of Bax expression in mice increases cerebellar purkinje cell numbers but not the number of granule cells. J Comp Neurol 436(1):82-91.

122. Fehrenbach RA, Wallesch CW, Claus D. 1984. Neuropsychologic findings in Friedreich's ataxia. Arch Neurol 41(3):306-308.

123. Ferguson JB, Andrews JR, Voynick IM, Fruton JS. 1973. The specificity of cathepsin D. J Biol Chem 248(19):6701-6708.

124. Fernandez-Gonzalez A, La Spada AR, Treadaway J, Higdon JC, Harris BS, Sidman RL, Morgan JI, Zuo J. 2002. Purkinje cell degeneration (pcd) phenotypes caused by mutations in the axotomy-induced gene, Nna1. Science 295(5561):1904-1906.

125. Filimonenko M, Stuffers S, Raiborg C, Yamamoto A, Malerod L, Fisher EM, Isaacs A, Brech A, Stenmark H, Simonsen A. 2007. Functional multivesicular bodies are required for autophagic clearance of protein aggregates associated with neurodegenerative disease. J Cell Biol 179(3):485-500.

126. Flechsig E, Hegyi I, Leimeroth R, Zuniga A, Rossi D, Cozzio A, Schwarz P, Rulicke T, Gotz J, Aguzzi A, Weissmann C. 2003. Expression of truncated PrP targeted to Purkinje cells of PrP knockout mice causes Purkinje cell death and ataxia. Embo J 22(12):3095-3101.

127. Ford MJ, Burton LJ, Morris RJ, Hall SM. 2002. Selective expression of prion protein in peripheral tissues of the adult mouse. Neuroscience 113(1):177-192.

128. Forloni G, Bugiani O, Tagliavini F, Salmona M. 1996. Apoptosis-mediated neurotoxicity induced by beta-amyloid and PrP fragments. Mol Chem Neuropathol 28(1-3):163-171.

129. Fournier JG, Escaig-Haye F, Billette de Villemeur T, Robain O. 1995. Ultrastructural localization of cellular prion protein (PrPc) in synaptic boutons of normal hamster hippocampus. C R Acad Sci III 318(3):339-344.

130. Frank-Cannon TC, Zeve DR, Abbott LC. 2007. Developmental expression of neuronal nitric oxide synthase in P/Q-type voltage-gated calcium ion channel mutant mice, leaner and tottering. Brain Res 1140:96-104.

131. Frank TC, Nunley MC, Sons HD, Ramon R, Abbott LC. 2003. Fluoro-jade identification of cerebellar granule cell and purkinje cell death in the alpha1A calcium ion channel mutant mouse, leaner. Neuroscience 118(3):667-680.

132. Fraser JR. 2002. What is the basis of transmissible spongiform encephalopathy induced neurodegeneration and can it be repaired? Neuropathol Appl Neurobiol 28(1):1-11.

133. Frischmuth S, Kranda K, Baurle J. 2006. Translocation of cytochrome c during cerebellar degeneration in Lurcher and weaver mutant mice. Brain Res Bull 71(1-3):139-148.

134. Fuhrmann M, Mitteregger G, Kretzschmar H, Herms J. 2007. Dendritic pathology in prion disease starts at the synaptic spine. J Neurosci 27(23):6224-6233.

135. Fukutani Y, Cairns NJ, Rossor MN, Lantos PL. 1996. Purkinje cell loss and astrocytosis in the cerebellum in familial and sporadic Alzheimer's disease. Neurosci Lett 214(1):33-36.

136. Gains MJ, Roth KA, LeBlanc AC. 2006. Prion protein protects against ethanol-induced Bax-mediated cell death in vivo. Neuroreport 17(9):903-906.

137. Galvan C, Camoletto PG, Dotti CG, Aguzzi A, Ledesma MD. 2005. Proper axonal distribution of PrP(C) depends on cholesterol-sphingomyelin-enriched membrane domains and is developmentally regulated in hippocampal neurons. Mol Cell Neurosci 30(3):304-315.

138. Garnett AP, Viles JH. 2003. Copper binding to the octarepeats of the prion protein. Affinity, specificity, folding, and cooperativity: insights from circular dichroism. J Biol Chem 278(9):6795-6802.

139. Gauczynski S, Peyrin JM, Haik S, Leucht C, Hundt C, Rieger R, Krasemann S, Deslys JP, Dormont D, Lasmezas CI, Weiss S. 2001. The 37-kDa/67-kDa laminin receptor acts as the cell-surface receptor for the cellular prion protein. Embo J 20(21):5863-5875.

140. Genoud N, Behrens A, Miele G, Robay D, Heppner FL, Freigang S, Aguzzi A. 2004. Disruption of Doppel prevents neurodegeneration in mice with extensive Prnp deletions. Proc Natl Acad Sci U S A 101(12):4198-4203.

141. German DC, Quintero EM, Liang CL, Ng B, Punia S, Xie C, Dietschy JM. 2001. Selective neurodegeneration, without neurofibrillary tangles, in a mouse model of Niemann-Pick C disease. J Comp Neurol 433(3):415-425.

142. Gillardon F, Baurle J, Grusser-Cornehls U, Zimmermann M. 1995a. DNA fragmentation and activation of c-Jun in the cerebellum of mutant mice (weaver, Purkinje cell degeneration). Neuroreport 6(13):1766-1768.

143. Gillardon F, Baurle J, Wickert H, Grusser-Cornehls U, Zimmermann M. 1995b. Differential regulation of bcl-2, bax, c-fos, junB, and krox-24 expression in the cerebellum of Purkinje cell degeneration mutant mice. J Neurosci Res 41(5):708-715.

144. Goffinet AM. 1983. The embryonic development of the inferior olivary complex in normal and reeler (rlORL) mutant mice. J Comp Neurol 219(1):10-24.

145. Goldowitz D, Hamre K. 1998. The cells and molecules that make a cerebellum. Trends Neurosci 21(9):375-382.

146. Gonzalez-Polo RA, Boya P, Pauleau AL, Jalil A, Larochette N, Souquere S, Eskelinen EL, Pierron G, Saftig P, Kroemer G. 2005. The apoptosis/autophagy paradox: autophagic vacuolization before apoptotic death. J Cell Sci 118(Pt 14):3091-3102.

147. Goodlett CR, Hamre KM, West JR. 1992. Dissociation of spatial navigation and visual guidance performance in Purkinje cell degeneration (pcd) mutant mice. Behav Brain Res 47(2):129-141.

148. Gounko NV, Gramsbergen A, van der Want JJ. 2007. The glutamate receptor delta 2 in relation to cerebellar development and plasticity. Neurosci Biobehav Rev 31(8):1095-1100.

149. Graner E, Mercadante AF, Zanata SM, Forlenza OV, Cabral AL, Veiga SS, Juliano MA, Roesler R, Walz R, Minetti A, Izquierdo I, Martins VR, Brentani RR. 2000. Cellular prion protein binds laminin and mediates neuritogenesis. Brain Res Mol Brain Res 76(1):85-92.

150. Griffith JS. 1967. Self-replication and scrapie. Nature 215(5105):1043-1044.

151. Griffith TS, Chin WA, Jackson GC, Lynch DH, Kubin MZ. 1998. Intracellular regulation of TRAIL-induced apoptosis in human melanoma cells. J Immunol 161(6):2833-2840.

152. Gross A, Jockel J, Wei MC, Korsmeyer SJ. 1998. Enforced dimerization of BAX results in its translocation, mitochondrial dysfunction and apoptosis. EMBO Journal 17(14):3878-3885.

153. Gross A, Yin XM, Wang K, Wei MC, Jockel J, Milliman C, Erdjument-Bromage H, Tempst P, Korsmeyer SJ. 1999. Caspase cleaved BID targets mitochondria and is required for cytochrome c release, while BCL-XL prevents this release but not tumor necrosis factor-R1/Fas death. Journal of Biological Chemistry 274(2):1156-1163.

154. Guenet JL, Sotelo C, Mariani J. 1983. Hyperspiny Purkinje cell, a new neurological mutation in the mouse. J Hered 74(2):105-108.

155. Guillery RW, Herrup K. 1997. Quantification without pontification: choosing a method for counting objects in sectioned tissues. J Comp Neurol 386(1):2-7.

156. Gutierrez MG, Munafo DB, Beron W, Colombo MI. 2004. Rab7 is required for the normal progression of the autophagic pathway in mammalian cells. J Cell Sci 117(Pt 13):2687-2697.

157. Hack I, Bancila M, Loulier K, Carroll P, Cremer H. 2002. Reelin is a detachment signal in tangential chain-migration during postnatal neurogenesis. Nat Neurosci 5(10):939-945.

158. Haeberle AM, Ribaut-Barassin C, Bombarde G, Mariani J, Hunsmann G, Grassi J, Bailly Y. 2000. Synaptic prion protein immuno-reactivity in the rodent cerebellum. Microsc Res Tech 50(1):66-75.

159. Hamann M, Rossi DJ, Mohr C, Andrade AL, Attwell D. 2005. The electrical response of cerebellar Purkinje neurons to simulated ischaemia. Brain 128(Pt 10):2408-2420.

160. Hamburger V, Levi-Montalcini R. 1949. Proliferation, differentiation and degeneration in the spinal ganglia of the chick embryo under normal and experimental conditions. J Exp Zool 111(3):457-501.

161. Hamilton BA, Frankel WN, Kerrebrock AW, Hawkins TL, FitzHugh W, Kusumi K, Russell LB, Mueller KL, van Berkel V, Birren BW, Kruglyak L, Lander ES. 1996. Disruption of the nuclear hormone receptor RORalpha in staggerer mice. Nature 379(6567):736-739.

162. Harding TM, Hefner-Gravink A, Thumm M, Klionsky DJ. 1996. Genetic and phenotypic overlap between autophagy and the cytoplasm to vacuole protein targeting pathway. J Biol Chem 271(30):17621-17624.

163. Harmey JH, Doyle D, Brown V, Rogers MS. 1995. The cellular isoform of the prion protein, PrPc, is associated with caveolae in mouse neuroblastoma (N2a) cells. Biochem Biophys Res Commun 210(3):753-759.

164. Harris DA, Lele P, Snider WD. 1993. Localization of the mRNA for a chicken prion protein by in situ hybridization. Proc Natl Acad Sci U S A 90(9):4309-4313.

165. Hashimoto K, Kano M. 2005. Postnatal development and synapse elimination of climbing fiber to Purkinje cell projection in the cerebellum. Neurosci Res 53(3):221-228.

166. Hauw JJ, Gray F, Baudrimont M, Escourolle R. 1981. Cerebellar changes in 50 cases of Creutzfeldt-Jakob disease with emphasis on granule cell atrophy variant. Acta Neuropathol Suppl 7:196-198.

167. Hawkes R, colonnier M, Leclerc N. 1985. Monoclonal antibodies reveal sagittal banding in the rodent cerebellar cortex. Brain Res 333(2):359-365.

168. Hayley S, Crocker SJ, Smith PD, Shree T, Jackson-Lewis V, Przedborski S, Mount M, Slack R, Anisman H, Park DS. 2004. Regulation of dopaminergic loss by Fas in a 1-methyl-4-phenyl-1,2,3,6-tetrahydropyridine model of Parkinson's disease. J Neurosci 24(8):2045-2053.

169. Heckroth JA, Goldowitz D, Eisenman LM. 1989. Purkinje cell reduction in the reeler mutant mouse: a quantitative immunohistochemical study. J Comp Neurol 279(4):546-555.

170. Hegde RS, Mastrianni JA, Scott MR, DeFea KA, Tremblay P, Torchia M, DeArmond SJ, Prusiner SB, Lingappa VR. 1998. A transmembrane form of the prion protein in neurodegenerative disease. Science 279(5352):827-834.

171. Heitz S, Lutz Y, Rodeau JL, Zanjani H, Gautheron V, Bombarde G, Richard F, Fuchs JP, Vogel MW, Mariani J, Bailly Y. 2007. BAX contributes to Doppel-induced apoptosis of prion-protein-deficient Purkinje cells. Developmental Neurobiology 67(5):670-686.

172. Heitz S, Gautheron V, Lutz Y, Rodeau JL, Zanjani HS, Sugihara I, Bombarde G, Richard F, Fuchs JP, Vogel MW, Mariani J, Bailly Y. 2008. BCL-2 counteracts Doppel-induced apoptosis of prion-protein-deficient Purkinje cells in the Ngsk Prnp(0/0) mouse. Dev Neurobiol 68(3):332-348.

173. Heitz S, Leschiera R, Haeberle AM, Demais V, Grant NJ, Bombarde G, Bailly Y. in review. Autophagy in Purkinje cells overexpressing Doppel in Ngsk Prnp-deficient mice. Brain Pathol.

174. Hendry IA. 1976. A method to correct adequately for the change in neuronal size when estimating neuronal numbers after nerve growth factor treatment. J Neurocytol 5(3):337-349.

175. Herms J, Tings T, Gall S, Madlung A, Giese A, Siebert H, Schurmann P, Windl O, Brose N, Kretzschmar H. 1999. Evidence of presynaptic location and function of the prion protein. J Neurosci 19(20):8866-8875.

176. Herms JW, Korte S, Gall S, Schneider I, Dunker S, Kretzschmar HA. 2000. Altered intracellular calcium homeostasis in cerebellar granule cells of prion protein-deficient mice. J Neurochem 75(4):1487-1492.

177. Herms JW, Tings T, Dunker S, Kretzschmar HA. 2001. Prion protein affects Ca2+-activated K+ currents in cerebellar purkinje cells. Neurobiol Dis 8(2):324-330.

178. Herrup K, Mullen RJ. 1979. Staggerer chimeras: intrinsic nature of Purkinje cell defects and implications for normal cerebellar development. Brain Res 178(2-3):443-457.

179. Herrup K, Wilczynski SL. 1982. Cerebellar cell degeneration in the leaner mutant mouse. Neuroscience 7(9):2185-2196.

180. Hickey MA, Chesselet MF. 2003. Apoptosis in Huntington's disease. Prog Neuropsychopharmacol Biol Psychiatry 27(2):255-265.

181. Hilber P, Jouen F, Delhaye-Bouchaud N, Mariani J, Caston J. 1998. Differential roles of cerebellar cortex and deep cerebellar nuclei in learning and retention of a spatial task: studies in intact and cerebellectomized lurcher mutant mice. Behav Genet 28(4):299-308.

182. Hilber P, Caston J. 2001. Motor skills and motor learning in Lurcher mutant mice during aging. Neuroscience 102(3):615-623.

183. Hirai H, Matsuda S. 1999. Interaction of the C-terminal domain of delta glutamate receptor with spectrin in the dendritic spines of cultured Purkinje cells. Neurosci Res 34(4):281-287.

184. Hirai H, Launey T, Mikawa S, Torashima T, Yanagihara D, Kasaura T, Miyamoto A, Yuzaki M. 2003. New role of delta2-glutamate receptors in AMPA receptor trafficking and cerebellar function. Nat Neurosci 6(8):869-876.

185. Hirano T, Kasono K, Araki K, Shinozuka K, Mishina M. 1994. Involvement of the glutamate receptor delta 2 subunit in the long-term depression of glutamate responsiveness in cultured rat Purkinje cells. Neurosci Lett 182(2):172-176.

186. Hironaka K, Umemori H, Tezuka T, Mishina M, Yamamoto T. 2000. The protein-tyrosine phosphatase PTPMEG interacts with glutamate receptor delta 2 and epsilon subunits. J Biol Chem 275(21):16167-16173.

187. Hofmann K, Bucher P, Tschopp J. 1997. The CARD domain: a new apoptotic signalling motif. Trends Biochem Sci 22(5):155-156.

188. Hollenbeck PJ. 1993. Products of endocytosis and autophagy are retrieved from axons by regulated retrograde organelle transport. J Cell Biol 121(2):305-315.

189. Horiuchi M, Ishiguro N, Nagasawa H, Toyoda Y, Shinagawa M. 1998. Genomic structure of the bovine PrP gene and complete nucleotide sequence of bovine PrP cDNA. Anim Genet 29(1):37-40.

190. Hundt C, Peyrin JM, Haik S, Gauczynski S, Leucht C, Rieger R, Riley ML, Deslys JP, Dormont D, Lasmezas CI, Weiss S. 2001. Identification of interaction domains of the prion protein with its 37-kDa/67-kDa laminin receptor. Embo J 20(21):5876-5886.

191. Hung AY, Sheng M. 2002. PDZ domains: structural modules for protein complex assembly. J Biol Chem 277(8):5699-5702.

192. Hussein MR, Haemel AK, Wood GS. 2003. Apoptosis and melanoma: molecular mechanisms. J Pathol 199(3):275-288.

193. Ichikawa R, Miyazaki T, Kano M, Hashikawa T, Tatsumi H, Sakimura K, Mishina M, Inoue Y, Watanabe M. 2002. Distal extension of climbing fiber territory and multiple innervation caused by aberrant wiring to adjacent spiny branchlets in cerebellar Purkinje cells lacking glutamate receptor delta 2. J Neurosci 22(19):8487-8503.

194. Ikeno K, Yamakura T, Yamazaki M, Sakimura K. 2001. The Lurcher mutation reveals Ca(2+) permeability and PKC modification of the GluRdelta channels. Neurosci Res 41(2):193-200.

195. Ino H. 2004. Immunohistochemical characterization of the orphan nuclear receptor ROR alpha in the mouse nervous system. J Histochem Cytochem 52(3):311-323.

196. Inouye M, Oda SI. 1980. Strain-specific variations in the folial pattern of the mouse cerebellum. J Comp Neurol 190(2):357-362.

197. Irmler M, Thome M, Hahne M, Schneider P, Hofmann K, Steiner V, Bodmer JL, Schroter M, Burns K, Mattmann C, Rimoldi D, French LE, Tschopp J. 1997. Inhibition of death receptor signals by cellular FLIP. Nature 388(6638):190-195.

198. Ishikura N, Clever JL, Bouzamondo-Bernstein E, Samayoa E, Prusiner SB, Huang EJ, DeArmond SJ. 2005. Notch-1 activation and dendritic atrophy in prion disease. Proc Natl Acad Sci U S A 102(3):886-891.

199. Ito M. 1984. The cerbellum and neural control New York(Raven):580.

200. Jeffrey M, Scott JR, Williams A, Fraser H. 1992. Ultrastructural features of spongiform encephalopathy transmitted to mice from three species of bovidae. Acta Neuropathol 84(5):559-569.

201. Jia L, Dourmashkin RR, Allen PD, Gray AB, Newland AC, Kelsey SM. 1997. Inhibition of autophagy abrogates tumour necrosis factor alpha induced apoptosis in human T-lymphoblastic leukaemic cells. Br J Haematol 98(3):673-685.

202. Jones CE, Abdelraheim SR, Brown DR, Viles JH. 2004. Preferential Cu2+ coordination by His96 and His111 induces beta-sheet formation in the unstructured amyloidogenic region of the prion protein. J Biol Chem 279(31):32018-32027.

203. Joyal CC, Meyer C, Jacquart G, Mahler P, Caston J, Lalonde R. 1996. Effects of midline and lateral cerebellar lesions on motor coordination and spatial orientation. Brain Res 739(1-2):1-11.

204. Kabeya Y, Mizushima N, Ueno T, Yamamoto A, Kirisako T, Noda T, Kominami E, Ohsumi Y, Yoshimori T. 2000. LC3, a mammalian homologue of yeast Apg8p, is localized in autophagosome membranes after processing. Embo J 19(21):5720-5728.

205. Kabeya Y, Kawamata T, Suzuki K, Ohsumi Y. 2007. Cis1/Atg31 is required for autophagosome formation in Saccharomyces cerevisiae. Biochemical & Biophysical Research Communications 356(2):405-410.

206. Kakegawa W, Miyazaki T, Emi K, Matsuda K, Kohda K, Motohashi J, Mishina M, Kawahara S, Watanabe M, Yuzaki M. 2008. Differential regulation of synaptic plasticity and cerebellar motor learning by the C-terminal PDZ-binding motif of GluRdelta2. J Neurosci 28(6):1460-1468.

207. Kamada Y, Funakoshi T, Shintani T, Nagano K, Ohsumi M, Ohsumi Y. 2000. Tor-mediated induction of autophagy via an Apg1 protein kinase complex. J Cell Biol 150(6):1507-1513.

208. Kanaani J, Prusiner SB, Diacovo J, Baekkeskov S, Legname G. 2005. Recombinant prion protein induces rapid polarization and development of synapses in embryonic rat hippocampal neurons in vitro. J Neurochem 95(5):1373-1386.

209. Kashiwabuchi N, Ikeda K, Araki K, Hirano T, Shibuki K, Takayama C, Inoue Y, Kutsuwada T, Yagi T, Kang Y, et al. 1995. Impairment of motor coordination, Purkinje cell synapse formation, and cerebellar long-term depression in GluR delta 2 mutant mice. Cell 81(2):245-252.

210. Kerr JF, Wyllie AH, Currie AR. 1972. Apoptosis: a basic biological phenomenon with wide-ranging implications in tissue kinetics. Br J Cancer 26(4):239-257.

211. Kihara A, Kabeya Y, Ohsumi Y, Yoshimori T. 2001. Beclin-phosphatidylinositol 3-kinase complex functions at the trans-Golgi network. EMBO Rep 2(4):330-335.

212. Kim BH, Lee HG, Choi JK, Kim JI, Choi EK, Carp RI, Kim YS. 2004. The cellular prion protein (PrPC) prevents apoptotic neuronal cell death and mitochondrial dysfunction induced by serum deprivation. Brain Res Mol Brain Res 124(1):40-50.

213. Kimberlin RH, Wilesmith JW. 1994. Bovine spongiform encephalopathy. Epidemiology, low dose exposure and risks. Ann N Y Acad Sci 724:210-220.

214. Kirisako T, Ichimura Y, Okada H, Kabeya Y, Mizushima N, Yoshimori T, Ohsumi M, Takao T, Noda T, Ohsumi Y. 2000. The reversible modification regulates the membrane-binding state of Apg8/Aut7 essential for autophagy and the cytoplasm to vacuole targeting pathway. J Cell Biol 151(2):263-276.

215. Kirschke H, Langner J, Wiederanders B, Ansorge S, Bohley P. 1977. Cathepsin L. A new proteinase from rat-liver lysosomes. Eur J Biochem 74(2):293-301.

216. Klein RM, Howe JR. 2004. Effects of the lurcher mutation on GluR1 desensitization and activation kinetics. J Neurosci 24(21):4941-4951.

217. Klewpatinond M, Davies P, Bowen S, Brown DR, Viles JH. 2008. Deconvoluting the Cu2+ binding modes of full-length prion protein. J Biol Chem 283(4):1870-1881.

218. Knight RS, Will RG. 2004. Prion diseases. J Neurol Neurosurg Psychiatry 75 Suppl 1:i36-42.

219. Ko DC, Milenkovic L, Beier SM, Manuel H, Buchanan J, Scott MP. 2005. Cell-autonomous death of cerebellar purkinje neurons with autophagy in Niemann-Pick type C disease. PLoS Genet 1(1):81-95.

220. Kocer A, Gallozzi M, Renault L, Tilly G, Pinheiro I, Le Provost F, Pailhoux E, Vilotte JL. 2007. Goat PRND expression pattern suggests its involvement in early sex differentiation. Developmental Dynamics 236(3):836-842.

221. Kohda K, Wang Y, Yuzaki M. 2000. Mutation of a glutamate receptor motif reveals its role in gating and delta2 receptor channel properties. Nat Neurosci 3(4):315-322.

222. Kohda K, Kamiya Y, Matsuda S, Kato K, Umemori H, Yuzaki M. 2003. Heteromer formation of delta2 glutamate receptors with AMPA or kainate receptors. Brain Res Mol Brain Res 110(1):27-37.

223. Kohda K, Kakegawa W, Matsuda S, Nakagami R, Kakiya N, Yuzaki M. 2007. The extreme C-terminus of GluRdelta2 is essential for induction of long-term depression in cerebellar slices. Eur J Neurosci 25(5):1357-1362.

224. Koike M, Iino M, Ozawa S. 1997. Blocking effect of 1-naphthyl acetyl spermine on Ca(2+)-permeable AMPA receptors in cultured rat hippocampal neurons. Neurosci Res 29(1):27-36.

225. Komatsu M, Waguri S, Chiba T, Murata S, Iwata J, Tanida I, Ueno T, Koike M, Uchiyama Y, Kominami E, Tanaka K. 2006. Loss of autophagy in the central nervous system causes neurodegeneration in mice. Nature 441(7095):880-884.

226. Kondo T, Kakegawa W, Yuzaki M. 2005. Induction of long-term depression and phosphorylation of the delta2 glutamate receptor by protein kinase C in cerebellar slices. Eur J Neurosci 22(7):1817-1820.

227. Korte S, Vassallo N, Kramer ML, Kretzschmar HA, Herms J. 2003. Modulation of L-type voltage-gated calcium channels by recombinant prion protein. J Neurochem 87(4):1037-1042.

228. Kothakota S, Azuma T, Reinhard C, Klippel A, Tang J, Chu K, McGarry TJ, Kirschner MW, Koths K, Kwiatkowski DJ, Williams LT. 1997. Caspase-3-generated fragment of gelsolin: effector of morphological change in apoptosis. Science 278(5336):294-298.

229. Kovacs GG, Kurucz I, Budka H, Adori C, Muller F, Acs P, Kloppel S, Schatzl HM, Mayer RJ, Laszlo L. 2001. Prominent stress response of Purkinje cells in Creutzfeldt-Jakob disease. Neurobiol Dis 8(5):881-889.

230. Krajewska M, Mai JK, Zapata JM, Ashwell KW, Schendel SL, Reed JC, Krajewski S. 2002. Dynamics of expression of apoptosis-regulatory proteins Bid, Bcl-2, Bcl-X, Bax and Bak during development of murine nervous system. Cell Death Differ 9(2):145-157.

231. Krajewski S, Tanaka S, Takayama S, Schibler MJ, Fenton W, Reed JC. 1993. Investigation of the subcellular distribution of the bcl-2 oncoprotein: residence in the nuclear envelope, endoplasmic reticulum, and outer mitochondrial membranes. Cancer Research 53(19):4701-4714.

232. Ku NO, Liao J, Omary MB. 1997. Apoptosis generates stable fragments of human type I keratins. J Biol Chem 272(52):33197-33203.

233. Kunz J, Henriquez R, Schneider U, Deuter-Reinhard M, Movva NR, Hall MN. 1993. Target of rapamycin in yeast, TOR2, is an essential phosphatidylinositol kinase homolog required for G1 progression. Cell 73(3):585-596.

234. Kurihara H, Hashimoto K, Kano M, Takayama C, Sakimura K, Mishina M, Inoue Y, Watanabe M. 1997. Impaired parallel fiber-->Purkinje cell synapse stabilization during cerebellar development of mutant mice lacking the glutamate receptor delta2 subunit. J Neurosci 17(24):9613-9623.

235. Kurschner C, Morgan JI. 1995. The cellular prion protein (PrP) selectively binds to Bcl-2 in the yeast two-hybrid system. Brain Res Mol Brain Res 30(1):165-168.

236. Kurschner C, Morgan JI. 1996. Analysis of interaction sites in homo- and heteromeric complexes containing Bcl-2 family members and the cellular prion protein. Brain Res Mol Brain Res 37(1-2):249-258.

237. Kuwahara C, Takeuchi AM, Nishimura T, Haraguchi K, Kubosaki A, Matsumoto Y, Saeki K, Matsumoto Y, Yokoyama T, Itohara S, Onodera T. 1999. Prions prevent neuronal cell-line death. Nature 400(6741):225-226.

238. Laine J, Marc ME, Sy MS, Axelrad H. 2001. Cellular and subcellular morphological localization of normal prion protein in rodent cerebellum. Eur J Neurosci 14(1):47-56.

239. Lalonde R, Botez MI. 1985. Exploration and habituation in nervous mutant mice. Behav Brain Res 17(2):83-86.

240. Lalonde R, Botez MI, Boivin D. 1986a. Spontaneous alternation and habituation in a t-maze in nervous mutant mice. Behav Neurosci 100(3):350-352.

241. Lalonde R, Lamarre Y, Smith AM, Botez MI. 1986b. Spontaneous alternation and habituation in lurcher mutant mice. Brain Res 362(1):161-164.

242. Lalonde R, Botez MI, Boivin D. 1987. Object exploration in staggerer mutant mice. Physiol Behav 41(2):115-117.

243. Lalonde R, Lamarre Y, Smith AM. 1988a. Does the mutant mouse lurcher have deficits in spatially oriented behaviours? Brain Res 455(1):24-30.

244. Lalonde R, Manseau M, Botez MI. 1988b. Spontaneous alternation and exploration in staggerer mutant mice. Behav Brain Res 27(3):273-276.

245. Lalonde R, Botez MI. 1990. The cerebellum and learning processes in animals. Brain Res Brain Res Rev 15(3):325-332.

246. Lalouette A, Guenet JL, Vriz S. 1998. Hotfoot mouse mutations affect the delta 2 glutamate receptor gene and are allelic to lurcher. Genomics 50(1):9-13.

247. Lalouette A, Lohof A, Sotelo C, Guenet J, Mariani J. 2001. Neurobiological effects of a null mutation depend on genetic context: comparison between two hotfoot alleles of the delta-2 ionotropic glutamate receptor. Neuroscience 105(2):443-455.

248. Landis SC. 1973. Ultrastructural changes in the mitochondria of cerebellar Purkinje cells of nervous mutant mice. J Cell Biol 57(3):782-797.

249. Landis SC, Mullen RJ. 1978. The development and degeneration of Purkinje cells in pcd mutant mice. J Comp Neurol 177(1):125-143.

250. Landsend AS, Amiry-Moghaddam M, Matsubara A, Bergersen L, Usami S, Wenthold RJ, Ottersen OP. 1997. Differential localization of delta glutamate receptors in the rat cerebellum: coexpression with AMPA receptors in parallel fiber-spine synapses and absence from climbing fiber-spine synapses. J Neurosci 17(2):834-842.

251. Lane DP. 1992. Cancer. p53, guardian of the genome. Nature 358(6381):15-16.

252. Larsell O. 1952. The morphogenesis and adult pattern of the lobules and fissures of the cerebellum of the white rat. J Comp Neurol 97(2):281-356.

253. Lau FC, Frank TC, Nahm SS, Stoica G, Abbott LC. 2004. Postnatal apoptosis in cerebellar granule cells of homozygous leaner (tg1a/tg1a) mice. Neurotox Res 6(4):267-280.

254. Lavrik I, Krueger A, Schmitz I, Baumann S, Weyd H, Krammer PH, Kirchhoff S. 2003. The active caspase-8 heterotetramer is formed at the CD95 DISC. Cell Death Differ 10(1):144-145.

255. Leclerc E, Serban H, Prusiner SB, Burton DR, Williamson RA. 2006. Copper induces conformational changes in the N-terminal part of cell-surface PrPC. Arch Virol 151(11):2103-2109.

256. Lee CY, Baehrecke EH. 2001. Steroid regulation of autophagic programmed cell death during development. Development 128(8):1443-1455.

257. Lee DC, Sakudo A, Kim CK, Nishimura T, Saeki K, Matsumoto Y, Yokoyama T, Chen SG, Itohara S, Onodera T. 2006. Fusion of Doppel to octapeptide repeat and N-terminal half of hydrophobic region of prion protein confers resistance to serum deprivation. Microbiology & Immunology 50(3):203-209.

258. Lee SW, Ko YG, Bang S, Kim KS, Kim S. 2000. Death effector domain of a mammalian apoptosis mediator, FADD, induces bacterial cell death. Mol Microbiol 35(6):1540-1549.

259. Lemaire-Vieille C, Schulze T, Podevin-Dimster V, Follet J, Bailly Y, Blanquet-Grossard F, Decavel JP, Heinen E, Cesbron JY. 2000. Epithelial and endothelial expression of the green fluorescent protein reporter gene under the control of bovine prion protein (PrP) gene regulatory sequences in transgenic mice. Proc Natl Acad Sci U S A 97(10):5422-5427.

260. Li A, Sakaguchi S, Atarashi R, Roy BC, Nakaoke R, Arima K, Okimura N, Kopacek J, Shigematsu K. 2000a. Identification of a novel gene encoding a PrP-like protein expressed as chimeric transcripts fused to PrP exon 1/2 in ataxic mouse line with a disrupted PrP gene. Cell Mol Neurobiol 20(5):553-567.

261. Li A, Sakaguchi S, Shigematsu K, Atarashi R, Roy BC, Nakaoke R, Arima K, Okimura N, Kopacek J, Katamine S. 2000b. Physiological expression of the gene for PrP-like protein, PrPLP/Dpl, by brain endothelial cells and its ectopic expression in neurons of PrP-deficient mice ataxic due to Purkinje cell degeneration. Am J Pathol 157(5):1447-1452.

262. Li H, Zhu H, Xu CJ, Yuan J. 1998. Cleavage of BID by caspase 8 mediates the mitochondrial damage in the Fas pathway of apoptosis. Cell 94(4):491-501.

263. Li P, Nijhawan D, Budihardjo I, Srinivasula SM, Ahmad M, Alnemri ES, Wang X. 1997. Cytochrome c and dATP-dependent formation of Apaf-1/caspase-9 complex initiates an apoptotic protease cascade.[see comment]. Cell 91(4):479-489.

264. Li YR, Li Q, Yang JM, Zhou XM, Yin XM, Zhao DM. 2008. Expression patterns of Doppel gene in golden hamster: Quantification using real-time RT-PCR. Mol Cell Probes 22(4):255-258.

265. Liang XH, Kleeman LK, Jiang HH, Gordon G, Goldman JE, Berry G, Herman B, Levine B. 1998. Protection against fatal Sindbis virus encephalitis by beclin, a novel Bcl-2-interacting protein. J Virol 72(11):8586-8596.

266. Liberski PP, Sikorska B, Bratosiewicz-Wasik J, Gajdusek DC, Brown P. 2004. Neuronal cell death in transmissible spongiform encephalopathies (prion diseases) revisited: from apoptosis to autophagy. Int J Biochem Cell Biol 36(12):2473-2490.

267. Liberski PP, Brown DR, Sikorska B, Caughey B, Brown P. 2008. Cell death and autophagy in prion diseases (transmissible spongiform encephalopathies). Folia Neuropathol 46(1):1-25.

268. Lima FR, Arantes CP, Muras AG, Nomizo R, Brentani RR, Martins VR. 2007. Cellular prion protein expression in astrocytes modulates neuronal survival and differentiation. J Neurochem 103(6):2164-2176.

269. Lipton P. 1999. Ischemic cell death in brain neurons. Physiol Rev 79(4):1431-1568.

270. Liss B, Neu A, Roeper J. 1999. The weaver mouse gain-of-function phenotype of dopaminergic midbrain neurons is determined by coactivation of wvGirk2 and K-ATP channels. J Neurosci 19(20):8839-8848.

271. Liu X, Kim CN, Yang J, Jemmerson R, Wang X. 1996. Induction of apoptotic program in cell-free extracts: requirement for dATP and cytochrome c. Cell 86(1):147-157.

272. Liu X, Zou H, Slaughter C, Wang X. 1997. DFF, a heterodimeric protein that functions downstream of caspase-3 to trigger DNA fragmentation during apoptosis. Cell 89(2):175-184.

273. Locht C, Chesebro B, Race R, Keith JM. 1986. Molecular cloning and complete sequence of prion protein cDNA from mouse brain infected with the scrapie agent. Proc Natl Acad Sci U S A 83(17):6372-6376.

274. Loftus SK, Morris JA, Carstea ED, Gu JZ, Cummings C, Brown A, Ellison J, Ohno K, Rosenfeld MA, Tagle DA, Pentchev PG, Pavan WJ. 1997. Murine model of Niemann-Pick C disease: mutation in a cholesterol homeostasis gene. Science 277(5323):232-235.

275. Lohof AM, Delhaye-Bouchaud N, Mariani J. 1996. Synapse elimination in the central nervous system: functional significance and cellular mechanisms. Rev Neurosci 7(2):85-101.

276. Lomeli H, Sprengel R, Laurie DJ, Kohr G, Herb A, Seeburg PH, Wisden W. 1993. The rat delta-1 and delta-2 subunits extend the excitatory amino acid receptor family. FEBS Lett 315(3):318-322.

277. Lopes MH, Hajj GN, Muras AG, Mancini GL, Castro RM, Ribeiro KC, Brentani RR, Linden R, Martins VR. 2005. Interaction of cellular prion and stress-inducible protein 1 promotes neuritogenesis and neuroprotection by distinct signaling pathways. J Neurosci 25(49):11330-11339.

278. Lu K, Wang W, Xie Z, Wong BS, Li R, Petersen RB, Sy MS, Chen SG. 2000. Expression and structural characterization of the recombinant human doppel protein. Biochemistry 39(44):13575-13583.

279. Lu W, Tsirka SE. 2002. Partial rescue of neural apoptosis in the Lurcher mutant mouse through elimination of tissue plasminogen activator. Development 129(8):2043-2050.

280. Lucassen PJ, Williams A, Chung WC, Fraser H. 1995. Detection of apoptosis in murine scrapie. Neurosci Lett 198(3):185-188.

281. Luiken JJ, Blommaart EF, Boon L, van Woerkom GM, Meijer AJ. 1994. Cell swelling and the control of autophagic proteolysis in hepatocytes: involvement of phosphorylation of ribosomal protein S6? Biochemical Society Transactions 22(2):508-511.

282. Lum JJ, Bauer DE, Kong M, Harris MH, Li C, Lindsten T, Thompson CB. 2005. Growth factor regulation of autophagy and cell survival in the absence of apoptosis. Cell 120(2):237-248.

283. Luo X, Budihardjo I, Zou H, Slaughter C, Wang X. 1998. Bid, a Bcl2 interacting protein, mediates cytochrome c release from mitochondria in response to activation of cell surface death receptors. Cell 94(4):481-490.

284. Ly CD, Roche KW, Lee HK, Wenthold RJ. 2002. Identification of rat EMAP, a delta-glutamate receptor binding protein. Biochem Biophys Res Commun 291(1):85-90.

285. Lyahyai J, Bolea R, Serrano C, Monleon E, Moreno C, Osta R, Zaragoza P, Badiola JJ, Martin-Burriel I. 2006. Correlation between Bax overexpression and prion deposition in medulla oblongata from natural scrapie without evidence of apoptosis. Acta Neuropathol 112(4):451-460.

286. Maiuri MC, Zalckvar E, Kimchi A, Kroemer G. 2007. Self-eating and self-killing: crosstalk between autophagy and apoptosis. Nat Rev Mol Cell Biol 8(9):741-752.

287. Malinow R, Malenka RC. 2002. AMPA receptor trafficking and synaptic plasticity. Annu Rev Neurosci 25:103-126.

288. Mandolesi G, Cesa R, Autuori E, Strata P. 2008. An orphan ionotropic glutamate receptor: The delta2 subunit. Neuroscience.

289. Mann SS, Hammarback JA. 1994. Molecular characterization of light chain 3. A microtubule binding subunit of MAP1A and MAP1B. J Biol Chem 269(15):11492-11497.

290. Manson J, West JD, Thomson V, McBride P, Kaufman MH, Hope J. 1992. The prion protein gene: a role in mouse embryogenesis? Development 115(1):117-122.

291. Manson JC, Clarke AR, Hooper ML, Aitchison L, McConnell I, Hope J. 1994. 129/Ola mice carrying a null mutation in PrP that abolishes mRNA production are developmentally normal. Mol Neurobiol 8(2-3):121-127.

292. Mariani J, Crepel F, Mikoshiba K, Changeux JP, Sotelo C. 1977. Anatomical, physiological and biochemical studies of the cerebellum from Reeler mutant mouse. Philos Trans R Soc Lond B Biol Sci 281(978):1-28.

293. Mariani J, Changeux JP. 1980. Multiple innervation of Purkinje cells by climbing fibers in the cerebellum of the adult staggerer mutant mouse. J Neurobiol 11(1):41-50.

294. Mariani J, Changeux JP. 1981. Ontogenesis of olivocerebellar relationships. I. Studies by intracellular recordings of the multiple innervation of Purkinje cells by climbing fibers in the developing rat cerebellum. J Neurosci 1(7):696-702.

295. Mariani J. 1982. Extent of multiple innervation of Purkinje cells by climbing fibers in the olivocerebellar system of weaver, reeler, and staggerer mutant mice. J Neurobiol 13(2):119-126.

296. Maricich SM, Soha J, Trenkner E, Herrup K. 1997. Failed cell migration and death of purkinje cells and deep nuclear neurons in the weaver cerebellum. J Neurosci 17(10):3675-3683.

297. Martin DN, Baehrecke EH. 2004. Caspases function in autophagic programmed cell death in Drosophila. Development 131(2):275-284.

298. Martinou JC, Dubois-Dauphin M, Staple JK, Rodriguez I, Frankowski H, Missotten M, Albertini P, Talabot D, Catsicas S, Pietra C, et al. 1994. Overexpression of BCL-2 in transgenic mice protects neurons from naturally occurring cell death and experimental ischemia. Neuron 13(4):1017-1030.

299. Mason CA, Christakos S, Catalano SM. 1990. Early climbing fiber interactions with Purkinje cells in the postnatal mouse cerebellum. J Comp Neurol 297(1):77-90.

300. Massimino ML, Ballarin C, Bertoli A, Casonato S, Genovesi S, Negro A, Sorgato MC. 2004. Human Doppel and prion protein share common membrane microdomains and internalization pathways. International Journal of Biochemistry & Cell Biology 36(10):2016-2031.

301. Matsuda I, Mishina M. 2000. Identification of a juxtamembrane segment of the glutamate receptor delta2 subunit required for the plasma membrane localization. Biochem Biophys Res Commun 275(2):565-571.

302. Matsuda S, Yuzaki M. 2002. Mutation in hotfoot-4J mice results in retention of delta2 glutamate receptors in ER. Eur J Neurosci 16(8):1507-1516.

303. Matsuda S, Hannen R, Matsuda K, Yamada N, Tubbs T, Yuzaki M. 2004. The C-terminal juxtamembrane region of the delta 2 glutamate receptor controls its export from the endoplasmic reticulum. Eur J Neurosci 19(7):1683-1690.

304. Matthews MR. 1973. An ultrastructural study of axonal changes following constriction of postganglionic branches of the superior cervical ganglion in the rat. Philos Trans R Soc Lond B Biol Sci 264(866):479-505.

305. Mayat E, Petralia RS, Wang YX, Wenthold RJ. 1995. Immunoprecipitation, immunoblotting, and immunocytochemistry studies suggest that glutamate receptor delta subunits form novel postsynaptic receptor complexes. J Neurosci 15(3 Pt 2):2533-2546.

306. Mayeux R. 2003. Epidemiology of neurodegeneration. Annu Rev Neurosci 26:81-104.

307. McFarland R, Blokhin A, Sydnor J, Mariani J, Vogel MW. 2007. Oxidative stress, nitric oxide, and the mechanisms of cell death in Lurcher Purkinje cells. Dev Neurobiol 67(8):1032-1046.

308. McKenzie MD, Carrington EM, Kaufmann T, Strasser A, Huang DC, Kay TW, Allison J, Thomas HE. 2008. Proapoptotic BH3-only protein Bid is essential for death receptor-induced apoptosis of pancreatic beta-cells. Diabetes 57(5):1284-1292.

309. Mead S, Beck J, Dickinson A, Fisher EM, Collinge J. 2000. Examination of the human prion protein-like gene doppel for genetic susceptibility to sporadic and variant Creutzfeldt-Jakob disease. Neurosci Lett 290(2):117-120.

310. Medina JF, Repa JC, Mauk MD, LeDoux JE. 2002. Parallels between cerebellum- and amygdala-dependent conditioning. Nat Rev Neurosci 3(2):122-131.

311. Meijer AJ, Codogno P. 2004. Regulation and role of autophagy in mammalian cells. Int J Biochem Cell Biol 36(12):2445-2462.

312. Middleton FA, Strick PL. 2000. Basal ganglia and cerebellar loops: motor and cognitive circuits. Brain Res Brain Res Rev 31(2-3):236-250.

313. Mihailoff GA, Burne RA, Azizi SA, Norell G, Woodward DJ. 1981. The pontocerebellar system in the rat: an HRP study. II. Hemispheral components. J Comp Neurol 197(4):559-577.

314. Mills KR, Reginato M, Debnath J, Queenan B, Brugge JS. 2004. Tumor necrosis factor-related apoptosis-inducing ligand (TRAIL) is required for induction of autophagy during lumen formation in vitro. Proc Natl Acad Sci U S A 101(10):3438-3443.

315. Mironov A, Jr., Latawiec D, Wille H, Bouzamondo-Bernstein E, Legname G, Williamson RA, Burton D, DeArmond SJ, Prusiner SB, Peters PJ. 2003. Cytosolic prion protein in neurons. J Neurosci 23(18):7183-7193.

316. Miyagi Y, Yamashita T, Fukaya M, Sonoda T, Okuno T, Yamada K, Watanabe M, Nagashima Y, Aoki I, Okuda K, Mishina M, Kawamoto S. 2002. Delphilin: a novel PDZ and formin homology domain-containing protein that synaptically colocalizes and interacts with glutamate receptor delta 2 subunit. J Neurosci 22(3):803-814.

317. Miyashita T, Reed JC. 1995. Tumor suppressor p53 is a direct transcriptional activator of the human bax gene. Cell 80(2):293-299.

318. Mizushima N, Sugita H, Yoshimori T, Ohsumi Y. 1998. A new protein conjugation system in human. The counterpart of the yeast Apg12p conjugation system essential for autophagy. J Biol Chem 273(51):33889-33892.

319. Mizushima N, Yoshimori T, Ohsumi Y. 2003. Role of the Apg12 conjugation system in mammalian autophagy. Int J Biochem Cell Biol 35(5):553-561.

320. Mobley WC, Neve RL, Prusiner SB, McKinley MP. 1988. Nerve growth factor increases mRNA levels for the prion protein and the beta-amyloid protein precursor in developing hamster brain. Proc Natl Acad Sci U S A 85(24):9811-9815.

321. Molinari M, Petrosini L, Gremoli T. 1990. Hemicerebellectomy and motor behaviour in rats. II. Effects of cerebellar lesion performed at different developmental stages. Exp Brain Res 82(3):483-492.

322. Molinari M, Grammaldo LG, Petrosini L. 1997. Cerebellar contribution to spatial event processing: right/left discrimination abilities in rats. Eur J Neurosci 9(9):1986-1992.

323. Moore RC, Lee IY, Silverman GL, Harrison PM, Strome R, Heinrich C, Karunaratne A, Pasternak SH, Chishti MA, Liang Y, Mastrangelo P, Wang K, Smit AF, Katamine S, Carlson GA, Cohen FE, Prusiner SB, Melton DW, Tremblay P, Hood LE, Westaway D. 1999. Ataxia in prion protein (PrP)-deficient mice is associated with upregulation of the novel PrP-like protein doppel. J Mol Biol 292(4):797-817.

324. Moore RC, Mastrangelo P, Bouzamondo E, Heinrich C, Legname G, Prusiner SB, Hood L, Westaway D, DeArmond SJ, Tremblay P. 2001. Doppel-induced cerebellar degeneration in transgenic mice. Proc Natl Acad Sci U S A 98(26):15288-15293.

325. Morando L, Cesa R, Rasetti R, Harvey R, Strata P. 2001. Role of glutamate delta -2 receptors in activity-dependent competition between heterologous afferent fibers. Proc Natl Acad Sci U S A 98(17):9954-9959.

326. Morara S, van der Want JJ, de Weerd H, Provini L, Rosina A. 2001. Ultrastructural analysis of climbing fiber-Purkinje cell synaptogenesis in the rat cerebellum. Neuroscience 108(4):655-671.

327. Moser M, Colello RJ, Pott U, Oesch B. 1995. Developmental expression of the prion protein gene in glial cells. Neuron 14(3):509-517.

328. Mouillet-Richard S, Ermonval M, Chebassier C, Laplanche JL, Lehmann S, Launay JM, Kellermann O. 2000. Signal transduction through prion protein. Science 289(5486):1925-1928.

329. Mukae N, Enari M, Sakahira H, Fukuda Y, Inazawa J, Toh H, Nagata S. 1998. Molecular cloning and characterization of human caspase-activated DNase. Proc Natl Acad Sci U S A 95(16):9123-9128.

330. Nakagawa T, Zhu H, Morishima N, Li E, Xu J, Yankner BA, Yuan J. 2000. Caspase-12 mediates endoplasmic-reticulum-specific apoptosis and cytotoxicity by amyloid-beta. Nature 403(6765):98-103.

331. Namura S, Zhu J, Fink K, Endres M, Srinivasan A, Tomaselli KJ, Yuan J, Moskowitz MA. 1998. Activation and cleavage of caspase-3 in apoptosis induced by experimental cerebral ischemia. J Neurosci 18(10):3659-3668.

332. Newmeyer DD, Ferguson-Miller S. 2003. Mitochondria: releasing power for life and unleashing the machineries of death.[erratum appears in Cell. 2003 Mar 21;(112)6:873]. Cell 112(4):481-490.

333. Nicolas O, Gavin R, Braun N, Urena JM, Fontana X, Soriano E, Aguzzi A, del Rio JA. 2007. Bcl-2 overexpression delays caspase-3 activation and rescues cerebellar degeneration in prion-deficient mice that overexpress amino-terminally truncated prion. Faseb J 21(12):3107-3117.

334. Nishida N, Tremblay P, Sugimoto T, Shigematsu K, Shirabe S, Petromilli C, Erpel SP, Nakaoke R, Atarashi R, Houtani T, Torchia M, Sakaguchi S, DeArmond SJ, Prusiner SB, Katamine S. 1999. A mouse prion protein transgene rescues mice deficient for the prion protein gene from purkinje cell degeneration and demyelination. Lab Invest 79(6):689-697.

335. Nishino I, Fu J, Tanji K, Yamada T, Shimojo S, Koori T, Mora M, Riggs JE, Oh SJ, Koga Y, Sue CM, Yamamoto A, Murakami N, Shanske S, Byrne E, Bonilla E, Nonaka I, DiMauro S, Hirano M. 2000. Primary LAMP-2 deficiency causes X-linked vacuolar cardiomyopathy and myopathy (Danon disease). Nature 406(6798):906-910.

336. Nixon RA, Wegiel J, Kumar A, Yu WH, Peterhoff C, Cataldo A, Cuervo AM. 2005. Extensive involvement of autophagy in Alzheimer disease: an immuno-electron microscopy study. J Neuropathol Exp Neurol 64(2):113-122.

337. Nixon RA. 2006. Autophagy in neurodegenerative disease: friend, foe or turncoat? Trends Neurosci 29(9):528-535.

338. Norman DJ, Feng L, Cheng SS, Gubbay J, Chan E, Heintz N. 1995. The lurcher gene induces apoptotic death in cerebellar Purkinje cells. Development 121(4):1183-1193.

339. Northington FJ, Ferriero DM, Flock DL, Martin LJ. 2001. Delayed neurodegeneration in neonatal rat thalamus after hypoxia-ischemia is apoptosis. Journal of Neuroscience 21(6):1931-1938.

340. Nunomura A, Moreira PI, Lee HG, Zhu X, Castellani RJ, Smith MA, Perry G. 2007. Neuronal death and survival under oxidative stress in Alzheimer and Parkinson diseases. CNS Neurol Disord Drug Targets 6(6):411-423.

341. Oesch B, Westaway D, Walchli M, McKinley MP, Kent SB, Aebersold R, Barry RA, Tempst P, Teplow DB, Hood LE, et al. 1985. A cellular gene encodes scrapie PrP 27-30 protein. Cell 40(4):735-746.

342. Ohsumi Y, Mizushima N. 2004. Two ubiquitin-like conjugation systems essential for autophagy. Semin Cell Dev Biol 15(2):231-236.

343. Ona VO, Li M, Vonsattel JP, Andrews LJ, Khan SQ, Chung WM, Frey AS, Menon AS, Li XJ, Stieg PE, Yuan J, Penney JB, Young AB, Cha JH, Friedlander RM. 1999. Inhibition of caspase-1 slows disease progression in a mouse model of Huntington's disease. Nature 399(6733):263-267.

344. Orrenius S. 2007. Reactive oxygen species in mitochondria-mediated cell death. Drug Metab Rev 39(2-3):443-455.

345. Paisley D, Banks S, Selfridge J, McLennan NF, Ritchie AM, McEwan C, Irvine DS, Saunders PT, Manson JC, Melton DW. 2004. Male infertility and DNA damage in Doppel knockout and prion protein/Doppel double-knockout mice. American Journal of Pathology 164(6):2279-2288.

346. Paitel E, Alves da Costa C, Vilette D, Grassi J, Checler F. 2002. Overexpression of PrPc triggers caspase 3 activation: potentiation by proteasome inhibitors and blockade by anti-PrP antibodies. J Neurochem 83(5):1208-1214.

347. Paitel E, Fahraeus R, Checler F. 2003. Cellular prion protein sensitizes neurons to apoptotic stimuli through Mdm2-regulated and p53-dependent caspase 3-like activation. J Biol Chem 278(12):10061-10066.

348. Paitel E, Sunyach C, Alves da Costa C, Bourdon JC, Vincent B, Checler F. 2004. Primary cultured neurons devoid of cellular prion display lower responsiveness to staurosporine through the control of p53 at both transcriptional and post-transcriptional levels. J Biol Chem 279(1):612-618.

349. Palay S, Chan-Palay V. 1974. Cerebellar Cortex: Cytology andorganisation(Springer Verlag).

350. Pan T, Wong BS, Liu T, Li R, Petersen RB, Sy MS. 2002. Cell-surface prion protein interacts with glycosaminoglycans. Biochem J 368(Pt 1):81-90.

351. Pankiv S, Clausen TH, Lamark T, Brech A, Bruun JA, Outzen H, Overvatn A, Bjorkoy G, Johansen T. 2007. p62/SQSTM1 binds directly to Atg8/LC3 to facilitate degradation of ubiquitinated protein aggregates by autophagy. J Biol Chem 282(33):24131-24145.

352. Papa S, Bubici C, Zazzeroni F, Pham CG, Kuntzen C, Knabb JR, Dean K, Franzoso G. 2006. The NF-kappaB-mediated control of the JNK cascade in the antagonism of programmed cell death in health and disease. Cell Death Differ 13(5):712-729.

353. Patil N, Cox DR, Bhat D, Faham M, Myers RM, Peterson AS. 1995. A potassium channel mutation in weaver mice implicates membrane excitability in granule cell differentiation. Nat Genet 11(2):126-129.

354. Pattingre S, Tassa A, Qu X, Garuti R, Liang XH, Mizushima N, Packer M, Schneider MD, Levine B. 2005. Bcl-2 antiapoptotic proteins inhibit Beclin 1-dependent autophagy. Cell 122(6):927-939.

355. Peng J, Wu Z, Wu Y, Hsu M, Stevenson FF, Boonplueang R, Roffler-Tarlov SK, Andersen JK. 2002. Inhibition of caspases protects cerebellar granule cells of the weaver mouse from apoptosis and improves behavioral phenotype. J Biol Chem 277(46):44285-44291.

356. Peoc'h K, Serres C, Frobert Y, Martin C, Lehmann S, Chasseigneaux S, Sazdovitch V, Grassi J, Jouannet P, Launay JM, Laplanche JL. 2002. The human "prion-like" protein Doppel is expressed in both Sertoli cells and spermatozoa. J Biol Chem 277(45):43071-43078.

357. Peoc'h K, Volland H, De Gassart A, Beaudry P, Sazdovitch V, Sorgato MC, Creminon C, Laplanche JL, Lehmann S. 2003. Prion-like protein Doppel expression is not modified in scrapie-infected cells and in the brains of patients with Creutzfeldt-Jakob disease. FEBS Lett 536(1-3):61-65.

358. Petrakis S, Sklaviadis T. 2006. Identification of proteins with high affinity for refolded and native PrPC. Proteomics 6(24):6476-6484.

359. Petrosini L, Molinari M, Gremoli T. 1990. Hemicerebellectomy and motor behaviour in rats. I. Development of motor function after neonatal lesion. Exp Brain Res 82(3):472-482.

360. Petrosini L, Molinari M, Dell'Anna ME. 1996. Cerebellar contribution to spatial event processing: Morris water maze and T-maze. Eur J Neurosci 8(9):1882-1896.

361. Phillips r. 1960. 'Lurcher,' a new gene in linkage groupe XI of the house mouse. J Genet 57:35-42.

362. Pijpers A, Apps R, Pardoe J, Voogd J, Ruigrok TJ. 2006. Precise spatial relationships between mossy fibers and climbing fibers in rat cerebellar cortical zones. J Neurosci 26(46):12067-12080.

363. Premzl M, Sangiorgio L, Strumbo B, Marshall Graves JA, Simonic T, Gready JE. 2003. Shadoo, a new protein highly conserved from fish to mammals and with similarity to prion protein. Gene 314:89-102.

364. Prestori F, Rossi P, Bearzatto B, Laine J, Necchi D, Diwakar S, Schiffmann SN, Axelrad H, D'Angelo E. 2008. Altered neuron excitability and synaptic plasticity in the cerebellar granular layer of juvenile prion protein knock-out mice with impaired motor control. J Neurosci 28(28):7091-7103.

365. Prusiner SB. 1982. Novel proteinaceous infectious particles cause scrapie. Science 216(4542):136-144.

366. Prusiner SB, Groth DF, Bolton DC, Kent SB, Hood LE. 1984. Purification and structural studies of a major scrapie prion protein. Cell 38(1):127-134.

367. Prusiner SB. 1998. Prions. Proc Natl Acad Sci U S A 95(23):13363-13383.

368. Puig B, Ferrer I. 2001. Cell death signaling in the cerebellum in Creutzfeldt-Jakob disease. Acta Neuropathol 102(3):207-215.

369. Punnonen EL, Autio S, Marjomaki VS, Reunanen H. 1992. Autophagy, cathepsin L transport, and acidification in cultured rat fibroblasts. J Histochem Cytochem 40(10):1579-1587.

370. Purkinyé JE. 1877. Bericht über die Versammlung deutscher Naturforscher und Ärzte in Prag in September. Prague: Anatomisch-Physiologische Verhandlungen 3(5):177-180.

371. Puro DG, Woodward DJ. 1977. The climbing fiber system in the Weaver mutant. Brain Res 129(1):141-146.

372. Puthalakath H, Strasser A. 2002. Keeping killers on a tight leash: transcriptional and post-translational control of the pro-apoptotic activity of BH3-only proteins. Cell Death & Differentiation 9(5):505-512.

373. Pyo JO, Jang MH, Kwon YK, Lee HJ, Jun JI, Woo HN, Cho DH, Choi B, Lee H, Kim JH, Mizushima N, Oshumi Y, Jung YK. 2005. Essential roles of Atg5 and FADD in autophagic cell death: dissection of autophagic cell death into vacuole formation and cell death. J Biol Chem 280(21):20722-20729.

374. Qin K, Yang DS, Yang Y, Chishti MA, Meng LJ, Kretzschmar HA, Yip CM, Fraser PE, Westaway D. 2000. Copper(II)-induced conformational changes and protease resistance in recombinant and cellular PrP. Effect of protein age and deamidation. J Biol Chem 275(25):19121-19131.

375. Qin K, Coomaraswamy J, Mastrangelo P, Yang Y, Lugowski S, Petromilli C, Prusiner SB, Fraser PE, Goldberg JM, Chakrabartty A, Westaway D. 2003. The PrP-like protein Doppel binds copper. J Biol Chem 278(11):8888-8896.

376. Qin K, Zhao L, Tang Y, Bhatta S, Simard JM, Zhao RY. 2006. Doppel-induced apoptosis and counteraction by cellular prion protein in neuroblastoma and astrocytes. Neuroscience 141(3):1375-1388.

377. Quaglio E, Chiesa R, Harris DA. 2001. Copper converts the cellular prion protein into a protease-resistant species that is distinct from the scrapie isoform. J Biol Chem 276(14):11432-11438.

378. Ramón y Cajal S. 1911. Histologie du Système nerveux. Maloine Vols I and II.

379. Rao RV, Poksay KS, Castro-Obregon S, Schilling B, Row RH, del Rio G, Gibson BW, Ellerby HM, Bredesen DE. 2004a. Molecular components of a cell death pathway activated by endoplasmic reticulum stress. Journal of Biological Chemistry 279(1):177-187.

380. Rao RV, Ellerby HM, Bredesen DE. 2004b. Coupling endoplasmic reticulum stress to the cell death program. Cell Death & Differentiation 11(4):372-380.

381. Ravikumar B, Vacher C, Berger Z, Davies JE, Luo S, Oroz LG, Scaravilli F, Easton DF, Duden R, O'Kane CJ, Rubinsztein DC. 2004. Inhibition of mTOR induces autophagy and reduces toxicity of polyglutamine expansions in fly and mouse models of Huntington disease. Nat Genet 36(6):585-595.

382. Ravikumar B, Acevedo-Arozena A, Imarisio S, Berger Z, Vacher C, O'Kane CJ, Brown SD, Rubinsztein DC. 2005. Dynein mutations impair autophagic clearance of aggregate-prone proteins. Nat Genet 37(7):771-776.

383. Ricci JE, Munoz-Pinedo C, Fitzgerald P, Bailly-Maitre B, Perkins GA, Yadava N, Scheffler IE, Ellisman MH, Green DR. 2004. Disruption of mitochondrial function during apoptosis is mediated by caspase cleavage of the p75 subunit of complex I of the electron transport chain. Cell 117(6):773-786.

384. Rideout HJ, Lang-Rollin I, Stefanis L. 2004. Involvement of macroautophagy in the dissolution of neuronal inclusions. Int J Biochem Cell Biol 36(12):2551-2562.

385. Rieger R, Edenhofer F, Lasmezas CI, Weiss S. 1997. The human 37-kDa laminin receptor precursor interacts with the prion protein in eukaryotic cells. Nat Med 3(12):1383-1388.

386. Rieger R, Lasmezas CI, Weiss S. 1999. Role of the 37 kDa laminin receptor precursor in the life cycle of prions. Transfus Clin Biol 6(1):7-16.

387. Riek R, Hornemann S, Wider G, Glockshuber R, Wuthrich K. 1997. NMR characterization of the full-length recombinant murine prion protein, mPrP(23-231). FEBS Lett 413(2):282-288.

388. Robinson KO, Petersen AM, Morrison SN, Elso CM, Stubbs L. 2005. Two reciprocal translocations provide new clues to the high mutability of the Grid2 locus. Mamm Genome 16(1):32-40.

389. Roche KW, Ly CD, Petralia RS, Wang YX, McGee AW, Bredt DS, Wenthold RJ. 1999. Postsynaptic density-93 interacts with the delta2 glutamate receptor subunit at parallel fiber synapses. J Neurosci 19(10):3926-3934.

390. Rodda RA. 1981. Cerebellar atrophy in Huntington's disease. J Neurol Sci 50(1):147-157.

391. Rondi-Reig L, Lohof A, Dubreuil YL, Delhaye-Bouchaud N, Martinou JC, Caston J, Mariani J. 1999. Hu-Bcl-2 transgenic mice with supernumerary neurons exhibit timing impairment in a complex motor task. Eur J Neurosci 11(7):2285-2290.

392. Ross CA, Poirier MA. 2004. Protein aggregation and neurodegenerative disease. Nat Med 10 Suppl:S10-17.

393. Rossi D, Cozzio A, Flechsig E, Klein MA, Rulicke T, Aguzzi A, Weissmann C. 2001. Onset of ataxia and Purkinje cell loss in PrP null mice inversely correlated with Dpl level in brain. Embo J 20(4):694-702.

394. Rossi F, Jankovski A, Sotelo C. 1995. Target neuron controls the integrity of afferent axon phenotype: a study on the Purkinje cell-climbing fiber system in cerebellar mutant mice. J Neurosci 15(3 Pt 1):2040-2056.

395. Roucou X, Guo Q, Zhang Y, Goodyer CG, LeBlanc AC. 2003. Cytosolic prion protein is not toxic and protects against Bax-mediated cell death in human primary neurons. J Biol Chem 278(42):40877-40881.

396. Roucou X, Giannopoulos PN, Zhang Y, Jodoin J, Goodyer CG, LeBlanc A. 2005. Cellular prion protein inhibits proapoptotic Bax conformational change in human neurons and in breast carcinoma MCF-7 cells. Cell Death Differ 12(7):783-795.

397. Rowland AM, Richmond JE, Olsen JG, Hall DH, Bamber BA. 2006. Presynaptic terminals independently regulate synaptic clustering and autophagy of GABAA receptors in Caenorhabditis elegans. J Neurosci 26(6):1711-1720.

398. Ruigrok TJ, Voogd J. 2000. Organization of projections from the inferior olive to the cerebellar nuclei in the rat. J Comp Neurol 426(2):209-228.

399. Rusten TE, Lindmo K, Juhasz G, Sass M, Seglen PO, Brech A, Stenmark H. 2004. Programmed autophagy in the Drosophila fat body is induced by ecdysone through regulation of the PI3K pathway. Dev Cell 7(2):179-192.

400. Safar JG, Kellings K, Serban A, Groth D, Cleaver JE, Prusiner SB, Riesner D. 2005. Search for a prion-specific nucleic acid. J Virol 79(16):10796-10806.

401. Sagne C, Agulhon C, Ravassard P, Darmon M, Hamon M, El Mestikawy S, Gasnier B, Giros B. 2001. Identification and characterization of a lysosomal transporter for small neutral amino acids. Proc Natl Acad Sci U S A 98(13):7206-7211.

402. Sailer A, Bueler H, Fischer M, Aguzzi A, Weissmann C. 1994. No propagation of prions in mice devoid of PrP. Cell 77(7):967-968.

403. Sakaguchi S, Katamine S, Shigematsu K, Nakatani A, Moriuchi R, Nishida N, Kurokawa K, Nakaoke R, Sato H, Jishage K, et al. 1995. Accumulation of proteinase K-resistant prion protein (PrP) is restricted by the expression level of normal PrP in mice inoculated with a mouse-adapted strain of the Creutzfeldt-Jakob disease agent. J Virol 69(12):7586-7592.

404. Sakaguchi S, Katamine S, Nishida N, Moriuchi R, Shigematsu K, Sugimoto T, Nakatani A, Kataoka Y, Houtani T, Shirabe S, Okada H, Hasegawa S, Miyamoto T, Noda T. 1996. Loss of cerebellar Purkinje cells in aged mice homozygous for a disrupted PrP gene. Nature 380(6574):528-531.

405. Sakudo A, Lee DC, Nishimura T, Li S, Tsuji S, Nakamura T, Matsumoto Y, Saeki K, Itohara S, Ikuta K, Onodera T. 2005a. Octapeptide repeat region and N-terminal half of hydrophobic region of prion protein (PrP) mediate PrP-dependent activation of superoxide dismutase. Biochemical & Biophysical Research Communications 326(3):600-606.

406. Sakudo A, Lee DC, Nakamura I, Taniuchi Y, Saeki K, Matsumoto Y, Itohara S, Ikuta K, Onodera T. 2005b. Cell-autonomous PrP-Doppel interaction regulates apoptosis in PrP gene-deficient neuronal cells. Biochemical & Biophysical Research Communications 333(2):448-454.

407. Sales N, Rodolfo K, Hassig R, Faucheux B, Di Giamberardino L, Moya KL. 1998. Cellular prion protein localization in rodent and primate brain. Eur J Neurosci 10(7):2464-2471.

408. Salvesen GS, Dixit VM. 1997. Caspases: intracellular signaling by proteolysis. Cell 91(4):443-446.

409. Sanchez I, Xu CJ, Juo P, Kakizaka A, Blenis J, Yuan J. 1999. Caspase-8 is required for cell death induced by expanded polyglutamine repeats. Neuron 22(3):623-633.

410. Santuccione A, Sytnyk V, Leshchyns'ka I, Schachner M. 2005. Prion protein recruits its neuronal receptor NCAM to lipid rafts to activate p59fyn and to enhance neurite outgrowth. J Cell Biol 169(2):341-354.

411. Sarna JR, Hawkes R. 2003. Patterned Purkinje cell death in the cerebellum. Prog Neurobiol 70(6):473-507.

412. Scaffidi C, Fulda S, Srinivasan A, Friesen C, Li F, Tomaselli KJ, Debatin KM, Krammer PH, Peter ME. 1998. Two CD95 (APO-1/Fas) signaling pathways. Embo J 17(6):1675-1687.

413. Scaffidi C, Schmitz I, Krammer PH, Peter ME. 1999. The role of c-FLIP in modulation of CD95-induced apoptosis. J Biol Chem 274(3):1541-1548.

414. Scelfo B, Strata P. 2005. Correlation between multiple climbing fibre regression and parallel fibre response development in the postnatal mouse cerebellum. Eur J Neurosci 21(4):971-978.

415. Schatzl HM, Laszlo L, Holtzman DM, Tatzelt J, DeArmond SJ, Weiner RI, Mobley WC, Prusiner SB. 1997. A hypothalamic neuronal cell line persistently infected with scrapie prions exhibits apoptosis. J Virol 71(11):8821-8831.

416. Schilling K. 2000. Lineage, development and morphogenesis of cerebellar interneurons. Prog Brain Res 124:51-68.

417. Schmahmann JD, Pandya DN. 1989. Anatomical investigation of projections to the basis pontis from posterior parietal association cortices in rhesus monkey. J Comp Neurol 289(1):53-73.

418. Schmahmann JD, Pandya DN. 1997. Anatomic organization of the basilar pontine projections from prefrontal cortices in rhesus monkey. J Neurosci 17(1):438-458.

419. Schmahmann JD, Sherman JC. 1997. Cerebellar cognitive affective syndrome. Int Rev Neurobiol 41:433-440.

420. Schmeiser K, Hammond EM, Roberts S, Grand RJ. 1998. Specific cleavage of gamma catenin by caspases during apoptosis. FEBS Lett 433(1-2):51-57.

421. Schmitt-Ulms G, Legname G, Baldwin MA, Ball HL, Bradon N, Bosque PJ, Crossin KL, Edelman GM, DeArmond SJ, Cohen FE, Prusiner SB. 2001. Binding of neural cell adhesion molecules (N-CAMs) to the cellular prion protein. J Mol Biol 314(5):1209-1225.

422. Schwartz LM, Smith SW, Jones ME, Osborne BA. 1993. Do all programmed cell deaths occur via apoptosis? Proc Natl Acad Sci U S A 90(3):980-984.

423. Schwarz MK, Pawlak V, Osten P, Mack V, Seeburg PH, Kohr G. 2001. Dominance of the lurcher mutation in heteromeric kainate and AMPA receptor channels. Eur J Neurosci 14(5):861-868.

424. Schweichel JU, Merker HJ. 1973. The morphology of various types of cell death in prenatal tissues. Teratology 7(3):253-266.

425. Scorrano L, Oakes SA, Opferman JT, Cheng EH, Sorcinelli MD, Pozzan T, Korsmeyer SJ. 2003. BAX and BAK regulation of endoplasmic reticulum Ca2+: a control point for apoptosis.[see comment]. Science 300(5616):135-139.

426. Selimi F, Campana A, Weitzman J, Vogel MW, Mariani J. 2000a. Bax and p53 are differentially involved in the regulation of caspase-3 expression and activation during neurodegeneration in Lurcher mice. C R Acad Sci III 323(11):967-973.

427. Selimi F, Doughty M, Delhaye-Bouchaud N, Mariani J. 2000b. Target-related and intrinsic neuronal death in Lurcher mutant mice are both mediated by caspase-3 activation. J Neurosci 20(3):992-1000.

428. Selimi F, Vogel MW, Mariani J. 2000c. Bax inactivation in lurcher mutants rescues cerebellar granule cells but not purkinje cells or inferior olivary neurons. J Neurosci 20(14):5339-5345.

429. Selimi F, Lohof AM, Heitz S, Lalouette A, Jarvis CI, Bailly Y, Mariani J. 2003. Lurcher GRID2-induced death and depolarization can be dissociated in cerebellar Purkinje cells. Neuron 37(5):813-819.

430. Settanni G, Hoang TX, Micheletti C, Maritan A. 2002. Folding pathways of prion and doppel. Biophys J 83(6):3533-3541.

431. Shi Y. 2002. Mechanisms of caspase activation and inhibition during apoptosis. Mol Cell 9(3):459-470.

432. Shibata M, Lu T, Furuya T, Degterev A, Mizushima N, Yoshimori T, MacDonald M, Yankner B, Yuan J. 2006. Regulation of intracellular accumulation of mutant Huntingtin by Beclin 1. J Biol Chem 281(20):14474-14485.

433. Shimizu S, Kanaseki T, Mizushima N, Mizuta T, Arakawa-Kobayashi S, Thompson CB, Tsujimoto Y. 2004. Role of Bcl-2 family proteins in a non-apoptotic programmed cell death dependent on autophagy genes. Nat Cell Biol 6(12):1221-1228.

434. Shmerling D, Hegyi I, Fischer M, Blattler T, Brandner S, Gotz J, Rulicke T, Flechsig E, Cozzio A, von Mering C, Hangartner C, Aguzzi A, Weissmann C. 1998. Expression of amino-terminally truncated PrP in the mouse leading to ataxia and specific cerebellar lesions. Cell 93(2):203-214.

435. Shyng SL, Huber MT, Harris DA. 1993. A prion protein cycles between the cell surface and an endocytic compartment in cultured neuroblastoma cells. J Biol Chem 268(21):15922-15928.

436. Shyng SL, Heuser JE, Harris DA. 1994. A glycolipid-anchored prion protein is endocytosed via clathrin-coated pits. J Cell Biol 125(6):1239-1250.

437. Shyng SL, Moulder KL, Lesko A, Harris DA. 1995. The N-terminal domain of a glycolipid-anchored prion protein is essential for its endocytosis via clathrin-coated pits. J Biol Chem 270(24):14793-14800.

438. Sikorska B, Liberski PP, Giraud P, Kopp N, Brown P. 2004. Autophagy is a part of ultrastructural synaptic pathology in Creutzfeldt-Jakob disease: a brain biopsy study. Int J Biochem Cell Biol 36(12):2563-2573.

439. Sillitoe RV, Joyner AL. 2007. Morphology, molecular codes, and circuitry produce the three-dimensional complexity of the cerebellum. Annu Rev Cell Dev Biol 23:549-577.

440. Silverman GL, Qin K, Moore RC, Yang Y, Mastrangelo P, Tremblay P, Prusiner SB, Cohen FE, Westaway D. 2000. Doppel is an N-glycosylated, glycosylphosphatidylinositol-anchored protein. Expression in testis and ectopic production in the brains of Prnp(0/0) mice predisposed to Purkinje cell loss. J Biol Chem 275(35):26834-26841.

441. Sjobeck M, Englund E. 2001. Alzheimer's disease and the cerebellum: a morphologic study on neuronal and glial changes. Dement Geriatr Cogn Disord 12(3):211-218.

442. Sklan EH, Podoly E, Soreq H. 2006. RACK1 has the nerve to act: structure meets function in the nervous system. Progress in Neurobiology 78(2):117-134.

443. Smeyne RJ, Goldowitz D. 1989. Development and death of external granular layer cells in the weaver mouse cerebellum: a quantitative study. J Neurosci 9(5):1608-1620.

444. Sotelo C. 1975. Dendritic abnormalities of Purkinje cells in the cerebellum of neurologic mutant mice (weaver and staggerer). Adv Neurol 12:335-351.

445. Sotelo C, Triller A. 1979. Fate of presynaptic afferents to Purkinje cells in the adult nervous mutant mouse: a model to study presynaptic stabilization. Brain Res 175(1):11-36.

446. Sotelo C. 1990a. Cerebellar synaptogenesis: what we can learn from mutant mice. J Exp Biol 153:225-249.

447. Sotelo C. 1990b. Axonal abnormalities in cerebellar Purkinje cells of the 'hyperspiny Purkinje cell' mutant mouse. J Neurocytol 19(5):737-755.

448. Sotelo C, Wassef M. 1991. Cerebellar development: afferent organization and Purkinje cell heterogeneity. Philos Trans R Soc Lond B Biol Sci 331(1261):307-313.

449. Spielhaupter C, Schatzl HM. 2001. PrPC directly interacts with proteins involved in signaling pathways. J Biol Chem 276(48):44604-44612.

450. Steele AD, Emsley JG, Ozdinler PH, Lindquist S, Macklis JD. 2006. Prion protein (PrPc) positively regulates neural precursor proliferation during developmental and adult mammalian neurogenesis. Proc Natl Acad Sci U S A 103(9):3416-3421.

451. Steele AD, King OD, Jackson WS, Hetz CA, Borkowski AW, Thielen P, Wollmann R, Lindquist S. 2007. Diminishing apoptosis by deletion of Bax or overexpression of Bcl-2 does not protect against infectious prion toxicity in vivo. J Neurosci 27(47):13022-13027.

452. Stefanis L, Larsen KE, Rideout HJ, Sulzer D, Greene LA. 2001. Expression of A53T mutant but not wild-type alpha-synuclein in PC12 cells induces alterations of the ubiquitin-dependent degradation system, loss of dopamine release, and autophagic cell death. J Neurosci 21(24):9549-9560.

453. Stefanis L. 2005. Caspase-dependent and -independent neuronal death: two distinct pathways to neuronal injury. Neuroscientist 11(1):50-62.

454. Stennicke HR, Jurgensmeier JM, Shin H, Deveraux Q, Wolf BB, Yang X, Zhou Q, Ellerby HM, Ellerby LM, Bredesen D, Green DR, Reed JC, Froelich CJ, Salvesen GS. 1998. Pro-caspase-3 is a major physiologic target of caspase-8. J Biol Chem 273(42):27084-27090.

455. Stewart RS, Piccardo P, Ghetti B, Harris DA. 2005. Neurodegenerative illness in transgenic mice expressing a transmembrane form of the prion protein. J Neurosci 25(13):3469-3477.

456. Stockel J, Safar J, Wallace AC, Cohen FE, Prusiner SB. 1998. Prion protein selectively binds copper(II) ions. Biochemistry 37(20):7185-7193.

457. Stoppini L, Buchs PA, Muller D. 1991. A simple method for organotypic cultures of nervous tissue. J Neurosci Methods 37(2):173-182.

458. Suda T, Takahashi T, Golstein P, Nagata S. 1993. Molecular cloning and expression of the Fas ligand, a novel member of the tumor necrosis factor family. Cell 75(6):1169-1178.

459. Sugihara I, Wu H, Shinoda Y. 1999. Morphology of single olivocerebellar axons labeled with biotinylated dextran amine in the rat. J Comp Neurol 414(2):131-148.

460. Sugihara I, Bailly Y, Mariani J. 2000. Olivocerebellar climbing fibers in the granuloprival cerebellum: morphological study of individual axonal projections in the X-irradiated rat. J Neurosci 20(10):3745-3760.

461. Sugihara I, Wu HS, Shinoda Y. 2001. The entire trajectories of single olivocerebellar axons in the cerebellar cortex and their contribution to Cerebellar compartmentalization. J Neurosci 21(19):7715-7723.

462. Swisher DA, Wilson DB. 1977. Cerebellar histogenesis in the lurcher (Lc) mutant mouse. J Comp Neurol 173(1):205-218.

463. Szegezdi E, Fitzgerald U, Samali A. 2003. Caspase-12 and ER-stress-mediated apoptosis: the story so far. Annals of the New York Academy of Sciences 1010:186-194.

464. Takayama C, Nakagawa S, Watanabe M, Mishina M, Inoue Y. 1995. Light- and electron-microscopic localization of the glutamate receptor channel delta 2 subunit in the mouse Purkinje cell. Neurosci Lett 188(2):89-92.

465. Takayama C, Nakagawa S, Watanabe M, Mishina M, Inoue Y. 1996. Developmental changes in expression and distribution of the glutamate receptor channel delta 2 subunit according to the Purkinje cell maturation. Brain Res Dev Brain Res 92(2):147-155.

466. Takeuchi T, Miyazaki T, Watanabe M, Mori H, Sakimura K, Mishina M. 2005. Control of synaptic connection by glutamate receptor delta2 in the adult cerebellum. J Neurosci 25(8):2146-2156.

467. Takio K, Towatari T, Katunuma N, Titani K. 1980. Primary structure study of rat liver cathepsin B -- a striking resemblance to papain. Biochem Biophys Res Commun 97(1):340-346.

468. Tanida I, Tanida-Miyake E, Ueno T, Kominami E. 2001. The human homolog of Saccharomyces cerevisiae Apg7p is a Protein-activating enzyme for multiple substrates including human Apg12p, GATE-16, GABARAP, and MAP-LC3. J Biol Chem 276(3):1701-1706.

469. Tanida I, Tanida-Miyake E, Komatsu M, Ueno T, Kominami E. 2002. Human Apg3p/Aut1p homologue is an authentic E2 enzyme for multiple substrates, GATE-16, GABARAP, and MAP-LC3, and facilitates the conjugation of hApg12p to hApg5p. J Biol Chem 277(16):13739-13744.

470. Tartaglia LA, Ayres TM, Wong GH, Goeddel DV. 1993. A novel domain within the 55 kd TNF receptor signals cell death. Cell 74(5):845-853.

471. Taylor DR, Watt NT, Perera WS, Hooper NM. 2005. Assigning functions to distinct regions of the N-terminus of the prion protein that are involved in its copper-stimulated, clathrin-dependent endocytosis. J Cell Sci 118(Pt 21):5141-5153.

472. Taylor DR, Hooper NM. 2007. The low-density lipoprotein receptor-related protein 1 (LRP1) mediates the endocytosis of the cellular prion protein. Biochem J 402(1):17-23.

473. Teismann P, Tieu K, Cohen O, Choi DK, Wu DC, Marks D, Vila M, Jackson-Lewis V, Przedborski S. 2003. Pathogenic role of glial cells in Parkinson's disease. Mov Disord 18(2):121-129.

474. Thach WT, Bastian AJ. 2004. Role of the cerebellum in the control and adaptation of gait in health and disease. Prog Brain Res 143:353-366.

475. Tiller-Borcich JK, Urich H. 1986. Abnormal arborizations of Purkinje cell dendrites in Creutzfeldt-Jakob disease: a manifestation of neuronal plasticity? J Neurol Neurosurg Psychiatry 49(5):581-584.

476. Tobler I, Gaus SE, Deboer T, Achermann P, Fischer M, Rulicke T, Moser M, Oesch B, McBride PA, Manson JC. 1996. Altered circadian activity rhythms and sleep in mice devoid of prion protein. Nature 380(6575):639-642.

477. Tobler I, Deboer T, Fischer M. 1997. Sleep and sleep regulation in normal and prion protein-deficient mice. J Neurosci 17(5):1869-1879.

478. Toni M, Spisni E, Griffoni C, Santi S, Riccio M, Lenaz P, Tomasi V. 2006. Cellular prion protein and caveolin-1 interaction in a neuronal cell line precedes fyn/erk 1/2 signal transduction. J Biomed Biotechnol 2006(5):69469.

479. Tranulis MA, Espenes A, Comincini S, Skretting G, Harbitz I. 2001. The PrP-like protein Doppel gene in sheep and cattle: cDNA sequence and expression. Mamm Genome 12(5):376-379.

480. Troncoso JC, Sukhov RR, Kawas CH, Koliatsos VE. 1996. In situ labeling of dying cortical neurons in normal aging and in Alzheimer's disease: correlations with senile plaques and disease progression. J Neuropathol Exp Neurol 55(11):1134-1142.

481. Tsujimoto Y, Croce CM. 1986. Analysis of the structure, transcripts, and protein products of bcl-2, the gene involved in human follicular lymphoma. Proc Natl Acad Sci U S A 83(14):5214-5218.

482. Tsujimoto Y, Shimizu S. 2005. Another way to die: autophagic programmed cell death. Cell Death Differ 12 Suppl 2:1528-1534.

483. Turmaine M, Raza A, Mahal A, Mangiarini L, Bates GP, Davies SW. 2000. Nonapoptotic neurodegeneration in a transgenic mouse model of Huntington's disease. Proc Natl Acad Sci U S A 97(14):8093-8097.

484. Uchiyama Y. 2001. Autophagic cell death and its execution by lysosomal cathepsins. Arch Histol Cytol 64(3):233-246.

485. Uemura T, Mori H, Mishina M. 2004. Direct interaction of GluRdelta2 with Shank scaffold proteins in cerebellar Purkinje cells. Mol Cell Neurosci 26(2):330-341.

486. Uemura T, Kakizawa S, Yamasaki M, Sakimura K, Watanabe M, Iino M, Mishina M. 2007. Regulation of long-term depression and climbing fiber territory by glutamate receptor delta2

at parallel fiber synapses through its C-terminal domain in cerebellar Purkinje cells. J Neurosci 27(44):12096-12108.

487. Unterberger U, Voigtlander T, Budka H. 2005. Pathogenesis of prion diseases. Acta Neuropathol 109(1):32-48.

488. Valenti P, Cozzio A, Nishida N, Wolfer DP, Sakaguchi S, Lipp HP. 2001. Similar target, different effects: late-onset ataxia and spatial learning in prion protein-deficient mouse lines. Neurogenetics 3(4):173-184.

489. Vey M, Pilkuhn S, Wille H, Nixon R, DeArmond SJ, Smart EJ, Anderson RG, Taraboulos A, Prusiner SB. 1996. Subcellular colocalization of the cellular and scrapie prion proteins in caveolae-like membranous domains. Proc Natl Acad Sci U S A 93(25):14945-14949.

490. Volsen SG, Day NC, McCormack AL, Smith W, Craig PJ, Beattie R, Ince PG, Shaw PJ, Ellis SB, Gillespie A, et al. 1995. The expression of neuronal voltage-dependent calcium channels in human cerebellum. Brain Res Mol Brain Res 34(2):271-282.

491. Voogd J, Glickstein M. 1998. The anatomy of the cerebellum. Trends Neurosci 21(9):370-375.

492. Voogd J, Ruigrok TJ. 2004. The organization of the corticonuclear and olivocerebellar climbing fiber projections to the rat cerebellar vermis: the congruence of projection zones and the zebrin pattern. J Neurocytol 33(1):5-21.

493. Wallesch CW, Horn A. 1990. Long-term effects of cerebellar pathology on cognitive functions. Brain Cogn 14(1):19-25.

494. Walter ED, Chattopadhyay M, Millhauser GL. 2006. The affinity of copper binding to the prion protein octarepeat domain: evidence for negative cooperativity. Biochemistry 45(43):13083-13092.

495. Walter ED, Stevens DJ, Visconte MP, Millhauser GL. 2007. The prion protein is a combined zinc and copper binding protein: Zn2+ alters the distribution of Cu2+ coordination modes. J Am Chem Soc 129(50):15440-15441.

496. Wang CW, Klionsky DJ. 2003. The molecular mechanism of autophagy. Mol Med 9(3-4):65-76.

497. Wang QJ, Ding Y, Kohtz DS, Mizushima N, Cristea IM, Rout MP, Chait BT, Zhong Y, Heintz N, Yue Z. 2006. Induction of autophagy in axonal dystrophy and degeneration. J Neurosci 26(31):8057-8068.

498. Wang X. 2001. The expanding role of mitochondria in apoptosis. Genes Dev 15(22):2922-2933.

499. Wang Y, Matsuda S, Drews V, Torashima T, Meisler MH, Yuzaki M. 2003. A hot spot for hotfoot mutations in the gene encoding the delta2 glutamate receptor. Eur J Neurosci 17(8):1581-1590.

500. Wassef M, Simons J, Tappaz ML, Sotelo C. 1986. Non-Purkinje cell GABAergic innervation of the deep cerebellar nuclei: a quantitative immunocytochemical study in C57BL and in Purkinje cell degeneration mutant mice. Brain Res 399(1):125-135.

501. Wassef M, Sotelo C, Cholley B, Brehier A, Thomasset M. 1987. Cerebellar mutations affecting the postnatal survival of Purkinje cells in the mouse disclose a longitudinal pattern of differentially sensitive cells. Dev Biol 124(2):379-389.

502. Wassef M, Cholley B, Heizmann CW, Sotelo C. 1992. Development of the olivocerebellar projection in the rat: II. Matching of the developmental compartmentations of the cerebellum and inferior olive through the projection map. J Comp Neurol 323(4):537-550.

503. Watts JC, Drisaldi B, Ng V, Yang J, Strome B, Horne P, Sy MS, Yoong L, Young R, Mastrangelo P, Bergeron C, Fraser PE, Carlson GA, Mount HT, Schmitt-Ulms G, Westaway D. 2007. The CNS glycoprotein Shadoo has PrP(C)-like protective properties and displays reduced levels in prion infections. Embo J 26(17):4038-4050.

504. Watts JC, Westaway D. 2007. The prion protein family: diversity, rivalry, and dysfunction. Biochimica et biophysica acta 1772(6):654-672.

505. Webb JL, Ravikumar B, Atkins J, Skepper JN, Rubinsztein DC. 2003. Alpha-Synuclein is degraded by both autophagy and the proteasome. J Biol Chem 278(27):25009-25013.

506. Weber CH, Vincenz C. 2001. A docking model of key components of the DISC complex: death domain superfamily interactions redefined. FEBS Lett 492(3):171-176.

507. Wegiel J, Wisniewski HM, Morys J, Tarnawski M, Kuchna I, Dziewiatkowski J, Pirttila T, Krivimaki T, Lehtimaki T, Lach B. 1999. Neuronal loss and beta-amyloid removal in the amygdala of people with Down syndrome. Neurobiol Aging 20(3):259-269.

508. Weise J, Sandau R, Schwarting S, Crome O, Wrede A, Schulz-Schaeffer W, Zerr I, Bahr M. 2006. Deletion of cellular prion protein results in reduced Akt activation, enhanced postischemic caspase-3 activation, and exacerbation of ischemic brain injury. Stroke 37(5):1296-1300.

509. Weissmann C. 1991. A 'unified theory' of prion propagation. Nature 352(6337):679-683.

510. Weissmann C, Aguzzi A. 1999. Perspectives: neurobiology. PrP's double causes trouble. Science 286(5441):914-915.

511. Wells MA, Jackson GS, Jones S, Hosszu LL, Craven CJ, Clarke AR, Collinge J, Waltho JP. 2006a. A reassessment of copper(II) binding in the full-length prion protein. Biochem J 399(3):435-444.

512. Wells MA, Jelinska C, Hosszu LL, Craven CJ, Clarke AR, Collinge J, Waltho JP, Jackson GS. 2006b. Multiple forms of copper (II) co-ordination occur throughout the disordered N-terminal region of the prion protein at pH 7.4. Biochem J 400(3):501-510.

513. Welsh JP, Yuen G, Placantonakis DG, Vu TQ, Haiss F, O'Hearn E, Molliver ME, Aicher SA. 2002. Why do Purkinje cells die so easily after global brain ischemia? Aldolase C, EAAT4, and the cerebellar contribution to posthypoxic myoclonus. Adv Neurol 89:331-359.

514. Wen LP, Fahrni JA, Troie S, Guan JL, Orth K, Rosen GD. 1997. Cleavage of focal adhesion kinase by caspases during apoptosis. J Biol Chem 272(41):26056-26061.

515. Wetts R, Herrup K. 1982. Interaction of granule, Purkinje and inferior olivary neurons in lurcher chimaeric mice. I. Qualitative studies. J Embryol Exp Morphol 68:87-98.

516. White AR, Collins SJ, Maher F, Jobling MF, Stewart LR, Thyer JM, Beyreuther K, Masters CL, Cappai R. 1999. Prion protein-deficient neurons reveal lower glutathione reductase activity and increased susceptibility to hydrogen peroxide toxicity. Am J Pathol 155(5):1723-1730.

517. White FA, Keller-Peck CR, Knudson CM, Korsmeyer SJ, Snider WD. 1998. Widespread elimination of naturally occurring neuronal death in Bax-deficient mice. J Neurosci 18(4):1428-1439.

518. Whittington MA, Sidle KC, Gowland I, Meads J, Hill AF, Palmer MS, Jefferys JG, Collinge J. 1995. Rescue of neurophysiological phenotype seen in PrP null mice by transgene encoding human prion protein. Nat Genet 9(2):197-201.

519. Wollmuth LP, Kuner T, Jatzke C, Seeburg PH, Heintz N, Zuo J. 2000. The Lurcher mutation identifies delta 2 as an AMPA/kainate receptor-like channel that is potentiated by Ca(2+). J Neurosci 20(16):5973-5980.

520. Wolter KG, Hsu YT, Smith CL, Nechushtan A, Xi XG, Youle RJ. 1997. Movement of Bax from the cytosol to mitochondria during apoptosis. Journal of Cell Biology 139(5):1281-1292.

521. Wong BS, Liu T, Paisley D, Li R, Pan T, Chen SG, Perry G, Petersen RB, Smith MA, Melton DW, Gambetti P, Brown DR, Sy MS. 2001. Induction of HO-1 and NOS in doppel-expressing mice devoid of PrP: implications for doppel function. Mol Cell Neurosci 17(4):768-775.

522. Wullner U, Loschmann PA, Weller M, Klockgether T. 1995. Apoptotic cell death in the cerebellum of mutant weaver and lurcher mice. Neurosci Lett 200(2):109-112.

523. Wullner U, Weller M, Schulz JB, Krajewski S, Reed JC, Klockgether T. 1998. Bcl-2, Bax and Bcl-x expression in neuronal apoptosis: a study of mutant weaver and lurcher mice. Acta Neuropathol 96(3):233-238.

524. Xu Y, Kim SO, Li Y, Han J. 2006. Autophagy contributes to caspase-independent macrophage cell death. J Biol Chem 281(28):19179-19187.

525. Yamamoto N, Kurotani T, Toyama K. 1989. Neural connections between the lateral geniculate nucleus and visual cortex in vitro. Science 245(4914):192-194.

526. Yamashita A, Makita K, Kuroiwa T, Tanaka K. 2006. Glutamate transporters GLAST and EAAT4 regulate postischemic Purkinje cell death: an in vivo study using a cardiac arrest model in mice lacking GLAST or EAAT4. Neurosci Res 55(3):264-270.

527. Yang Z, Huang J, Geng J, Nair U, Klionsky DJ. 2006. Atg22 recycles amino acids to link the degradative and recycling functions of autophagy. Mol Biol Cell 17(12):5094-5104.

528. Yap CC, Muto Y, Kishida H, Hashikawa T, Yano R. 2003a. PKC regulates the delta2 glutamate receptor interaction with S-SCAM/MAGI-2 protein. Biochem Biophys Res Commun 301(4):1122-1128.

529. Yap CC, Murate M, Kishigami S, Muto Y, Kishida H, Hashikawa T, Yano R. 2003b. Adaptor protein complex-4 (AP-4) is expressed in the central nervous system neurons and interacts with glutamate receptor delta2. Mol Cell Neurosci 24(2):283-295.

530. Yasumura M, Uemura T, Yamasaki M, Sakimura K, Watanabe M, Mishina M. 2008. Role of the internal Shank-binding segment of glutamate receptor delta2 in synaptic localization and cerebellar functions. Neurosci Lett 433(2):146-151.

531. Yawata S, Tsuchida H, Kengaku M, Hirano T. 2006. Membrane-proximal region of glutamate receptor delta2 subunit is critical for long-term depression and interaction with protein interacting with C kinase 1 in a cerebellar Purkinje neuron. J Neurosci 26(14):3626-3633.

532. Yedidia Y, Horonchik L, Tzaban S, Yanai A, Taraboulos A. 2001. Proteasomes and ubiquitin are involved in the turnover of the wild-type prion protein. Embo J 20(19):5383-5391.

533. Yin SM, Sy MS, Yang HY, Tien P. 2004. Interaction of Doppel with the full-length laminin receptor precursor protein. Archives of Biochemistry & Biophysics 428(2):165-169.

534. Yoshida T, Katoh A, Ohtsuki G, Mishina M, Hirano T. 2004. Oscillating Purkinje neuron activity causing involuntary eye movement in a mutant mouse deficient in the glutamate receptor delta2 subunit. J Neurosci 24(10):2440-2448.

535. Yoshikawa D, Kopacek J, Yamaguchi N, Ishibashi D, Yamanaka H, Yamaguchi Y, Katamine S, Sakaguchi S. 2007. Newly established in vitro system with fluorescent proteins shows that abnormal expression of downstream prion protein-like protein in mice is probably due to functional disconnection between splicing and 3' formation of prion protein pre-mRNA. Gene 386(1-2):139-146.

536. Yousefi S, Perozzo R, Schmid I, Ziemiecki A, Schaffner T, Scapozza L, Brunner T, Simon HU. 2006. Calpain-mediated cleavage of Atg5 switches autophagy to apoptosis. Nat Cell Biol 8(10):1124-1132.

537. Yu L, Alva A, Su H, Dutt P, Freundt E, Welsh S, Baehrecke EH, Lenardo MJ. 2004. Regulation of an ATG7-beclin 1 program of autophagic cell death by caspase-8. Science 304(5676):1500-1502.

538. Yu WH, Cuervo AM, Kumar A, Peterhoff CM, Schmidt SD, Lee JH, Mohan PS, Mercken M, Farmery MR, Tjernberg LO, Jiang Y, Duff K, Uchiyama Y, Naslund J, Mathews PM, Cataldo AM, Nixon RA. 2005. Macroautophagy--a novel Beta-amyloid peptide-generating pathway activated in Alzheimer's disease. J Cell Biol 171(1):87-98.

539. Yuan J, Shaham S, Ledoux S, Ellis HM, Horvitz HR. 1993. The C. elegans cell death gene ced-3 encodes a protein similar to mammalian interleukin-1 beta-converting enzyme. Cell 75(4):641-652.

540. Yuan J, Yankner BA. 2000. Apoptosis in the nervous system. Nature 407(6805):802-809.

541. Yue Z, Horton A, Bravin M, DeJager PL, Selimi F, Heintz N. 2002. A novel protein complex linking the delta 2 glutamate receptor and autophagy: implications for neurodegeneration in lurcher mice. Neuron 35(5):921-933.

542. Yuzaki M. 2003. The delta2 glutamate receptor: 10 years later. Neurosci Res 46(1):11-22.

543. Zanata SM, Lopes MH, Mercadante AF, Hajj GN, Chiarini LB, Nomizo R, Freitas AR, Cabral AL, Lee KS, Juliano MA, de Oliveira E, Jachieri SG, Burlingame A, Huang L, Linden R, Brentani RR, Martins VR. 2002. Stress-inducible protein 1 is a cell surface ligand for cellular prion that triggers neuroprotection. Embo J 21(13):3307-3316.

544. Zanjani H, Rondi-Reig L, Vogel M, Martinou JC, Delhaye-Bouchaud N, Mariani J. 1998a. Overexpression of a Hu-bcl-2 transgene in Lurcher mutant mice delays Purkinje cell death. C R Acad Sci III 321(8):633-640.

545. Zanjani HS, Vogel MW, Delhaye-Bouchaud N, Martinou JC, Mariani J. 1996. Increased cerebellar Purkinje cell numbers in mice overexpressing a human bcl-2 transgene. J Comp Neurol 374(3):332-341.

546. Zanjani HS, Vogel MW, Martinou JC, Delhaye-Bouchaud N, Mariani J. 1998b. Postnatal expression of Hu-bcl-2 gene in Lurcher mutant mice fails to rescue Purkinje cells but protects inferior olivary neurons from target-related cell death. J Neurosci 18(1):319-327.

547. Zhang Y, Qin K, Wang J, Hung T, Zhao RY. 2006. Dividing roles of prion protein in staurosporine-mediated apoptosis. Biochem Biophys Res Commun 349(2):759-768.

548. Zhao HM, Wenthold RJ, Wang YX, Petralia RS. 1997. Delta-glutamate receptors are differentially distributed at parallel and climbing fiber synapses on Purkinje cells. J Neurochem 68(3):1041-1052.

549. Zhao L, Longo-Guess C, Harris BS, Lee JW, Ackerman SL. 2005. Protein accumulation and neurodegeneration in the woozy mutant mouse is caused by disruption of SIL1, a cochaperone of BiP. Nat Genet 37(9):974-979.

550. Zheng TS, Flavell RA. 2000. Divinations and surprises: genetic analysis of caspase function in mice. Exp Cell Res 256(1):67-73.

551. Zhu W, Cowie A, Wasfy GW, Penn LZ, Leber B, Andrews DW. 1996. Bcl-2 mutants with restricted subcellular location reveal spatially distinct pathways for apoptosis in different cell types. EMBO Journal 15(16):4130-4141.

552. Zidar J, Pirc ET, Hodoscek M, Bukovec P. 2008. Copper(II) ion binding to cellular prion protein. J Chem Inf Model 48(2):283-287.

553. Zion C, Auvray N, Caston J, Reber A, Stelz T. 1990. Effects of cerebellectomy at day 15 on the ontogenesis of the equilibrium behavior in the rat. Brain Res 515(1-2):104-110.

554. Zong WX, Li C, Hatzivassiliou G, Lindsten T, Yu QC, Yuan J, Thompson CB. 2003. Bax and Bak can localize to the endoplasmic reticulum to initiate apoptosis. Journal of Cell Biology 162(1):59-69.

555. Zong WX, Ditsworth D, Bauer DE, Wang ZQ, Thompson CB. 2004. Alkylating DNA damage stimulates a regulated form of necrotic cell death. Genes Dev 18(11):1272-1282.

556. Zou H, Henzel WJ, Liu X, Lutschg A, Wang X. 1997. Apaf-1, a human protein homologous to C. elegans CED-4, participates in cytochrome c-dependent activation of caspase-3.[see comment]. Cell 90(3):405-413.

557. Zuo J, De Jager PL, Takahashi KA, Jiang W, Linden DJ, Heintz N. 1997. Neurodegeneration in Lurcher mice caused by mutation in delta2 glutamate receptor gene. Nature 388(6644):769-773.

Communications

Scientific articles

2008 Heitz S, Leschiera R, Haeberlé A-M, Demais V, Grant N, Bombarde G, Bailly Y. Autophagy and cell death of Purkinje cells overexpressing Doppel in Ngsk Prnp-deficient mice. **Brain Pathol,** *in review*

Heitz S, Gautheron V, Lutz Y, Rodeau J-L, Zanjani HS, Sugihara I, Bombarde G, Richard F, Fuchs J-P, Vogel MW, Mariani J, Bailly Y
BCL-2 counteracts Dpl-induced apoptosis of prion protein-deficient Purkinje cells in the Ngsk $Prnp^{0/0}$ mouse. **Dev Neurobiol**, (2008) 68:332-348

2007 Heitz S, Zanjani H, Lutz Y, Gautheron V, Bombarde G, Richard F, Fuchs JP, Vogel M, Mariani J, Bailly Y.
Bax contributes to Doppel-induced apoptosis of prion protein-deficient Purkinje cells. **Dev Neurobiol** (2007) 67:670-686.

2003 Selimi F, Lohof AM, Heitz S, Lalouette A, Jarvis CI, Bailly Y, Mariani J.
Lurcher GRID2-induced death and depolarization can be dissociated in cerebellar Purkinje cells. **Neuron** (2003) 37:813-9.

Oral communications

2005 Communication at « II international symposium on the new prion biology » (Venice, avril 2005)
Heitz S, Bailly Y. Bax mediated neurotoxicity of Doppel in the Purkinje cells of the *NgskPrnp*KO mouse line.

Posters

2008

Poster at the FENS 6th forum (Geneva, July 2008)
Bailly Y, Haeberle AM, Demais V, Grant N, Bombarde G, Heitz S.
Autophagic cell death of Purkinje cells in Doppel-expressing prion protein-deficient mice.

Poster at « first European synapse meeting » (Bordeaux, march 2008)
Gambino F, Pavlowsky A, Heitz S, Billuart P, Poulain B, Chelly J and Humeau Y. Cerebellar synaptic transmission in a mouse model of mental retardation.

2007

Poster at Abcam meeting « Molecular mechanisms of neurodegeneration » (Antigua, december 2007)
Heitz S, Haeberlé AM, Bombarde G, Richard F, Dron M, Dandoy-Dron F, Bailly Y. Doppel-induced cell death mechanism(s) in prion protein deficient Purkinje cells: apoptosis or autophagy?

Poster at the Colloque de la Société des Neurosciences (Montpellier, mai 2007)
Heitz S, Kapfhammer J, Bailly Y. Synaptic and dendritic development of the cerebellar Purkinje cells in GluRδ2 (GRID2) mutant mice: focus on autophagy and glutamate receptors.

2006

Poster at the FENS 5th forum (Vienna, july 2006)
Heitz S, Zanjani H, Mariani J, Bailly Y. *Bax* knock-out as well as HuBcl-2 save Purkinje cells from Doppel-induced apoptosis *in vivo*.

2005

Poster at the « Society for Neurosciences » 35th meeting (Washington, november 2005)
Bailly Y, Heitz S, Zanjani H, Mariani J. *Bax* knock-out as well as HuBcl-2 save Purkinje cells from Doppel-induced apoptosis *in vivo*.

Poster at the Colloque de la société des Neurosciences (Lille, mai 2005)
Bailly Y, Zanjani H, Mariani J, Heitz S. HuBcl-2 saves Purkinje cells from Dpl-induced apoptosis in the cerebellum of the NgskPrnp$^{0/0}$ mouse.

Poster at the « II international symposium on the new prion biology » (Venice, april 2005)
Poster at the Neurex meeting (Strasbourg, april 2005)
Heitz S, Bailly Y. Bax mediated neurotoxicity of Doppel in the Purkinje cells of the *NgskPrnp*KO mouse line.

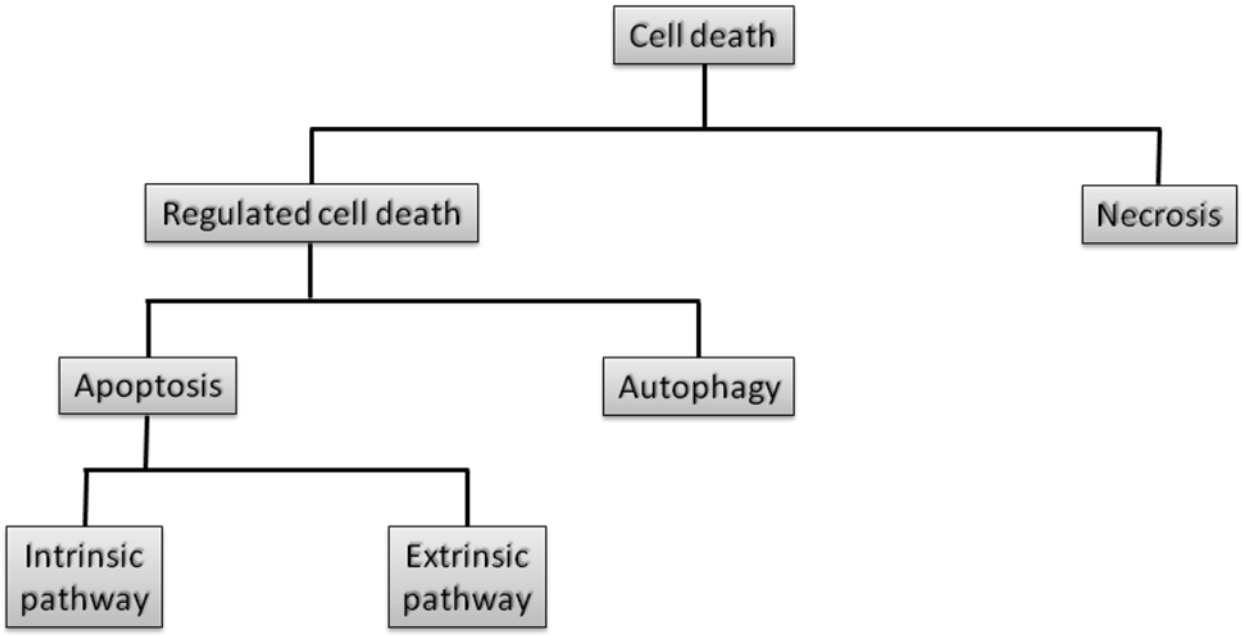

Figure 1. Cell death pathways. (Modified from Chowdhury et al., 2006)

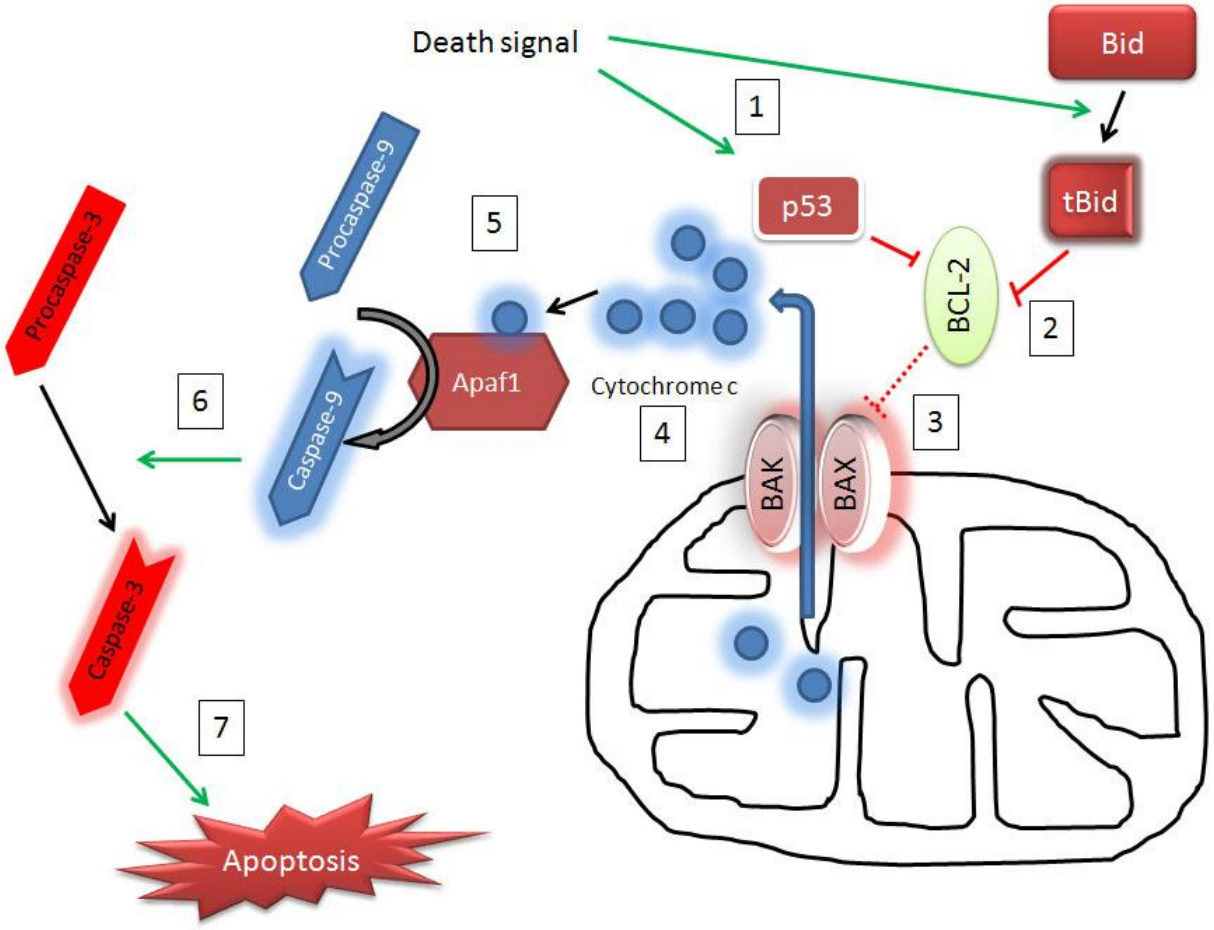

Figure 2. The intrinsic apoptotic pathway.

A death signal (1) will either activate p53 or induce the cleavage of the BH3-only pro-apoptotic factor Bid, resulting in the inhibition of BCL-2. The inhibitor effect of BCL-2 on BAX or BAK (3) will be suppressed, allowing BAX and BAK to form heterodimers and a pore in the mitochondrial outer membrane, resulting in the massive liberation of cytochrome c (4). Cytochrome c-bound Apaf1 will cleave the procaspase-9 into an active initiator caspase-9 (5) which in turn will cleave the effector procaspase-3 (6) into active caspase-3. (7) Active caspase-3 will induce DNA damages, dismantling of the cellular architecture and cell death.

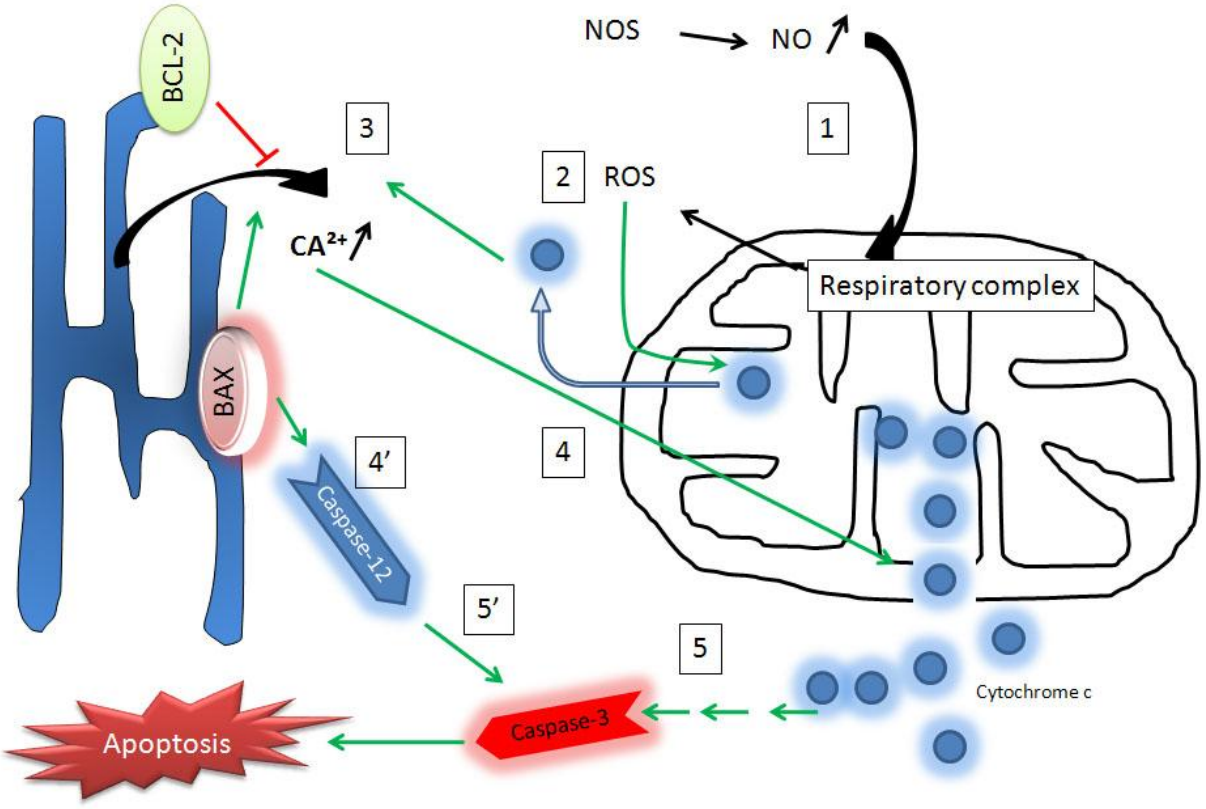

Figure 3. ROS induces ER stress and a caspases-dependent apoptotis.

Nitric oxide activates the mitochondrial respiratory complex (1) and the production of ROS. ROS-mediated MOMP will induce cytochrome c efflux to the cytoplasm (2) resulting in the massive liberation of Ca^{2+} from the ER (3). This Ca^{2+} liberation is regulated by BCL-2 and BAX. The massive liberation of Ca^{2+} will potentiate the MOMP resulting in a massive liberation of mitochondrial cytochrome c (4) and in caspase-3 dependent apoptosis (5). Activated BAX in the ER membrane can itself induce the caspase 12 activation (4') and subsequent caspase 3 activation (5').

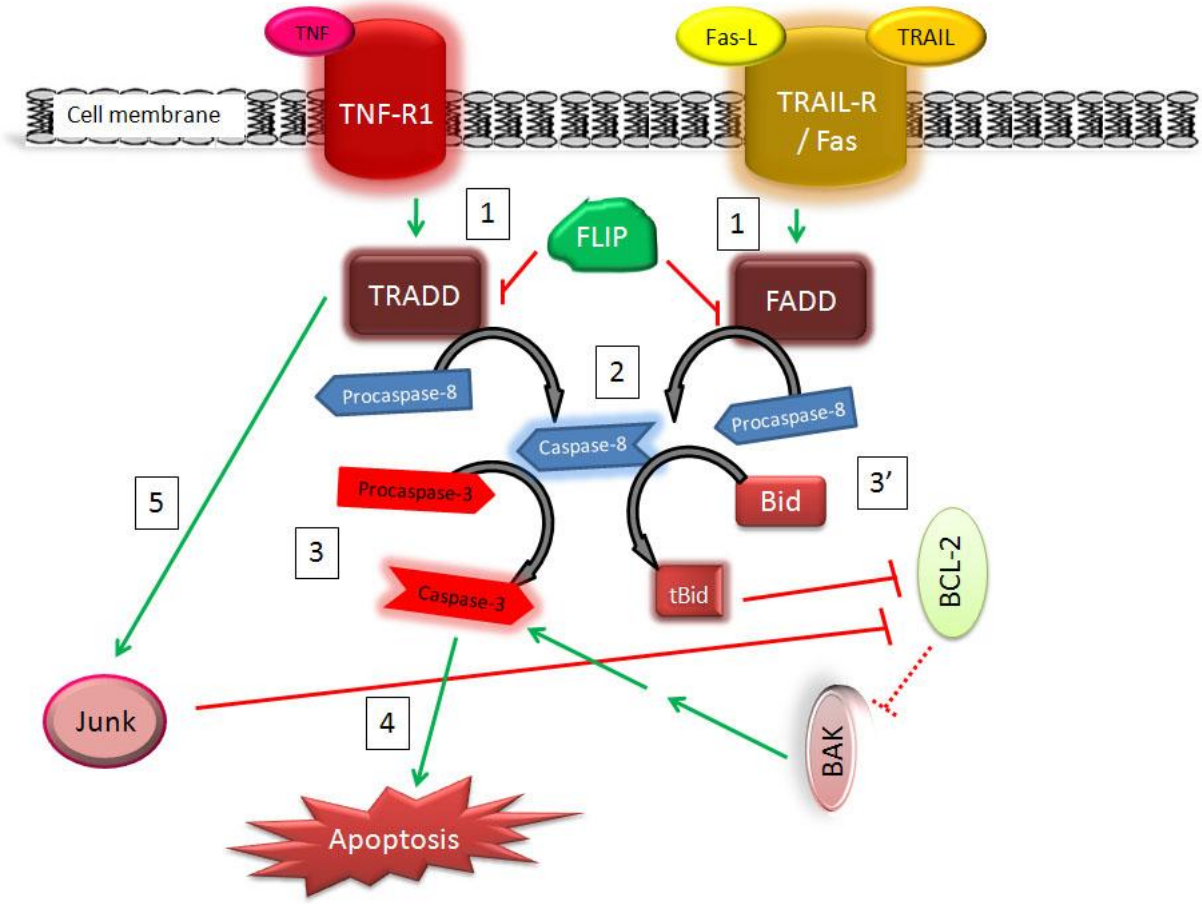

Figure 4. The apoptotic extrinsic pathways.

Death receptors TNF-R1, TRAIL-R and Fas are activated by their ligands and activate TRADD or FADD (1) via their death domain. TRADD and FADD will activate caspase-8 (2). The activate caspase-8 will directly activate caspase-3 (3). Caspase-8 can also cleave Bid into truncated Bid (3'), which inhibits BCL-2. This activates the intrinsic pathway and ultimately to caspase-3-dependent apoptosis (4). Potentiation of the apoptosis can also result from BCL-2 inhibition by TRADD-activated JUNK (5).

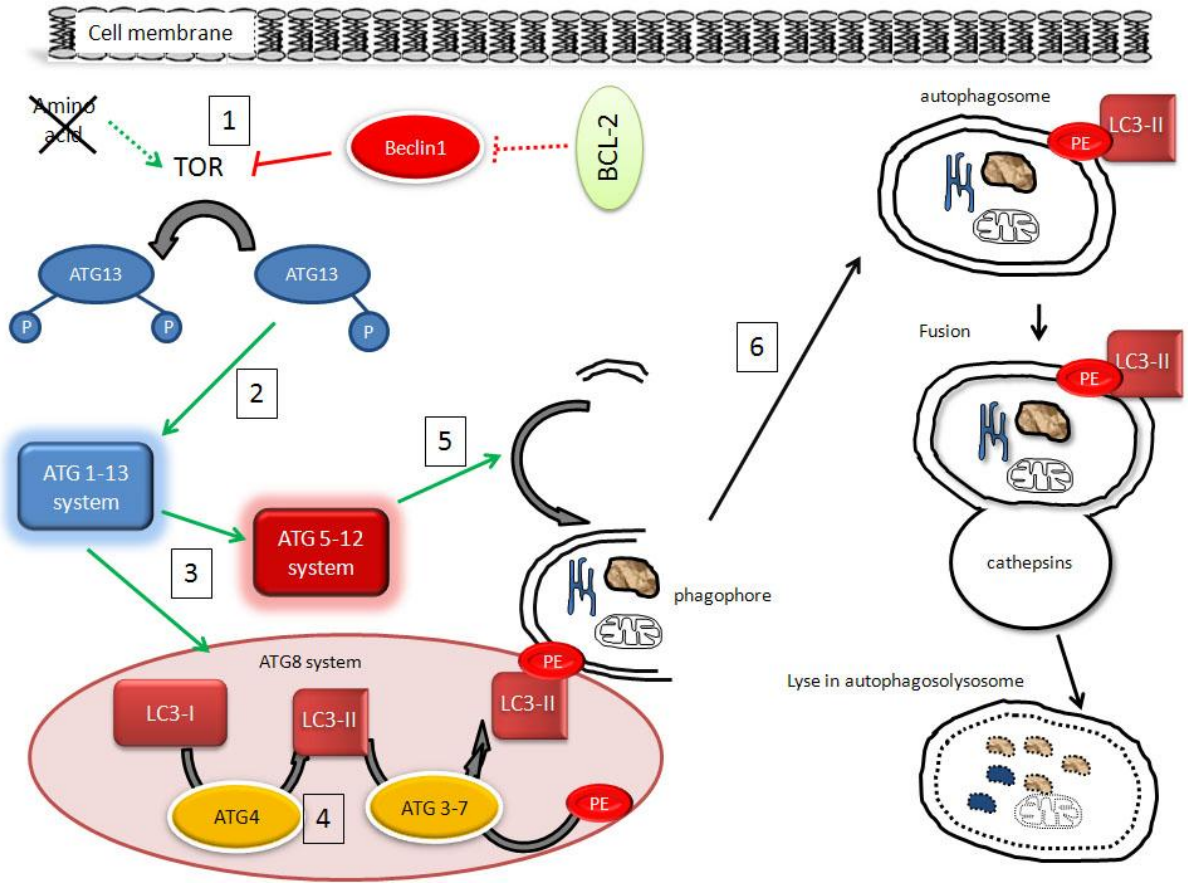

Figure 5. Induction and completion of the autophagic cascade.

(1) In the absence of nutrients and under Beclin1-dependent inhibition, TOR cannot maintain ATG13 phosphorylation. The dephosphorylated ATG13 will form an ATG 1-13 complex (2) which activates the ATG 5-12 and the ATG8 conjugation systems (3). ATG 5-12 will recruit an isolation membrane (5) while LC3-I is cleaved by ATG4 into its LC3-II form (4) in the ATG8 conjugation system. A phosphatidylethanolamine (PE) will be bound to LC3-II by ATG3 and 7. This allows the sequestration of cytoplasm in a double-membraned autophagic vacuole or autophagosome (6) The autophagosome resulting from the isolation membrane elongation will fuse with a lysosome to form an autophagolysosome. The lysosomal cathepsins will finally degrade the autophagic body.

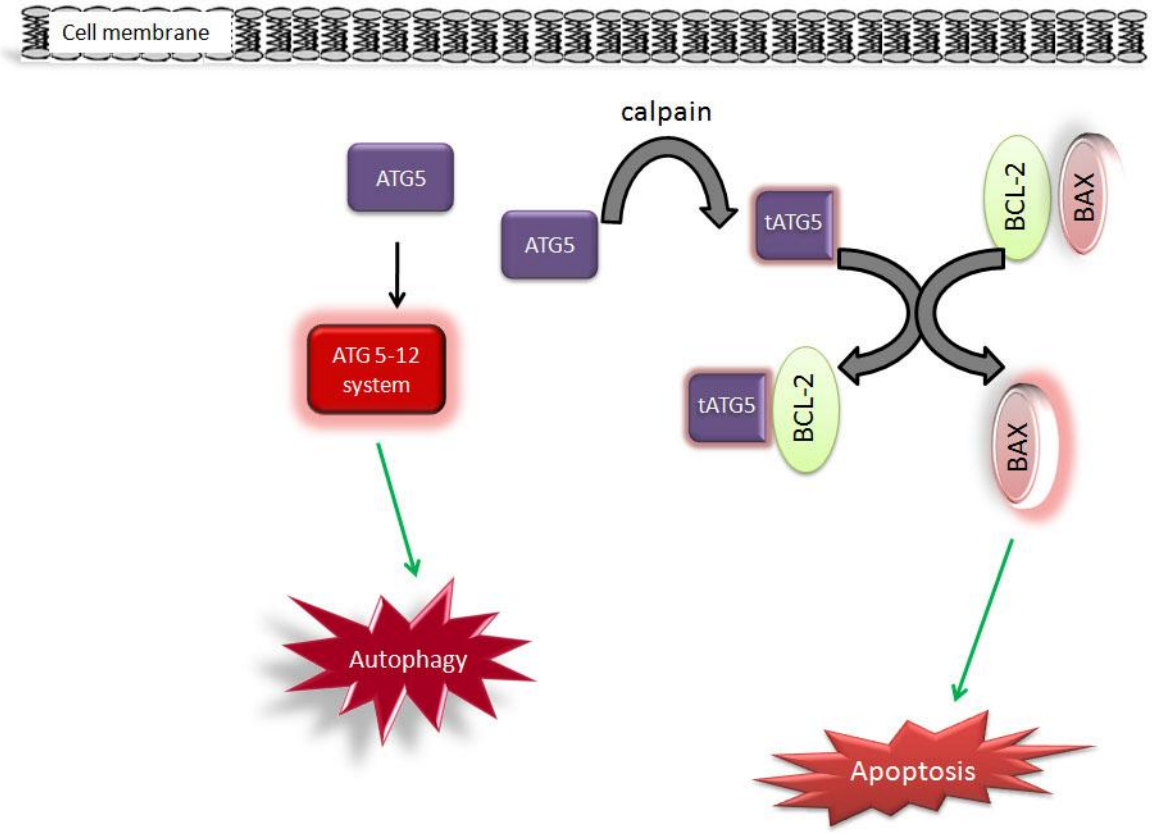

Figure 6. ATG5 mediates interplay between autophagic and intrinsic apoptotic pathways.

Truncated tATG5 resulting from the cleavage of ATG5 by calpains is able to dissociate the BCL-2/BAX complex. This allows tATG5 to bind BCL-2 via a BH3-like domain and BAX to exert pro-apoptotic activity.

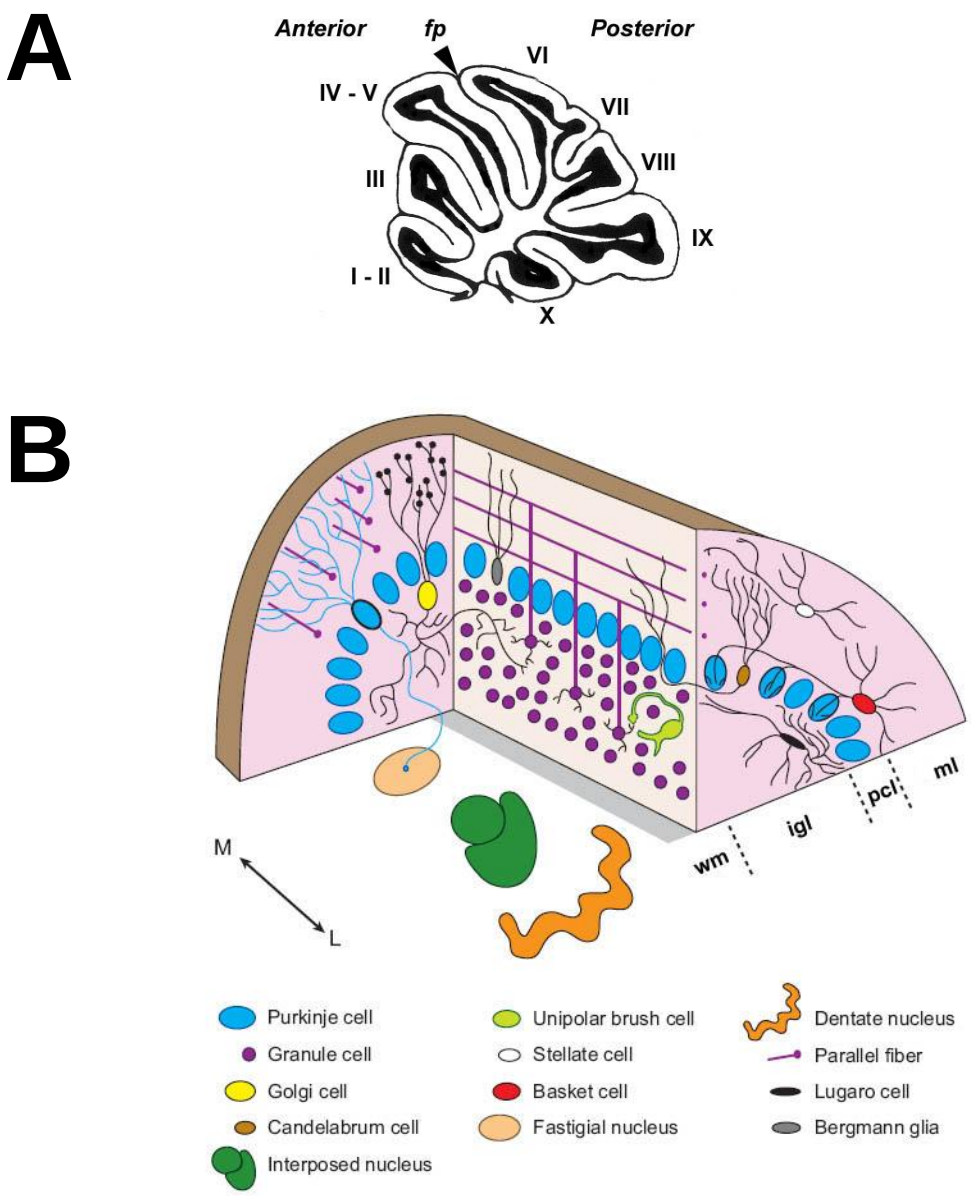

Figure 7. Anatomical organization of the cerebellar cortex.

A. Foliation of the C57Bl6 mouse cerebellum. The cerebellum is divided into anterior and posterior lobes by the fissura principalis (fp). Supplemental fissures further subdivide the anterior and posterior lobes into transversally oriented lobules I to X (Modified from Inouye and Oda, 1980).

B. Neuronal composition of the cerebellar cortex. ml, molecular layer. pcl, Purkinje cell layer. igl, internal granular layer. wm, white matter (Modified from Sillitoe and Joyner, 2007).

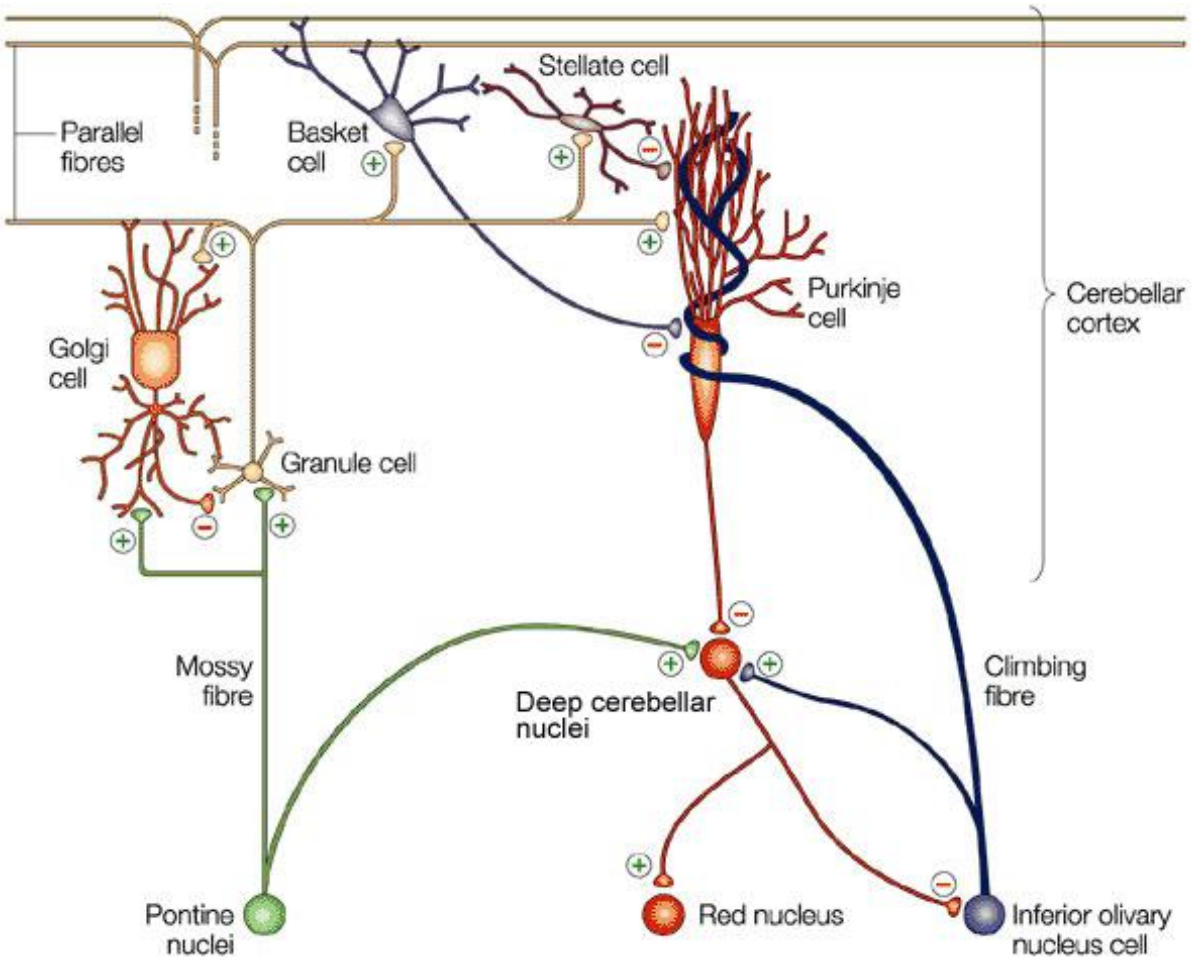

Figure 8. Schematic diagram of the cerebellar circuit with marked excitatory (+) and inhibitory (-) innervation (Modified from Medina et al., 2002)

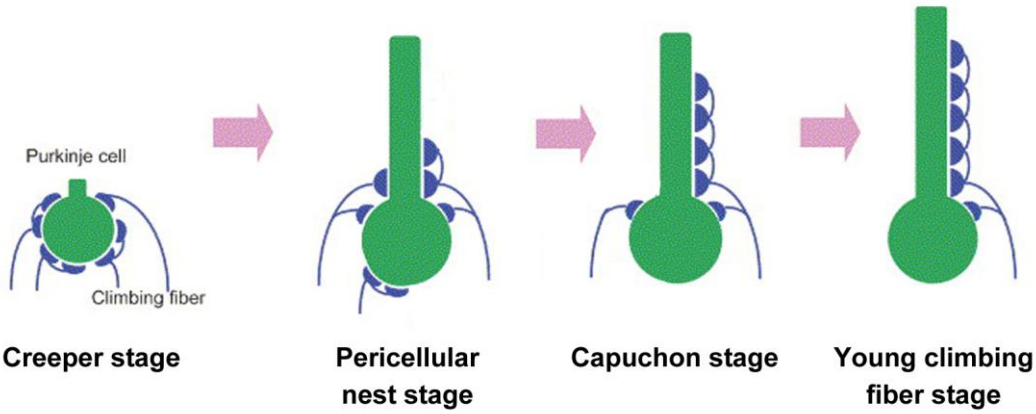

Figure 9. Climbing fiber differentiation during postnatal development. (Modified from Hashimoto and Kano, 2005)

At the “creeper stage” (P3), most Purkinje cells are innervated by 3 or more climbing fibers. Around P5, the peak of the “nest stage” corresponds to the peak of multiple innervation of Purkinje cells by climbing fibers. During the “capuchon stage” (P7-P10), the climbing fiber somato-dendritic translocation correlates with an abrupt decline of the multiple innervation. Then, the adult numerical relationship of one climbing fiber per one Purkinje cell is finally established.

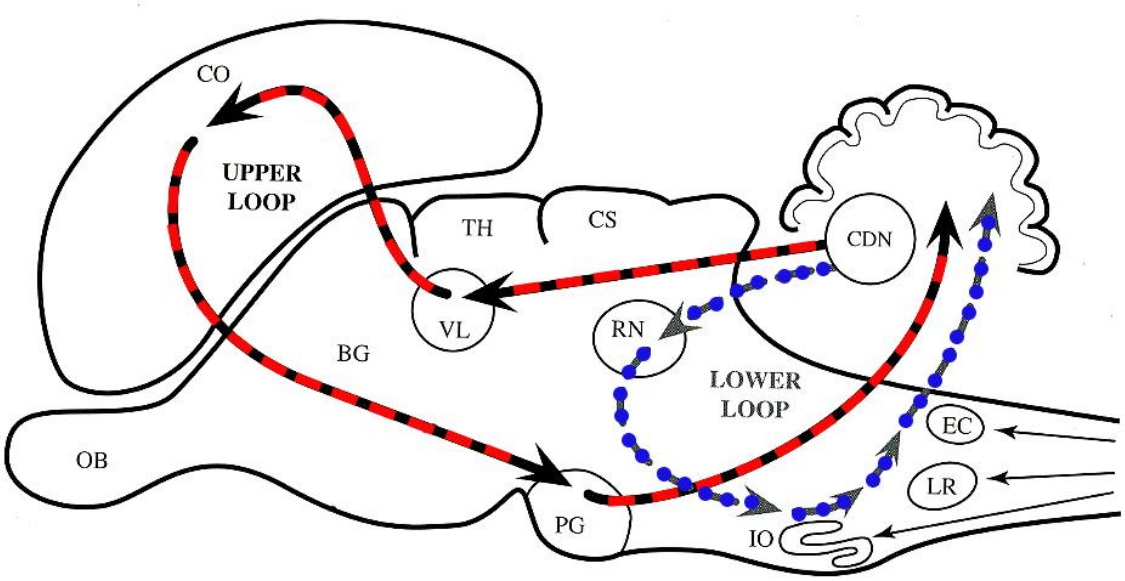

Figure 10. Schematic diagram outlining the major efferent pathways of the deep cerebellar nuclei. (Modified from Altman and Bayer, 1997)

Within the lower closed loop (blue), there are also projections from the red nucleus to the deep cerebellar nuclei (direct) or via the precerebellar nuclei to the deep cerebellar nuclei (indirect). The upper closed loop (red) predominantly involves the thalamus, cerebral cortex and pontine grey nuclei.

CO=cerebral cortex, BG=basal ganglia, TH=Thalamus, VL=ventrolateral thalamus, CS=superior colliculus, RN=red nucleus, PG=pontine grey nucleus, IO=inferior olive, DCN=deep cerebellar nuclei, LR=lateral reticular nucleus, EC=external cuneate nucleus.

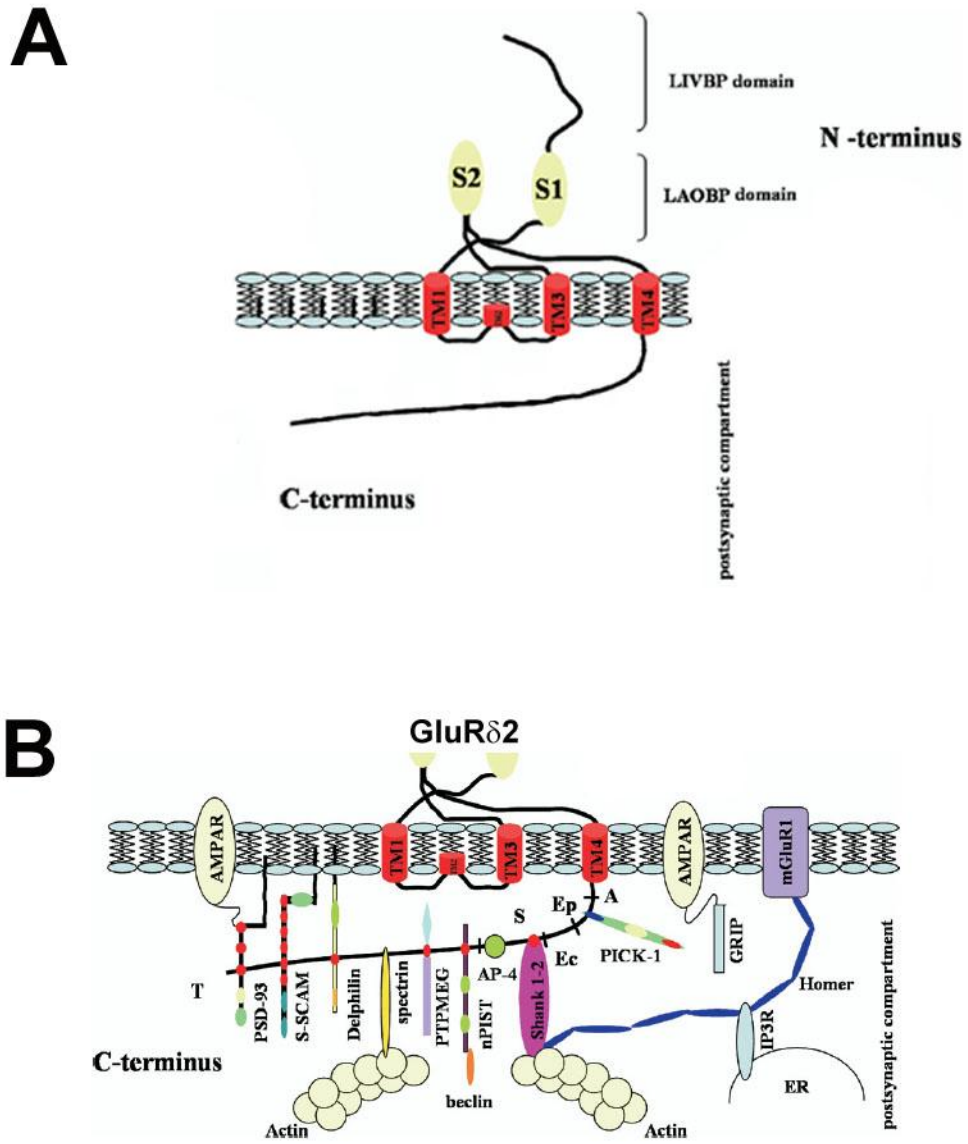

Figure 11. Structure of GluRδ2 and C-terminal partners. (Modified from Mandolesi et al., 2008)

A. The N-terminus region of GluRδ2 contains a LIVBP-like domain, a LAOBP-like domain which is divided in two parts by transmembrane domains (TM) 1 to 3 and a TM4. TM2 forms the ion-channel re-entrant loop segment.

B. The intracellular C-terminus of GluRδ2 interacts with PICK-1, AP-4, spectrin and PDZ domain-containing proteins PSD93, PTP-MEG, delphilin, S-SCAM, nPIST and Shank.

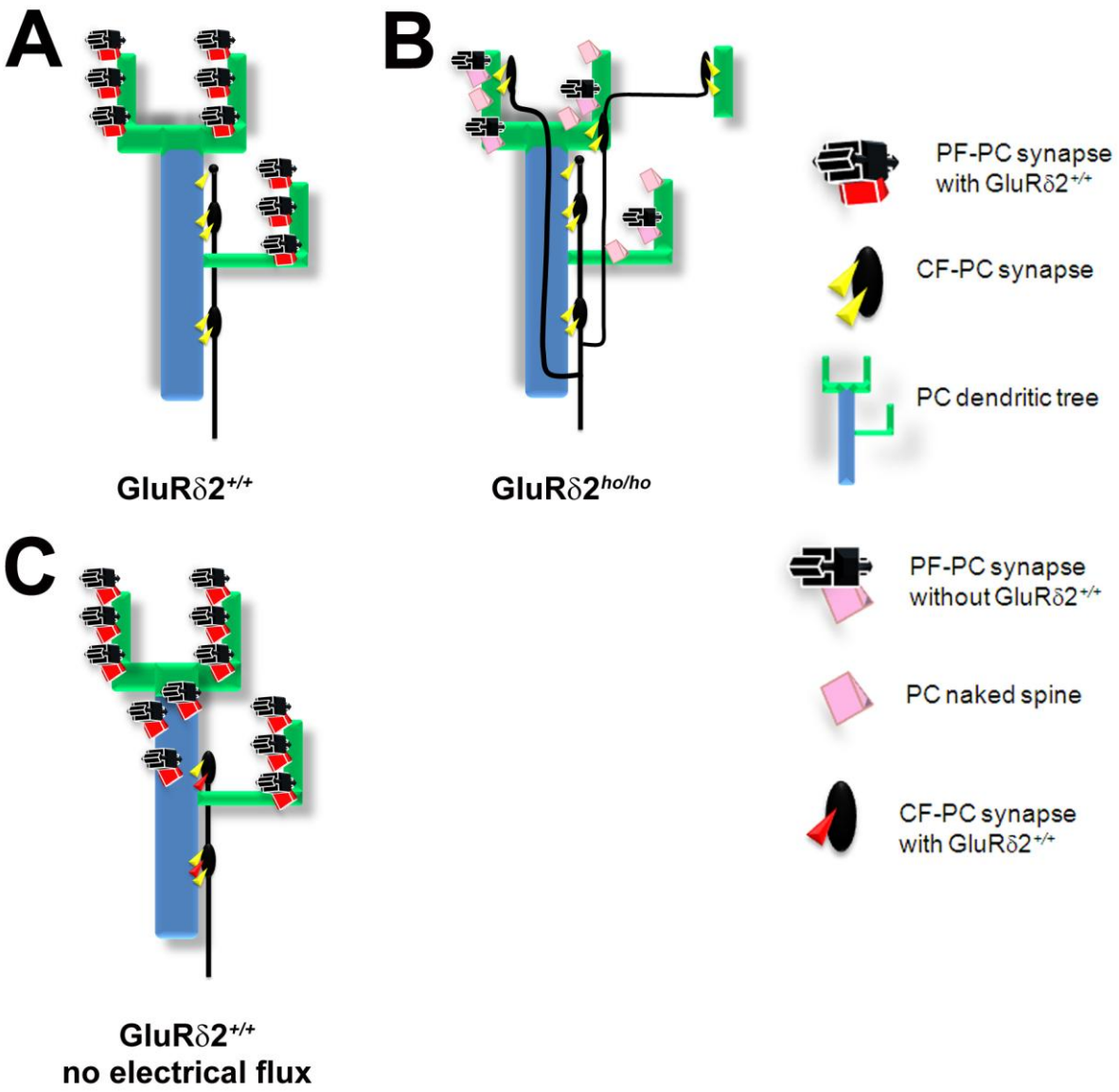

Figure 12. Parallel fiber and climbing fiber projection domains on Purkinje cell dendrites of the wild-type and GluRδ2$^{ho/ho}$ Purkinje cells (Modified from Ichikawa et al., 2002).

A. In the adult wild-type (GluRδ2$^{+/+}$) mouse, climbing fibers innervate proximal primary and secondary dendrites (blue) while parallel fibers innervate tertiary branchlet spines (green). GluRδ2 receptors are expressed at the parallel fiber synapses.

B. In the adult GluRδ2-deficient *hotfoot* (GluRδ2$^{ho/ho}$) mouse, climbing fibers emit collaterals distally extending to abnormally innervate tertiary branchlets. Numerous Purkinje cell dendritic spines remain devoid of innervation. Climbing fibers often jump to form synapses on spiny branchlets of adjacent Purkinje cells.

C. blocking the electrical activity afferent to wild-type Purkinje cells allows the parallel fibers to extend their territory to the proximal dendrite. This leads to the climbing fiber atrophy and restoration of GluRδ2 expression in the adult climbing fiber synapses.

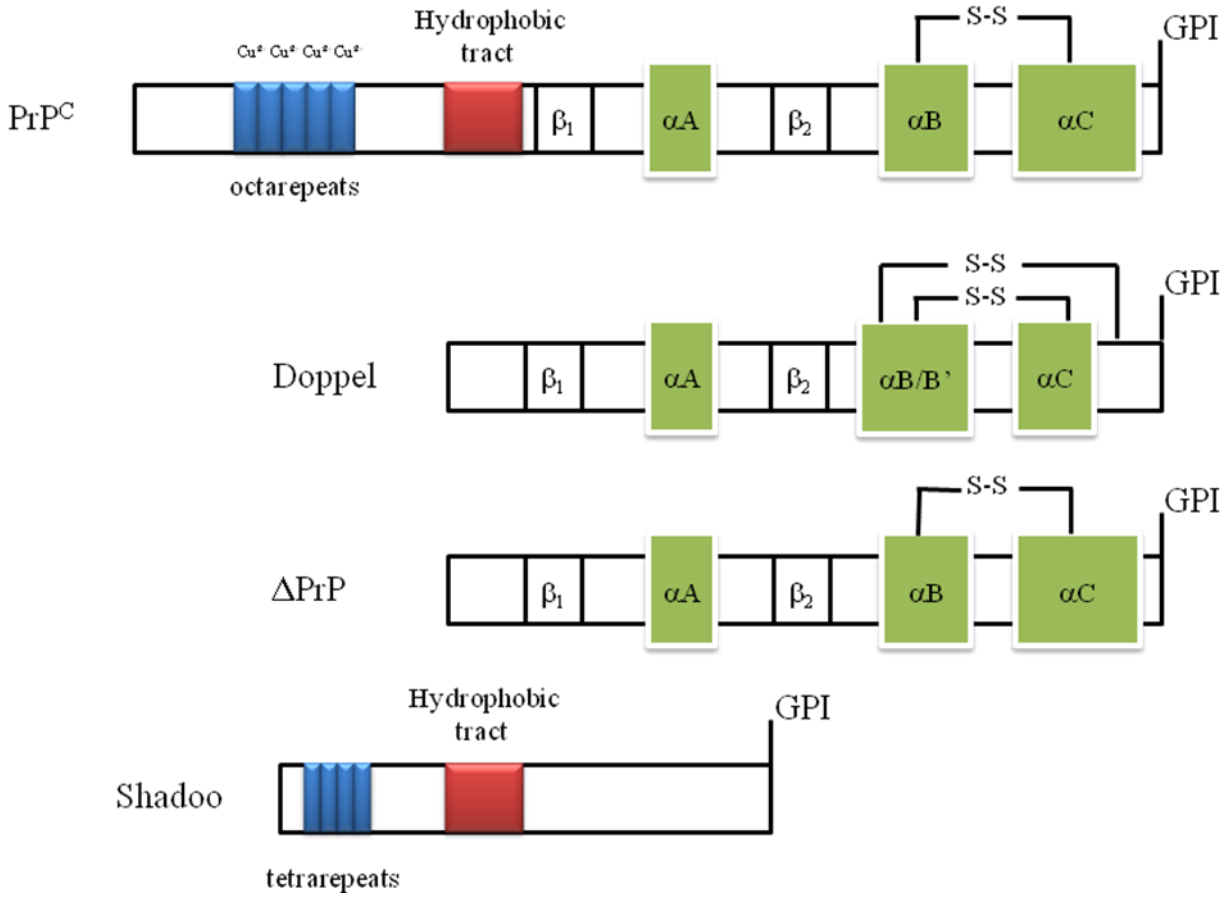

Figure 13: Structure of PrP^C, Dpl, ΔPrP and Shadoo. (Modified from Watts and Westaway, 2007).

PrP^C, Dpl and ΔPrP have a structured C-terminal domain including 3 α-helices and 2 β-sheets which are absent in Shadoo. Dpl has two disulfide bonds (S-S) when only one is present in PrP^C and ΔPrP. Hydrophobic tract and repetitive regions are conserved in PrP^C (octarepeats) and Shadoo (tetrarepeats).

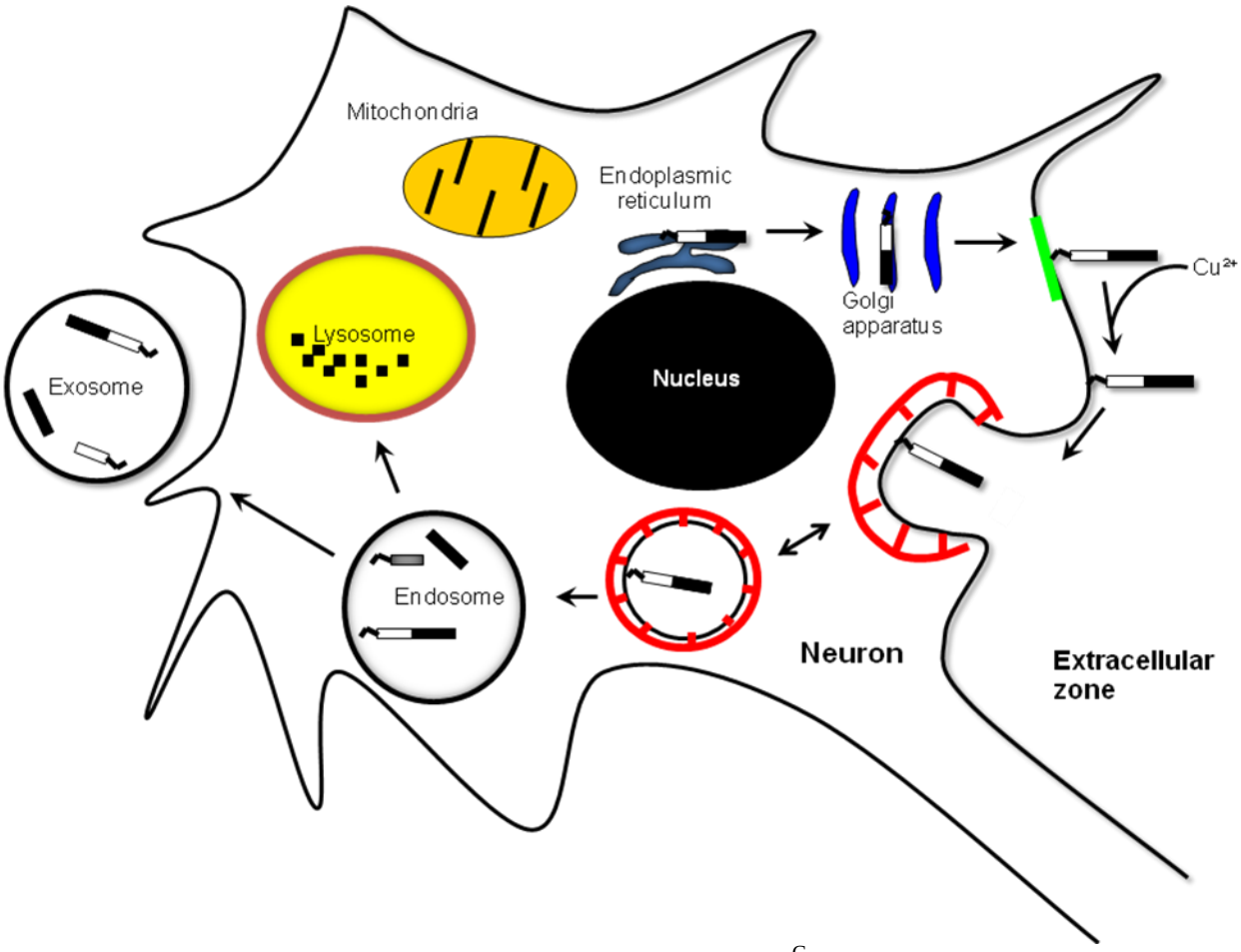

Figure 14: Intracellular and plasma membrane trafficking of PrP^C. (Modified from Shyng et al., 1993)

After ER synthesis, PrP^C is post-translationally modified in the ER and the Golgi apparatus before trafficked to the cell surface in a lipid raft microdomain (green). Copper-binding makes PrP^C to exit the lipid raft to be internalized by clathrin-mediated endocytosis and submitted to constitutive cycling. A part of the internalized molecules are cleaved within endosomes and either externalized via exosomes or degraded by lysosomes.

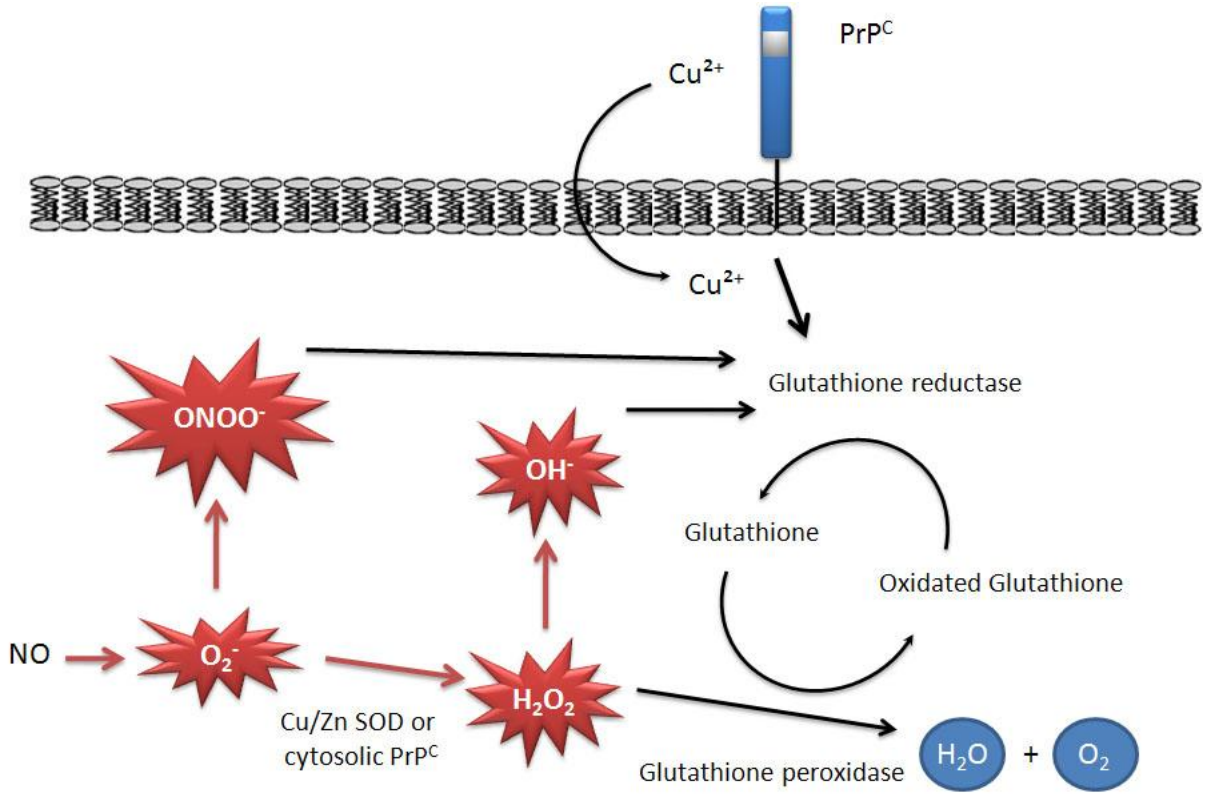

Figure 15: Schematic representation of Cu/ZnSOD and glutathione anti-oxidant pathways and putative interaction with PrP^{C}-Cu^{2+}. (Modified from White et al., 1999)

PrP^{C} might facilitate the reduction of glutathione by the glutathione reductase which ultimately reduces reactive oxygen species. In the absence of PrP^{C}, the reduction of oxidative species is impaired leading to a less efficient protection against oxidative stress.

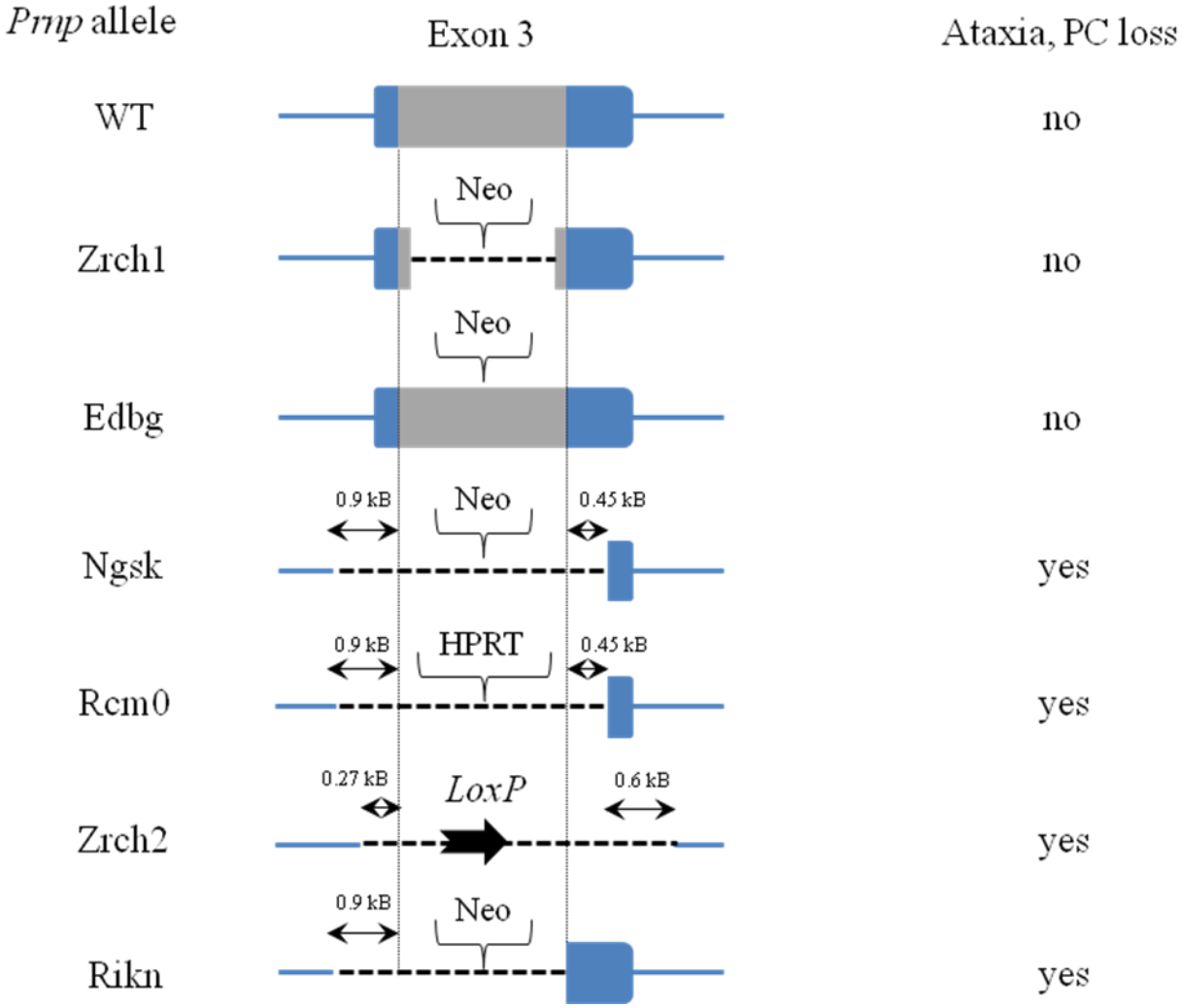

Figure 16: Various strategies used to disrupt the locus of the *Prnp* gene to generate different strains of *Prnp* knockout mice. (Modified from Rossi et al., 2001)

Prnp ORF is in grey and non-coding sequences are in blue. The dotted line indicates the deleted *Prnp* sequence and the brace indicates an inserted neomycine phosphotransferase (Neo) or a hypoxanthine phosphoribosyltransferase (HPRT). *LoxP* is a 34 Kb recombination site from phage 1.

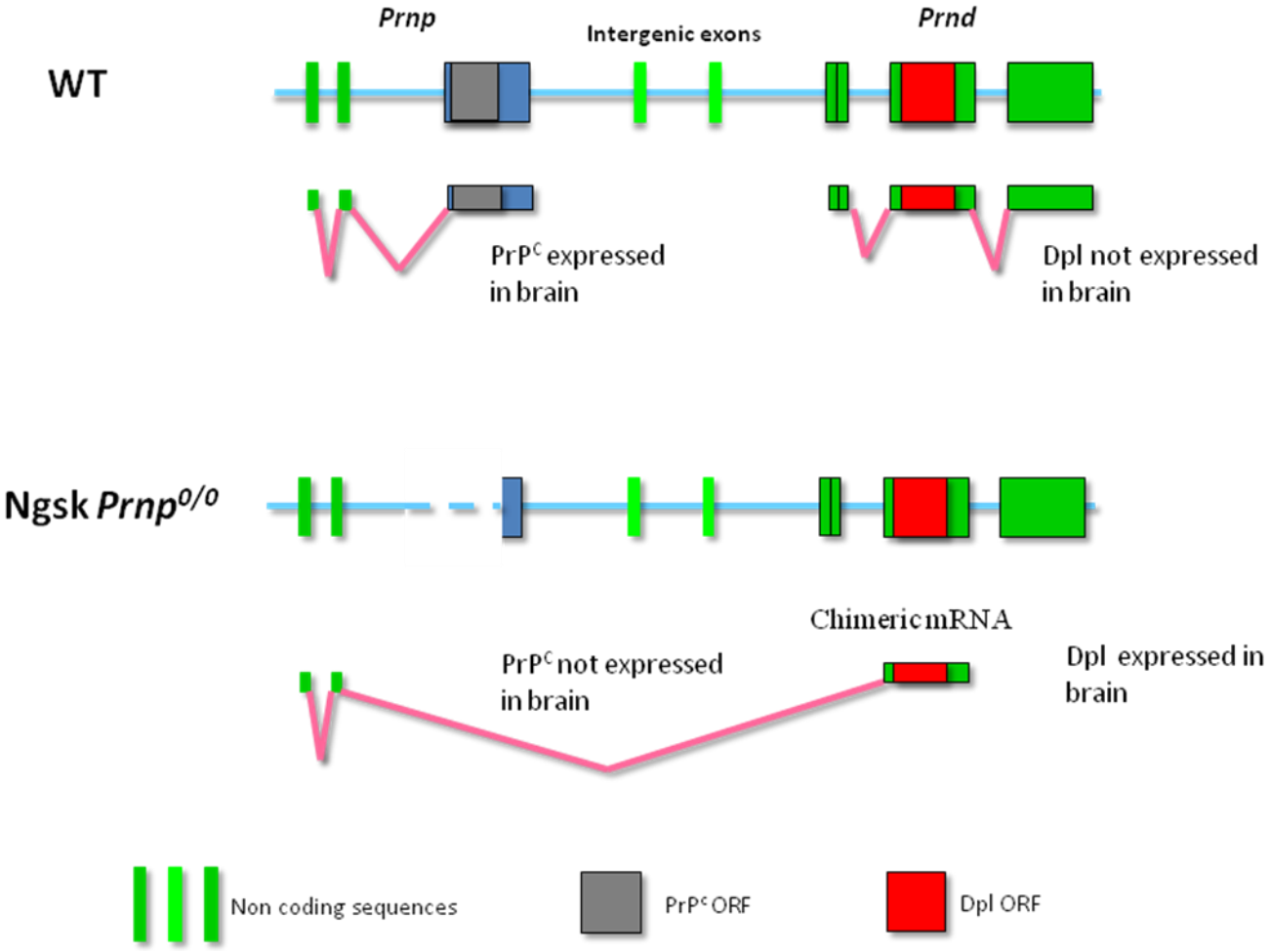

Figure 17: *Prnd* expression depends on *Prnp* promoter in Nagasaki *Prnp*$^{0/0}$ (*NP*$^{0/0}$) mouse. (Modified from Weissmann and Aguzzi, 1999)

When deletion of *Prnp* coding region and flanking regions includes the splice acceptor of intron 2, the resulting chimerical mRNAs comprising *Prnp* exons 1 and 2 are spliced to the Dpl-coding *Prnd* exon.

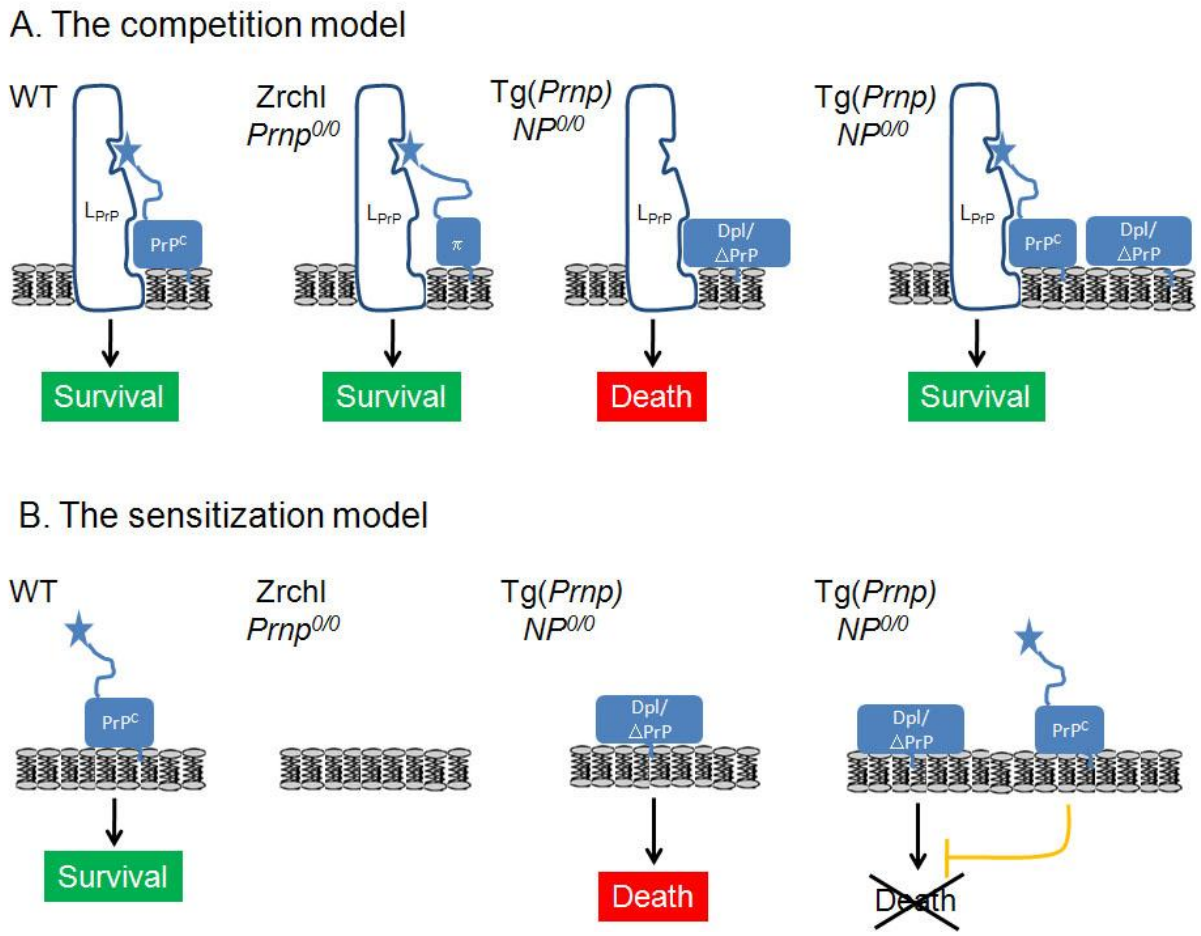

Figure 18: Dpl-PrP^C interaction models. (Modified from Watts and Westaway, 2007)

A. The competition model. In wild-type mouse, PrP^C binds to a hypothetical ligand L_{PrP} and elicits a survival signal. In *Prnp*$^{0/0}$ mouse such as ZrchI, a hypothetical PrP^C-like protein π binds to L_{PrP} with a lower affinity and induces the same survival signal. When Dpl or ΔPrP bind to L_{PrP}, an improper signal leading to cell death is initiated. It is counteracted by reintroduction of PrP^C.

B. The sensitization model. PrP^C favors cell survival in wild-type mouse and its absence in ZrchI mouse has no specific effect. In *NP*$^{0/0}$ mice, Dpl like ΔPrP initiates a cell death signal which is directly abrogated by PrP^C.

A

Group	Treatment schedule	Mean number of NASP treated PCs	Mean number of untreated PCs
WT 1	12 days treatment	429.4 ± 90.8	423 ± 60.7
GluRδ2$^{Lc/+}$ 2	12 days treatment	446.7 ± 36.7	258.24 ± 22.9
WT 3	6 days treatment	512 ± 62.2	453 ± 43.1
GluRδ2$^{Lc/+}$ 4	6 days treatment	530.7 ± 163	494 ± 58
GluRδ2$^{Lc/+}$ 5	10 days feeding and 2 days treatment	324.3 ± 35	258.24 ± 29.9
GluRδ2$^{Lc/+}$ 6	8 days feeding and 4 days treatment	388.6 ± 49.14	
GluRδ2$^{Lc/+}$ 7	6 days feeding and 6 days treatment	401 ± 41	
GluRδ2$^{Lc/+}$ 8	6 days treatment and 6 days feeding	252 ± 24	

B

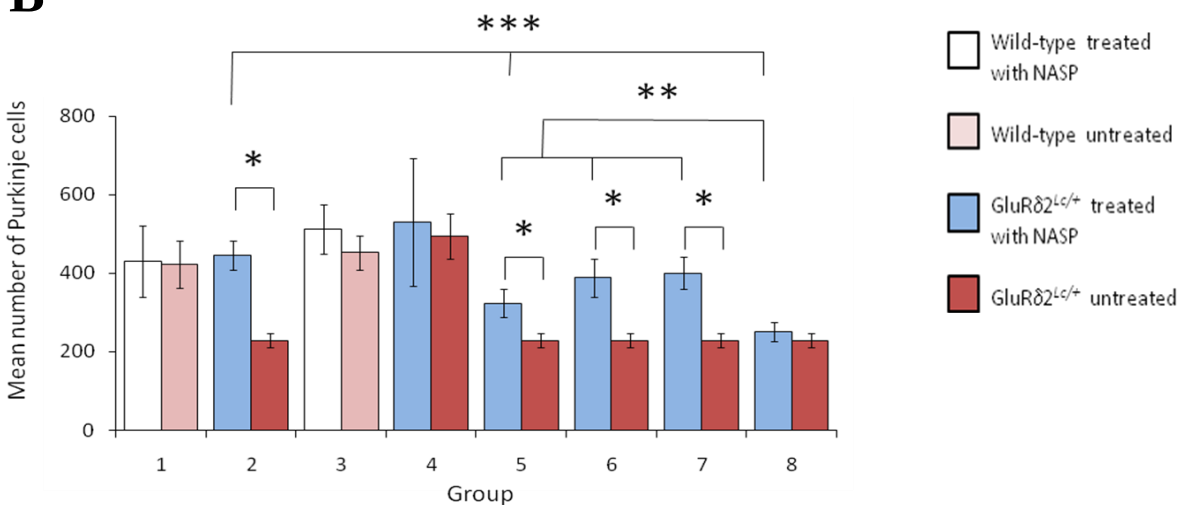

Figure 19.

A. Mean numbers of GluRδ2$^{Lc/+}$ and wild-type Purkinje cells submitted to different NASP treatment schedules ± SD.

B. Blockade of GluRδ2$^{Lc/+}$-induced excitotoxicity by NASP treatment is efficient to significantly rescue GluRδ2$^{Lc/+}$ Purkinje cells after at least 6 DIV in organotypic cerebellar cultures from P0 cerebellum. 1 to 8 are groups of wild-type and GluRδ2$^{Lc/+}$ mice indicated in A.

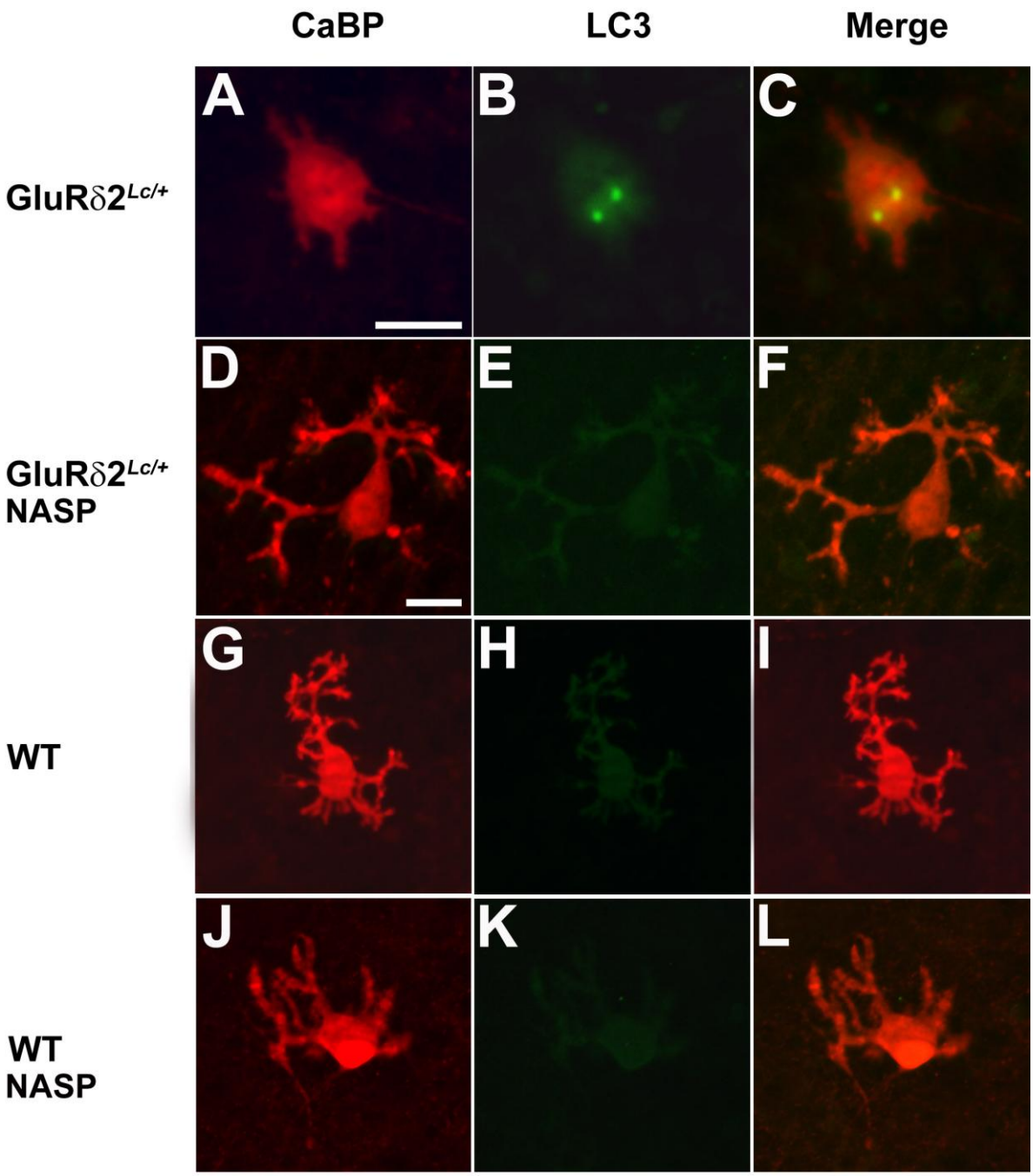

Figure 20. Somatic dots of LC3-immunofluorescent labeling (B, C) reveal autophagy in the CaBP-immunofluorescent GluRδ2$^{Lc/+}$ Purkinje cells (A, C) displaying dendritic atrophy in 12 DIV organotypic cerebellar cultures. Autophagy could not be detected (E, F) in GluRδ2$^{Lc/+}$ Purkinje cells treated with NASP for 12 DIV (D, F). This treatment also restored the dendritic tree of GluRδ2$^{Lc/+}$ Purkinje cells to its wild-type dimension but had no effect on wild-type Purkinje cells (G-L). Bar = 20μm for A-L.

A

Group	Treatment schedule	Mean dendritic area of treated PCs	Mean dendritic area of untreated PCs	Mean maximum dendritic length of treated PCs	Mean maximum dendritic length of untreated PCs
WT 1	12 days treatment	1584.6 ± 142.8	1516.5 ± 191.5	23.9 ± 1.3	24.1 ± 1.2
GluRδ2$^{Lc/+}$ 2	12 days treatment	1483.4 ± 117	933.32 ± 127.05	23.5 ± 1.27	18.23 ± 1.18
GluRδ2$^{Lc/+}$ 5	10 days feeding and 2 days treatment	1068.18 ± 116		20.77 ± 2.3	
GluRδ2$^{Lc/+}$ 6	8 days feeding and 4 days treatment	1085.4 ± 120.85		22.55 ± 2.1	
GluRδ2$^{Lc/+}$ 7	6 days feeding and 6 days treatment	1451.7 ± 116.9		23.54 ± 1.09	
GluRδ2$^{Lc/+}$ 8	6 days treatment and 6 days feeding	878.13 ± 36.32		15.69 ± 0.85	

B

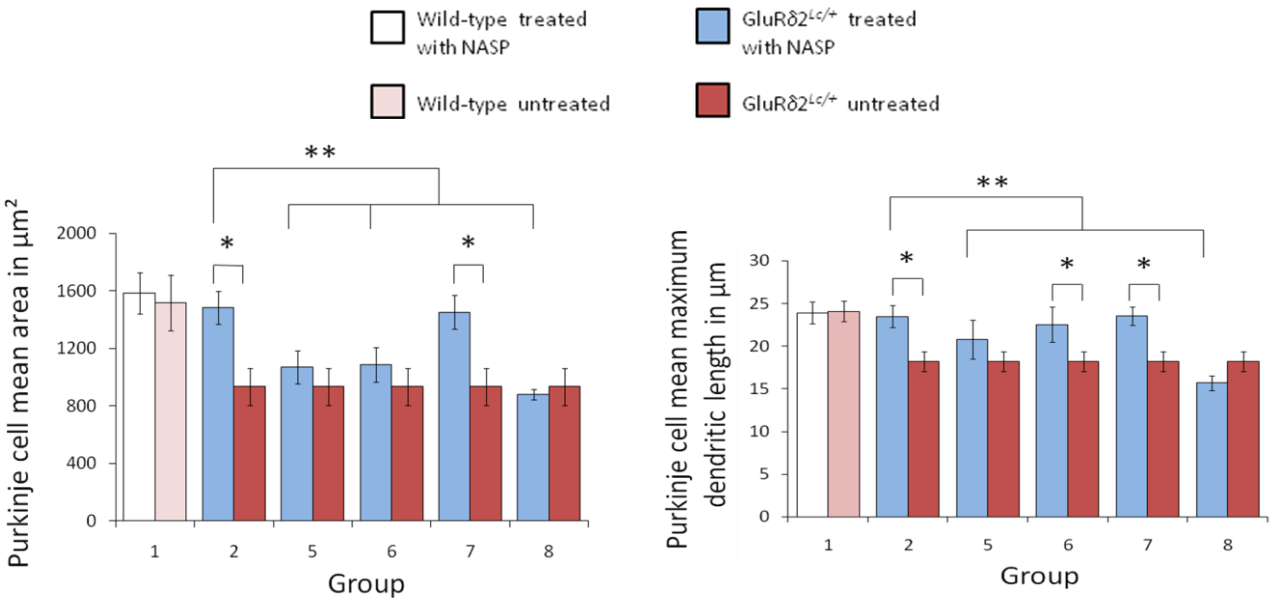

Figure 21. A. Mean area (µm²) and maximum dendritic length (µm) ± SD of GluRδ2$^{Lc/+}$ and wild-type Purkinje cells submitted to different NASP treatment schedules in 12 DIV organotypic cerebellar cultures.

B. Blockade of GluRδ2$^{Lc/+}$-induced excitotoxicity by NASP treatment is efficient to significantly restore GluRδ2$^{Lc/+}$ Purkinje cell dendritic growth after at least 6 DIV in organotypic cerebellar cultures from P0 cerebellum. 1 to 8 are groups of wild-type and GluRδ2$^{Lc/+}$ mice indicated in A.

Genotype	Mean number of Purkinje cells	Mean dendritic area	Mean maximum dendritic length	Mean numbers of primary dendrites	Mean numbers of secondary dendrites	Mean numbers of tertiary dendrites
WT	998 ± 116	3138 ± 272	98 ± 1	1.58 ± 0.7	4.87 ± 1.59	53.2 ± 11
GluRδ2$^{ho/ho}$	681 ± 173	3037 ± 819	83 ± 5	1.61 ± 0.8	3.95 ± 1.4	18.13 ± 4.7

Table 1. Mean number of Purkinje cells, mean area and maximum length of Purkinje cell dendritic tree and mean numbers of primary, secondary and tertiary dendrites of GluRδ2$^{ho/ho}$ and wild-type Purkinje cells ± SD.

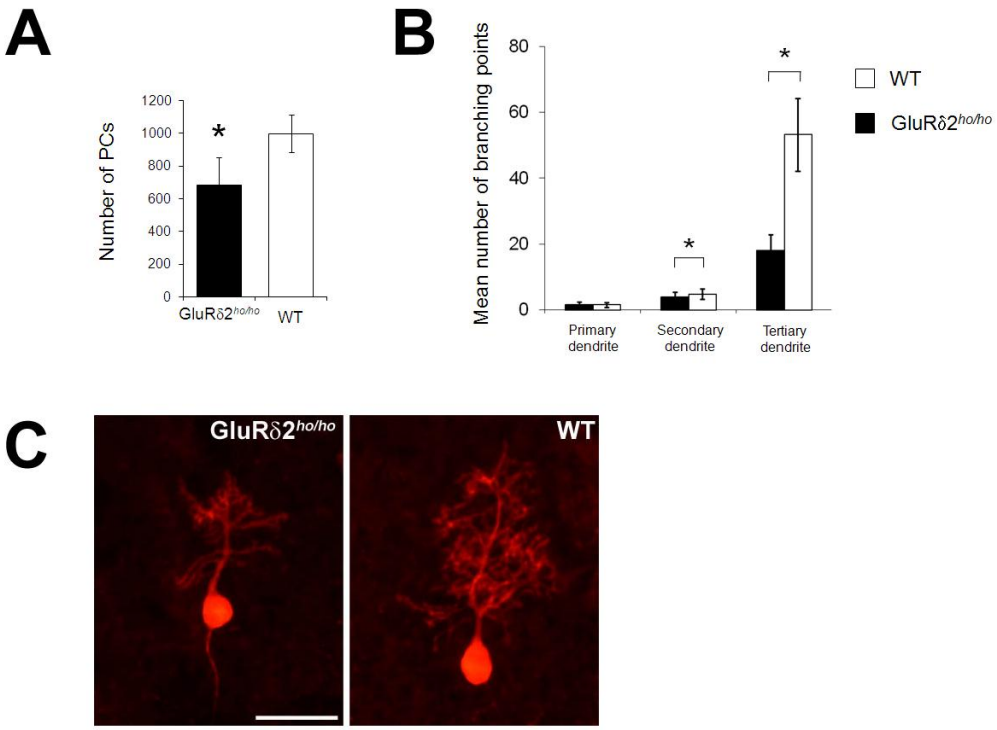

Figure 22. A and B. Significant Purkinje cell loss and atrophy of secondary and tertiary Purkinje cell dendrites in GluRδ2$^{ho/ho}$ cerebellar cultures. C. Representative CaBP-immunofluorescent Purkinje cells in GluRδ2$^{ho/ho}$ and wild-type organotypic cerebellar cultures. Bar = 50 µm.

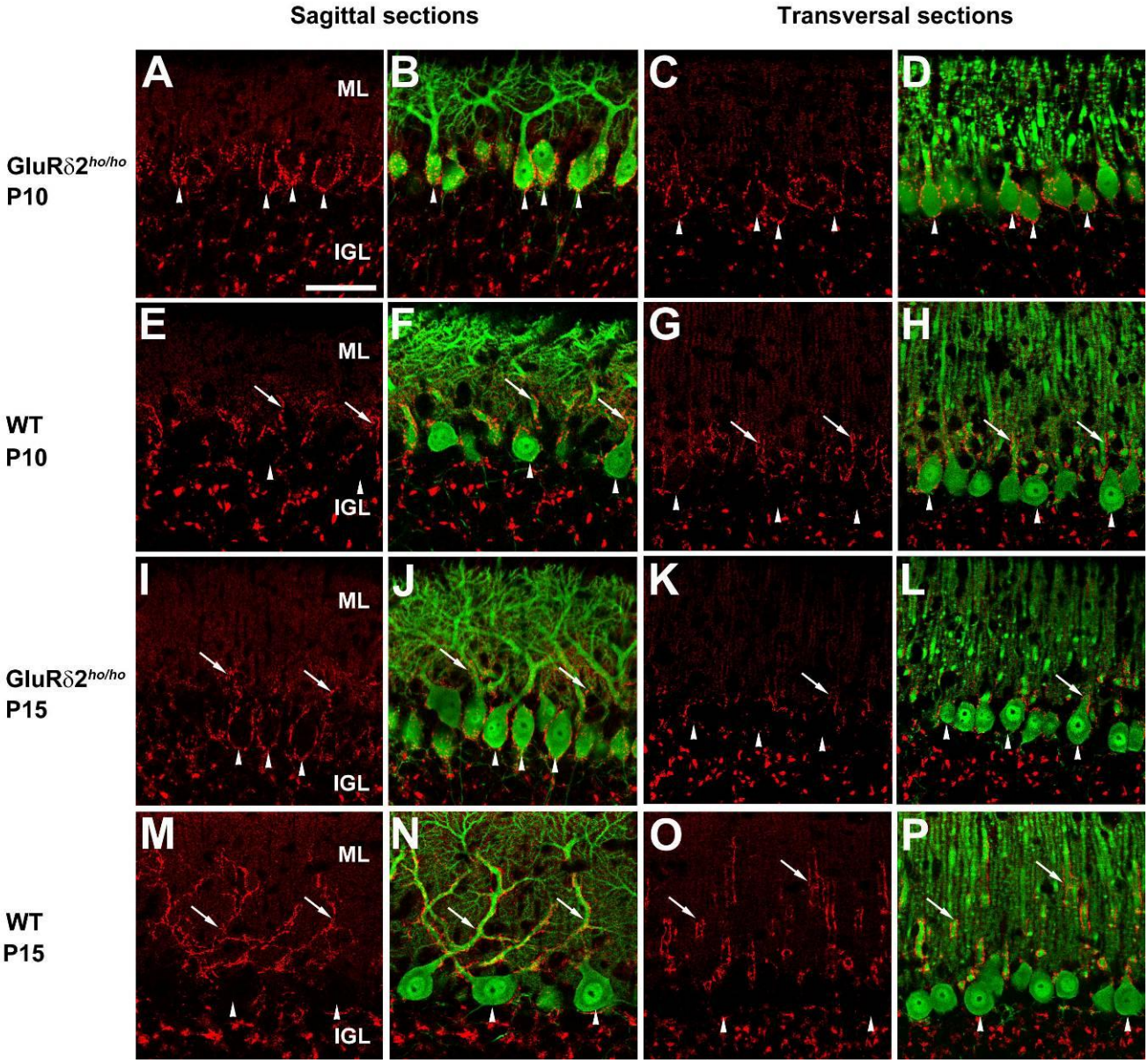

Figure 23. Climbing fiber (arrows) translocation along the soma and dendrites of the Purkinje cells (arrowheads) is impaired in GluRδ2$^{ho/ho}$ mice.

A-H. At P10, VGlut 2-immunofluorescent (red) climbing fibers (A-D) innervate the soma but not the dendrites of the CaBP-immunofluorescent (green) GluRδ2$^{ho/ho}$ Purkinje cells (B, D) whereas climbing fiber somato-dendritic translocation (E-H) has already occurred on the proximal dendrite of the wild-type Purkinje cells (F, H). Fifteen day-old GluRδ2$^{ho/ho}$ Purkinje cells (J, L) exhibit somatic and limited dendritic climbing fiber innervation (I-L) while climbing fiber translocation to the primary and secondary dendrites is completed on the wild-type Purkinje cells (M-P). Bar = 50µm for A-P.

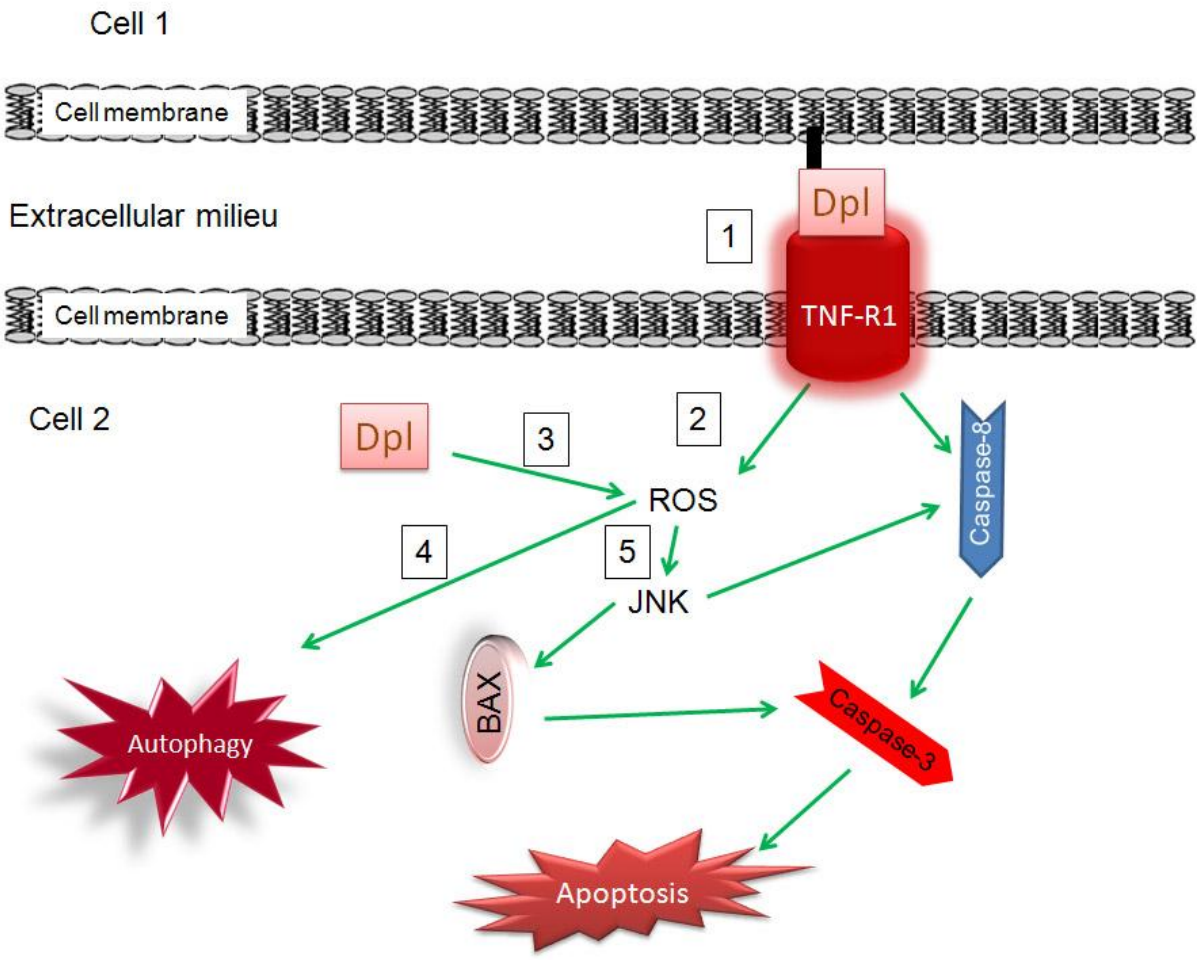

Figure 24. Hypothesis for a Dpl-induced neurotoxic mechanism.

(1) Extracellular Dpl, bound to cell membrane, can activate TNF-R1, leading to the production of ROS (2) by an unidentified mechanism (Papa et al., 2006). (3) In parallel, cytosolic Dpl can induce production of ROS by a possible calcium-dependent pathway (Brini et al., 2005). The produced ROS will either induce autophagy (4) (Djavaheri-Mergny et al., 2007) or activate JNK (5) (Papa et al., 2006) leading to the activation of caspase-8-dependent apoptosis and BAX-dependent apoptosis.

Primary antibody	**Company**	**Dilution**	**Secondary antibody**	**Company**	**Dilution**	**Experiment**
Mouse anti-CaBP	Sigma Aldrich	1/1000	Alexa 546 goat anti-mouse	Molecular Probes	1/1000	Immuno-fluorescence
Mouse anti-CaBP	Sigma Aldrich	1/1000	Alexa 488 goat anti-mouse	Molecular Probes	1/1000	Immuno-fluorescence
Rabbit anti-CaBP	From Mrs Thomasset	1/1000	Alexa 546 goat anti-rabbit	Molecular Probes	1/1000	Immuno-fluorescence
Guinea pig anti-VGlut2	Chemicon	1/3000	Alexa 546 goat anti-Guinea pig	Molecular Probes	1/1000	Immuno-fluorescence
Mouse anti-GFAP	Sigma Aldrich	1/500	Byotinilated horse anti-mouse	Vector Labs	1/200	Immuno-peroxidase
Mouse anti-GFAP	Sigma Aldrich	1/500	Alexa 546 goat anti-mouse	Molecular Probes	1/1000	Immuno-fluorescence
Rabbit anti-GFAP	Dako	1/500	Alexa 488 goat anti-rabbit	Molecular Probes	1/1000	Immuno-fluorescence
Rabbit anti-aldolase C	From Dr Sugihara	160ng/mL	Byotinilated horse anti-rabbit	Vector Labs	1/200	Immuno-peroxidase
Rabbit anti-aldolase C	From Dr Sugihara	160ng/mL	Alexa 488 goat anti-rabbit	Molecular Probes	1/1000	Immuno-fluorescence
Mouse anti-*Hu-bcl-2*	BD Biosciences	1/50	Byotinilated horse anti-mouse	Vector Labs	1/200	Immuno-peroxidase
Rabbit anti-Scrg1	From Dr Dron	1/60	Alexa 488 goat anti-rabbit	Molecular Probes	1/1000	Immuno-fluorescence
Mouse anti-LC3B	Nanotools	1/10	Alexa 488 goat anti-mouse	Molecular Probes	1/1000	Immuno-fluorescence
Mouse anti-p62	BD Transduction Labs	1/100	Alexa 488 goat anti-mouse	Molecular Probes	1/1000	Immuno-fluorescence

Table 3. Antibodies used for immunohistochemical staining experiments.

Method	Fixative
Transmission electron microscopy for ultrastructural analysis	4% paraformaldehyde – 2% glutaraldehyde in PB
Scrapie responsive gene 1 (Scrg1) pre-embedding immunogold	1% paraformaldehyde in PB
γ amino butyric acid (GABA) post-embedding immunogold	2% paraformaldehyde - 2% glutaraldehyde in PB

Table 4. Fixative used for transmission electron microscopy and immunocytochemistry.

	GluRδ2$^{Lc/+}$ mouse		$NP^{0/0}$ mouse	
		Reference		Reference
Apoptosis	Increased Bax IR in GluRδ2$^{Lc/+}$ Purkinje cells	523	DNA fragmentation in Dpl-overexpressing hippocampal neurons	237
	TUNEL labeling of GluRδ2$^{Lc/+}$ Purkinje cells	522, 338	TUNEL labelling of Dpl overexpressing granule cells	324
	Caspase-3 IF in GluRδ2$^{Lc/+}$ Purkinje cells	427	ROS producing enzymes upregulation in Dpl-overexpressing neurons	94, 521
	Delayed death of *Bax*$^{-/-}$:GluRδ2$^{Lc/+}$ Purkinje cell	428	Activation of caspases 3 and 10 by Dpl in N2A and astrocytes	376
	Inactivation of extrinsic pathway delays *tPA*$^{-/-}$:GluRδ2$^{Lc/+}$ Purkinje cell death	279	*Bcl-2* overexpression delays caspase-3 activation in the cerebellum of ΔPrP transgenic mouse	333
	ROS are induced in GluRδ2$^{Lc/+}$ Purkinje cells	307	*Bcl-2* overexpression and *Bax*$^{-/-}$ partly rescue $NP^{0/0}$ Purkinje cells	171, 172
Autophagy	GluRδ2 is linked to Beclin1 via nPIST in cerebellar extracts and HEK cells	541	Scrg1 IR of $NP^{0/0}$ Purkinje cells	111, 173
	LC3 IR of GluRδ2$^{Lc/+}$ Purkinje cells *in vivo* and *in vitro*	499		
	GluRδ2^{Lc} induces autophagy *in vitro* in HEK cells and *in vivo* in *Lurcher* Purkinje cells	541	Early autophagy in $NP^{0/0}$ Purkinje cells	173
	Autophagy is induced by GluRδ2^{Lc} in GluRδ2$^{Lc/ho}$ Purkinje cells	429		
	Induction of axonal autophagy in GluRδ2$^{Lc/+}$ Purkinje cell	499	Upregulation of p62 in $NP^{0/0}$ Purkinje cells	173
	Absence of p62 upregulation in GluRδ2$^{Lc/+}$ Purkinje cells	499		

Table 2. Experimental evidences for apoptosis and autophagy in *Grid2* mutant mice and in Nagasaki *Prnp*-deficient mice overexpressing Dpl.

Neuron, Vol. 37, 813–819, March 6, 2003, Copyright ©2003 by Cell Press

Lurcher GRID2-Induced Death and Depolarization Can Be Dissociated in Cerebellar Purkinje Cells

Fekrije Selimi,[1] Ann M. Lohof,[1] Stéphane Heitz,[2] Alexis Lalouette,[1] Christopher I. Jarvis,[1] Yannick Bailly,[2] and Jean Mariani[1,*]
[1]Laboratoire Développement et Vieillissement du Système Nerveux
CNRS-UMR 7102
Université Pierre et Marie Curie
75005 Paris
[2]UPR 2356
CNRS
IFR37 des Neurosciences
67084 Strasbourg
France

Summary

The Lurcher mutation transforms the GRID2 receptor into a constitutively opened channel. In Lurcher heterozygous mice, cerebellar Purkinje cells are permanently depolarized, a characteristic that has been thought to be the primary cause of their death, which occurs from the second postnatal week onward. The more dramatic phenotype of Lurcher homozygotes is thought to be due to a simple gene dosage effect of the mutant allele. We have analyzed the phenotype of Lurcher/hotfoot heteroallelic mutants bearing only one copy of the Lurcher allele and no wild-type *Grid2*. Our results show that the absence of wild-type GRID2 receptors in these heteroallelic mutants induces an early and massive Purkinje cell death that is correlated with early signs of autophagy. This neuronal death is independent of depolarization and can be explained by the direct activation of autophagy by Lurcher GRID2 receptors through the recently discovered signaling pathway formed by GRID2, n-PIST, and Beclin1.

Introduction

Glutamate receptor overactivation leads to neuronal death through a process known as excitotoxicity and contributes to numerous acute pathologies such as ischemia (Lee et al., 1999) and chronic ones such as amyotrophic lateral sclerosis (Lancelot and Beal, 1998). The depolarization and the perturbed ion homeostasis, in particular increased calcium concentration, that result from glutamate receptor overactivation have been given a central role in the molecular events inducing neuronal death during excitotoxicity (Reynolds, 1998).

Glutamate ionotropic receptors can be divided into four subfamilies: the AMPA, NMDA, kainate, and δ (GRID1 and GRID2) receptors. GRID receptors were cloned by sequence homology with other glutamate receptors, but no ligand has yet been found to activate these putative channels (Araki et al., 1993; Mayat et al., 1995). However, the Lurcher point mutation (Lc) transforms the GRID2 receptor into a constitutively opened channel (Zuo et al., 1997), thus supporting a role as a gated ion channel. In Lurcher heterozygous mice, the expression of the *Grid2*^{Lc} allele in cerebellar Purkinje cells (PCs) leads to the permanent depolarization of these neurons (Zuo et al., 1997) and their degeneration from the second postnatal week onward (Caddy and Biscoe, 1979). The permanent depolarization of *Grid2*^{Lc}/*Grid2*$^{+}$ PCs has been proposed to be the primary cause of their death through an excitotoxic-like process (Zuo et al., 1997). Only a small number of PCs are still present in neonatal Lurcher homozygotes (Cheng and Heintz, 1997; Resibois et al., 1997); death of PCs thus takes place at least 2 weeks earlier than in heterozygotes, suggesting a gene dosage effect of the Lurcher allele. GRID2 is expressed as early as E15 in developing PCs (Takayama et al., 1996), and GRID2^{Lc} channels induce depolarization when expressed in heterologous cells (Kohda et al., 2000; Zuo et al., 1997), raising the question of what controls the onset of PC death and, in particular, whether it is simply depolarization.

We generated and analyzed heteroallelic mutant mice expressing only one copy of the Lurcher allele and no wild-type allele. Hotfoot (*Grid2*^{ho}/*Grid2*^{ho}) mice are "natural" *Grid2* knock-out mice (Lalouette et al., 1998). The hotfoot-Nancy strain has a deletion of 948 bp in the coding sequence of *Grid2*. These mice do not express the GRID2 protein and have a behavioral and morphological phenotype similar to the *Grid2* targeted knockout mouse (Lalouette et al., 2001). We crossed *Grid2*^{Lc}/*Grid2*$^{+}$ mice with *Grid2*^{ho}/*Grid2*^{ho} mice in order to obtain *Grid2*^{Lc}/*Grid2*^{ho} mice, which have only one copy of the Lurcher allele and no wild-type allele. Our data provide in vivo evidence that the Lurcher GRID2 receptors can induce neuronal death and activate autophagy independently of their depolarization effect.

Results

Early Onset of Neurodegeneration in the Grid2^{Lc}/Grid2^{ho} Cerebellum

Grid2^{Lc}/*Grid2*^{ho} animals were viable but ataxic, suggesting a cerebellar defect. At P21, the cerebellum of *Grid2*^{Lc}/*Grid2*^{ho} animals was clearly atrophic when compared to the cerebella of *Grid2*$^{+}$/*Grid2*^{ho} and *Grid2*$^{+}$/*Grid2*$^{+}$ control mice (Figure 1). This atrophy is much more severe than that of the *Grid2*^{Lc}/*Grid2*$^{+}$ cerebellum at the same age. While numerous PCs are still detected by calbindin immunostaining in *Grid2*^{Lc}/*Grid2*$^{+}$ cerebella, almost none are found in *Grid2*^{Lc}/*Grid2*^{ho} cerebella (only 66 ± 39 per hemicerebellum).

To determine whether the more severe loss of PCs in P21 *Grid2*^{Lc}/*Grid2*^{ho} cerebella was a consequence of an accelerated process or due to an earlier onset of degeneration, we counted the number of PCs in *Grid2*^{Lc}/*Grid2*^{ho}, *Grid2*^{Lc}/*Grid2*$^{+}$, *Grid2*$^{+}$/*Grid2*^{ho}, and *Grid2*$^{+}$/*Grid2*$^{+}$ cerebella of P5 and P10 animals in sections stained with an anti-calbindin antibody (specifically staining PCs in the cerebellum) and with cresyl-violet (Figures 1 and 2A). In *Grid2*^{Lc}/*Grid2*$^{+}$ mice, the number

*Correspondence: jean.mariani@snv.jussieu.fr

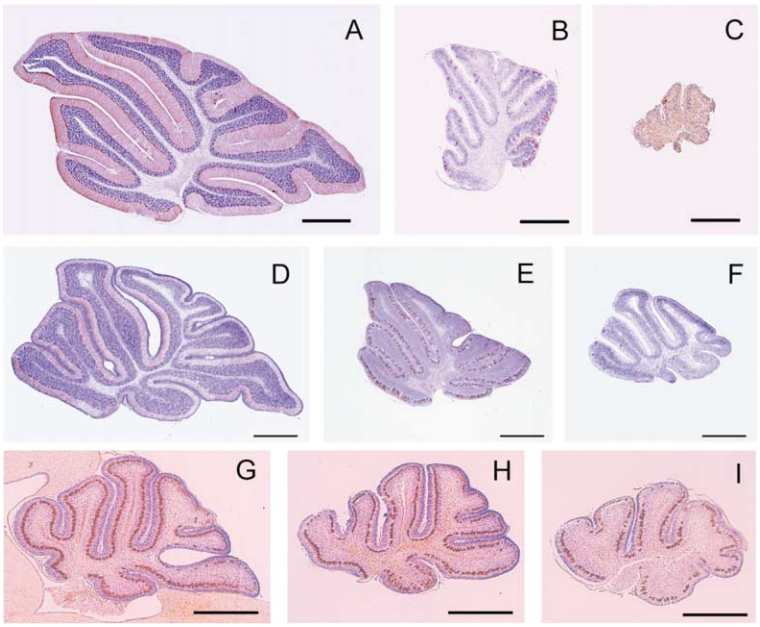

Figure 1. Early Onset of Purkinje Cell Degeneration in *Grid2^{Lc}/Grid2^{ho}* Mice

At P21, almost no calbindin-immunopositive Purkinje cells and very few granule cells are still detected in the cerebellum of *Grid2^{Lc}/Grid2^{ho}* mice (C), in contrast with the cerebellum of *Grid2^{+}/Grid2^{ho}* (A) and *Grid2^{Lc}/Grid2^{+}* mice (B). At P10, only a very few Purkinje cells still survive in the cerebellum of the *Grid2^{Lc}/Grid2^{ho}* double mutants (compare [F] with the *Grid2^{+}/Grid2^{ho}* [D] and *Grid2^{Lc}/Grid2^{+}* cerebella [E]). At P5, the cerebellum of the *Grid2^{Lc}/Grid2^{ho}* mice (I) is smaller and less foliated than the cerebellum of *Grid2^{+}/Grid2^{ho}* (G) and *Grid2^{Lc}/Grid2^{+}* (H) mice. Scale bars = 500 μm.

of PCs per hemicerebellum decreased slightly from 52,923 ± 2,381 at P5 to 52,509 ± 4,479 at P10. The number of PCs in *Grid2^{Lc}/Grid2^{+}* cerebellum was significantly lower than that found in *Grid2^{+}/Grid2^{+}* controls at both ages (Tukey-Kramer test, $p < 0.05$), but was significantly lower compared to *Grid2^{+}/Grid2^{ho}* cerebella only at P10. Loss of one wild-type allele of *Grid2* seems to delay PC development, as the number of PCs in *Grid2^{+}/Grid2^{ho}* cerebella is significantly reduced compared to *Grid2^{+}/Grid2^{+}* cerebella at P5, but reaches control level at P10. Thus, a delay in PC development probably also contributes to the reduced number of PCs in P5 *Grid2^{Lc}/Grid2^{+}* cerebella, suggesting that PC death has barely begun in those mutants by that age. In contrast, the cerebella of *Grid2^{Lc}/Grid2^{ho}* mice displayed a striking atrophy by P5 and were less foliated than the cerebella of age-matched *Grid2^{Lc}/Grid2^{+}*, *Grid2^{+}/Grid2^{ho}*, and *Grid2^{+}/Grid2^{+}* animals (Figure 1). The number of PCs in *Grid2^{Lc}/Grid2^{ho}*cerebella decreased from 20,455 ± 1,140 at P5 to 12,947 ± 1,593 at P10, significantly reduced when compared to the numbers found in all other genotypes at both ages (Figure 2A; Tukey-Kramer test, $p < 0.05$).

These results show that PC death has already very significantly affected *Grid2^{Lc}/Grid2^{ho}* cerebella by P5, an age at which *Grid2^{Lc}/Grid2^{+}* cerebella are not yet obviously affected. Thus, the absence of the *Grid2* wild-type allele leads to an earlier onset of PC degeneration in mice expressing one allele of *Grid2^{Lc}*.

At P21, the internal granule cell layer is still well defined in *Grid2^{Lc}/Grid2^{+}* cerebella and contains numerous granule cells, whereas it has almost completely disappeared in the cerebellum of *Grid2^{Lc}/Grid2^{ho}* animals (Figure 1). While the presence of an external granule cell layer (EGL) containing granule cell precursors is clear in the cerebellum of P10 *Grid2^{Lc}/Grid2^{+}* mice, this layer has almost disappeared in P10 *Grid2^{Lc}/Grid2^{ho}* cerebella (Figure 1). At P5, the thickness of the EGL in *Grid2^{Lc}/Grid2^{ho}* mice was only 26.0 ± 0.9 μm, which was significantly less than in both *Grid2^{+}/Grid2^{ho}* and *Grid2^{Lc}/Grid2^{+}* cerebella (40.9 ± 1.9 μm and 42.5 ± 1.5 μm, respectively; ANOVA followed by the Scheffé's post hoc test, $p < 0.001$). This shows that the early onset of PC degeneration leads to a deficit in the genesis of granule cells, in addition to the target-related death of these neurons (Wetts and Herrup, 1982). This is in accordance with the known trophic support provided by PCs to the granule cell precursors (Feddersen et al., 1992; Smeyne et al., 1995).

Lurcher GRID2 Induces PC Death and Autophagy Independent of Depolarization

PCs of *Grid2^{Lc}/Grid2^{+}* mice are chronically depolarized due to a constitutively active inward current (Zuo et al., 1997). We hypothesized that in the absence of the wild-type *Grid2* allele, this depolarization might be more severe or show an earlier developmental onset, explaining the accelerated PC death in *Grid2^{Lc}/Grid2^{ho}* mice. We therefore made patch-clamp recordings from PCs in slices prepared from *Grid2^{+}/Grid2^{+}*, *Grid2^{+}/Grid2^{ho}*, *Grid2^{Lc}/Grid2^{+}*, or *Grid2^{Lc}/Grid2^{ho}* cerebella at P5–P6 and P9–P12 (Figure 2B). As shown by Zuo et al. (1997), *Grid2^{Lc}/Grid2^{+}* Purkinje cells at P9–P12 had very large holding currents (−1.67 ± 0.11 nA), significantly different from *Grid2^{+}/Grid2^{ho}* and *Grid2^{+}/Grid2^{+}* values (Tukey-Kramer test, $p < 0.05$). *Grid2^{Lc}/Grid2^{ho}* PCs also had higher holding currents than controls at P9–P12 (−1.35 ± 0.24 nA; $p < 0.05$). The tendency was toward lower holding currents than in *Grid2^{Lc}/Grid2^{+}* Purkinje cells, although this difference was not statistically significant ($p > 0.05$). At P5–P6, the *Grid2^{Lc}/Grid2^{+}* PCs had larger holding currents (−0.66 ± 0.13 nA; $p < 0.05$) than those of their control littermates, but were less depolarized than *Grid2^{Lc}/Grid2^{+}* PCs at P9–P12. A striking finding was that at P5–P6, PCs of *Grid2^{Lc}/Grid2^{ho}* mice had holding currents equivalent to those of control animals (−0.22 ± 0.07 versus −0.24 ± 0.03 nA for *Grid2^{+}/Grid2^{ho}*, −0.11 ± 0.03 nA for *Grid2^{+}/Grid2^{+}*; $p >$

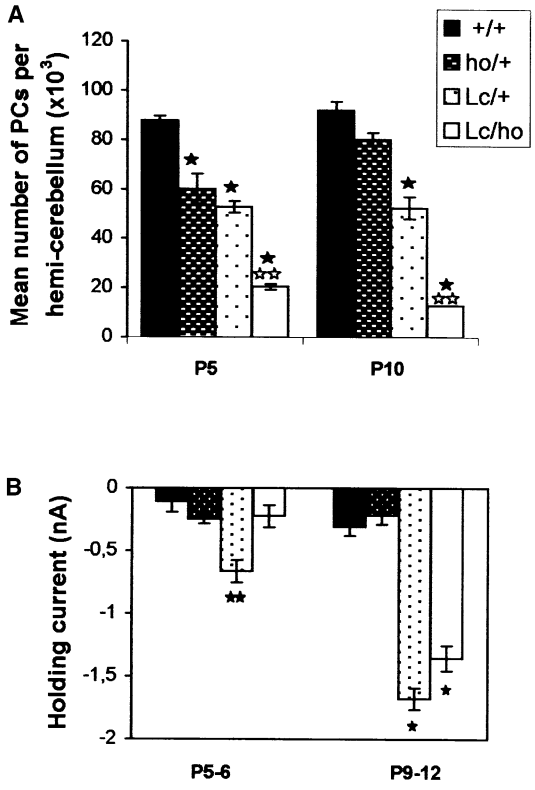

Figure 2. Purkinje Cell Death Is Not Correlated with Depolarization in *Grid2*^{Lc}/*Grid2*^{ho} Cerebellum

(A) Purkinje cell number per hemicerebellum was assessed using calbindin-immunostained sections (*$p < 0.05$, significantly different from *Grid2*$^{+}$/*Grid2*$^{+}$ values; **$p < 0.05$, significantly different from *Grid2*^{Lc}/*Grid2*$^{+}$ values, Tukey-Kramer test; n = 3–5 animals per genotype).

(B) Holding currents are significantly larger at P9–P12 for *Grid2*^{Lc}/*Grid2*$^{+}$ and *Grid2*^{Lc}/*Grid2*^{ho} Purkinje cells (*$p < 0.05$, Welch ANOVA followed by Tukey-Kramer test) compared to the same genotypes at P5–P6 and compared to *Grid2*$^{+}$/*Grid2*^{ho} and *Grid2*$^{+}$/*Grid2*$^{+}$ at both ages. *Grid2*^{Lc}/*Grid2*$^{+}$ holding currents at P5–P6 are significantly different from any other group (**$p < 0.05$).

0.05) and significantly lower than those of *Grid2*^{Lc}/*Grid2*$^{+}$ mice. Thus the earlier PC death is not correlated with an early depolarization.

To verify the expression of GRID2 in the *Grid2*^{Lc}/*Grid2*^{ho} PCs, we performed immunohistochemistry on cerebellar sections of P5 mutants (see Supplemental Data at http://www.neuron.org/cgi/content/full/37/5/813/DC1). In *Grid2*^{ho}/*Grid2*^{ho} cerebella, no immunostaining was detected in PCs, supporting the results of Lalouette et al. (2001) and further confirming that *hotfoot* mice can be considered a functional knock-out for *Grid2*. In *Grid2*^{Lc}/*Grid2*^{ho} cerebella, GRID2 immunoreactivity could be detected in PCs in a pattern similar to that seen in *Grid2*$^{+}$/*Grid2*^{ho} and *Grid2*^{Lc}/*Grid2*$^{+}$ cerebella. Although Lurcher GRID2 is expressed in PCs of *Grid2*^{Lc}/*Grid2*^{ho} mice at P5, depolarization of these neurons is only detected at P9. However PC death is already massive at P5 in *Grid2*^{Lc}/*Grid2*^{ho} mice. Recently, the presence of autophagy has been revealed in PCs of Lurcher heterozygotes (Yue et al., 2002). In order to see whether the early death of PCs in our heteroallelic mutants was still associated with signs of autophagy, we analyzed by electron microscopy the cerebellar morphology of our different mutants (Figure 3). Numerous autophagic vesicles were detected in all the PCs analyzed from P5 *Grid2*^{Lc}/*Grid2*^{ho} cerebella. This was not the case for PCs from age-matched *Grid2*$^{+}$/*Grid2*^{ho} and *Grid2*^{Lc}/*Grid2*$^{+}$ cerebella, which contained few or no autophagic profiles. This shows that the expression of GRID2^{Lc} protein can induce autophagy in correlation with PC death, even in a situation where it is not able to induce depolarization of these neurons.

Effects of Lurcher Allele Dosage

As *Grid2*^{Lc}/*Grid2*^{Lc} mice die perinatally (Cheng and Heintz, 1997), the gene dosage effect of the Lurcher allele was studied through the comparison of the cerebellar phenotype of our different mutants to that of *Grid2*^{Lc}/*Grid2*^{Lc} mice at P0 (Figure 4). The *Grid2*^{Lc}/*Grid2*^{Lc} cerebellum is clearly atrophic, in accordance with previously published results (Cheng and Heintz, 1997; Resibois et al., 1997); folia are barely distinguishable, while they are clearly visible in the cerebella of age-matched *Grid2*^{ho}/*Grid2*$^{+}$ controls and *Grid2*^{Lc}/*Grid2*$^{+}$ mice. The number of calbindin-positive PCs is also dramatically reduced in the cerebella of *Grid2*^{Lc}/*Grid2*^{Lc} mice compared to *Grid2*^{ho}/*Grid2*$^{+}$ and *Grid2*^{Lc}/*Grid2*$^{+}$ cerebella. The morphology of *Grid2*^{Lc}/*Grid2*^{ho} cerebella at P0 differs markedly from that of P0 *Grid2*^{Lc}/*Grid2*^{Lc} mice; folia are clearly formed, and the number of PCs is superior to that detected in *Grid2*^{Lc}/*Grid2*^{Lc} mice (compare Figures 4C and 4D). No neuronal death was apparent in the brainstem of *Grid2*^{Lc}/*Grid2*^{ho} animals (data not shown) in contrast to what has been described for *Grid2*^{Lc}/*Grid2*^{Lc} animals (Cheng and Heintz, 1997). These striking results show that there is a gene dosage effect of the Lurcher allele leading to accelerated PC death in *Grid2*^{Lc}/*Grid2*^{Lc} cerebella compared to the PC death observed in *Grid2*^{Lc}/*Grid2*^{ho} cerebella.

Discussion

The expression of GRID2^{Lc} in PCs causes a massive degeneration of these neurons accompanied by target-related death of PC afferents during the first postnatal month in *Grid2*^{Lc}/*Grid2*$^{+}$ mice (Caddy and Biscoe, 1979; Dumesnil-Bousez and Sotelo, 1992). The observation that *Grid2*^{Lc}/*Grid2*$^{+}$ PCs are depolarized due to the constitutive inward current induced by the expression of the mutant GRID2 receptors (Zuo et al., 1997) led to the hypothesis that this permanent depolarization causes the death of PCs by an excitotoxic mechanism. Our results show that the Lurcher GRID2 receptor can trigger autophagy and PC death without inducing depolarization of these neurons and that, although gene dosage partially determines the onset of PC degeneration, the loss of the wild-type *Grid2* allele greatly increases the vulnerability of PCs expressing Lurcher GRID2.

Numerous studies have focused on the role of depolarization and the concomitant ionic flux in the process leading to excitotoxicity (Iihara et al., 2001; Reynolds, 1998). However, it remains to be proven that massive depolarization and ionic flux are the only factors contributing to excitotoxicity in vivo. For example, the in-

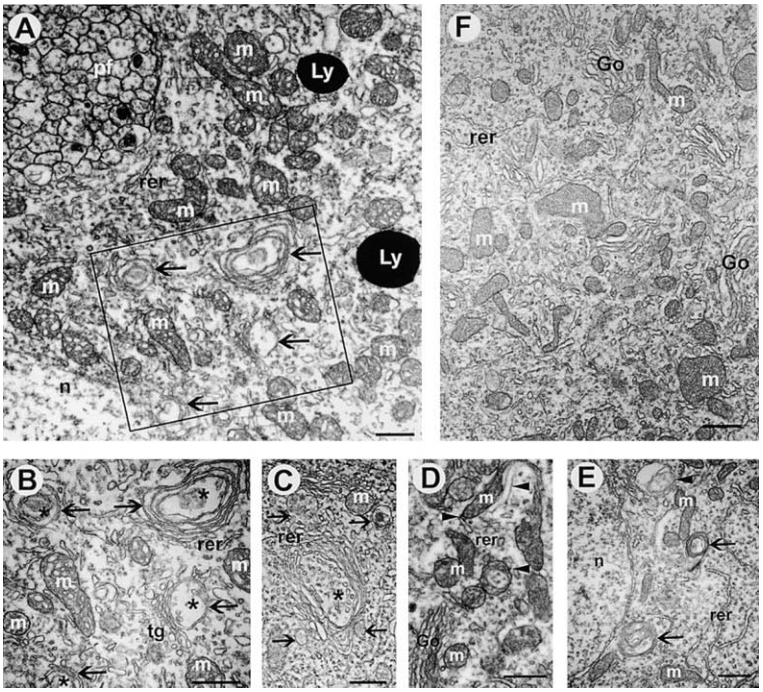

Figure 3. Activation of Autophagy in P5 *Grid2*^{Lc}/*Grid2*^{ho} Purkinje Cells

(A) Double-membrane vesicles (arrows) typical of autophagy have formed in the apical cytoplasm of a *Grid2*^{Lc}/*Grid2*^{ho} Purkinje cell.
(B) Magnification of inset in (A).
(C–E) Examples of autophagosomes at different stages in other *Grid2*^{Lc}/*Grid2*^{ho} Purkinje cells.
(F) Representative view of the somatic cytoplasm of *Grid2*^{ho}/*Grid2*$^{+}$ Purkinje cells. Go, Golgi dictyosome; m, mitochodrion; n, nucleus; rer, rough endoplasmic reticulum; tg, trans-Golgi; Ly, lysosome; pf, parallel fibers. Scale bars = 500 nm.

creased calcium permeability of AMPA receptors in GluR2-deficient mice does not influence the vulnerability of their neurons to kainate in vivo (Iihara et al., 2001). What triggers membrane depolarization and death in *Grid2*^{Lc}/*Grid2*$^{+}$ PCs remains unknown. The expression of GRID2 is detected as early as E15 in cerebellar PCs (Takayama et al., 1996). Expression of the *Grid2*^{Lc} allele in heterologous cells such as *Xenopus* oocytes or HEK293 cells leads to a permanent depolarization of these cells (Kohda et al., 2000; Zuo et al., 1997), raising the question of why *Grid2*^{Lc}/*Grid2*$^{+}$ PCs begin to die only after P5.

Our electrophysiological study of PC membrane potential shows that at P5, *Grid2*^{Lc}/*Grid2*$^{+}$ PCs are slightly depolarized when compared to control PCs. From P9 onward, this difference becomes highly significant, the mean holding current for *Grid2*^{Lc}/*Grid2*$^{+}$ PCs at this age being -1.67 ± 0.11 nA, while control holding current remains at -0.30 ± 0.02 nA. This result is in agreement with the results of Kohda et al. (2000), describing that *Grid2*^{Lc}/*Grid2*$^{+}$ PC depolarization is lower at P6–P7 than at P10. In *Grid2*^{Lc}/*Grid2*$^{+}$ mice, PC loss is not obvious at P5, but is approximately 35% at P10. This temporal correlation points toward a direct causality between membrane depolarization and PC death in *Grid2*^{Lc}/*Grid2*$^{+}$ mice, as had been proposed previously (Zuo et al., 1997). PC death occurs much earlier in *Grid2*^{Lc}/*Grid2*^{ho} cerebella than in *Grid2*^{Lc}/*Grid2*$^{+}$ cerebella, while the copy number of the *Grid2*^{Lc} allele is the same in both animals. In *Grid2*^{Lc}/*Grid2*^{ho} mutants, the number of PCs is already reduced by approximately 66% at P5, 84% at P10, and reaches almost 0 at P21. The phenotype of our heteroallelic mutants could have been explained in the context of depolarization if the absence of the wild-type allele led to an earlier onset of depolarization. However, our study shows that at P5, the holding current for *Grid2*^{Lc}/*Grid2*^{ho} PCs is equivalent to the control value and lower than for *Grid2*^{Lc}/*Grid2*$^{+}$ PCs. The loss of the *Grid2* wild-type allele does not affect the ability of GRID2^{Lc} channels to induce depolarization of PCs later during development, as *Grid2*^{Lc}/*Grid2*^{ho} PCs become depolarized at P9–P12. In *Grid2* knock-out mice, no PC degeneration has been detected. This is also true for *hotfoot* homozygotes, for which the number of PCs is not different from the wild-type (H. Zanjani et al., personal communication). *Grid2* knock-out mice display fewer parallel fiber/Purkinje cell synapses (Kashiwabuchi et al., 1995; Kurihara et al., 1997). This is unlikely to be a cause of the phenotype of the *Grid2*^{Lc}/*Grid2*^{ho} mice, as reduction of this input by X-irradiation does not alter the time course of PC death in *Grid2*^{Lc}/*Grid2*$^{+}$ animals (Doughty et al., 1999). Moreover, a significant part of

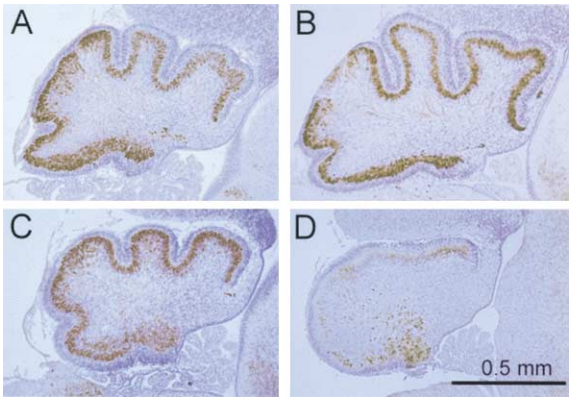

Figure 4. Comparison of Cerebellar Degeneration in P0 Mutants

The P0 *Grid2*^{Lc}/*Grid2*^{ho} cerebellum (C) is less developed than control *Grid2*$^{+}$/*Grid2*^{ho} (A) and *Grid2*^{Lc}/*Grid2*$^{+}$ (B) cerebella, suggesting that some Purkinje cell death might already have occurred at this age. The P0 *Grid2*^{Lc}/*Grid2*^{Lc} cerebellum (D) shows a much more dramatic loss of Purkinje cells than the other genotypes.

PC death in *Grid2^{Lc}/Grid2^{ho}* mice occurs before the bulk of synaptogenesis between granule cells and PCs (between P5 and P15). Thus, the earlier onset of PC degeneration in *Grid2^{Lc}/Grid2^{ho}* animals is not due to an increased ability of Lurcher GRID2 to form leaky channels in the absence of the wild-type GRID2, nor to a reduced number of synapses. In this case, membrane depolarization is not correlated with the degenerative process.

Studies have revealed that glutamate ionotropic receptors are not only gated ion channels, but also platforms for signaling pathways (Grant and O'Dell, 2001; Sheng and Pak, 2000). Recently, a direct link between GRID2 receptors and the process of autophagy has been found through the interaction of GRID2 with Beclin1 via n-PIST (Yue et al., 2002). Autophagy overactivation can lead to neuronal death and has been observed in various developmental and pathological paradigms (Anglade et al., 1997; Clarke, 1990). Although apoptotic characteristics have been detected in Lurcher PCs (Selimi et al., 2000a; Wullner et al., 1995), apoptosis inhibition by *bax* inactivation or BCL-2 overexpression only delays PC death in the Lurcher heterozygous mutants, suggesting that alternative death pathways are induced in Lurcher PCs (Doughty et al., 2000; Selimi et al., 2000b; Zanjani et al., 1998). Expression of GRID2^{Lc} in heterologous cells induces autophagy, and morphological signs of autophagy have been found in PCs from P10 Lurcher heterozygotes, suggesting that autophagy could be the alternative death pathway induced by GRID2^{Lc} receptors in PCs (Yue et al., 2002). We have shown here that GRID2^{Lc} is able to induce autophagy and death in PCs that are not depolarized. The concomitant expression of the wild-type receptor delays the overactivation of autophagy, as few signs of autophagy are detected in P5 Lurcher heterozygotes. When the quantity of these proteins is low, as is the case before P10 (Zhao et al., 1998), the coexpression of the wild-type GRID2 with the Lurcher GRID2 seems to be sufficient to prevent cell death. However, when the quantity of these proteins is increased, the activation of autophagy might be too overwhelming to be inhibited by the presence of the wild-type GRID2. Moreover, the depolarization and impaired ion homeostasis that starts after P5 in *Grid2^{Lc}/Grid2^{+}* PCs might also contribute to an enhanced sensitivity to the death signal induced by the Lurcher GRID2 receptor and/or induce parallel death pathways.

Our results show that GRID2 receptors can modulate neuronal death through a pathway that does not require depolarization of the neurons and which might involve direct molecular signaling pathways. Our data taken together with those of Yue et al. (2002) give strong in vivo evidence that this pathway is autophagy, whose overactivation can be directly induced by the interaction of GRID2^{Lc} with Beclin1 via n-PIST (Yue et al., 2002). It is interesting in this regard to note that in ischemia, direct inhibition of NMDA receptors or of calcium channels has been proven unsuccessful as a therapeutic strategy (Lee et al., 1999). Very recently, it has been shown that blocking the interaction between NMDA receptors and the scaffolding protein PSD-95 reduces focal ischemic brain damage in rats (Aarts et al., 2002). Altogether, these data highlight the possibility that in the different pathologies involving excitotoxicity, glutamate receptor activation might induce cell death not only through their channel function but also through direct molecular signaling pathways.

Experimental Procedures

Animals and Genotyping

Grid2^{Lc}/Grid2^{+} mice (B6CBA strain) were mated with *Grid2^{ho}/Grid2^{ho}* homozygotes (C57Bl6 strain ho-Nancy allele described in Lalouette et al. [2001]). *Grid2^{Lc}/Grid2^{ho}* animals identified by their ataxic phenotype were then further mated to *Grid2^{ho}/Grid2^{+}* or *Grid2^{Lc}/Grid2^{+}* animals to obtain *Grid2^{Lc}/Grid2^{ho}*, *Grid2^{Lc}/Grid2^{+}*, *Grid2^{ho}/Grid2^{+}*, and *Grid2^{Lc}/Grid2^{Lc}* animals in the same litter. *Grid2^{+}/Grid2^{+}* controls were obtained by crossing B6CBA mice with C57Bl6 mice. Litters were sacrificed at different ages from postnatal day 0 (P0) to P21 according to the guidelines from the NIH Guide for the Care and Use of Laboratory Animals. Genotyping was performed by polymerase chain reaction (PCR) followed by analysis of single-strand conformation polymorphism (SSCP) as described previously (Selimi et al., 2000b; Zuo et al., 1997). PCR was performed using 200–300 ng of genomic DNA and the following primers: 5′-TAAAAGCATATTGAT GTTGTTG-3′; 5′-CAGCATTTGTCAGGTTTGGTGAC-3′. At P0, morphological analysis of the brainstem was performed to differentiate between *Grid2^{Lc}/Grid2^{ho}* and *Grid2^{Lc}/Grid2^{Lc}* animals.

Histology and Neuronal Counts

10 μm-thick brain sections were obtained and stained with an anti-calbindin antibody and cresyl violet as previously described (Selimi et al., 2000b). The number of PCs per hemicerebellum was determined by counting the number of calbindin-immmunopositive PCs every 40th section at 1000× magnification. The total number of PCs was obtained from a graph of the number of PCs in each counted section plotted against the distance of the section from the midline. Corrections were made for double-counting PCs based on the method of Hendry (1976). We chose to use this traditional correction factor for our cell counts rather than more recently developed stereological techniques so that our results would be directly comparable with previously published counts. The external granule cell layer (EGL) thickness was measured in at least eight regions of the primary fissure in three vermal sections per cerebellum at 1000× magnification using a CCD camera and the NIH Image software. These measurements were made for three animals of each genotype to obtain the mean EGL thickness.

Immunohistochemistry and Electron Microscopy

GRID2 immunohistochemistry was performed based on the protocol of Takayama et al. (1995). 20 μm thick cryostat sections from P5 litters of a *Grid2^{Lc}/Grid2^{ho}* × *Grid2^{ho}/Grid2^{+}* cross were processed using an anti-GRID2 antibody (Chemicon, Temecula, CA) followed by an FITC conjugated anti-rabbit IgG and were analyzed using confocal microscopy.

Grid2^{Lc}/Grid2^{ho} (n = 3), *Grid2^{Lc}/Grid2^{+}* (n = 2), *Grid2^{ho}/Grid2^{+}* (n = 2), and *Grid2^{ho}/Grid2^{ho}* (n = 2) mice were perfused with a mixture of 4% paraformaldehyde and 2% glutaraldehyde in sodium phosphate buffer. Vibratome sagittal sections were postfixed with 2% osmium tetroxyde, then treated en bloc with uranyle acetate, and flat-embedded in Araldite M (Fluka). 60 nm ultrathin sections were examined with a Hitachi 7500 transmission electron microscope operated at 60kV.

Electrophysiology

250 μm thick cerebellar slices were prepared from P5–P12 mice using standard procedures (Llano et al., 1991). The slice recording chamber was continuously superfused with buffer containing 125 mM NaCl, 2.5 mM KCl, 1.25 mM NaH_2PO_4, 26 mM $NaHCO_3$, 2 mM $CaCl_2$, 1 mM $MgCl_2$, and 25 mM glucose, continuously bubbled with 95% O_2, 5% CO_2. Whole-cell patch-clamp recordings were made from PCs using an Axopatch 200 amplifier (Axon Instruments, Foster City, CA). Patch pipettes were filled with a solution containing 6 mM KCl, 140 mM K D-gluconate, 10 mM HEPES, 1 mM EGTA, 0.1 mM $CaCl_2$, 5 mM $MgCl_2$, 4 mM Na_2ATP, 0.4 mM NaGTP (pH 7.3, 290–300 mOsm). Purkinje cells were voltage clamped at −70mV while recording the holding current. In some cases, the superfusion buffer was replaced by a solution in which NaCl was substituted by 136

mM *N*-methyl-D-glucamine (NMDG) chloride (Zuo et al., 1997). This allowed confirmation that the leak current was indeed due to the Lurcher mutation and not to poor clamp quality. In the majority of recordings, 5 mg/ml biocytin was added to the pipette solution, and the slice was fixed (in 4% paraformaldehyde in PBS) to allow confirmation of the PC morphology using the ABC reaction (Elite ABC kit, Vectastain).

The number of animals and cells analyzed for each group was: at P5–P6, 9 $Grid2^{+}/Grid2^{ho}$ animals (45 cells), 4 $Grid2^{Lc}/Grid2^{+}$ (16), 4 $Grid2^{Lc}/Grid2^{ho}$ (16), 4 $Grid2^{+}/Grid2^{+}$ (17); at P9–P12, 10 $Grid2^{+}/Grid2^{ho}$ (23), 6 $Grid2^{Lc}/Grid2^{+}$ (17), 9 $Grid2^{Lc}/Grid2^{ho}$ (12), 3 $Grid2^{+}/Grid2^{+}$ (25).

Acknowledgments

We thank Pr. Nathaniel Heintz for helpful discussions concerning the manuscript. We also thank Pr. Jean-Louis Guénet for the use of his equipment, Mrs. P. Bouquet for her technical assistance with histology, the Centre de Traitement et de Production d'Images for help with digital figures, Dr. F. Frédéric for help with the statistics, and Mrs. P. Thouvenot for animal breeding. We are also grateful to S. Chasserot-Golaz, G. Bombarde, and the Plateforme Technique de Microscopie Confocale et Electronique (IFR37 de Neurosciences, Strasbourg). F.S. was supported by the Fondation Singer-Polignac. This work was also supported by NIH grant NS34309.

Received: July 8, 2002
Revised: January 24, 2003

References

Aarts, M., Liu, Y., Liu, L., Besshoh, S., Arundine, M., Gurd, J.W., Wang, Y.T., Salter, M.W., and Tymianski, M. (2002). Treatment of ischemic brain damage by perturbing NMDA receptor-PSD-95 protein interactions. Science *298*, 846–850.

Anglade, P., Vyas, S., Javoy-Agid, F., Herrero, M.T., Michel, P.P., Marquez, J., Mouatt-Prigent, A., Ruberg, M., Hirsch, E.C., and Agid, Y. (1997). Apoptosis and autophagy in nigral neurons of patients with Parkinson's disease. Histol. Histopathol. *12*, 25–31.

Araki, K., Meguro, H., Kushiya, E., Takayama, C., Inoue, Y., and Mishina, M. (1993). Selective expression of the glutamate receptor channel delta 2 subunit in cerebellar Purkinje cells. Biochem. Biophys. Res. Commun. *197*, 1267–1276.

Caddy, K.W., and Biscoe, T.J. (1979). Structural and quantitative studies on the normal C3H and Lurcher mutant mouse. Philos. Trans. R. Soc. Lond. B Biol. Sci. *287*, 167–201.

Cheng, S.S., and Heintz, N. (1997). Massive loss of mid- and hindbrain neurons during embryonic development of homozygous lurcher mice. J. Neurosci. *17*, 2400–2407.

Clarke, P.G. (1990). Developmental cell death: morphological diversity and multiple mechanisms. Anat. Embryol. (Berl.) *181*, 195–213.

Doughty, M.L., Lohof, A., Selimi, F., Delhaye-Bouchaud, N., and Mariani, J. (1999). Afferent-target cell interactions in the cerebellum: negative effect of granule cells on Purkinje cell development in lurcher mice. J. Neurosci. *19*, 3448–3456.

Doughty, M.L., De Jager, P.L., Korsmeyer, S.J., and Heintz, N. (2000). Neurodegeneration in lurcher mice occurs via multiple cell death pathways. J. Neurosci. *20*, 3687–3694.

Dumesnil-Bousez, N., and Sotelo, C. (1992). Early development of the Lurcher cerebellum: Purkinje cell alterations and impairment of synaptogenesis. J. Neurocytol. *21*, 506–529.

Feddersen, R.M., Ehlenfeldt, R., Yunis, W.S., Clark, H.B., and Orr, H.T. (1992). Disrupted cerebellar cortical development and progressive degeneration of Purkinje cells in SV40 T antigen transgenic mice. Neuron *9*, 955–966.

Grant, S.G., and O'Dell, T.J. (2001). Multiprotein complex signaling and the plasticity problem. Curr. Opin. Neurobiol. *11*, 363–368.

Hendry, I.A. (1976). A method to correct adequately for the change in neuronal size when estimating neuronal numbers after nerve growth factor treatment. J. Neurocytol. *5*, 337–349.

Iihara, K., Joo, D.T., Henderson, J., Sattler, R., Taverna, F.A., Lourensen, S., Orser, B.A., Roder, J.C., and Tymianski, M. (2001). The influence of glutamate receptor 2 expression on excitotoxicity in Glur2 null mutant mice. J. Neurosci. *21*, 2224–2239.

Kashiwabuchi, N., Ikeda, K., Araki, K., Hirano, T., Shibuki, K., Takayama, C., Inoue, Y., Kutsuwada, T., Yagi, T., Kang, Y., et al. (1995). Impairment of motor coordination, Purkinje cell synapse formation, and cerebellar long-term depression in GluR delta 2 mutant mice. Cell *81*, 245–252.

Kohda, K., Wang, Y., and Yuzaki, M. (2000). Mutation of a glutamate receptor motif reveals its role in gating and delta2 receptor channel properties. Nat. Neurosci. *3*, 315–322.

Kurihara, H., Hashimoto, K., Kano, M., Takayama, C., Sakimura, K., Mishina, M., Inoue, Y., and Watanabe, M. (1997). Impaired parallel fiber→Purkinje cell synapse stabilization during cerebellar development of mutant mice lacking the glutamate receptor delta2 subunit. J. Neurosci. *17*, 9613–9623.

Lalouette, A., Guenet, J.L., and Vriz, S. (1998). Hotfoot mouse mutations affect the delta 2 glutamate receptor gene and are allelic to lurcher. Genomics *50*, 9–13.

Lalouette, A., Lohof, A., Sotelo, C., Guenet, J., and Mariani, J. (2001). Neurobiological effects of a null mutation depend on genetic context: comparison between two hotfoot alleles of the delta-2 ionotropic glutamate receptor. Neuroscience *105*, 443–455.

Lancelot, E., and Beal, M.F. (1998). Glutamate toxicity in chronic neurodegenerative disease. Prog. Brain Res. *116*, 331–347.

Lee, J.M., Zipfel, G.J., and Choi, D.W. (1999). The changing landscape of ischaemic brain injury mechanisms. Nature *399*, A7–A14.

Llano, I., Marty, A., Armstrong, C.M., and Konnerth, A. (1991). Synaptic- and agonist-induced excitatory currents of Purkinje cells in rat cerebellar slices. J. Physiol. *434*, 183–213.

Mayat, E., Petralia, R.S., Wang, Y.X., and Wenthold, R.J. (1995). Immunoprecipitation, immunoblotting, and immunocytochemistry studies suggest that glutamate receptor delta subunits form novel postsynaptic receptor complexes. J. Neurosci. *15*, 2533–2546.

Resibois, A., Cuvelier, L., and Goffinet, A.M. (1997). Abnormalities in the cerebellum and brainstem in homozygous lurcher mice. Neuroscience *80*, 175–190.

Reynolds, I.J. (1998). Intracellular calcium and magnesium: critical determinants of excitotoxicity? Prog. Brain Res. *116*, 225–243.

Selimi, F., Doughty, M., Delhaye-Bouchaud, N., and Mariani, J. (2000a). Target-related and intrinsic neuronal death in Lurcher mutant mice are both mediated by caspase-3 activation. J. Neurosci. *20*, 992–1000.

Selimi, F., Vogel, M.W., and Mariani, J. (2000b). Bax inactivation in lurcher mutants rescues cerebellar granule cells but not Purkinje cells or inferior olivary neurons. J. Neurosci. *20*, 5339–5345.

Sheng, M., and Pak, D.T. (2000). Ligand-gated ion channel interactions with cytoskeletal and signaling proteins. Annu. Rev. Physiol. *62*, 755–778.

Smeyne, R., Chu, T., Lewin, A., Bian, F., S.-Crisman, S., Kunsch, C., Lira, S., and Oberdick, J. (1995). Local control of granule cell generation by cerebellar Purkinje cells. Mol. Cell. Neurosci. *6*, 230–251.

Takayama, C., Nakagawa, S., Watanabe, M., Mishina, M., and Inoue, Y. (1995). Light- and electron-microscopic localization of the glutamate receptor channel delta 2 subunit in the mouse Purkinje cell. Neurosci. Lett. *188*, 89–92.

Takayama, C., Nakagawa, S., Watanabe, M., Mishina, M., and Inoue, Y. (1996). Developmental changes in expression and distribution of the glutamate receptor channel delta 2 subunit according to the Purkinje cell maturation. Brain Res. Dev. Brain Res. *92*, 147–155.

Wetts, R., and Herrup, K. (1982). Interaction of granule, Purkinje and inferior olivary neurons in lurcher chimeric mice. II. Granule cell death. Brain Res. *250*, 358–362.

Wullner, U., Loschmann, P.A., Weller, M., and Klockgether, T. (1995). Apoptotic cell death in the cerebellum of mutant weaver and lurcher mice. Neurosci. Lett. *200*, 109–112.

Yue, Z., Horton, A., Bravin, M., DeJager, P.L., Selimi, F., and Heintz, N. (2002). A novel protein complex linking the delta 2 glutamate

receptor and autophagy: implications for neurodegeneration in lurcher mice. Neuron *35*, 921–933.

Zanjani, H.S., Rondi-Reig, L., Vogel, M., Martinou, J.C., Delhaye-Bouchaud, N., and Mariani, J. (1998). Overexpression of a Hu-bcl-2 transgene in Lurcher mutant mice delays Purkinje cell death. C. R. Acad. Sci. III *321*, 633–640.

Zhao, H.M., Wenthold, R.J., and Petralia, R.S. (1998). Glutamate receptor targeting to synaptic populations on Purkinje cells is developmentally regulated. J. Neurosci. *18*, 5517–5528.

Zuo, J., De Jager, P.L., Takahashi, K.A., Jiang, W., Linden, D.J., and Heintz, N. (1997). Neurodegeneration in Lurcher mice caused by mutation in delta2 glutamate receptor gene. Nature *388*, 769–773.

BAX Contributes to Doppel-Induced Apoptosis of Prion-Protein–Deficient Purkinje Cells

S. Heitz,[1] Y. Lutz,[2] J.-L. Rodeau,[3] H. Zanjani,[4] V. Gautheron,[4] G. Bombarde,[1] F. Richard,[1] J.-P. Fuchs,[2] M. W. Vogel,[5] J. Mariani,[4,6] Y. Bailly[1]

[1] Département Neurotransmission et Sécrétion Neuroendocrine, Institut des Neurosciences Cellulaires et Intégratives (UMR7168-LC2), CNRS/Université Louis Pasteur, IFR 37 des Neurosciences de Strasbourg, 5 Rue Blaise Pascal, 67084 Strasbourg, France

[2] Physiopathologie du Système Nerveux, INSERM U575, IFR 37 des Neurosciences de Strasbourg, 5 Rue Blaise Pascal, 67084 Strasbourg, France

[3] Département Nociception et Douleur, Institut des Neurosciences Cellulaires et Intégratives (UMR7168-LC2), CNRS/Université Louis Pasteur, IFR 37 des Neurosciences de Strasbourg, 21 Rue René Descartes, 67084 Strasbourg, France

[4] Neurobiologie des Processus Adaptatifs, Equipe Développement et Vieillissement du Système Nerveux (UMR7102), CNRS/Université Pierre et Marie Curie, 9 Quai Saint Bernard, 75005 Paris, France

[5] Maryland Psychiatric Research Center, University of Maryland, School of Medicine Baltimore, Maryland 21228

[6] APHP, Hôpital Charles Foix, UEF 94200 Ivry/Seine, France

Received 17 May 2006; revised 20 September 2006; accepted 17 October 2006

ABSTRACT: **Research efforts to deduce the function of the prion protein (PrP^c) in knock-out mouse mutants have revealed that large deletions in the PrP^c genome result in the ectopic neuronal expression of the prion-like protein Doppel (Dpl). In our analysis of one such line of mutant mice, Ngsk *Prnp*$^{0/0}$ (*NP*$^{0/0}$), we demonstrate that the ectopic expression of Dpl in brain neurons induces significant levels of cerebellar Purkinje cell (PC) death as early as six months after birth. To investigate the involvement of the mitochondrial proapoptotic factor BAX in the Dpl-induced apoptosis of PCs, we have analyzed the progression of PC death in aging *NP*$^{0/0}$:*Bax*$^{-/-}$ double knock-out mutants. Quantitative analysis of cell numbers showed that significantly more PCs survived in *NP*$^{0/0}$:*Bax*$^{-/-}$ double mutants than in the *NP*$^{0/0}$:*Bax*$^{+/+}$ mutants. However, PC numbers were not restored to wildtype levels or to the increased number of PCs observed in *Bax*$^{-/-}$ mutants. The partial rescue of *NP*$^{0/0}$ PCs suggests that the ectopic expression of Dpl induces both BAX-dependent and BAX-independent pathways of cell death. The activation of glial cells that is shown to be associated topographically with Dpl-induced PC death in the *NP*$^{0/0}$:*Bax*$^{+/+}$ mutants is abolished by the loss of *Bax* expression in the double mutant mice, suggesting that chronic inflammation is an indirect consequence of Dpl-induced PC death.** © 2007 Wiley Periodicals, Inc. Develop Neurobiol 67: 670–686, 2007

Keywords: **prion protein; Doppel; BAX; apoptosis; Purkinje cell**

Correspondence to: Dr. Y. Bailly (byan@neurochem.u-strasbg.fr).
Contract grant sponsor: G.I.S. Maladies à Prions.
Contract grant sponsor: National Institute of Health; contract grant number: NS34309.

Published online 20 February 2007 in Wiley InterScience (www.interscience.wiley.com).
DOI 10.1002/dneu.20366

INTRODUCTION

Doppel (Dpl) is the first identified homolog of the cellular prion protein, PrP^c, implicated in the pathogenesis of transmissible spongiform encephalopathies (TSE) (Prusiner, 1998). Dpl is an N-truncated form of PrP^c with common structural features as well as cellular trafficking pathways (Weissmann and Aguzzi, 1999; Silverman et al., 2000; Flechsig et al., 2003; Qin et al., 2003; Massimino et al., 2004). Targeted disruptions of the PrP^c coding gene (*Prnp*) that extend into the upstream region of intron 2 result in cis-activation of the Dpl gene (*Prnd*). Ectopic Dpl neuronal expression in $Prnp^{0/0}$ mouse lines such as Ngsk (Sakaguchi et al., 1996), Rcm0 (Moore et al., 1995), ZH-II (Rossi et al., 2001), and Rikn (Yokoyama et al., 2001) causes late onset Purkinje cell (PC) degeneration and ataxia. Dpl shares 25% identity to PrP^c, but lacks its flexible N-terminal sequence. Expression of the N-terminal truncated form of PrP (ΔPrP) in *Prnp*-ablated mouse lines (Flechsig et al., 2003) causes neurodegenerative effects in PCs similar to the overexpression of Dpl (Anderson et al., 2004; Yamaguchi et al., 2004), and the neurotoxic effects of Dpl and ΔPrP are both antagonized by PrP^c (Nishida et al., 1999; Cui et al., 2003; Flechsig et al., 2003; Anderson et al., 2004; Yamaguchi et al., 2004). These results suggest that Dpl and ΔPrP may cause cell death by the same mechanism, perhaps by interfering with a cellular signaling pathway essential for cell survival and normally controlled by full-length PrP^c (Shmerling et al., 1998; Anderson et al., 2004).

To date, only a few studies have investigated the mechanism by which Dpl kills neurons. PrP-deficient cells have been shown to undergo Dpl-induced apoptosis in a dose-dependent, cell autonomous manner (Sakudo et al., 2005). Furthermore, oxidative stress and glial activation may play a role in the death of neurons since NOS activity is induced by Dpl *in vitro* and *in vivo* (Wong et al., 2001; Cui et al., 2003) and ectopic expression of Dpl in Ngsk $Prnp^{0/0}$ ($NP^{0/0}$) mice is associated with an activation of glial cells (Atarashi et al., 2001). The normal prion protein, PrP^c, has a protective function since Dpl-induced apoptosis is inhibited by PrP^c either expressed endogenously or applied exogenously (Cui et al., 2003). The neuroprotective functions of PrP^c have been attributed to its BCL-2-like properties (Kuwahara et al., 1999). PrP^c binds to BCL-2 in the yeast two-hybrid system (Kurschner and Morgan, 1995) and PrP^c as well as BCL-2 protect yeast (Li and Harris, 2005) and neurons (Bounhar et al., 2001; Roucou et al., 2003) from BAX-induced apoptosis. PrP^c protects against cell death by preventing the conformational change of BAX that occurs during BAX activation (Roucou et al., 2005). Thus, PrP^c seems to have an antagonistic function on mitochondrial apoptotic pathways.

To investigate the involvement of BAX in the mechanism of Dpl-induced apoptosis, we have crossed $NP^{0/0}$:$Bax^{+/+}$ mice with $Bax^{-/-}$ mice to obtain $NP^{0/0}$:$Bax^{-/-}$ double mutant mice. The survival of cerebellar PCs was analyzed in these mice at a period of maximal PC death in $NP^{0/0}$:$Bax^{+/+}$ mice (i.e. 12–21 months). In addition, the distribution of PCs and activated astrocytes was analyzed by immunohistofluorescence in $NP^{0/0}$:$Bax^{+/+}$ and double mutant mice to investigate a causal link between PC loss and gliosis in the cerebellar cortex and the eventual effect of *Bax* inactivation in this process.

METHODS

Animals and Genotyping

As previously reported, $Bax^{-/-}$ mice were generated by deleting exons 2–5 (Knudson et al., 1995); further breeding strategies were designed taking into account that $Bax^{-/-}$ males are sterile. $NP^{0/0}$:$Bax^{+/+}$ mice were generated by deleting the entire open reading frame (ORF) of the *Prnp* gene, located in exon 3, as well as 5′ and 3′ noncoding flanking regions (Sakaguchi et al., 1995). In both cases the deleted sequences were replaced by a Neo cassette. Genotypes were determined by PCR. *Bax* mutants were identified as described earlier (Knudson et al., 1995). The *Prnp* ORF was identified using the following primers: forward 5′CCGCTACCCTAACCAAGTGT3′ and reverse 5′CCTAGACCACGAGAATGCGA3′, both located within the *Prnp* ORF. $NP^{0/0}$:$Bax^{+/+}$ mutants were identified using the following primers: forward 5′TGCCGCACTTCTTTGTGAAT3′ and reverse 5′CGGTGGATGTGGAATGTGT3′ (within Neo cassette).

For this study, founding mice have been first backcrossed with C57BL/6 mice for at least 10 generations. $NP^{0/0}$:$Bax^{+/+}$ males or females (gift from S. Katamine) were then crossed with $Bax^{+/-}$ males or females (gift from S. Korsmeyer) and offspring were identified by PCR genotyping using the aforementioned primer sets. $NP^{+/0}$:$Bax^{+/-}$ mice were further intercrossed, generating $NP^{0/0}$:$Bax^{-/-}$, $NP^{0/0}$:$Bax^{+/-}$, $NP^{0/0}$:$Bax^{+/+}$, $NP^{+/0}$:$Bax^{-/-}$, $NP^{+/0}$:$Bax^{+/-}$, $NP^{+/0}$:$Bax^{+/+}$, $NP^{+/+}$:$Bax^{+/+}$, NP^{+}:$Bax^{+/-}$, and $NP^{+/+}$:$Bax^{-/-}$ genotypes. The $NP^{0/0}$:$Bax^{-/-}$ double mutants were obtained by crossing $NP^{0/0}$:$Bax^{+/-}$ males with $NP^{0/0}$:$Bax^{-/-}$ or $NP^{0/0}$:$Bax^{+/-}$ females. Strict littermates of the different genotypes have been used throughout the study. All mice were submitted to footprint tests at 10, 12, 14, 16, and 18 months.

Mice were bred at the animal facilities of the Neurosciences IFR37 in Strasbourg and maintained according to the NIH guidelines (NIH Publication 80–23, revised 1996)

Table 1 Age and Number of Mutants and Normal Mice, Mean Area and Long Diameter ± SD of Purkinje Cell (PC) Nuclei and Mean Numbers ± SD of PC Counted in Groups of Age- and Genotype-Matched Mice

Genotype	Age (month)	No. of Mice	Mean Area of PC Nuclei (μm^2)	Mean Long Diameter of PC Nuclei (μm)	Mean no. of PC
Wildtype	12	3	93.52 ± 7.41	12.93 ± 0.73	135,554 ± 6760
	16	3	Not done	Not done	145,271 ± 6,657
	18	3	96.26 ± 6.24	13.08 ± 0.47	147,884 ±90,94
	21	3	77.56 ± 13.32	11.86 ± 1.06	143,303 ± 8,905
$Bax^{-/-}$	12	3	72.81 ± 1.78	11.99 ±0.2	200,197 ± 11,871
	16	3	Not done	Not done	173,518 ± 13,761
	18	3	88.35 ± 21.08	12.47 ± 1.55	138,083 ±10,423
$NP^{0/0}$:$Bax^{+/+}$	4	3	85.92 ± 8.82	12.94 ± 0.07	145,014 ± 10,472
	6	3	Not done	Not done	112,918 ± 8,419
	10	3	Not done	Not done	79,836 ± 1,853
	12	3	93.47 ± 11.58	13.20 ± 0.88	61,236 ± 671
	16	3	Not done	Not done	48,788 ± 763
	18	3	100.69 ± 5.32	13.75 ± 0.21	40,940 ± 1,695
	21	3	76.91 ± 10.5	12.48 ± 0.32	36,757 ± 3,464
$NP^{0/0}$:$Bax^{+/-}$	12	3	83.42 ± 9.13	12.35 ± 0.30	73,146 ± 7,230
	18	3	84.24 ± 18.2	12.63 ± 0.99	42,853 ± 4,377
	21	3	80.27 ± 13.82	12.55 ± 0.47	42,378 ± 6,987
$NP^{0/0}$:$Bax^{-/-}$	12	3	82.54 ± 12.2	12.44 ± 0.81	89,796 ± 6,019
	16	3	Not done	Not done	90,454 ± 6,607
	18	3	89.55 ± 2.81	12.82 ± 0.3	81,821 ± 2,208
	21	3	81.32 ± 12.09	12.19 ± 0.56	72,475 ± 5,172

and the European Communities Council Directive of November 24, 1986 (86/609/EEC). A minimal number of animals were used (Table 1) and handled with maximum care to minimize their suffering.

Histology

All mice (Table 1) were anesthetized with sodium pentobarbital (0.15 mL per 100 g, i.p.; Sanofi), after which brains were dissected and immersed overnight in Carnoy's fixative (60% ethanol, 30% chloroform, 10% acetic acid). Brains were dehydrated, embedded in paraffin, and sectioned in the sagittal plane at 10 μm.

In addition, 10- and 21-month-old $NP^{0/0}$:$Bax^{+/+}$ mice ($n = 3$/age) were anesthetized as described earlier and perfused with 4% paraformaldehyde in 0.1 M phosphate buffer (PB), pH 7.3. The brains were dissected and immersed for 4 h in the same fixative at 4°C before cryoprotective treatment by immersion in 0.44 M sucrose in PB at 4°C overnight. After freezing the brains in liquid nitrogen, transverse sections were cut (10 μm thick) with a cryostat (Leica).

Size of the Cerebellar Vermis

The size of the cerebellar vermis was estimated by measuring the mean area of seven sagittal cresyl-violet—stained sections (ImageJ) separated from each other by 400 mm (total sampling distance, 2470 μm) in the 18- and 21-month-old wildtype, $NP^{0/0}$:$Bax^{+/+}$, $NP^{0/0}$:$Bax^{+/-}$, $NP^{0/0}$:$Bax^{-/-}$, and $Bax^{-/-}$ mice ($n = 3$/genotype).

Cell Counts

The PC population was quantified in all mice aged from 4 to 21 months (Table 1). The cresyl-violet—stained PCs were counted in 10-μm-thick paraffin sections using a 63× objective (final magnification, 630×) in every 40th sagittal section (from a random start) through the entire cerebellum as described previously (Wetts and Herrup, 1982; Herrup and Sunter, 1986; Zanjani et al., 2004). In brief, the PC nuclei profiles were counted along the entire length of the PC layer in each section. PCs were identified as neurons in the PC layer with a large soma and some portion of their nuclei in the plane of the section [black arrowheads in Fig. 1(C,F,I,L,O)]. The total number of PCs was estimated by graphing the number of visible PC nuclei per section as a function of the distance of each section from the midline and then integrating the area under the polygon to calculate the raw total. The raw total was adjusted for double counting errors using the Hendry correction (Hendry, 1976) because it was specifically designed to account for experimental changes in the size of the cells being counted (Zanjani et al., 2004). The Hendry correction factor is calculated in each cerebellum from measurements of the nuclear profile area and long diameter of over 300 PCs using ImageJ. We chose to use this classical correction factor for our cell counts instead of more recently developed stereological

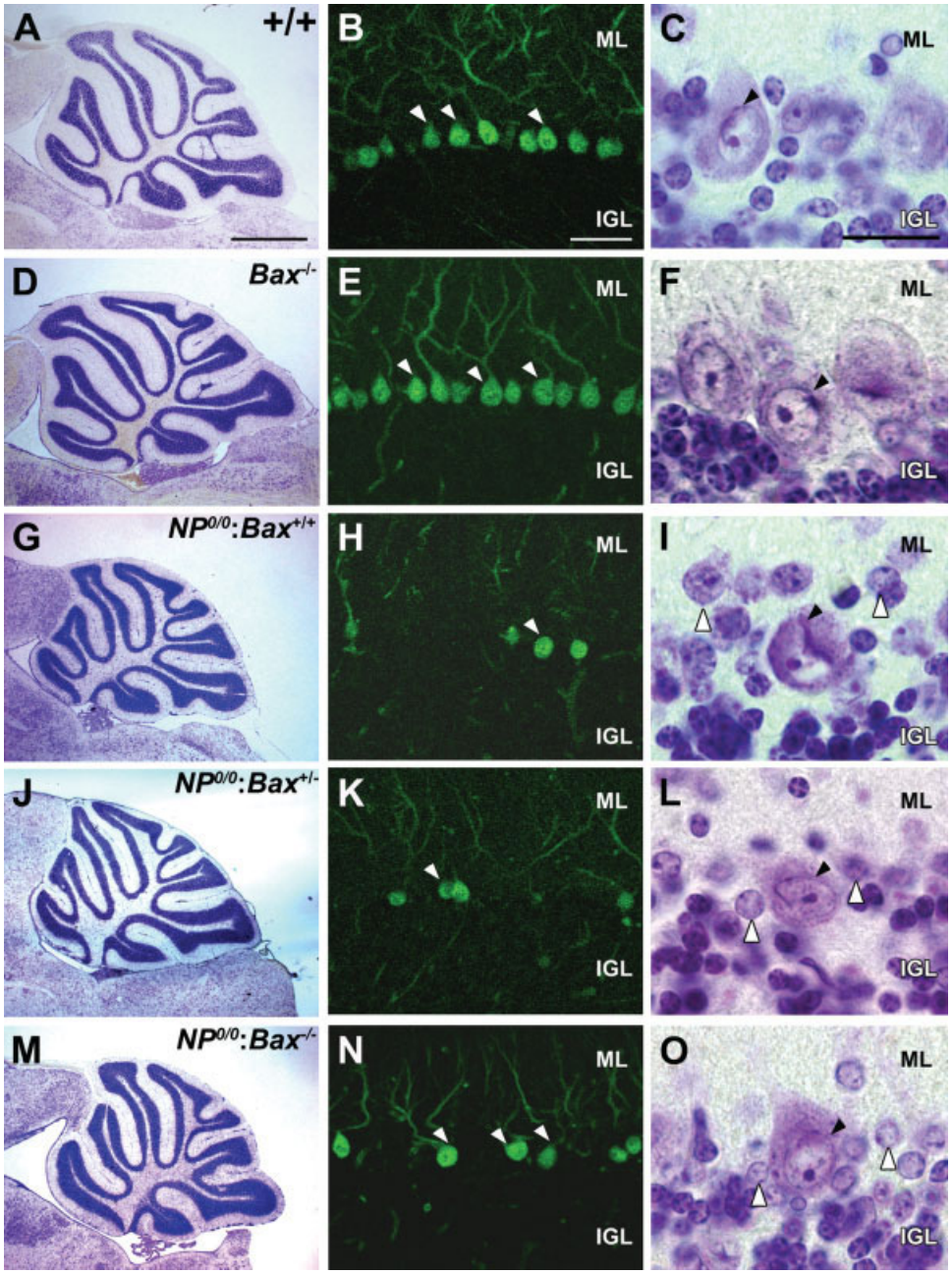

Figure 1 Histology of the cerebellum of the 18-month-old wildtype (A,B,C), $Bax^{-/-}$ (D,E,F), $NP^{0/0}$:$Bax^{+/+}$ (G,H,I), $NP^{0/0}$:$Bax^{+/-}$ (J,K,L), and $NP^{0/0}$:$Bax^{-/-}$ (M,N,O) mice. Cresyl-violet staining (A,C,D,F,G,I,J,L,M,O) and calcium-binding protein 28 kDa (CaBP) immunofluorescence (B,E,H,K,N) in sagittal sections of the median vermis. The cerebellum appears smaller in the $NP^{0/0}$:$Bax^{+/+}$, $NP^{0/0}$:$Bax^{+/-}$, and the $NP^{0/0}$:$Bax^{-/-}$ than in the wildtype and $Bax^{-/-}$ genotypes. The CaBP-immunofluorescent PCs (white arrowheads) form a dense monolayer between the molecular (ML) and the internal granular (IGL) layers in the wildtype (B) and $Bax^{-/-}$ (E) cerebellar cortex. PC loss is moderate in the $NP^{0/0}$:$Bax^{-/-}$ cerebellar cortex (N) and almost complete in the $NP^{0/0}$:$Bax^{+/+}$ (H) and $NP^{0/0}$:$Bax^{+/-}$ (K) cerebellar cortex. In the cerebellar cortex of all mice (C,F,I,L,O), PCs display a normal aspect and location between ML and IGL. Black arrowheads point to the PC nuclei. White arrowheads point to nuclei of presumptive astrocytes, the number of which is increased around PC soma in the cerebellar cortex of the $NP^{0/0}$:$Bax^{+/+}$ (I), $NP^{0/0}$:$Bax^{+/-}$ (L), and $NP^{0/0}$:$Bax^{-/-}$ (O) mice. A,D,G,J,M, ×17; bar = 1 mm. B,E,H,K,N, ×200; bar = 50 μm. C,F,I,L,O, ×630; bar = 20 μm. [Color figure can be viewed in the online issue, which is available at www.interscience.wiley.com.]

techniques since the profile counting method provides data on the transversal distribution of PCs. None of the nuclear profile area and long diameter measurements varied significantly between age-matched groups of different genotypes and between groups of the same genotype at different ages (Table 1).

The lateral distribution of PC loss and of PC rescue was estimated in age-matched $NP^{0/0}$:$Bax^{+/+}$mutants versus wildtype and $NP^{0/0}$:$Bax^{-/-}$ double mutants by comparing PC numbers between corresponding sagittal levels (2 levels/hemisphere and 7 vermal levels). The rostrocaudal distribution of PC loss in age-matched $NP^{0/0}$:$Bax^{+/+}$ versus wildtype cerebellum and of PC rescue in age-matched $NP^{0/0}$:$Bax^{-/-}$ versus $NP^{0/0}$:$Bax^{+/+}$ cerebellum was estimated by comparing the PC numbers ratios between the anterior cerebellum (lobules I to V) and the posterior cerebellum (lobules VI to X) in the corresponding sagittal levels (2 levels/hemisphere and 7 vermal levels).

All the PC counts were performed by the same person (SH), with the genetic identity of the animals masked.

Statistics

Data are given as mean ± standard deviation (SD). Statistical comparisons of group means (cerebellar size, PC numbers, PC numbers anterior/posterior ratio, PC nuclear area and long diameter, $n = 3$ mice per group) were performed with Minitab 13.20. Depending on the context, either two-way ANOVA (factor "genotype", factor "age" and within factors "brain region" and "parasagittal level") or one-way ANOVA (factor "genotype", factor "age") was used, followed by *post hoc* Tukey test for multiple comparisons when justified. The significance threshold was set at $p = 0.05$.

Statistical significance of the difference in PC numbers between 4-month-old $NP^{0/0}$:$Bax^{+/+}$ and 12-month-old wildtype as well as between astrogliotic and nonastrogliotic areas of the 4-month-old $NP^{0/0}$:$Bax^{+/+}$ cerebellar cortex was determined by using Student's test ($p < 0.05$). The same test was applied to compare PC numbers between cerebellar cortex areas with intense versus normal GFAP immunostaining in the 4-month-old $NP^{0/0}$:$Bax^{+/+}$ mice.

Immunoperoxidase for Glial Fibrillary Acidic Protein

Brain sections of wildtype (4 and 18 months), $NP^{0/0}$:$Bax^{+/+}$ (4, 10, and 18 months), $NP^{0/0}$:$Bax^{-/-}$ (10 and 18 months), and $Bax^{-/-}$ (18 months) mice were deparaffinized in toluene and rehydrated in decreasing concentrations of ethanol. The sections were incubated in 1% H_2O_2 in 0.1 *M* phosphate-buffered saline (PBS) for 20 min. After rinsing in PBS, the sections were preincubated for 45 min in blocking solution made of 0.5% Triton X-100 and 3% normal horse serum (NHS) in PBS (PBST). The sections were then incubated overnight at 4°C in PBST containing 0.3% NHS and mouse monoclonal antibody against glial fibrillary acidic protein (GFAP; Sigma) diluted 1/500. The sections were then rinsed in PBS (2 × 10 min) and incubated with biotinylated horse anti-mouse immunoglobulins (Vector Labs). The GFAP-bound biotinylated horse anti-mouse immunoglobulins were visualized using the ABC method (Hsu et al., 1981) with 3,3′-diamino-benzidine tetra-hydrochloride (Fast-DAB, Sigma) as the chromogen. Six sections separated from each other by 400 μm were selected in the cerebellar vermis of the three 4-month-old $NP^{0/0}$:$Bax^{+/+}$ mice to be immunostained for GFAP and counterstained with cresyl violet. Stained sections were rinsed in PBS, dehydrated in graded ethanol and toluene, and mounted with Eukitt. The sections were examined under a light microscope equipped with differential interference contrast illumination (Axioskop-II, Zeiss, Jena, Germany). In each section, Purkinje cells (PCs) with a visible nucleus were counted in 1–5 cortical areas delineated sharply by intense GFAP immunostaining of activated astrocytes as well as in equivalent areas of cerebellar cortex with normal intensity of GFAP staining. Similar lengths of astrocytotic and unreactive cerebellar cortex (1–2 mm) were analyzed in each animal.

Immunofluorescence Staining for Calcium-Binding Protein

Brain sections of 18-month-old wildtype, $NP^{0/0}$:$Bax^{+/+}$, $NP^{0/0}$:$Bax^{-/-}$, $NP^{0/0}$:$Bax^{+/-}$, and $Bax^{-/-}$ mice were deparaffinized in toluene and rehydrated in decreasing concentrations of ethanol. After rinsing in PBS, the sections were preincubated for 45 min in blocking solution made of 0.5% Triton X-100 and 3% normal goat serum (NGS) in PBS (PBST). The sections were then incubated overnight at 4°C in PBST containing 0.3% NGS and mouse monoclonal antibody against calcium-binding protein (CaBP; Sigma) diluted 1/500. The sections were then rinsed in PBS (2 × 10 min) and incubated with green fluorescent Alexa 488 goat anti-mouse immunoglobulins (Molecular Probes) diluted 1/500 in PBS containing 0.3% NGS.

Double Immunofluorescence Staining for GFAP and CaBP

Frozen brain sections of paraformaldehyde-fixed 4–21-month-old $NP^{0/0}$:$Bax^{+/+}$ mice were rinsed in PBS and were preincubated for 45 min in blocking solution made of 0.5% Triton X-100 and NGS in PBS (PBST). The sections were then incubated overnight at 4°C in PBST containing 0.3% NGS, rabbit polyclonal antibody against GFAP (Dako) diluted 1/500, and mouse monoclonal antibody against CaBP (Sigma) diluted 1/500. The next day, sections were rinsed in PBS (2 × 10 min) and then incubated with second antibodies: green fluorescent Alexa 488 goat anti-rabbit immunoglobulins (Molecular Probes) and red fluorescent Alexa 546 goat anti-mouse immunoglobulins (Molecular Probes) diluted 1/500 in PBS containing 0.3% NGS.

After rinsing in PBS, single and double immunofluorescent sections were mounted in Mowiol before examination under a fluorescence microscope (Axioskop-II, Zeiss, Jena, Germany).

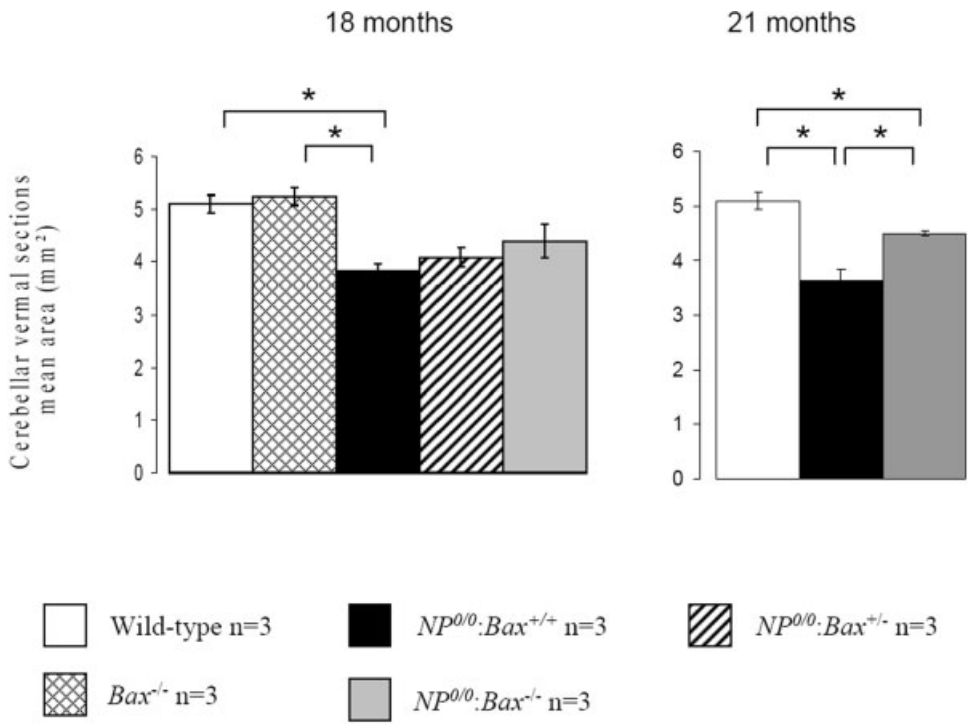

Figure 2 The 18-month-old $NP^{0/0}$:$Bax^{+/+}$ mice have a significantly smaller cerebellum (estimated size by the mean area (mm^2) of 7 sagittal sections in the vermis) than the wildtype and $Bax^{-/-}$ mice ($F_{4,10} = 8.07$, $p < 0.01$) of the same age. At 21 months, the $NP^{0/0}$:$Bax^{-/-}$ mice have a significantly larger cerebellum than do $NP^{0/0}$:$Bax^{+/+}$ mice ($F_{2,6} = 76.27$, $p < 0.01$).

Digital Images

Digital micrographs were stored using Zeiss Axiovision software. Photoshop 7.0 was used for final adjustments of contrast and brightness.

RESULTS

Bax Deletion Rescues $NP^{0/0}$ PCs From Doppel Neurotoxicity

Bax Deletion Has No Significant Effect on $NP^{0/0}$ Ataxia and Cerebellar Atrophy. The abnormal cerebral expression of Dpl has been shown to be responsible for premature death of PCs in the PrP-deficient mice of the Ngsk line (Moore et al., 2001; Anderson et al., 2004). To determine whether the proapoptotic BCL-2 family member BAX is required for $NP^{0/0}$ PC death, we have analyzed some features of the motor behavior and cerebellar anatomy of $NP^{0/0}$:$Bax^{-/-}$ double mutants and controls through the period of cerebellar degeneration in $NP^{0/0}$:$Bax^{+/+}$ mutants. All pups developed normally into the 12th postnatal month when $NP^{0/0}$:$Bax^{+/+}$ mutants and double mutants began to exhibit motor impairment characteristic of the $NP^{0/0}$:$Bax^{+/+}$ condition, as shown by hind footprints analysis (a trembling of the hindquarters on initiation of movement and during walking; Sakaguchi et al., 1996). No difference was observed in the timing of the onset of ataxia between $NP^{0/0}$:$Bax^{-/-}$, $NP^{0/0}$:$Bax^{+/+}$, and $NP^{0/0}$:$Bax^{+/-}$ mutants (data not shown). The folial pattern and cytoarchitecture of the cerebellum of the $Bax^{-/-}$, $NP^{0/0}$:$Bax^{+/+}$, $NP^{0/0}$:$Bax^{+/-}$, and $NP^{0/0}$:$Bax^{-/-}$ mutants were normal when compared with that of wildtype mice at all ages studied (Fig. 1). There were no obvious differences between the wildtype and $Bax^{-/-}$ mice in the overall size of the cerebella (Fig. 2) or in the histological aspect of the molecular and internal granular layers [Fig. 1(B,E)]. However, the size of the cerebellar vermis was significantly reduced in the 18- and 21-month-old $NP^{0/0}$:$Bax^{+/+}$ mice (Fig. 2). The size of the cerebellar vermis of the 21-month-old $NP^{0/0}$:$Bax^{-/-}$ mice was intermediate between that of wildtype mice and $NP^{0/0}$:$Bax^{+/+}$ mutants (Fig. 2). PCs in the mutants were arrayed normally at the interface between the molecular and the internal granular layers [Fig. 1(E-F,H-I,K-L,N-O)], and they were indistinguishable from wildtype PCs [Fig. 1(B,C)]. However, the PC monolayer appeared to contain fewer neurons in the $NP^{0/0}$:$Bax^{+/+}$, the

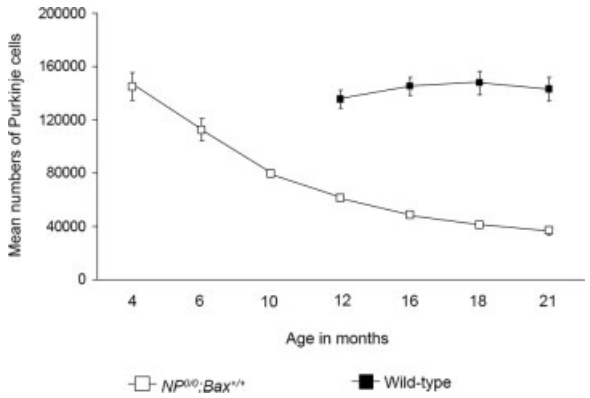

Figure 3 Time course of PCs mean numbers in the cerebellum of wildtype and $NP^{0/0}$:$Bax^{+/+}$ mutant mice during adulthood and aging. PC numbers of 4-month-old $NP^{0/0}$:$Bax^{+/+}$ mutant mice were not significantly different from those of wildtype mice at 12 months ($t_4 = 1.29$, $p > 0.25$).

$NP^{0/0}$:$Bax^{-/-}$, and the $NP^{0/00/0}$:$Bax^{-/-}$ mice [Fig. 1(H,K,N)] than in the wildtype and $Bax^{-/-}$ mice [Fig. 1(B,E)].

PC Death Is Already Significant in the 6-Month-Old $NP^{0/0}$:$Bax^{+/+}$ Cerebellum. The neurotoxic effect of Dpl overexpression was evaluated by estimating PC loss in the cerebellum of the $NP^{0/0}$:$Bax^{+/+}$ mice from 4 to 21 months. PC loss induced by Dpl was previously detected at 20 months in the cerebellum of the $NP^{0/0}$:$Bax^{+/+}$ mice (Sakaguchi et al., 1996). An earlier decrease in mRNA expression of the PC specific IP3R1 was detected in the cerebellum of 8-month-old $NP^{0/0}$:$Bax^{+/+}$ mice (Atarashi et al., 2001). In this study, the number of PCs remained stable in wildtype mice from 12 to 21 months ($F_{3,8} = 1.46$, $p > 0.2$, Table 1, Fig. 3). In contrast, although PC numbers were normal in the 4-month-old $NP^{0/0}$:$Bax^{+/+}$ mutants, the PC population declined thereafter until 21 months, PC loss slowing between 12 and 21 months ($F_{6,14} = 172.67$, $p < 0.001$, Table 1, Fig. 3).

Bax Deletion Protects PCs from Dpl-Induced Apoptosis. The role of *Bax* expression in the apoptotic mechanism triggered by Dpl in the PrP-deprived PCs was investigated by comparing the total number of PCs between $NP^{0/0}$:$Bax^{-/-}$, $NP^{0/0}$:$Bax^{+/-}$, $NP^{0/0}$:$Bax^{+/+}$, $Bax^{-/-}$ and wildtype mice at 10, 12, 16, 18, and 21 months of age (Table 1).

When comparing $NP^{0/0}$:$Bax^{-/-}$ and $NP^{0/0}$:$Bax^{+/+}$ at 10–21 months, two-way ANOVA showed a significant effect of genotype ($F_{1,20} = 666.77$, $p < 0.001$) and age ($F_{4,20} = 120.33$, $p < 0.001$) and of their interaction ($F_{4,20} = 3.37$, $p < 0.05$). The cerebellum of the 12-month-old $NP^{0/0}$:$Bax^{-/-}$ double mutants contained 47% more PCs than the cerebellum of the $NP^{0/0}$:$Bax^{+/+}$ mutants of the same age (Fig. 4). This difference increased with age up to 97% at 21 months, suggesting that *Bax* deletion protects PCs from Dpl-mediated toxicity. Although the number of PCs did not change significantly between 10 and 18 months in the $NP^{0/0}$:$Bax^{-/-}$ double mutants, there is a significant decrease between 12 and 21 months (Fig. 4), indicating that some PC loss still occurs in spite of *Bax* deletion.

The mean number of PCs was also higher in $NP^{0/0}$:$Bax^{+/-}$ mice than in $NP^{0/0}$:$Bax^{+/+}$ mice (significant effect of genotype: $F_{1,12} = 8.29$, $p = 0.014$, and of age: $F_{2,12} = 61.7$, $p < 0.001$). The interaction term was not significant ($F_{2,12} = 1.68$, $p > 0.2$, Fig. 4), which means that this relative increase was similar at 12 (20%), 18 (5%), and 21 (3.5%) months (Table 1).

Spatial Extent of Dpl Neurotoxicity and Bax Knock-Out Neuroprotection. Although significant PC loss occurred at each parasagittal level in the $NP^{0/0}$:$Bax^{+/+}$ cerebellum at any age studied [Fig. 5(A)], normalizing values of PC numbers at the different parasagittal levels counted in the cerebellar vermis and hemispheres of the 12-, 16-, and 18 [Fig 5(B)]-month-old $NP^{0/0}$:$Bax^{+/+}$ and wildtype mice did not disclose significant differences in PC loss along the transversal dimension of the $NP^{0/0}$:$Bax^{+/+}$ cerebellum.

Two-way repeated measures ANOVA with factors "genotype" and "brain region" (anterior/posterior, within-subject) showed a significant rostrocaudal difference similar in wildtype, $NP^{0/0}$:$Bax^{+/+}$ and $NP^{0/0}$:$Bax^{-/-}$ mice at 12 (data not shown, factor genotype: $F_{2,6} = 28.47$, $p < 0.001$, factor region: $F_{1,6} = 101.09$, $p < 0.001$, interaction term: $F_{2,6} = 1.38$, $p = 0.322$)

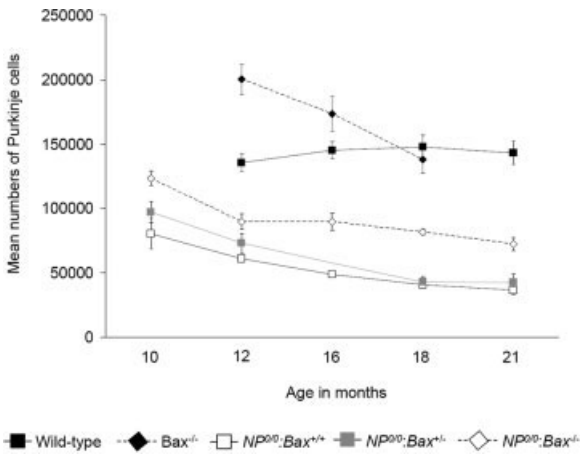

Figure 4 Time course of PCs mean numbers in the cerebellum of wildtype and different mutant mice during aging.

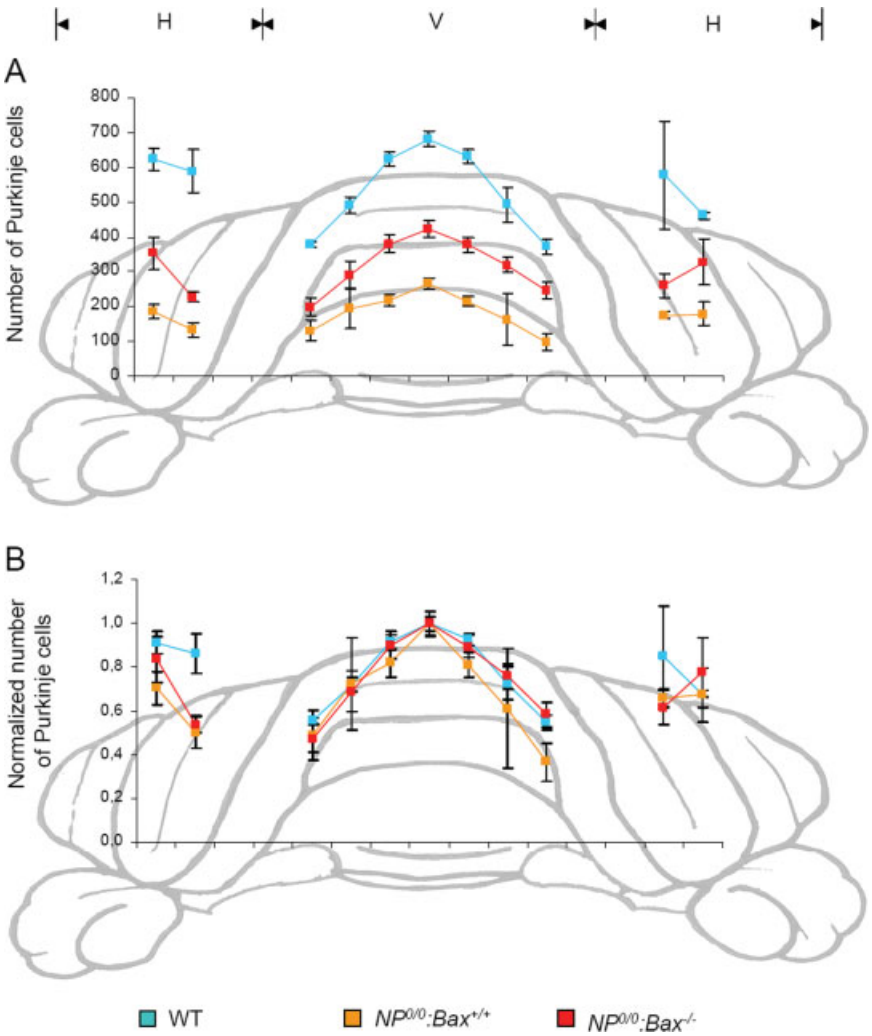

Figure 5 A. At any of the 11 parasagittal levels analyzed in the cerebellar vermis (V) and left (LH) and right (RH) hemispheres PC numbers are significantly different in the 18-month-old wild-type (blue), $NP^{0/0}$:$Bax^{-/-}$ (red) and $NP^{0/0}$:$Bax^{+/+}$ (orange) mice (two-way ANOVA with repeated measures on parasagittal levels: effect of genotype: $F_{2,60} = 113.17$, $p < 0.001$; effect of level: $F_{10,60} = 20.79$, $p < 0.001$; effect of interaction: $F_{20,60} = 2.23$, $p < 0.01$). B. The same data are normalized within each group to the mean value ($n = 3$) of PC numbers at the sagittal level. Two-way ANOVA (effect of genotype: $F_{2,66} = 12.19$, $p < 0.001$; effect of parasagittal level: $F_{10,66} = 21.87$, $p < 0.001$; effect of interaction: $F_{20,66} = 1.72$, $p > 0.05$) failed to disclose any significant difference at any parasagittal level analyzed.

and 18 [Fig. 6(A); factor genotype: $F_{2,6} = 220.17$, $p < 0.001$, factor region: $F_{1,6} = 105.92$, $p < 0.001$, interaction term: $F_{2,6} = 1{,}75$, $p = 0.253$] months. However, calculation of the anterior/posterior PC numbers ratio for each mouse indicated a significantly lower ratio (one-way ANOVA) in the 12 ($F_{2,6} = 17.25$, $p < 0.01$)- and 18 [Fig. 6(B); $F_{2,6} = 6.21$, $p < 0.05$]-month-old $NP^{0/0}$:$Bax^{+/+}$ mice, revealing that the anterior (I-V) cerebellar lobules have lost relatively more PCs than the posterior (VI-X) ones.

Significant rescue of PCs occurred at each parasagittal level in the $NP^{0/0}$:$Bax^{-/-}$ cerebellum at any age studied [Fig. 5(A)]. Normalizing values of PC numbers at the different parasagittal levels counted in the cerebellar vermis and hemispheres of the 12-, 16-, and 18 [Fig 5(B)]-month-old $NP^{0/0}$:$Bax^{+/+}$ and $NP^{0/0}$:$Bax^{-/-}$ mice did not disclose significant differences in PC rescue along the transversal dimension of the $NP^{0/0}$:$Bax^{-/-}$ cerebellum. The anterior/posterior PC numbers ratios of $NP^{0/0}$:$Bax^{-/-}$ and $NP^{0/0}$:$Bax^{+/+}$ were not signifi-

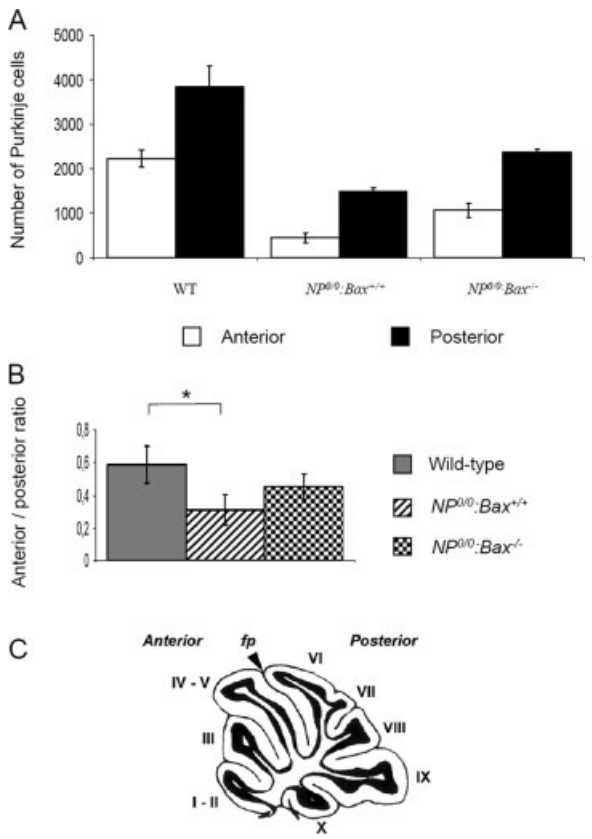

Figure 6 Purkinje cell numbers in the cortex of the anterior (lobules I–V) and posterior (lobules VI–X) cerebellum of the 18-month-old wildtype, $NP^{0/0}$:$Bax^{+/+}$ and $NP^{0/0}$:$Bax^{-/-}$ mice. Mean numbers from three mice per genotype were estimated in sagittal cerebellar sections separated from each other by 400 μm (2 sections in the right and in the left hemispheres and 7 sections in the vermis). A. The posterior (black) cerebellar cortex contains many more PCs than the anterior (white) cerebellar cortex in all genotypes. B. Significantly different wildtype and $NP^{0/0}$:$Bax^{+/+}$ anterior/posterior PC numbers ratios show a greater PC loss in the anterior $NP^{0/0}$:$Bax^{+/+}$ cerebellum ($F_{2,6} = 6.21$, $p < 0.05$, Tukey: $p < 0.01$). The anterior/posterior PC numbers ratios in the $NP^{0/0}$:$Bax^{+/+}$ and $NP^{0/0}$:$Bax^{-/-}$ cerebella are not significantly different ($F_{2,6} = 6.21$, $p < 0.05$, Tukey: $p > 0.2$), indicating that *Bax* knock-out rescues PC evenly along the rostrocaudal dimension of the cerebellum. C. Sagittal section through the median line in the cerebellar vermis showing the 10 lobules and the *fissura prima* (fp) separating the anterior cerebellum from the posterior cerebellum between lobule V and lobule VI.

cantly different at 12 months (data not shown; $F_{2,6} = 17.25, p < 0.01$; Tukey: $p > 0.5$) and 18 months [Fig. 6(B); $F_{2,6} = 6.21, p < 0.01$; Tukey: $p > 0.2$], suggesting that *Bax* knock-out rescued PCs evenly throughout the rostrocaudal axis of the cerebellum.

Supernumerary PCs of the $Bax^{-/-}$ Transgenic Mice Die During Aging and Cannot Account for the Protective Effect of *Bax* Deletion on the $NP^{0/0}$:$Bax^{+/+}$ PCs

Elimination of *Bax* expression in mice has been previously shown to increase cerebellar PC numbers by more than 30%, which supports the hypothesis that BAX plays a role in naturally occurring PC death (Fan et al., 2001). Comparing $Bax^{-/-}$ and wildtype mice at 12, 16, and 18 months, two-way ANOVA showed significant effects of genotype ($F_{1,12} = 33.86$, $p < 0.001$), age ($F_{2,12} = 9.42$, $p < 0.005$), and interaction ($F_{2,12} = 20.39$, $p < 0.001$). A 48% larger PC population was indeed counted in our 12-month-old $Bax^{-/-}$ mice when compared with the wildtype mice (Fig. 4). However, the number of supernumerary $Bax^{-/-}$ PCs decreased thereafter. By 16 months, $Bax^{-/-}$ mutants contain only 19% more PCs than the wildtype mice (Fig. 4). The number of PCs in $Bax^{-/-}$ mutants and wildtype mice was not significantly different by 18 months (Fig. 4). The decline in PC numbers in $Bax^{-/-}$ mutants between 12 and 18 months (Fig. 4) suggests that the loss of *Bax* expression is no longer sufficient to maintain the survival of the supernumerary PCs in the aging mice.

One possible explanation for the rescue of PCs in the $NP^{0/0}$:$Bax^{-/-}$ double mutants is that it is simply due to the presence of supernumerary $Bax^{-/-}$ PCs rescued from developmental cell death. At 12 months the $NP^{0/0}$:$Bax^{-/-}$ cerebellum contains 47% more PCs than the $NP^{0/0}$:$Bax^{+/+}$ cerebellum, which is similar to the percent increase in PCs in the $Bax^{-/-}$ mutant when compared with wildtype mice (48%, Fig. 4). Nevertheless, this explanation no longer holds at 16 months since the $Bax^{-/-}$ cerebellum contains only 19% more PCs than the wildtype against 85% more PCs in the $NP^{0/0}$:$Bax^{-/-}$ than in the $NP^{0/0}$:$Bax^{+/+}$ mutant (Fig. 4). Finally, at 18 months, when the $Bax^{-/-}$ cerebellum contains the same number of PCs as wildtype mice, the $NP^{0/0}$:$Bax^{-/-}$ double mutant contains almost twice as many PCs as in $NP^{0/0}$:$Bax^{+/+}$ mutants (Fig. 4), suggesting that the survival of these cells results from a specific rescue effect of *Bax* deletion (effect of genotype : $F_{3,24} = 452.21$, $p < 0.001$; effect of age: $F_{2,24} = 20.02$, $p < 0.001$; effect of interaction: $F_{6,24} = 12.87$, $p < 0.001$; Tukey: $p > 0.5$ between 18-month-old wildtype and $Bax^{-/-}$ mice and $p < 0.001$ between 18-month-old $NP^{0/0}$:$Bax^{-/-}$ and $NP^{0/0}$:$Bax^{+/+}$ mice).

Bax Deletion Prevents Abnormal Activation of $NP^{0/0}$ Astrocytes

Activation of Astrocytes in the 4-Month-Old $NP^{0/0}$:$Bax^{+/+}$ Cerebellar Cortex Correlates Topographi-

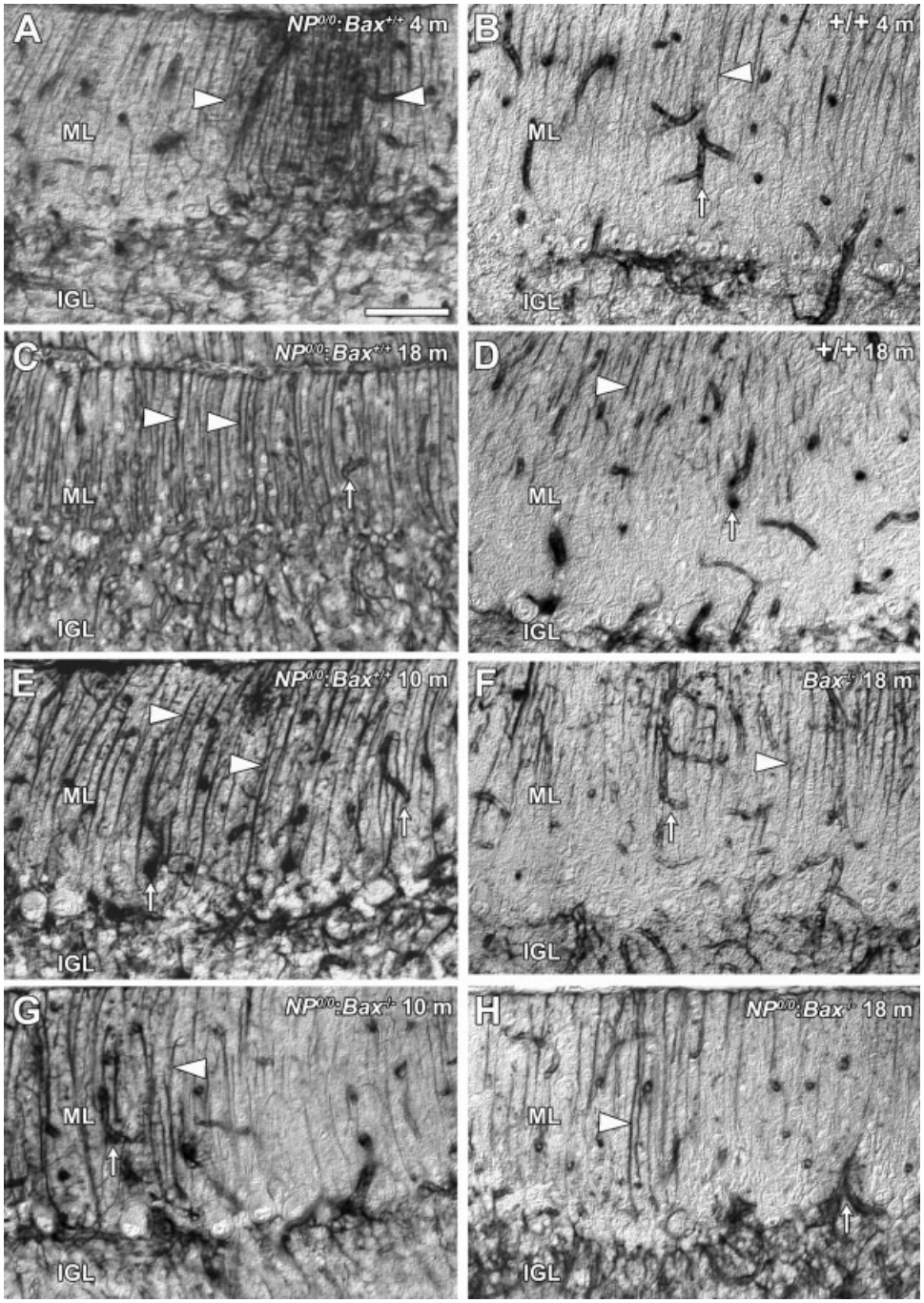

Figure 7 A. Immunohistochemistry for the astrocyte marker GFAP discloses patches of gliosis (between arrowheads) in the molecular layer (ML) of the 4- (A) month-old $NP^{0/0}$:$Bax^{+/+}$ cerebellar cortex. C, E. Gliosis has propagated throughout the ML in the older 10- (E) and 18- (C) month-old $NP^{0/0}$:$Bax^{+/+}$ mice. See also glial activation throughout the internal granular layer (IGL). B,D,F. GFAP staining of radial Bergmann glia (arrowheads) and IGL astrocytes remains weak in the 4- (B) and 18 (D)-month-old wildtype cerebellar cortex. GFAP immunoreactivity of the cerebellar cortex of the 18-month-old $Bax^{-/-}$ (F) and wildtype (B,D) mice (F) is similar at all ages studied. G,H. Bax deletion has restored normal intensity of GFAP immunoreactivity in ML of the 10- (G) and 18 (H)-month-old $NP^{0/0}$:$Bax^{-/-}$ cerebellar cortex, although astrogliosis still occurs in parts of ML and throughout IGL at both ages. Arrow shows nonspecific GFAP staining of blood vessel walls in all mice. Bar = 50 μm, $\times$200.

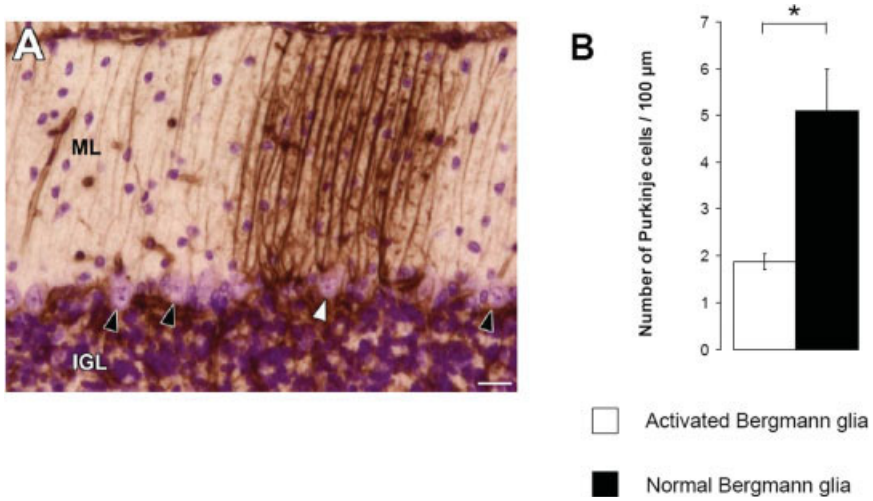

Figure 8 A. Area of intensely GFAP immunoreactive radial Bergmann glia in the cerebellar molecular layer (ML) of a 4-month-old $NP^{0/0}$:$Bax^{+/+}$ mouse. In this astrogliotic area, very few PCs (white arrowhead) can be stained by cresyl violet than elsewhere (black arrowheads) in the cerebellar cortex. IGL, internal granular layer, bar = 50 μm. B. Areas of activated Bergmann glia (with increased intensity of GFAP immunostaining, white bar) have lost significantly more PCs than areas with normal Bergmann glia (with normal intensity of GFAP immunostaining, black bar) in the 4-month-old $NP^{0/0}$:$Bax^{+/+}$ mice (paired t-test, $t_4 = 6.07$, $p < 0.03$; $n = 3$).

cally with PC Loss. Glial cells (including astrocytes) become activated in the cerebellar cortex of the $NP^{0/0}$:$Bax^{+/+}$ mutants as early as the third postnatal week as shown by increased GFAP and lysozyme M (LM) mRNA levels and by intense GFAP immunohistochemical staining of astrocytes at the 20th month (Atarashi et al., 2001). In the present GFAP immunohistochemical study, the cerebellar cortex of the 4-month-old $NP^{0/0}$:$Bax^{+/+}$ mice displayed activation of astrocytes in restricted areas of the molecular and the internal granular layers [Figs. 7(A,B) and 8(A)]. PC counts showed that these areas contained fewer PCs than in areas with normal GFAP immunoreactivity (Fig. 8). In 10- [Fig. 7(E)] and 18 [Fig. 7(C,D)]-month-old $NP^{0/0}$:$Bax^{+/+}$ mice, astrogliosis extended throughout the cerebellar cortex, suggesting that astrogliosis and PC death kinetics were correlated. Moreover, double GFAP and CaBP immunohistofluorescence studies showed that astrogliosis and PC loss topography systematically overlapped in the cerebellar cortex of the $NP^{0/0}$:$Bax^{+/+}$ mice at all ages studied (Fig. 9): indeed, GFAP labeling was the most intense in regions devoid of PCs. This strongly suggests that the gliosis relates to PC loss.

Activation of Astrocytes Is Moderated by Bax Deletion in the $NP^{0/0}$:$Bax^{-/-}$ Cerebellar Cortex. Astrogliosis did not occur in the cerebellar cortex of the $Bax^{-/-}$ mice at any ages studied [Fig. 7(F)], indicating that *Bax* deletion itself has no effect on astrocytes. In the cerebellar cortex of the 10- [Fig. 7(G)] and 18 [Fig. 7(H)]-month-old $NP^{0/0}$:$Bax^{-/-}$ double mutant mice, GFAP immunohistochemistry revealed a much less intense, patchy astrogliosis than in age-matched $NP^{0/0}$:$Bax^{+/+}$ mice [Fig. 7(C,E)]. This indicated that *Bax* deletion could prevent the activation of astrocytes in the presence of ectopic Dpl in $NP^{0/0}$:$Bax^{+/+}$mutants.

DISCUSSION

To investigate whether the proapoptotic factor BAX is necessary for the premature death of cerebellar PCs in $NP^{0/0}$ mice with overexpression of the PrP^c paralog Dpl (Moore et al., 1999; Weissmann and Aguzzi, 1999; Li et al., 2000), we crossed $NP^{0/0}$ mutants with *Bax* knock-out mutants and analyzed PC numbers and glial activation. The results from our analysis of $Bax^{-/-}$ mutants and $NP^{0/0}$:$Bax^{-/-}$ double mutants suggest three conclusions. First, the supernumerary PCs rescued from developmental cell death in $Bax^{-/-}$ mice eventually die during aging. Second, deletion of *Bax* expression rescues many PCs from Dpl-induced cell death in the $NP^{0/0}$:$Bax^{-/-}$ double mutant. Third, deletion of *Bax* expression blocks the activation of astrocytes induced by the $NP^{0/0}$ deletion. These studies demonstrate an important role for BAX in Dpl-mediated death of PrP^c-deficient PCs.

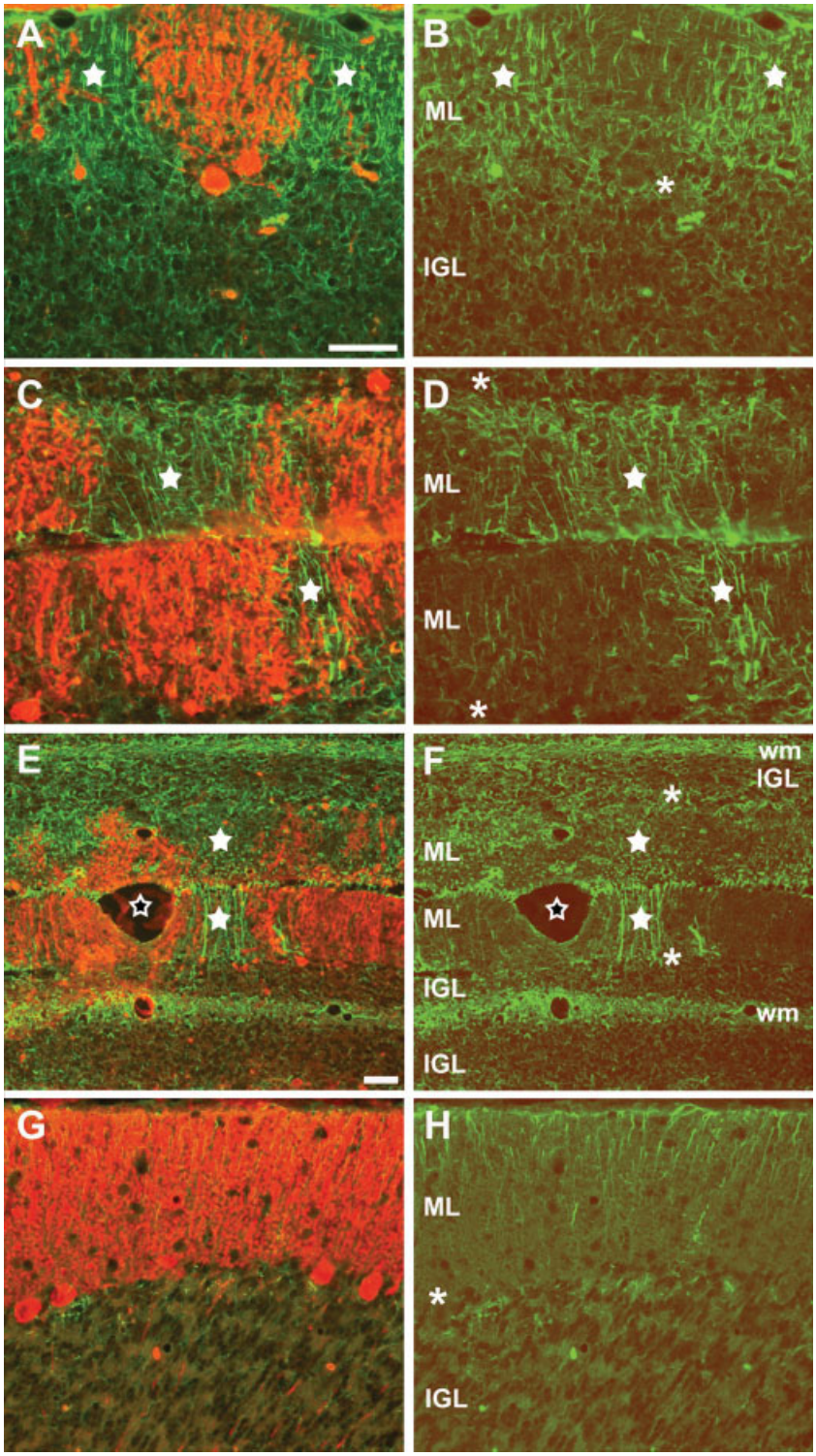

Figure 9 Double immunofluorescence staining for GFAP (green in A–H) and CaBP (red in A,C,E,G) in the cerebellar cortex of a 21-month-old $NP^{0/0}$:$Bax^{+/+}$ mutant mouse (A–F) and a 12-month-old wildtype mouse (G,H). A,B,G,H and C,D,E,F show cortical areas from respectively anterior and posterior cerebellum. Asterisks indicate PCs location between the molecular (ML) and internal granular (IGL) layers of the cerebellar cortex and white stars indicate intense GFAP immunostaining. Black stars show a large pial blood vessel. wm, white matter. A,B,C,D,G,H, ×200; E,F, ×100; bar = 50 μm.

Loss of Supernumerary PCs in *Bax*$^{-/-}$ Mutants

Elimination of *Bax* increases PC numbers in adult *Bax*$^{-/-}$ mice (Fan et al., 2001), presumably by rescuing PCs that are believed to die from BAX-mediated naturally occurring cell death during development. The present study shows that these supernumerary PCs undergo BAX-independent cell death during aging, thereby restoring the PC population to levels in wildtype by 18 months in *Bax*$^{-/-}$ mutants. Since we did not have any *Bax*$^{-/-}$ mice older than 18 months for this study, we did not estimate PC numbers in older mice. However, the number of PCs may stabilize after 18 months. This is strongly suggested by the similar phenomenon that occurs in the cerebellum of transgenic mice that overexpress a human *Bcl-2* transgene (Zanjani et al., 2004). In these mice, a significant number of PCs that are likely rescued from naturally occurring cell death (Zanjani et al., 1996) has been shown to decline from 6 to 12 months, to approach wildtype levels by 18 months like in the *Bax*$^{-/-}$ mutants and stabilizing thereafter by 24 months (Zanjani et al., 2004). The failure to sustain the survival of supernumerary PCs in *Bax*$^{-/-}$ mutants with aging suggests that PC survival may gradually become independent of apoptotic mechanisms involving BCL-2 family members. The transition to alternative survival/death mechanisms may be correlated with the decreased expression with age of survival factors such as BCL-2, which normally antagonize BAX. Indeed, BCL-2, a direct BAX antagonist that has been shown to favor PC survival during the same period as observed in *Bax*-deficient mice (Zanjani et al., 1996; Fan et al., 2001), undergoes decreased expression by 5 months in wildtype mice (Merry et al., 1994; Zanjani et al., 2004). *Bax* expression also has been shown to decline with age in the CNS, although this decrease has already occurred by 3 months (Vekrellis et al., 1997).

Bax Deletion Rescues *NP*$^{0/0}$ PCs from Doppel Neurotoxicity

Previous studies have shown a loss of *NP*$^{0/0}$ PCs by 20 months (Sakaguchi et al., 1996) whereas a decrease of the PC marker IP_3R1 mRNA was detected in 8-month-old *NP*$^{0/0}$:*Bax*$^{+/+}$ mice (Atarashi et al., 2001). Our study extends the latter data by demonstrating a significant reduction of PCs numbers in *NP*$^{0/0}$:*Bax*$^{+/+}$ cerebella by 6 months, i.e., much sooner than previously believed. However, footprint analyses only revealed motor impairments in *NP*$^{0/0}$:*Bax*$^{+/+}$ mutants by 12 months, suggesting either that substantial numbers of PCs must be lost before ataxia is apparent or that the development of the ataxic phenotype may also depend on neurodegeneration in other parts of the brain. The *NP*$^{0/0}$:*Bax*$^{-/-}$ and *NP*$^{0/0}$:*Bax*$^{+/-}$ mice displayed ataxia at the same time as the *NP*$^{0/0}$:*Bax*$^{+/+}$ mice. This suggests that this phenotype is not solely a function of the number of surviving PCs since the *NP*$^{0/0}$:*Bax*$^{-/-}$ double mutants have more PCs than *NP*$^{0/0}$:*Bax*$^{+/+}$ mutants do at 12 months.

The participation of BAX in Dpl-mediated apoptosis in PCs was investigated by assessing PC numbers through the lifespan of *NP*$^{0/0}$:*Bax*$^{-/-}$ double transgenic mice. The double transgenics contain many more PCs than do the *NP*$^{0/0}$:*Bax*$^{+/+}$ single mutants during the period studied (12–21 months). While the number of PCs in the *Bax*$^{-/-}$ mutant declines from 12 to 18 months, the number of PCs in the *NP*$^{0/0}$:*Bax*$^{-/-}$ mutant is stable during this period. Thus, the rescue of PCs from developmental cell death by deleting *Bax* expression cannot account for the long-lasting effect of the loss of *Bax* expression on the *NP*$^{0/0}$ PC population. Thus the absence of BAX enables some PCs to resist Dpl neurotoxicity and indicates that BAX plays a role in Dpl-mediated cell death. There was a tendency for *NP*$^{0/0}$:*Bax*$^{+/-}$ PCs to resist Dpl-induced neurotoxicity, although this has disappeared by 18 months. A *Bax* gene dose effect might exist in the regulation of Dpl-mediated PC death, although it was not observed in the regulation of developmental PC death (Fan et al., 2001).

The graduate decline in the *NP*$^{0/0}$:*Bax*$^{-/-}$ PC population during the 9-month-long study indicated that *Bax* deletion was not effective enough to oppose Dpl-mediated apoptosis of all PCs. At all ages, the number of *NP*$^{0/0}$:*Bax*$^{-/-}$ PCs was significantly less than in wildtype cerebella. This suggests that *Bax*-independent death mechanisms can be activated by Dpl specifically in the PrP^c-deficient Ngsk PCs. Indeed, PCs survive in Zürich-1 (ZH-I) (Büeler et al., 1993) and Edbr (Manson et al., 1994) *Prnp*-knock-out mice that do not overexpress Dpl, ruling out PrP-deficiency as a cause of PC death in the *NP*$^{0/0}$:*Bax*$^{-/-}$ mice.

The ectopic expression of Dpl may induce BAX-dependent and BAX-independent mechanisms in the same PCs. Alternatively, the two pathways could be mutually exclusive such that Dpl may selectively stimulate one pathway or the other in different PCs. Against this hypothesis, neither Dpl-induced PC loss nor PC rescue induced by *Bax* deletion showed significant variations along the lateral axis of the cerebellum in the *NP*$^{0/0}$:*Bax*$^{+/+}$ and *NP*$^{0/0}$:*Bax*$^{-/-}$ mice, suggesting that the neurotoxicity of Dpl, and in particular its BAX-mediated component, is evenly dis-

tributed along the lateral axis of the cerebellum and is not related to the parasagittal compartmentation of the PC population (Eisenman and Hawkes, 1993; Bailly et al., 1995). Nevertheless in favor of the existence of cell-specific differential sensitivity of PCs to Dpl neurotoxicity, PC loss was increased in the anterior cerebellum. This suggests that Dpl neurotoxicity varies along the rostrocaudal axis of the cerebellum and could be related to the anteroposterior compartmentation of the PC population (Duchala et al., 2004). However, since PC survival in the anterior and posterior cerebellum of the $NP^{0/0}$:$Bax^{-/-}$ was similar, the rescue effect of *Bax* knock-out did not change between anterior and posterior PCs, suggesting that BAX-mediated effect of Dpl is not related to the rostrocaudal compartmentation of PC population.

The structural properties shared by Dpl and PrP^c and the increasing amount of data connecting PrP^c and apoptosis (Bounhar et al., 2001; Roucou et al., 2003 2004; Diarra-Mehrpour et al., 2004; Kim et al., 2004; Paitel et al., 2004; Solforosi et al., 2004) suggest that the analysis of Dpl-induced neurodegeneration might help to understand the biology and pathology of prior proteins (Aguzzi and Polymenidou, 2004). However, the molecular basis of Dpl and PrP^c antagonism still have not been clarified (Hundt and Weiss, 2004). Dpl and PrP^c might compete for a common but still unknown ligand provisionally termed L_{PrP} whose binding with Dpl might cause cell death. Or Dpl and PrP^c may have noncompetitive antagonistic functions and Dpl might cause cell death in the absence of PrP^c opposition (Behrens, 2003).

In both cases, according to our present results, Dpl-induced cell death would include BAX-dependent as well as BAX-independent pathways. Besides signal transduction and antioxidant activity, PrP^c is neuroprotective like BCL-2 as a potent BAX inhibitor. Although not exactly acting like BCL-2, PrP^c could functionally replace it when BCL-2 decreases in the aging brain (see review in Roucou et al., 2005). Interestingly, BAX has been recently shown to mediate neuronal apoptosis of cerebellar granule cells induced by the 14 octapeptide repeats-containing Tg(PG14)PrP (Chiesa et al., 2005). The survival of PCs could be explained by the fact that the transgenic vector does not drive the expression of the pathogenic Tg(PG14)PrP in these neurons (Fischer et al., 1996). On the other hand, BAX-induced apoptosis cannot be counteracted by PrP^c devoid of its N-terminal octapeptide repeats, suggesting that this domain, partially homologous to the BH2 domain of the BCL-2 family of proteins (Yin et al., 1994; Roucou et al., 2004), is crucial for the neuroprotective functions of PrP^c. Interestingly, an important function of BCL-2 is to antagonize the proapoptotic effect of BAX through direct interaction at this BH2 domain (Oltvai et al., 1993; Gross et al., 1999; Cheng et al., 2001), which is lacking in both Dpl and ΔPrP (Shmerling et al., 1998; Flechsig et al., 2003) and impaired in Tg(PG14)PrP (Chiesa et al., 1998). A direct interaction of PrP^c with BAX is however not likely the mechanism by which PrP^c prevents *Bax*-mediated apoptosis, since cellular compartmentalization would prevent a direct interaction between PrP^c and the BCL-2 family of proteins. Nevertheless, cytosolic localization of PrP^c has been recently described and could interfere directly with *Bax*-mediated death (Ma and Lindquist, 2001; Yedidia et al., 2001; Roucou et al., 2003).

Bax Deletion Rescues $NP^{0/0}$ Astrocytes from Activation

In the present study, we observed increased immunolabeling for GFAP in the cerebellum of 4-month-old $NP^{0/0}$:$Bax^{+/+}$ mutants, indicating activation of astrocytes which agrees with previous observations (Atarashi et al., 2001). At this age, astrogliosis occurred in patches with a stripy shape reminiscent of the parasagittal compartments delineated by PC clusters in the cerebellar cortex (Eisenman and Hawkes, 1993; Bailly et al., 1995). By 10 months and beyond, astrogliosis propagated throughout the cerebellar cortex following a parallel time course with PC loss.

The presence of abnormally high GFAP mRNA levels, well before PC injury could be detected by the decrease of IP_3R1 mRNA levels in the cerebellar cortex of the $NP^{0/0}$:$Bax^{+/+}$ mouse, has led to the suggestion that in the absence of PrP^c, Dpl originating either from the astrocytes (Atarashi et al., 2001) or from the neurons (Radovanovic et al., 2005) could actively induce gliosis in the brain of these mutants. Thus, either induced intrinsically by astroglial Dpl or by ectopic Dpl expressed on the neuronal surface, glial-cell activation, together with the loss of PrP^c, may in turn contribute to neurodegeneration. In addition, microglia are thought to be involved in the etiology of various neurodegenerative conditions. They are known to be activated in the CNS of $NP^{0/0}$:$Bax^{+/+}$ mice and they may play a role in PC death (Atarashi et al., 2001).

As an alternative to the glial-mediated neuronal death hypothesis exposed earlier, the recent demonstration that astrocytic activation itself was unable to induce neuronal death *in vivo* (Mallucci et al., 2003) makes conceivable that gliosis occurs as a consequence of PC damage in the cerebellum of the $NP^{0/0}$:$Bax^{+/+}$ mice. This is supported by the topographic

coincidence of astrogliosis and PC loss evidenced by the present study. In all cases, regions with gliosis overlapped PC-free areas whereas regions with normal GFAP fluorescence of glial cells contained surviving PCs, suggesting that activation of astrocytes could result from PC degeneration signals. Even in the cerebellar cortex of the 4-month-old $NP^{0/0}$:$Bax^{+/+}$ mice where the present global quantitative analysis could not detect significant PC loss, we showed that the astrocytic areas contained fewer PCs than regions with unreactive astroglia. This indicates that neuronal death and astrocyte activation follow the same temporal and regional patterns. The activation of astrocytes was greatly moderated by *Bax* deletion in the cerebellar cortex of the $NP^{0/0}$:$Bax^{-/-}$ mice. Consistent glial expression of BAX could not be detected in mouse and human brain (Hara et al., 1996; Shin et al., 2000), suggesting that *Bax* deletion indirectly represses astrocytic activation through a primary effect counteracting Dpl neurotoxicity in PCs. Nevertheless, a direct antagonistic effect of *Bax* knock-out in activated astrocytes cannot be definitely ruled out since ischemia has been shown to upregulate *Bax* in astrocytes (Imura and Shimohama, 2000; Giffard and Swanson, 2005). Further investigations to elucidate the mechanisms of glial cell activation in $NP^{0/0}$:$Bax^{+/+}$ mice might provide insight into PrP^{c} and Dpl physiology as well as pathogenesis of prion diseases.

We thank Laure Rondi-Reig for footprint tests expertise and Jean-Luc Dupont for immunofluorescence experiments.

REFERENCES

Aguzzi A, Polymenidou M. 2004. Mammalian prion biology: One century of evolving concepts. Cell 116:313–327.

Anderson L, Rossi D, Linehan J, Brandner S, Weissmann C. 2004. Transgene-driven expression of the Doppel protein in Purkinje cells causes Purkinje cell degeneration and motor impairment. Proc Natl Acad Sci USA 101: 3644–3649.

Atarashi R, Sakaguchi S, Shigematsu K, Arima K, Okimura N, Yamaguchi N, Li A, et al. 2001. Abnormal activation of glial cells in the brains of prion protein-deficient mice ectopically expressing prion protein-like protein, PrPLP/Dpl. Mol Med 7:803–809.

Bailly Y, Schoen SW, Delhaye-Bouchaud N, Kreutzberg GW, Mariani J. 1995. 5′-nucleotidase activity as a synaptic marker of parasagittal compartmentation in the mouse cerebellum. J Neurocytol 24:879–890.

Behrens A. 2003. Physiological and pathological functions of the prion protein homologue Dpl. Br Med Bull 66:35–42.

Bounhar Y, Zhang Y, Goodyer CG, LeBlanc A. 2001. Prion protein protects human neurons against Bax-mediated apoptosis. J Biol Chem 276:39145–39149.

Büeler H, Aguzzi A, Sailer A, Greiner RA, Autenried P, Aguet M, Weissmann C. 1993. Mice devoid of PrP are resistant to scrapie. Cell 73:1339–1347.

Cheng EH, Wei MC, Weiler S, Flavell RA, Mak TW, Lindsten T, Korsmeyer SJ. 2001. BCL-2, BCL-X(L) sequester BH3 domain-only molecules preventing BAX- and BAK-mediated mitochondrial apoptosis. Mol Cell 8:705–711.

Chiesa R, Piccardo P, Dossena S, Nowoslawski L, Roth KA, Ghetti B, Harris DA. 2005. Bax deletion prevents neuronal loss but not neurological symptoms in a transgenic model of inherited prion disease. Proc Natl Acad Sci USA 102:238–243.

Chiesa R, Piccardo P, Ghetti B, Harris DA. 1998. Neurological illness in transgenic mice expressing a prion protein with an insertional mutation. Neuron 21:1339–1351.

Cui T, Holme A, Sassoon J, Brown DR. 2003. Analysis of doppel protein toxicity. Mol Cell Neurosci 23:144–155.

Diarra-Mehrpour M, Arrabal S, Jalil A, Pinson X, Gaudin C, Piétu G, Pitaval A, et al. 2004. Prion protein prevents human breast carcinoma cell line from tumor necrosis factor a-induced cell death. Cancer Res 64:719–727.

Duchala CS, Shick HE, Garcia J, Deweese DM, Sun X, Stewart VJ, Macklin WB. 2004. The toppler mouse: A novel mutant exhibiting loss of Purkinje cells. J Comp Neurol 476:113–129.

Eisenman L, Hawkes R. 1993. Antigenic compartmentation in the mouse cerebellar cortex: Zebrin and HNK-1 reveal a complex, overlapping molecular topography. J Comp Neurol 335:586–605.

Fan H, Favero M, Vogel MW. 2001. Elimination of Bax expression in mice increases cerebellar Purkinje cell numbers but not the number of granule cells. J Comp Neurol 436:82–91.

Fischer M, Rülicke T, Raeber A, Sailer A, Moser M, Oesch B, Brandner S, et al. 1996. Prion protein (PrP) with amino-proximal deletions restoring susceptibility of μPrP knockout mice to scrapie. EMBO J 15:1255–1264.

Flechsig E, Hegyi I, Leimeroth R, Zuniga A, Rossi D, Cozzio A, Schwarz P, et al. 2003. Expression of truncated PrP targeted to Purkinje cells of PrP knockout mice causes Purkinje cell death and ataxia. EMBO J 22:3095–3101.

Giffard RG, Swanson RA. 2005. Ischemia-induced programmed cell death in astrocytes. Glia 50:299–306.

Gross A, McDonnell JM, Korsmeyer SJ. 1999. BCL-2 family members and the mitochondria in apoptosis. Genes Dev 13:1899–1911.

Hara A, Hirose Y, Wang A, Yoshimi N, Tanaka T, Mori H. 1996. Localization of Bax and Bcl-2 proteins, regulators of programmed cell death, in the human central nervous system. Virchows Arch 429:249–253.

Hendry IA. 1976. A method to correct adequately for the change in neuronal size when estimating neuronal numbers after nerve growth factor treatment. J Neurocytol 5:337–349.

Herrup K, Sunter K. 1986. Cell lineage dependent and independent control of Purkinje cell number in the mammalian CNS: Further quantitative studies of lurcher chimeric mice. Dev Biol 117:417–427.

Hsu SM, Raine L, Fanger H. 1981. Use of avidin-biotin-peroxidase complex (ABC) in immunoperoxidase technics. J Histochem Cytochem 29:577–580.

Hundt C, Weiss S. 2004. The prion-like protein Doppel fails to interact with itself, the prion protein and the 37 kDa/67 kDa laminin receptor in the yeast two-hybrid system. Biochim Biophys Acta 1689:1–5.

Imura T, Shimohama S. 2000. Opposing effects of adenosine on the survival of glial cells exposed to chemical ischemia. J Neurosci Res 62:539–546.

Kim BH, Lee HG, Choi JK, Kim JI, Choi EK, Carp RI, Kim YS. 2004. The cellular prion protein (PrPC) prevents apoptotic neuronal cell death and mitochondrial dysfunction induced by serum deprivation. Brain Res Mol Brain Res 124:40–50.

Knudson CM, Tung KS, Tourtellotte WG, Brown GA, Korsmeyer SJ. 1995. Bax-deficient mice with lymphoid hyperplasia and male germ cell death. Science 270:96–99.

Kurschner C, Morgan JI. 1995. The cellular prion protein (PrP) selectively binds to Bcl-2 in the yeast two-hybrid system. Brain Res Mol Brain Res 30:165–168.

Kuwahara C, Takeuchi A, Nishimura T, Haraguchi K, Kubosaki A, Matsumoto Y, Saeki K, et al. 1999. Prions prevent neuronal cell-line death. Nature 400:225–226.

Li A, Harris DA. 2005. Mammalian prion protein suppresses BAX-induced cell death in yeast. J Biol Chem 280:17430–17434.

Li A, Sakaguchi S, Ryuichiro A, Bhabesh CR, Ryota N, Kazuhiko A, Nobuhiko O, et al. 2000. Identification of a novel gene encoding a PrP-like protein expressed as chimeric transcripts fused to PrP exon 1/2 in ataxic mouse line with a disrupted PrP gene. Cell Mol Biol 20:553–567.

Ma J, Lindquist S. 2001. Wild-type PrP and a mutant associated with prion disease are subject to retrograde transport and proteasome degradation. Proc Natl Acad Sci USA 98:14955–14960.

Mallucci G, Dickinson A, Linehan J, Klöhn P-C, Brandner S, Collinge J. 2003. Depleting neuronal PrP in prion infection prevents disease and reverses spongiosis. Science 302:871–874.

Manson JC, Clarke AR, Hooper ML, Aitchison L, McConnell I, Hope J. 1994. 129/Ola mice carrying a null mutation in PrP that abolishes mRNA production are developmentally normal. Mol Neurobiol 8:121–127.

Massimino ML, Ballarin C, Bertoli A, Casonato S, Genovesi S, Negro A, Sorgato MC. 2004. Human Doppel and prion protein share common membrane microdomains and internalization pathways. Int J Biochem Cell Biol 36:2016–2031.

Merry DE, Veis DJ, Hickey WF, Kormeyer SJ. 1994. Bcl-2 protein expression is widespread in the developing nervous system and retained in the adult PNS. Development 120:301–311.

Moore RC, Mastrangelo P, Bouzamondo E, Heinrich C, Legname G, Prusiner SB, Hood L, et al. 2001. Doppel-induced cerebellar degeneration in transgenic mice. Proc Natl Acad Sci USA 98:15288–15293.

Moore RC, Lee IT, Bouzamondo E, Silverman GL, Harisson PM, Strome R, Heinrich C, et al. 1999. Ataxia in prion protein (PrP)-deficient mice is associated with upregulation of the novel PrP-like protein doppel. J Mol Biol 292:797–817.

Moore RC, Redhead NJ, Selfridge J, Hope J, Manson JC, Melton DW. 1995. Double replacement gene targeting for the production of a series of mouse strains with different prion protein gene alterations. Biotechnology (NY) 13:999–1004.

Nishida N, Tremblay P, Sugimoto T, Shigematsu K, Shirabe S, Petromilli C, Erpel SP, et al. 1999. A mouse prion protein transgene rescues mice deficient for the prion protein gene from Purkinje cell degeneration and demyelination. Lab Invest 79:689–697.

Oltvai ZN, Milliman CL, Korsmeyer SJ. 1993. Bcl-2 heterodimerizes in vivo with a conserved homolog, Bax, that accelerates programmed cell death. Cell 74:609–619.

Paitel E, Sunyach C, Alves da Costa C, Bourdon JC, Vincent B, Checler F. 2004. Primary cultured neurons devoid of cellular prion display lower responsiveness to staurosporine through the control of p53 at both transcriptional and post-transcriptional levels. J Biol Chem 279:612–618.

Prusiner SB. 1998. Prions. Proc Natl Acad Sci USA 95: 13363–13364.

Qin K, Coomaraswamy J, Mastrangelo P, Yang Y, Lugowski S, Petromilli C, Prusiner SB, et al. 2003. The PrP-like protein Doppel binds copper. J Biol Chem 278:8888–8896.

Radovanovic I, Braun N, Giger O, Mertz K, Miele G, Prinz M, Navarro B, Aguzzi A. 2005. Truncated prion protein and Doppel are myelinotoxic in the absence of oligodendrocytic PrP^{c}. J Neurosci 25:4879–4888.

Rossi D, Cozzio A, Flechsig E, Klein MA, Rulicke T, Aguzzi A, Weissmann C. 2001. Onset of ataxia and Purkinje cell loss in PrP null mice inversely correlated with Dpl level in brain. EMBO J 20:694–702.

Roucou X, Giannopoulos PN, Zhang Y, Jodoin J, Goodyer CG, LeBlanc A. 2005. Cellular prion protein inhibits proapoptotic Bax conformational change in human neurons and in breast carcinoma MCF-7 cells. Cell Death Differ 12:783–795.

Roucou X, Gains M, LeBlanc AC. 2004. Neuroprotective functions of prion protein. J Neurosci Res 75:153–161.

Roucou X, Guo Q, Zhang Y, Goodyer CG, LeBlanc AC. 2003. Cytosolic prion protein is not toxic and protects against Bax-mediated cell death in human primary neurons. J Biol Chem 278:40877–40881.

Sakaguchi S, Katamine S, Nishida N, Moriuchi R, Shigematsu K, Sugimoto T, Nakatani A, et al. 1996. Loss of cerebellar Purkinje cells in aged mice homozygous for a disrupted PrP gene. Nature 380:528–531.

Sakaguchi S, Katamine S, Shigematsu K, Nakatani A, Moriuchi R, Nishida N, Kurokawa K, et al. 1995. Accumula-

tion of proteinase K-resistant prion protein (PrP) is restricted by the expression level of normal PrP in mice inoculated with a mouse-adapted strain of the Creutzfeldt-Jakob disease agent. J Virol 69:7586–7592.

Sakudo A, Lee DC, Nakamura I, Taniuchi Y, Saeki K, Matsumoto Y, Itohara S, et al. 2005. Cell-autonomous PrP-Doppel interaction regulates apoptosis in PrP gene-deficient neuronal cells. Biochem Biophys Res Commun 333:448–454.

Shin C-M, Chung YH, Kim MJ, Shin DH, Kim YS, Gurney ME, Lee KW, et al. 2000. Immunohistochemical study on the distribution of Bcl-2 and Bax in the central nervous system of the transgenic mice expressing a human Cu/Zn SOD mutation. Brain Res 887:309–315.

Shmerling D, Hegyi I, Fischer M, Blattler T, Brandner S, Gotz J, Rulicke T, et al. 1998. Expression of amino-terminally truncated PrP in the mouse leading to ataxia and specific cerebellar lesions. Cell 93:203–214.

Silverman GL, Qin K, Moore RC, Yang Y, Mastrangelo P, Tremblay P, Prusiner SB, et al. 2000. Doppel is an N-glycosylated, glycosylphosphatidylinositol-anchored protein. Expression in testis and ectopic production in the brains of Prnp(0/0) mice predisposed to Purkinje cell loss. J Biol Chem 275:26834–26841.

Solforosi L, Criado JR, McGavern DB, Wirz S, Sanchez-Alavez M, Sugama S, DeGiorgio LA, et al. 2004. Cross-linking cellular prion protein triggers neuronal apoptosis in vivo. Science 303:1514–1516.

Vekrellis K, Mc Carthy MJ, Watson A, Whitfield J, Rubin LL, Ham J. 1997. Bax promotes neuronal cell death and is downregulated during the development of the nervous system. Development 124:1239–1249.

Weissmann C, Aguzzi A. 1999. PrP double causes trouble. Science 286:914–915.

Wetts R, Herrup K. 1982. Cerebellar Purkinje cells are descended from a small number of progenitors committed during early development: Quantitative analysis of lurcher chimeric mice. J Neurosci 2:1494–1498.

Wong BS, Liu T, Paisley D, Li R, Pan T, Chen SG, Perry G, et al. 2001. Induction of HO-1 and NOS in doppel-expressing mice devoid of PrP: Implications for doppel function. Mol Cell Neurosci 17:768–775.

Yamaguchi N, Sakaguchi S, Shigematsu K, Okimura N, Katamine S. 2004. Doppel-induced Purkinje cell death is stoichiometrically abrogated by prion protein. Biochem Biophys Res Commun 319:1247–1252.

Yedidia Y, Horontchik L, Tzaban S, Yanai A, Taraboulos A. 2001. Proteasomes and ubiquitin are involved in the turnover of the wild-type prion protein. EMBO J 20: 5383–5391.

Yin XM, Oltvai ZN, Korsmeyer SJ. 1994. BH1 and BH2 domains of Bcl-2 are required for inhibition of apoptosis and heterodimerization with Bax. Nature 369:321–323.

Yokoyama T, Kimura KM, Ushiki Y, Yamada S, Morooka A, Nakashiba T, Sassa T, et al. 2001. In vivo conversion of cellular prion protein to pathogenic isoforms, as monitored by conformation-specific antibodies. J Biol Chem 276:11265–11271.

Zanjani H, Lemaigre-Dubreuil Y, Tillakaratne NJ, Blokhin A, McMahon RP, Tobin AJ, Vogel MW, et al. 2004. Cerebellar Purkinje cell loss in aging Hu-Bcl-2 transgenic mice. J Comp Neurol 475:481–492.

Zanjani HS, Vogel MW, Delhaye-Bouchaud N, Martinou JC, Mariani J. 1996. Increased cerebellar Purkinje cell numbers in mice overexpressing a human bcl-2 transgene. J Comp Neurol 374:332–341.

BCL-2 Counteracts Doppel-Induced Apoptosis of Prion-Protein-Deficient Purkinje Cells in the Ngsk *Prnp$^{0/0}$* Mouse

S. Heitz,[1] V. Gautheron,[2] Y. Lutz,[3] J.-L. Rodeau,[4] H.S. Zanjani,[2,5] I. Sugihara,[6] G. Bombarde,[1] F. Richard,[1] J.-P. Fuchs,[3] M.W. Vogel,[5] J. Mariani,[2,7] Y. Bailly[1]

[1] Institut des Neurosciences Cellulaires et Intégratives, Département Neurotransmission et Sécrétion Neuroendocrine, UMR7168-LC2 CNRS and Université Louis Pasteur, IFR 37 des Neurosciences de Strasbourg, 5 rue Blaise Pascal 67084 Strasbourg cedex, France

[2] Neurobiologie des Processus Adaptatifs, Equipe Développement et Vieillissement du Système Nerveux, UMR7102, CNRS and Université Pierre et Marie Curie, 9 quai Saint Bernard 75005 Paris, France

[3] Physiopathologie du Système Nerveux, INSERM U575, IFR 37 des Neurosciences de Strasbourg, 5 rue Blaise Pascal, 67084 Strasbourg, France

[4] Institut des Neurosciences Cellulaires et Intégratives, Département Nociception et Douleur, UMR7168-LC2 CNRS and Université Louis Pasteur, IFR 37 des Neurosciences de Strasbourg, 21 rue René Descartes, 67084 Strasbourg, France

[5] Maryland Psychiatric Research Center, University of Maryland School of Medicine, Baltimore, Maryland 21228

[6] Department of Systems Neurophysiology, Tokyo Medical and Dental University, Graduate School of Medicine, Tokyo 113-8519, Japan

[7] APHP, Hôpital Charles Foix, UEF 94200 Ivry/Seine, France

Received 20 February 2007; accepted 14 June 2007

ABSTRACT: **The pro-apoptotic factor BAX has recently been shown to contribute to Purkinje cell (PC) apoptosis induced by the neurotoxic prion-like protein Doppel (Dpl) in the prion-protein-deficient Ngsk *Prnp$^{0/0}$* (*NP$^{0/0}$*) mouse. In view of cellular prion protein (PrP^{c}) ability to counteract Dpl neurotoxicity and favor neuronal survival like BCL-2, we investigated the effects of the anti-apoptotic factor BCL-2 on Dpl neurotoxicity by studying the progression of PC death in aging *NP$^{0/0}$-Hu-bcl-2* double mutant mice overexpressing human BCL-2 (*Hu-bcl-2*). Quantitative analysis showed that significantly more PCs survived in *NP$^{0/0}$-Hu-bcl-2* double mutants compared with the *NP$^{0/0}$* mutants. However, number of PCs remained inferior to wild-type levels and to the increased number of PCs observed in *Hu-bcl-2* mutants. In the *NP$^{0/0}$* mutants, Dpl-induced PC death**

Correspondence to: S. Heitz (heitz@neurochem.u-strasbg.fr).
Contract grant sponsor: G.I.S. Maladies à Prions.
Contract grant sponsor: National Institute of Health; contract grant number: NS34309.
Contract grant sponsor: Neurex Network.

Published online 17 December 2007 in Wiley InterScience (www.interscience.wiley.com).
DOI 10.1002/dneu.20555

occurred preferentially in the aldolase C-negative parasagittal compartments of the cerebellar cortex. Activation of glial cells exclusively in these compartments, which was abolished by the expression of *Hu-bcl-2* in the double mutants, suggested that chronic inflammation is an indirect consequence of Dpl-induced PC death. This partial rescue of $NP^{0/0}$ PCs by *Hu-bcl-2* expression was similar to that observed in $NP^{0/0}$:$Bax^{-/-}$ double mutants with *bax* deletion. Taken together, these data strongly support the involvement of BCL-2 family-dependent apoptotic pathways in Dpl neurotoxicity. The capacity of BCL-2 to compensate PrP^c deficiency by rescuing PCs from Dpl-induced death suggests that the BCL-2-like property of PrP^c may impair Dpl-like neurotoxic pathways in wild-type neurons. Develop Neurobiol 68: 332–348, 2008

Keywords: **Purkinje cell; Doppel; neurodegeneration; apoptosis; prion protein; BCL-2**

INTRODUCTION

Doppel (Dpl) is the first identified homolog of the cellular prion protein, PrP^c, which is implicated in the pathogenesis of transmissible spongiform encephalopathies (TSE) (Prusiner, 1998). Dpl is an N-truncated form of PrP^c with common structural features and function roles in cellular trafficking pathways (Weissmann and Aguzzi, 1999; Silverman et al., 2000; Flechsig et al., 2003; Qin et al., 2003; Massimino et al., 2004). Targeted disruptions of the PrP^c coding gene (*Prnp*) that extend into the upstream region of intron 2 result in cis-activation of the Dpl gene (*Prnd*). Ectopic Dpl neuronal expression in $Prnp^{0/0}$ mouse lines such as Ngsk (Sakaguchi et al., 1996), Rcm0 (Moore et al., 1995), ZH-II (Rossi et al., 2001), and Rikn (Yokoyama et al., 2001) causes late onset Purkinje cell (PC) degeneration and ataxia. Dpl shares 25% identity with PrP^c, but lacks its flexible N-terminal sequence. Expression of the N-terminal truncated form of PrP (ΔPrP) in *Prnp*-ablated mouse lines (Flechsig et al., 2003) causes neurodegenerative effects in PCs similar to the overexpression of Dpl (Anderson et al., 2004; Yamaguchi et al., 2004), and the neurotoxic effects of Dpl and ΔPrP are both antagonized by PrP^c (Nishida et al., 1999; Cui et al., 2003; Flechsig et al., 2003; Anderson et al., 2004; Yamaguchi et al., 2004). These results suggest that Dpl and ΔPrP may cause cell death by the same mechanism, perhaps by interfering with a cellular signaling pathway essential for cell survival and normally controlled by full-length PrP^c (Shmerling et al., 1998; Anderson et al., 2004).

To date, only a few studies have investigated the mechanism by which Dpl kills neurons. PrP-deficient cells have been shown to undergo Dpl-induced apoptosis in a dose-dependent, cell autonomous manner (Sakudo et al., 2005). Furthermore, oxidative stress may play a role in the death of neurons because NOS activity is induced by Dpl both *in vitro* and *in vivo* (Wong et al., 2001; Cui et al., 2003). In addition, an activation of glial cells is associated with ectopic expression of Dpl in Ngsk $Prnp^{0/0}$ ($NP^{0/0}$) mice (Atarashi et al., 2001).

PrP^c itself has recently been shown to have neuroprotective function. PrP^c, either expressed endogenously or applied exogenously, inhibited Dpl-induced apoptosis (Cui et al., 2003) and introduction of a *Prnp* transgene rescued the $NP^{0/0}$ phenotype (i.e. PC degeneration and ataxia, Sakaguchi et al., 1996; Nishida et al., 1999). Quantitative analysis of the PC population in the cerebellum of the $NP^{0/0}$:$Bax^{-/-}$ double mutant mice significantly improved PC survival, demonstrating the contribution of the pro-apoptotic factor BAX to Dpl neurotoxicity (Heitz et al., 2007).

Interestingly, overexpression of the *bcl-2* gene can also rescue PrP-deprived hippocampal cell lines from serum deprivation-induced apoptosis (Kuwahara et al., 1999). PrP^c also binds to BCL-2 in the yeast two-hybrid system (Kurschner and Morgan, 1995) and both PrP^c and BCL-2 protect yeast (Li and Harris, 2005) and neurons (Bounhar et al., 2001; Roucou et al., 2003) from BAX-induced apoptosis suggesting that the BAX-dependent component of Dpl neurotoxicity could be antagonized by PrP^c as well as BCL-2.

Here, we investigate the mechanism underlying Dpl-induced apoptosis and PrP^c neuroprotective properties. The ability of exogenous BCL-2 overexpression to antagonize Dpl neurotoxicity was tested in $NP^{0/0}$-*Hu-bcl-2* double mutant mice obtained by crossing $NP^{0/0}$ mice with NSE73a *Hu-bcl-2* mice (Martinou et al., 1994). The survival of cerebellar PCs was analyzed in these mice during adulthood (i.e. 4–24 months) including the period of PC death in $NP^{0/0}$ mice (i.e. 4–16 months). In parallel, the activation of astrocytes in the cerebellar cortex of the $NP^{0/0}$-*Hu-bcl-2* double mutant mice was analyzed by immunohistochemistry in order to determine if *Hu-bcl-2* overexpression affected astrogliosis induced by the $NP^{0/0}$ condition (Atarashi et al., 2001; Heitz et al., 2007).

MATERIALS AND METHODS

Animals and Genotyping

As previously reported, *Hu-bcl-2* mice from the NSE73a strain were generated by injecting embryos with the EB-2

Table 1 Age and Number of Mutants and Normal Mice, Mean Area and Long Diameter ± SD of Purkinje Cell Nuclei and Mean Number ± SD of Purkinje Cells Counted in Groups of Age- and Genotype-Matched Mice

Genotype	Age in Months	Number of Mice	Mean Area of PC Nuclei (μm^2)	Mean Long Diameter of PC Nuclei (μm)	Mean Number of PCs
Wild-Type	6	3	Not done	Not done	142,728 ± 3356
	12	3	93.52 ± 7.41	12.93 ± 0.73	135,554 ± 6760
	16	3	Not done	Not done	145,271 ± 6657
	18	3	96.26 ± 6.24	13.08 ± 0.47	147,884 ± 9094
	21	3	77.56 ± 13.32	11.86 ± 1.06	143,303 ± 8905
Hu-bcl-2	6	3	Not done	Not done	202,720 ± 6508
	12	3	105.63 ± 0.43	13.62 ± 0.01	170,790 ± 6722
	16	3	Not done	Not done	158,228 ± 7895
	21	3	97.45 ± 13.2	13.2 ± 0.35	157,823 ± 14745
$NP^{0/0}$	4	3	85.92 ± 8.82	12.94 ± 0.07	145,014 ± 10,472
	6	3	Not done	Not done	112,918 ± 8419
	10	3	Not done	Not done	79,836 ± 1853
	12	3	93.47 ± 11.58	13.20 ± 0.88	61,236 ± 671
	16	3	Not done	Not done	48,788 ± 763
	18	3	100.69 ± 5.32	13.75 ± 0.21	40940 ± 1695
	21	3	76.91 ± 10.5	12.48 ± 0.32	36757 ± 3464
$NP^{0/0}$-*Hu-bcl-2*	4	3	92.11 ± 6.85	13.01 ± 0.32	159,737 ± 12,424
	10	3	Not done	Not done	97,416 ± 24,930
	12	3	90.81 ± 3.7	12.75 ± 0.44	86,749 ± 3269
	16	3	Not done	Not done	62,585 ± 608
	18	3	86.13 ± 5.73	12.35 ± 0.36	70,572 ± 11,701
	21	3	81.8 ± 5.91	12.07 ± 0.51	64,494 ± 2035
	24	3	Not done	Not done	68,481 ± 1158

In brief, the PC nuclei profiles were counted along the entire length of the PC layer in each section. PCs were identified as neurons in the PC layer with a large soma and some portion of their nuclei in the plane of the section (black arrowheads in Fig. 1 C, F, I, L). The total number of PCs was estimated by graphing the number of visible PC nuclei per section as a function of the distance of each section from the midline and then integrating the area under the polygon to calculate the raw total. The raw total was adjusted for double counting errors using the Hendry correction (Hendry, 1976) because it was specifically designed to account for experimental changes in the size of the cells being counted. The Hendry correction factor was calculated in each cerebellum from measurements of the nuclear profile area and long diameter of over 300 PCs using ImageJ. We chose to use this classical correction factor for our cell counts, instead of more recently developed stereological techniques, since the profile counting method provides data on the transversal distribution of PCs. None of the nuclear profile area and long diameter measurements varied significantly between age-matched groups of different genotypes and between groups of the same genotype at different ages.

construct in the cloning vector pSK+ containing the human BCL-2 coding region (Tsujimito and Croce, 1986; Martinou et al., 1994). Further breeding strategies were designed taking in account that *Hu-bcl-2* females are sterile. *Hu-bcl-2* detection by Southern blot was achieved using a BamH1-Pst1 253 bp probe (Martinou et al., 1994). $NP^{0/0}$ mice were generated by deleting the entire open reading frame (ORF) of the *Prnp* gene, located in exon 3, as well as 5′ and 3′ non-coding flanking regions (Sakaguchi et al., 1995). The deleted sequences were replaced by a Neo cassette. The *Prnp* ORF was identified using the following primers: forward 5′-CCGCTACCCTAACCAAGTGT-3′ and reverse 5′-CCTAGACCACGAGAATGCGA-3′, both located within *Prnp* ORF. $NP^{0/0}$ mutants were identified using the following primers: forward 5′-TGCCGCACTTCTTTG TGAAT-3′ and reverse 5′-CGGTGGATGTGGAATGTGT-3′ (within Neo cassette).

For this study, founding mice were first backcrossed with C57BL/6 mice for at least 10 generations. $NP^{0/0}$ females (gift from S. Katamine) were then crossed with *Hu-bcl-2* males and offspring were identified using the aforementioned probes and primer sets. $NP^{+/0}$-*Hu-bcl-2* males were further crossed with $NP^{0/0}$ females to generate $NP^{0/0}$-*Hu-bcl-2* offspring. Mice were bred at the animal facility of the IFR37 de Neurosciences in Strasbourg and maintained according to the NIH guidelines (NIH Publication 80-23, revised 1996) and the European Communities Council Directive of November 24, 1986 (86/609/EEC). A minimal number of animals were used (Table 1) and handled with maximum care to minimize their suffering.

Footprint Analysis

All mice used in this study were submitted for footprint analysis. Ink was applied to the fore (green) and hind (red) paws of individual mice. Mice were induced to walk forward on a white paper in a dark narrow alley. Ataxic gait was detected when the line linking the middle of the step

width (left-right distance) of the hind paws swerved from the straight line gait of the non-ataxic animal.

Histology

All mice (Table 1) were anaesthetized with sodium pentobarbital (0.15 mL/100 g i.p., Sanofi), after which brains were dissected and immersed overnight in Carnoy's fixative (60% ethanol, 30% chloroform, 10% acetic acid). Brains were dehydrated, embedded in paraffin, and sectioned in the sagittal plane at 10 μm.

Size of the Cerebellar Vermis

The size of the cerebellar vermis was estimated by measuring the mean area of 7 sagittal cresyl violet-stained sections (Image J) separated from each other by 400 μm (total sampling distance 2470 μm) in the 12-, 18-, and 21-month-old wild-type, *NP$^{0/0}$*, *NP$^{0/0}$-Hu-bcl-2*, and *Hu-bcl-2* mice ($n = 3$/genotype).

Cell Counts

The PC population was quantified in all mice aged 4–24 months (Table 1). The cresyl violet-stained PCs were counted in 10 μm-thin paraffin sections using a $\times$63 objective (final magnification $\times$630) in every 40th sagittal section (from a random start) through the entire cerebellum as described previously (Wetts and Herrup, 1982; Herrup and Sunter, 1986; Zanjani et al., 2004; Heitz et al, 2007 and Table 1). In brief, the PC nuclei profiles were counted along the entire length of the PC layer in each section. PCs were identified as neurons in the PC layer with a large soma and some portion of their nuclei in the plane of the section [white arrowheads in Fig. 1(C,F,I,L)]. The total number of PCs was estimated by graphing the number of visible PC nuclei per section as a function of the distance of each section from the midline and then integrating the area under the polygon to calculate the raw total. The raw total was adjusted for double counting errors using the Hendry correction (Hendry, 1976) because it was specifically designed to account for experimental changes in the size of the cells being counted (Zanjani et al., 2004). The Hendry correction factor was calculated in each cerebellum from measurements of the nuclear profile area and long diameter of over 300 PCs using Image J. We chose to use this classical correction factor for our cell counts instead of more recently developed stereological techniques since the profile counting method provides data on the transversal distribution of PCs. None of the nuclear profile area and long diameter measurements varied significantly between age-matched groups of different genotypes and between groups of the same genotype at different ages (Table 1). The ratio of anterior (lobules I–V) to posterior (lobules VI–X) Purkinje cell numbers in corresponding sagittal levels (two levels/hemisphere and seven vermal levels) was calculated in order to compare the rostro-caudal distribution of PC survival in age-matched *NP$^{0/0}$-Hu-bcl-2* double mutants *versus* *NP$^{0/0}$* mutants (Fig. 4A). The lateral distribution of PC survival was estimated in age-matched *NP$^{0/0}$* mutants *versus* *NP$^{0/0}$-Hu-bcl-2* double mutants by comparing Purkinje cell numbers between corresponding sagittal levels (two levels/hemisphere and seven vermal levels). To investigate a possible link between Dpl neurotoxicity and the aldolase C-specific parasagittal compartmentation of the PC population (Hawkes and Leclerc, 1987), we compared the PC loss estimated in the aldolase C-positive and -negative compartments of the wild-type and *NP$^{0/0}$* cerebellar cortex. This was achieved in one of three transverse cerebellar cryostat sections cut at seven levels along the rostro-caudal dimension of the cerebellum (Eisenman and Hawkes, 1993) and double stained for aldolase C and cresyl violet.

All the PC counts were performed by the same person (S.H.) with the genetic identity of the animals masked.

Statistics

Data are given as mean values $\pm$ standard deviation (SD). Statistical comparisons of group means (cerebellar size, PC number, PC number anterior/posterior ratio, PC nuclear area and long diameter, $n = 3$ mice per group) were performed with Minitab 13.20. Depending on context, either two-way ANOVA (factors "genotype," "aldolase C expression," "age" and within factors "brain region," "parasagittal levels" and "Aldolase C compartments") or one-way ANOVA (factor "genotype," factor "age") was used, followed by *post hoc* Tukey test for multiple comparisons when justified. Missing values in the experimental design precluded a global statistical analysis comparing the four genotypes at all ages. The significance threshold was set at $p = 0.05$. Aldolase positive/negative PC number ratios between 12-month-old wild-type and *NP$^{0/0}$* mice were compared with Student's test ($p < 0.05$).

Immunohistochemistry

Immunoperoxidase Detection of GFAP. Brain sections of 18-month-old wild-type, *NP$^{0/0}$*, *NP$^{0/0}$-Hu-bcl-2*, and *Hu-bcl-2* mice were deparaffinized in toluene and rehydrated in decreasing concentrations of ethanol. The sections were incubated in 1% H_2O_2 in 0.1 M phosphate buffer saline (PBS) for 20 min. After rinsing in PBS, the sections were pre-incubated for 45 min in blocking solution made of 0.5% Triton X-100, 3% normal horse serum (NHS) in PBS (PBST). The sections were then incubated overnight at 4°C in PBST containing 0.3% NHS and mouse monoclonal antibody against GFAP (Sigma) diluted 1/500. The sections were then rinsed in PBS (2x, 10 min) and incubated with biotinylated horse anti-mouse immunoglobulins (Vector Labs). The GFAP-bound biotinylated horse anti-mouse immunoglobulins were visualized using the ABC method (Hsu et al., 1981) with 3, 3′-diamino-benzidine tetra-hydrochloride (Fast-DAB, Sigma) as the chromogen. Stained sections were rinsed in PBS, dehydrated in graded ethanol and toluene and mounted with Eukitt. The sections were examined with a light microscope equipped with differential in-

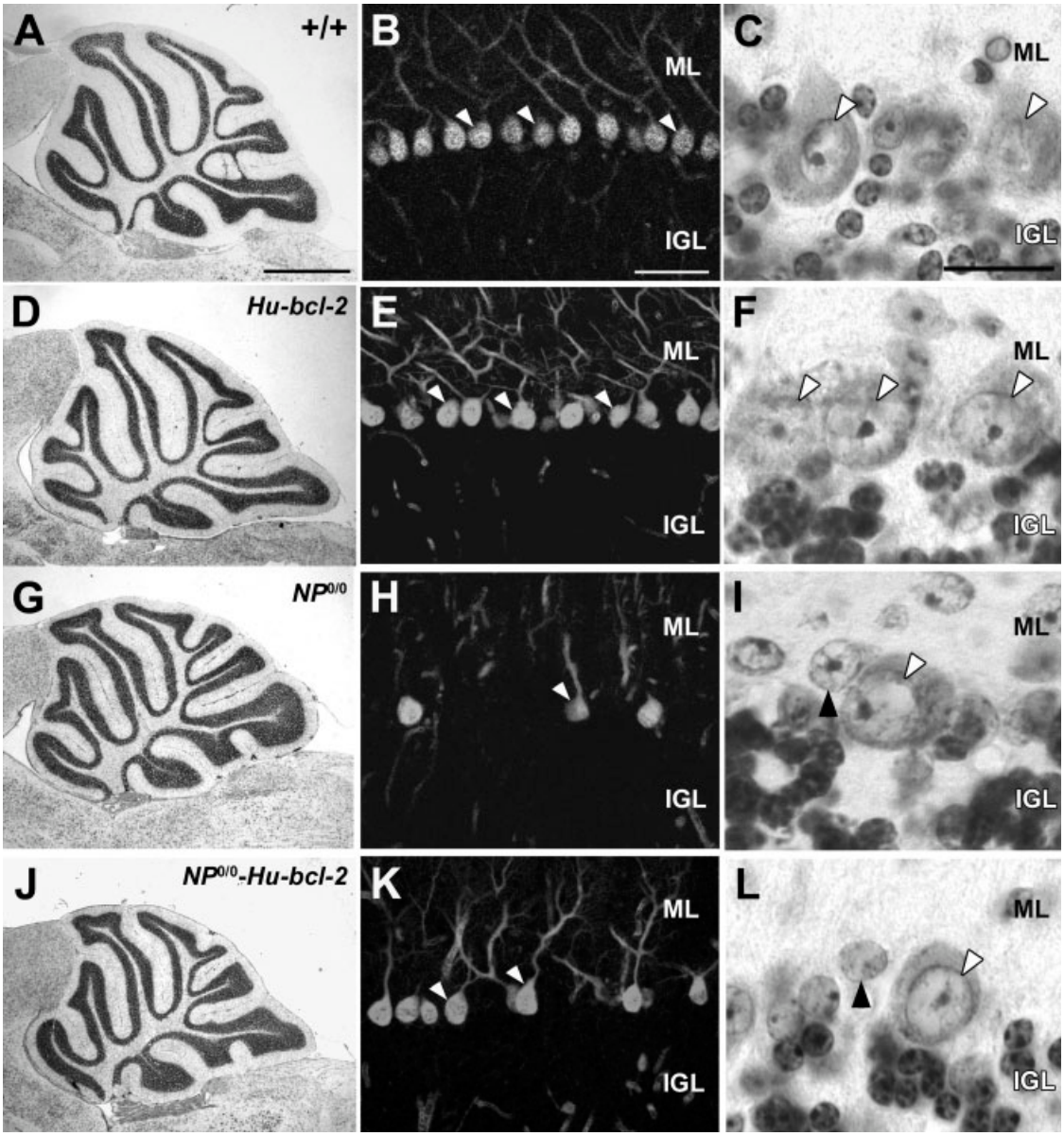

Figure 1 Histology of the cerebellum of the 18-month-old wild-type (A,B,C), *Hu-bcl-2* (D,E,F), $NP^{0/0}$ (G,H,I), and $NP^{0/0}$-*Hu-bcl-2* (J,K,L) mice. Cresyl violet-stained sagittal sections in the median vermis (A,C,D,F,G,I,J,L) and immunofluorescence staining for CaBP (B,E,H,K). A,D,G,J: The cerebellum appears smaller in the $NP^{0/0}$ and the $NP^{0/0}$-*Hu-bcl-2* than in the wild-type and *Hu-bcl-2* genotypes. B–L: The Purkinje cells (white arrowheads) form a dense monolayer between the molecular (ML) and the internal granular (IGL) layers in the wild-type (B) and *Hu-bcl-2* (E) cerebellar cortex. Purkinje cell loss is moderate in the $NP^{0/0}$-*Hu-bcl-2* cerebellar cortex (K) and almost complete in the $NP^{0/0}$ (H) cerebellar cortex. In all genotypes, Purkinje cells display a normal aspect and location between ML and IGL (C,F,I,L). Black arrowheads point to nuclei of presumptive astrocytes the number of which is increased around Purkinje cell soma in the $NP^{0/0}$ (I) and $NP^{0/0}$-*Hu-bcl-2* (L) mice. A,D,G,J: ×17; bar, 1 mm; B,E,H,K: ×200; bar, 50 μm. C, F,I,L: ×630; bar, 20 μm.

terference contrast illumination (Axioskop-II, Zeiss, Jena, Germany).

Immunofluorescent Detection of CaBP. Brain sections of 18-month-old wild-type, $NP^{0/0}$, $NP^{0/0}$-*Hu-bcl-2*, and *Hu-bcl-2* mice were deparaffinized in toluene and rehydrated in decreasing concentrations of ethanol before rinsing in PBS and pre-incubating for 45 min in blocking solution made of 0.5% Triton X-100 and 3% normal goat serum (NGS) in PBS (PBST). The sections were then incubated overnight at

4°C in PBST containing 0.3% NGS and mouse monoclonal antibody against CaBP (Sigma) diluted 1/500. The next day, sections were rinsed in PBS (2x, 10 min) and then incubated with secondary antibody: green fluorescent Alexa 488 goat anti-mouse immunoglobulins (Molecular Probes) diluted 1/500 in PBS containing 0.3% NGS. After rinsing in PBS, the sections were mounted in Mowiol before examination with a fluorescence microscope (Axioskop-II, Zeiss, Jena, Germany).

Immunoperoxidase Detection of Hu-bcl-2. Brain sections of 12-month-old *NP$^{0/0}$-Hu-bcl-2*, and *Hu-bcl-2* mice were deparaffinized in toluene and rehydrated in decreasing concentrations of ethanol. The sections were post-fixed in paraformaldehyde 4% in 0.1 M phosphate buffer (PB) for 20 min. An antigene unmasking treatment was applied by heating the sections in 10 mM citrate buffer pH 6 in a 750 W microwave for 15 min. After 30 min cooling and rinsing in PBS, the sections were pre-incubated for 1 h in a blocking solution made of 10% NHS in PBST before incubation overnight at 4°C in PBST containing 2% NHS and *Hu-bcl-2*-specific mouse monoclonal antibody (1/50, BD Biosciences). Immunoperoxidase staining was then processed according to the ABC method described above for GFAP (Vectastain ABC staining kit, Vector Labs). In order to detect differences of PC immunostaining intensity between the mutants, the sections were incubated together in the same solutions throughout the whole immunohistochemical procedure.

Immunoperoxidase Detection of Aldolase C. Frozen transverse brain sections of paraformaldehyde-perfused 12-month-old wild-type ($n = 3$) and *NP$^{0/0}$* ($n = 3$) mice were rinsed in PBS and then processed for aldolase C immunoperoxidase staining as described by Sugihara and Shinoda (2004) using anti-aldolase C rabbit polyclonal antibodies (160 ng/mL) followed by ABC immunoperoxidase staining. The sections were counter-stained with cresyl violet and mounted as described above.

Double Immunofluorescent Detection of Aldolase C and GFAP. Paraffin transverse brain sections of paraformaldehyde-perfused 6-month-old *NP$^{0/0}$* mice were rehydrated as described above and pre-incubating for 45 min in blocking solution made of 0.25% Triton X-100 and 3% NGS in PBS. The sections were then incubated overnight at 4°C in PBST containing 0.3% NGS, anti-aldolase C rabbit polyclonal antibodies (160 ng/mL) and anti-GFAP mouse monoclonal antibody diluted 1/500. The next day, sections were rinsed in PBS (2x, 10 min) and then incubated with secondary antibody: green fluorescent Alexa 488 goat anti-rabbit and red fluorescent Alexa 546 goat anti-mouse immunoglobulins (Molecular Probes) diluted 1/500 in PBS containing 0.3% NGS. After rinsing in PBS, the sections were mounted in Mowiol before examination.

Negative controls of all immunohistochemical reactions were performed by omitting either the primary or the secondary antibodies in the staining protocols.

Digital Images

Digital micrographs were stored using Zeiss Axiovision software. Photoshop 7.0 was used for final adjustments of contrast and brightness.

RESULTS

Hu-bcl-2 Overexpression Rescues *NP$^{0/0}$* PCs from Doppel Neurotoxicity

Hu-bcl-2 ***Overexpression Cannot Rescue Ataxia and Cerebellar Atrophy in NP$^{0/0}$ Mice.*** The abnormal cerebral expression of Dpl has been shown to be responsible for the premature death of PCs in the PrP-deficient mice of the Ngsk line (Moore et al., 2001; Anderson et al., 2004). Interestingly, whereas PrP^{c} displays neuroprotective BCL-2-like properties, the PC degeneration phenotype can be partially rescued either by introduction of a *Prnp* transgene (Rossi et al., 2001; Yamaguchi et al., 2004) or by knocking-out the pro-apoptotic *Bax* gene (Heitz et al., 2007) in *NP$^{0/0}$* mice. To determine whether the anti-apoptotic factor BCL-2 is able to substitute for the protective effects of PrP^{c}, we analyzed selected features of the motor behavior and cerebellar anatomy of *NP$^{0/0}$-Hu-bcl-2* double mutants and controls through the period of cerebellar degeneration in *NP$^{0/0}$* mutants. All pups developed normally up to the 12th postnatal month when *NP$^{0/0}$* mutants and double mutants began to exhibit motor impairment characteristic of the *NP$^{0/0}$* condition as shown by hind footprint analysis (a trembling of the hindquarters on initiation of movement and during walking; Sakaguchi et al., 1996). No difference was observed in the timing of the onset of ataxia between *NP$^{0/0}$-Hu-bcl-2*, and *NP$^{0/0}$* mutants (data not shown). The folial pattern and cytoarchitecture of the cerebellum of the *Hu-bcl-2*, *NP$^{0/0}$*, and *NP$^{0/0}$-Hu-bcl-2* mutants were normal compared with that of wild-type mice at all ages studied (Fig. 1). There were no obvious differences between the wild-type and *Hu-bcl-2* mice in the overall size of the cerebella (Fig. 2) or in the histological aspect of the molecular and internal granular layers [Fig. 1(B,E)]. The size of the cerebellar vermis was significantly reduced in the 18 (data not shown) and 21 (Fig. 2) month-old *NP$^{0/0}$* mice. Finally, the cerebellar vermis of the *NP$^{0/0}$-Hu-bcl-2* double mutants was larger than the cerebellar vermis of the *NP$^{0/0}$* mutants at 18 and 21 months, although for the sample size this difference was not significant. In all mutants, PCs were distributed normally at the interface between the molecular and the internal granular layers [Fig. 1(E,F,H,I,K,L)], and they were indistin-

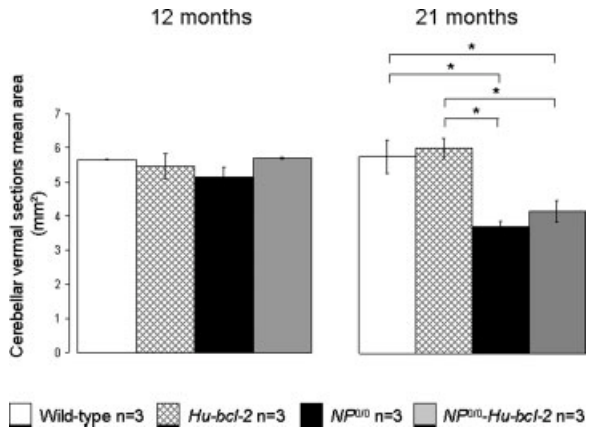

Figure 2 At 12 months of age, all genotypes have the same cerebellar size, estimated by the mean area of 7 sagittal sections in the vermis (one-way ANOVA; $F_{3,8} = 3.66$, $p > 0.05$). The 21-month-old $NP^{0/0}$ and $NP^{0/0}$-*Hu-bcl-2* mice have a significantly smaller cerebellum than the wild-type and *HuBcl-2* ($F_{3,8} = 28.24$, $p < 0.001$). The cerebellar sizes of the $NP^{0/0}$ and the $NP^{0/0}$-*Hu-bcl-2* mice are not significantly different.

guishable from wild-type PCs [Fig. 1(B,C)]. However, the PC monolayer appeared to contain fewer neurons in the $NP^{0/0}$ [Fig. 1(H)] and $NP^{0/0}$-*Hu-bcl-2* mice [Fig. 1(K)] than in the wild-type [Fig. 1(B)] and *Hu-bcl-2* [Fig. 1(E)] mice.

Overexpression of* Hu-bcl-2 *Partially Protects PCs from Doppel-Induced Apoptosis. The apoptotic mechanism triggered by Dpl in the PrP-deprived PCs was investigated by comparing the total number of PCs between $NP^{0/0}$-*Hu-bcl-2*, $NP^{0/0}$, *Hu-bcl-2*, and wild-type mice (Table 1, Fig. 3).

When comparing $NP^{0/0}$-*Hu-bcl-2* and $NP^{0/0}$, a two-way ANOVA test showed that a significant decrease of the PC number occurred between 4 and 21 months in both mutants (effect of age: $F_{5,24} = 109.02$, $p < 0.001$; Fig. 3). Thus, some PC loss still occurred in the $NP^{0/0}$-*Hu-bcl-2* double mutant in spite of *Hu-bcl-2* overexpression. However, the PC number was always higher in $NP^{0/0}$-*Hu-bcl-2* double mutant than in $NP^{0/0}$ mutant (effect of genotype: $F_{1,24} = 58.99$, $p < 0.001$; Fig. 3). This difference did not change significantly with time (interaction term: $F_{5,24} = 1.60$, $p = 0.2$). However, in relative terms, the cerebellum of the 12-month-old $NP^{0/0}$-*Hu-bcl-2* double mutants contained 41% more PCs than that of the $NP^{0/0}$ mutants at the same age, and the ratio increased with age up to 80% at 21–24 months, suggesting that *Hu-bcl-2* overexpression protects some PCs from Dpl-mediated toxicity. Nevertheless by 21 months, the number of surviving PCs in $NP^{0/0}$ mutants was 25.6% of wild-type compared with 45% in the $NP^{0/0}$-*Hu-bcl-2* double mutants indicating that overexpression of *Hu-bcl-2* rescued 20% of the wild-type number of PCs.

Spatial Extent of Neuroprotection Mediated by Hu-bcl-2 Overexpression. This loss of PCs in $NP^{0/0}$ and $NP^{0/0}$-*Hu-bcl-2* mutants compared with wild-type mice was also analyzed with two-way repeated measures ANOVA (taking into account a between-subject factor "genotype" and a within-subject factor "brain region"). The results showed a significant rostro-caudal difference that, in absolute terms, was similar in the three groups at 12 months (data not shown) and at 18 months [Fig. 4(B); factor genotype: $F_{2,12} = 127.36$, $p < 0.001$; factor region: $F_{1,12} = 136.74$, $p < 0.001$; interaction term: $F_{2,12} = 2.81$, $p = 0.1$]. In addition, calculation of the anterior/posterior ratio for each mouse indicated a significantly lower ratio in the $NP^{0/0}$ mice than in wild-type, at 12 (data not shown; $F_{2,6} = 8.5$, $P < 0.05$) and at 18 months [Fig. 4(C); $F_{2,6} = 8.26$, $p < 0.05$]. This reveals that the anterior (I–V) cerebellar lobules lost relatively more PCs than the posterior (VI–X) ones [Fig. 4(A)]. The anterior/posterior PC number ratios of $NP^{0/0}$ and $NP^{0/0}$-*Hu-bcl-2* were not significantly different at 12 and 18 months, suggesting that *Hu-bcl-2* overexpression rescued PCs evenly throughout the rostro-caudal axis of the cerebellum.

Significant PC loss occurred at each parasagittal level in the $NP^{0/0}$ cerebellum at all ages studied [Fig. 5(A)]. However, normalizing the values of PC numbers at the different parasagittal levels counted in the cerebellar vermis and hemispheres of the 12, 16, and 18 [Fig. 5(B)] month-old $NP^{0/0}$ and wild-type mice did not disclose any significant differences in PC loss

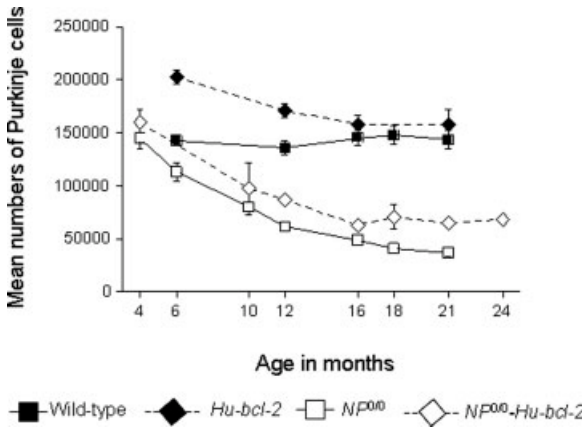

Figure 3 Time course of Purkinje cells mean numbers in the cerebellum of wild-type and different mutant mice during adulthood and aging.

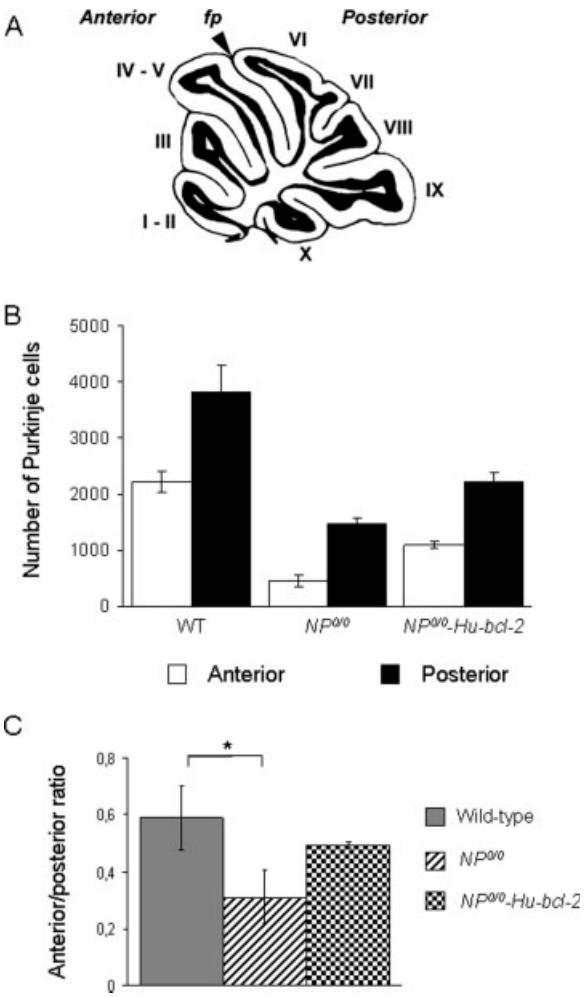

Figure 4 Purkinje cell numbers in the cortex of the anterior (lobules I–V) and posterior (lobules VI–X) cerebellum of the 18-month-old wild-type, $NP^{0/0}$ and $NP^{0/0}$-*Hu-bcl-2* mice. Mean numbers from three mice per genotype were estimated in sagittal cerebellar sections separated from each other by 400 μm (two sections in the right and in the left hemispheres and seven sections in the vermis). A: Sagittal section through the median line in the cerebellar vermis showing the 10 lobules and the fissura prima (fp) separating the anterior cerebellum from the posterior cerebellum between lobule V and lobule VI. B: The posterior (black) cerebellar cortex contains many more PCs than the anterior (white) cerebellar cortex in all genotypes. C: Significantly different wild-type and $NP^{0/0}$ anterior/posterior PC numbers ratios show a greater PC loss in the anterior $NP^{0/0}$ cerebellum. The anterior/posterior PC numbers ratios in the $NP^{0/0}$ and $NP^{0/0}$-*Hu-bcl-2* cerebella are not significantly different indicating that *Hu-bcl-2* overexpression rescues PC evenly along the rostro-caudal dimension of the cerebellum.

along the transversal dimension of the $NP^{0/0}$ cerebellum (Heitz et al., 2007). A significant PC rescue occurred at each parasagittal level in the $NP^{0/0}$-*Hu-bcl-2* cerebellum at all ages studied [Fig. 5(A)]. However, normalizing the values of PC numbers at the different parasagittal levels counted in the cerebellar vermis and hemispheres of the 12, 16, and 18 [Fig. 5(B)] month-old $NP^{0/0}$ and $NP^{0/0}$-*Hu-bcl-2* mice did not disclose significant differences in relative PC rescue along the transversal dimension of the $NP^{0/0}$-*Hu-bcl-2* cerebellum.

To determine a possible link between Dpl neurotoxicity and parasagittal compartmentation of the PC population in the cerebellar cortex, the transversal distribution pattern of PC loss was further investigated by comparing aldolase C-positive *versus* aldolase C-negative PC numbers [Fig. 6(A,B)] throughout the cerebellum of 12-month-old wild-type and

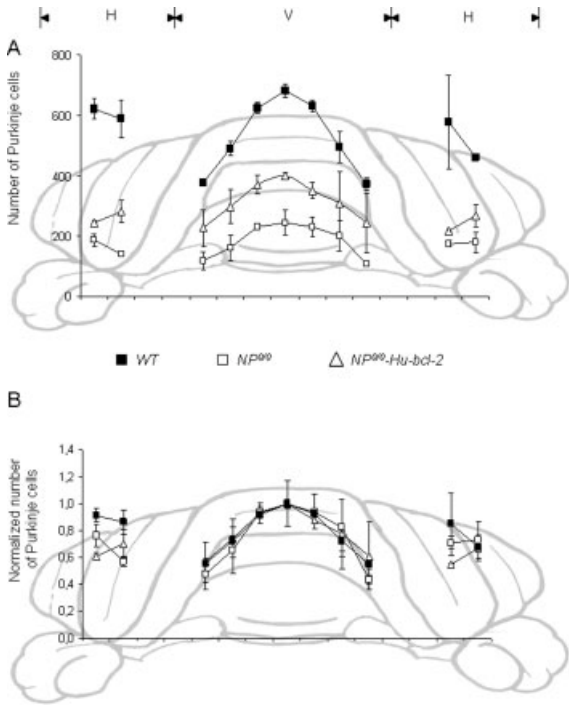

Figure 5 A: At any of the 11 parasagittal levels analyzed in the cerebellar vermis (V) and left (LH) and right (RH) hemispheres PC numbers are significantly different in the 18-month-old wild-type (■), $NP^{0/0}$-*Hu-bcl-2* (△) and $NP^{0/0}$ (□) mice (factor genotype: $F_{2,66} = 484.52$, $p < 0.001$; factor parasagittal level: $F_{10,66} = 16.02$, $p < 0.001$; interaction term: $F_{20,66} = 2.97$, $p < 0.001$). B: In the cerebellum of the 18-month-old wild-type (■), $NP^{0/0}$-*Hu-bcl-2* (△), and $NP^{0/0}$ (□) mice, PC number values at parasagittal levels of the vermis and hemispheres were normalized to the mean value of PC numbers ($n = 3$) at the sagittal level. No significant differences between genotypes were found at any level analyzed (factor genotype: $F_{2,66} = 2.96$, $p = 0.06$; factor parasagittal level: $F_{10,66} = 15.34$, $p < 0.001$; effect of interaction: $F_{20,66} = 1.64$, $p = 0.07$).

12- and 18-month-old $NP^{0/0}$ mice. Two-way repeated measures ANOVA with factors "group" (between; $F_{2,12} = 72.6$, $p < 0.001$) and "aldolase C expression" (within; $F_{1,12} = 62.6$, $p < 0.001$) showed a significant effect of both factors [Fig. 6(C)]. Doppel-induced PC loss occurred in both aldolase C-positive and -negative PC subpopulations but the proportion of aldolase C-negative PCs decreased from 41.4% in wild-type to 36.5% in 12-month-old $NP^{0/0}$ and 12.7% in 18-month-old $NP^{0/0}$. This indicated that relatively more aldolase C-negative PCs were lost from 12 to 18 months in the $NP^{0/0}$ cerebellum.

To further investigate the heterogeneity of this differential PC loss, we focused PC quantitative analysis to the cerebellar vermis where aldolase C compartmentation is best delineated [Fig. 6(D); Sugihara and Quy, 2007]. Two-way repeated measures ANOVA with factors "group" (between; $F_{2,48} = 62.4$, $p < 0.001$) and "aldolase C compartment" (within; $F_{7,48} = 15.5$, $p < 0.001$) confirmed that PC loss increased with age in aldolase C-negative compartments. The loss of aldolase C-positive PCs described in Figure 6(C) was found in the 1+ compartment, but not in other aldolase C-positive compartments.

In the $NP^{0/0}$ cerebellar cortex, GFAP immunohistofluorescent patches of PC death-related astrogliosis appeared exclusively in the aldolase C-negative compartments as early as 6 months in agreement with a stronger neurotoxic effect of Dpl in these compartments (Fig. 7). An alternative hypothesis is that *Hu-bcl-2* expression levels in the aldolase C-negative PCs are lower than in the aldolase C-positive PCs. This is not likely to be the case because *Hu-bcl-2* immunohistochemistry did not reveal any variations in staining intensities of PCs across the transversal dimension of the cerebellar cortex in either *Hu-bcl-2* mutant or $NP^{0/0}$-*Hu-bcl-2* double mutant mice (data not shown).

Supernumerary PCs of the *Hu-bcl-2* Transgenic Mice Die During Aging and Cannot Account for the Protective Effect of *Hu-bcl-2* Overexpression on the $NP^{0/0}$ PCs

Overexpression of *Hu-bcl-2* has been previously shown to increase cerebellar PC numbers by 43% in 6-month-old mice and 25% in 12-month-old mice, which supports the hypothesis that Hu-BCL-2 is able to counteract naturally occurring PC death (Martinou et al., 1994; Zanjani et al., 1996). After comparing *Hu-bcl-2* and wild-type mice at 6, 12, 16, and 21 months with a two-way ANOVA test, significant effects were measured for genotype ($F_{1,16} = 82.44$, $p < 0.001$), age ($F_{3,16} = 9.66$, $p < 0.01$) and their interaction ($F_{3,16} = 10.62$, $p < 0.001$). In our 6- and 12-month-old *Hu-bcl-2* mice, the PC population was respectively 42.5% and 25% larger than that of wild-type mice (Fig. 3) indicating that the number of supernumerary PCs decreased during aging. The number of PCs in *Hu-bcl-2* mutants and wild type mice was not significantly different at 16 months (Fig. 3). The decline in PC numbers in *Hu-bcl-2* mutants between 6 and 16 months (Fig. 3) suggests that *Hu-bcl-2* overexpression is no longer sufficient to maintain the survival of the supernumerary PCs in aging mice. In contrast, this was not the case in the $NP^{0/0}$-*Hu-bcl-2* double mutant, possibly due to an upregulation of *Hu-bcl-2* expression in the $NP^{0/0}$ condition which permitted supernumerary PCs to survive longer than in the *Hu-bcl-2* mutant. Nevertheless, similarities in the intensity of *Hu-bcl-2* immunoperoxidase staining of PCs in the cerebellar cortex of both the *Hu-bcl-2* mutant and the $NP^{0/0}$-*Hu-bcl-2* double mutant mice (data not shown) do not support this hypothesis.

One possible explanation for the rescue of PCs in the $NP^{0/0}$-*Hu-bcl-2* double mutants is that it is simply due to the presence of supernumerary *Hu-bcl-2* PCs rescued from developmental cell death. Global two-way ANOVA on the four genotypes at 12, 16, and 21 months confirmed the significant effects of genotype ($F_{3,24} = 523.01$, $p < 0.001$), age ($F_{2,24} = 8.62$, $p < 0.001$) and their interaction ($F_{6,24} = 6.22$, $p < 0.001$). However, in comparison to wild-type mice, the significantly higher increase in PCs in the cerebellum of the $NP^{0/0}$-*Hu-bcl-2* double mutant relative to the *Hu-bcl-2* mutant (42% vs. 25%, Fig. 3), is in contradiction with this explanation. Finally, between 16 and 21 months, when the *Hu-bcl-2* cerebellum contains similar numbers of PCs as wild-type mice, the $NP^{0/0}$-*Hu-bcl-2* double mutant contains significantly more PCs than the $NP^{0/0}$ mutants at 16 months (28%, $p < 0.01$), 18 months (57%) and 21 months (80%, $p < 0.01$) (Fig. 3) suggesting that the survival of these cells results from a specific rescue effect of *Hu-bcl-2* overexpression.

Hu-bcl-2 Overexpression Prevents Abnormal Activation of $NP^{0/0}$ Astrocytes

Glial cells (including astrocytes) become activated in the cerebellar cortex of the $NP^{0/0}$ mutants as early as the third postnatal week as shown by increased GFAP and lysozyme M (LM) mRNA levels and by intense GFAP immunohistochemical staining of astrocytes at

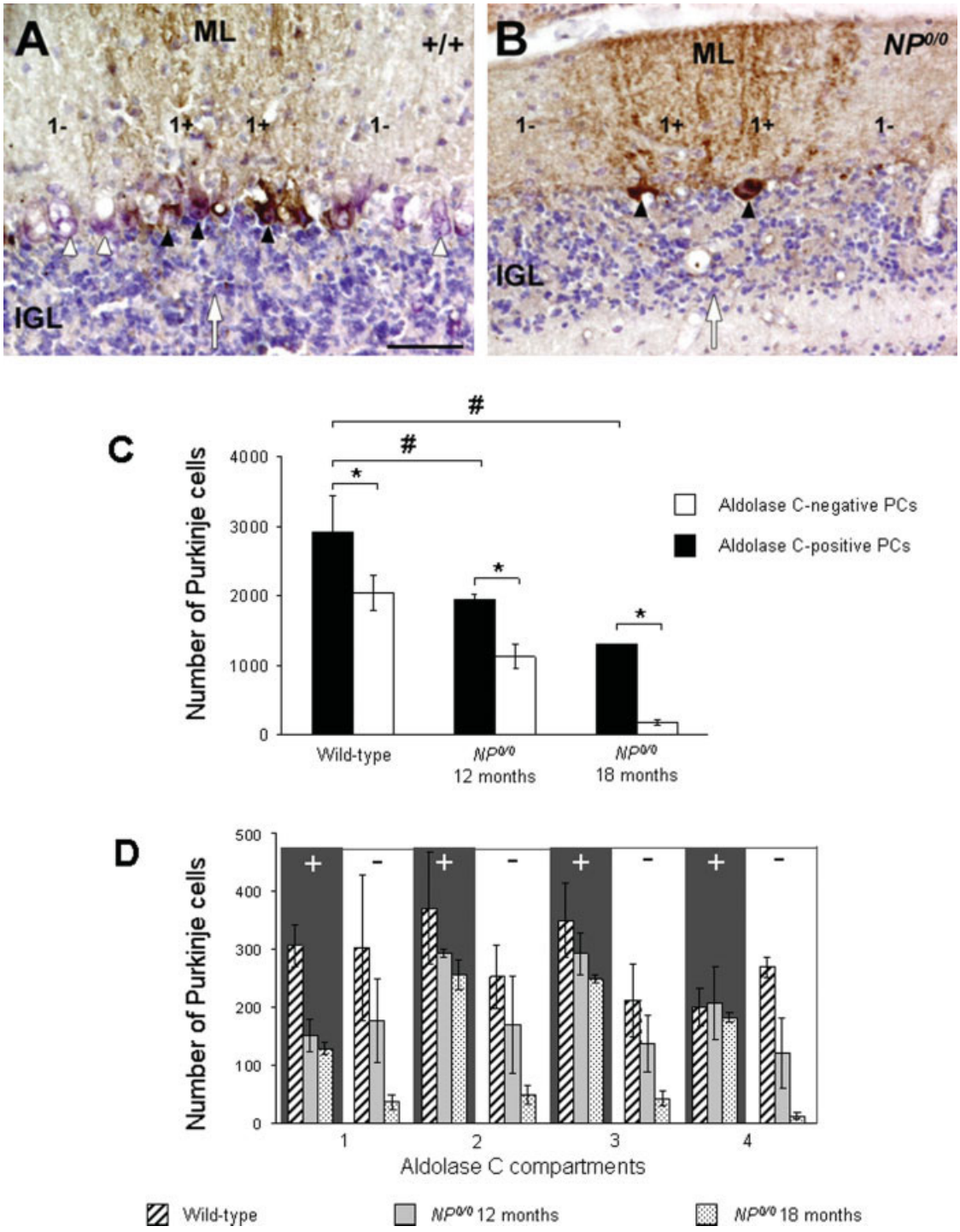

Figure 6 (See legend on following page)

the 20th month (Atarashi et al., 2001). In a recent GFAP immunohistochemical study, the cerebellar cortex of the 4-month-old $NP^{0/0}$ mice has been shown to display activation of astrocytes in restricted areas of the molecular and internal granular layers (Heitz et al., 2007). Correlation of astrogliosis and PC death kinetics was strongly suggested by the fact that these areas contained fewer PCs than areas with normal GFAP immunoreactivity and by the progressive extension of astrogliosis throughout the cerebellar cortex during aging. The systematic overlapping of astrogliosis and PC loss in the cerebellar cortex of the

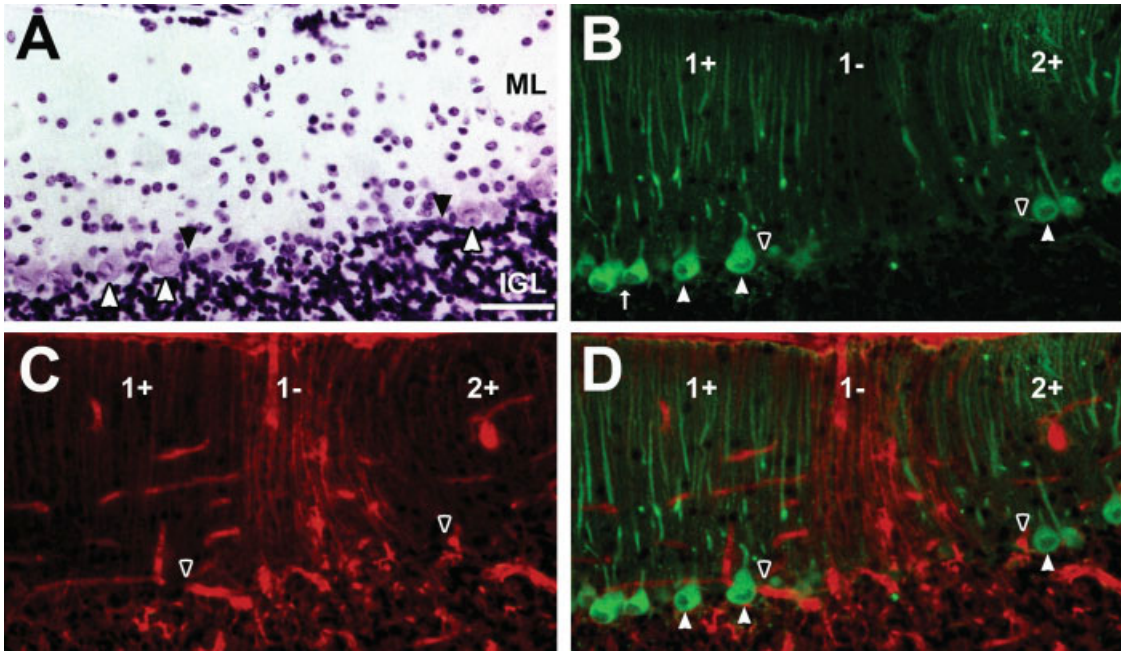

Figure 7 A: PC-deficient area (black arrowheads) between surviving PCs (white arrowheads) in the cerebellar cortex of the 6-month-old $NP^{0/0}$ mouse. ML, molecular layer; IGL internal granular layer. Cresyl violet staining. Bar, 50 μm. B: Aldolase-C immunohistofluorescence shows immunopositive PCs (white arrowheads) in the aldolase C-positive 1+ and 2+ compartments. Aldolase C-negative 1− compartment is included in the PC-deficient area viewed in A (black arrowheads). White arrow shows medial line of the cerebellum. C: The aldolase C-negative 1− compartment displays intense GFAP immunofluorescent astrogliosis. D: Merge of B and C.

$NP^{0/0}$ mice further strengthened gliosis as a consequence of PC loss (Heitz et al., 2007).

In the present study, astrogliosis occurred mostly in the aldolase C-negative compartments of the $NP^{0/0}$ cerebellar cortex as soon as 4 months, but it could not be detected in the cerebellar cortex of the *Hu-bcl-2* mice at any of the ages studied [Fig. 8(A,B)] indicating that *Hu-bcl-2* overexpression itself has no effect on astrocytes. In the cerebellar cortex of the 21-month-old $NP^{0/0}$-*Hu-bcl-2* double mutant mice [Fig. 8(D)], GFAP immunohistochemistry revealed a much less intense, patchy astrogliosis than in age-matched $NP^{0/0}$mice [Fig. 8(C)]. This indicated that *Hu-bcl-2* overexpression can prevent the activation of astrocytes in the presence of ectopic Dpl in $NP^{0/0}$ mutants.

Figure 6 Aldolase C parasagittal compartmentation of the $NP^{0/0}$ PC population. A, B: Aldolase C immunoperoxidase in the cerebellar cortex of the wild-type (A) and $NP^{0/0}$ (B) mice. A: Immunoperoxidase staining of the PC somata (black arrowheads) and dendrites of the aldolase C-positive 1+ compartments in the ventral side of the lobule IX in the median cerebellar vermis. White arrowheads point to unlabeled PC soma in the left and right aldolase C-negative 1− compartments flanking the 1+ compartments. ML, Molecular layer; IGL, Internal Granular Layer; white arrow at bottom points to the medial line of the cerebellum. B. $NP^{0/0}$ mutant mouse. Same legend as in A. See the dramatic loss of aldolase C-positive PCs (black arrowheads) in the 1+ compartments and of unlabeled PCs in the 1− compartments (white arrowhead). Bar, 50 μm. C: Aldolase C-positive and aldolase C-negative PCs in the cerebellum of the wild-type ($n = 3$) and the 12- and 18-month-old $NP^{0/0}$ mutants ($n = 3$ per age) mice. In any case, many more aldolase CP age positive than aldolase C-negative PCs were counted throughout the transverse extent of the cerebellum (*). Aldolase C-positive as well as aldolase C-negative PCs were lost in the 12- and 18-month-old $NP^{0/0}$ cerebellar cortex (#). D: PC numbers in the vermal aldolase C compartments of the wild-type and $NP^{0/0}$ cerebellum. Although $NP^{0/0}$ PC loss is observed in almost all aldolase C compartments, the difference with wild-type is not significant in any of the eight compartments.

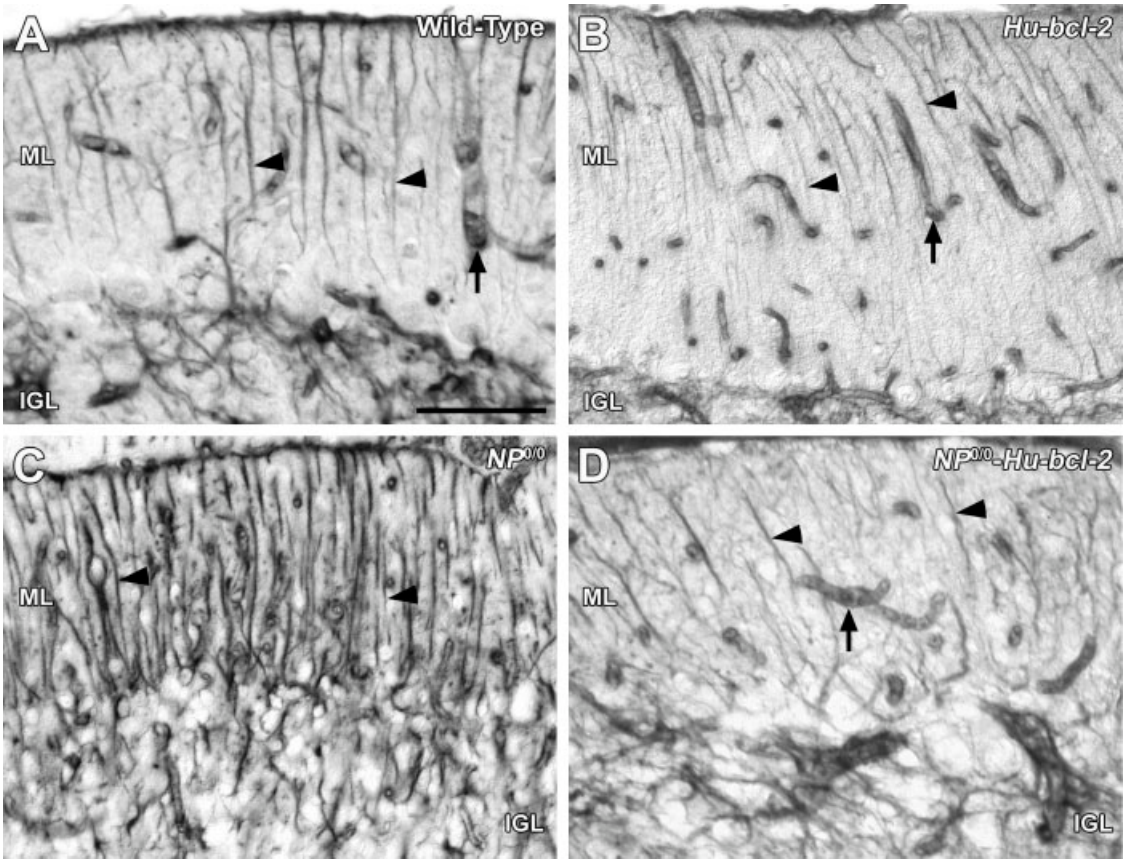

Figure 8 GFAP staining of radial Bergmann glia (black arrowheads) in the molecular layer (ML) and astrocytes in the internal granular layer (IGL) is weak in the 18-month-old wild-type (A) and *Hu-bcl-2* (B) cerebellar cortex. Gliosis disclosed in the ML and throughout the IGL of the 18-month-old $NP^{0/0}$ cerebellar cortex (C) is abolished by *Hu-bcl-2* which has restored normal intensity of GFAP immunoreactivity in ML of the 18-month-old $NP^{0/0}$-*Hu-bcl-2* cerebellar cortex (D) although astrogliosis still occurs in parts of ML and throughout IGL. Arrow shows nonspecific GFAP staining of blood vessel walls in all mice. Bar, 50 μm, $\times$200.

DISCUSSION

To investigate whether the anti-apoptotic factor BCL-2 is capable of preventing the premature death of cerebellar PCs in $NP^{0/0}$ mice caused by overexpression of the prion protein paralog Dpl (Moore et al., 1999; Weissmann and Aguzzi, 1999; Li et al., 2000), we crossed $NP^{0/0}$ mutants with *Hu-bcl-2* overexpressing mutants and analyzed PC numbers and glial activation in their cerebella. Our analysis of *Hu-bcl-2* mutants and $NP^{0/0}$-*Hu-bcl-2* double mutants suggest the following conclusions. Firstly, overexpression of *Hu-bcl-2* rescues many PCs from Dpl-induced cell death in the $NP^{0/0}$-*Hu-bcl-2* double mutant. Secondly, overexpression of *Hu-bcl-2* prevents the activation of astrocytes induced by the $NP^{0/0}$ deletion. Finally, Dpl neurotoxicity in PCs varies according to their aldolase C expression.

These studies confirm the contribution of a BAX-dependent mitochondrial pathway to Dpl-mediated PC death in the prion protein-deficient $NP^{0/0}$ mice. Furthermore, the capacity of Hu-BCL-2 to rescue some PCs from Dpl-induced neurotoxicity suggests that PrP^c may similarly protect neurons from Dpl in a BCL-2-like manner.

Hu-bcl-2 Overexpression Partially Rescues $NP^{0/0}$ PCs from Doppel Neurotoxicity

Our previous study of $NP^{0/0}$ mutants showed a significant reduction in PC numbers in the cerebellum at 6 months, but motor impairments were revealed by footprint analysis at 12 months only (Heitz et al., 2007). This suggested either that substantial numbers

of PCs must be lost before ataxia becomes apparent or that the development of the ataxic phenotype also depends on neurodegeneration in other parts of the brain. As observed in the $NP^{0/0}$:$Bax^{-/-}$ double mutants, the $NP^{0/0}$-*Hu-bcl-2* mice displayed ataxia at the same time as the $NP^{0/0}$ mice. This suggests that this phenotype is not solely a function of the number of surviving PCs, because both $NP^{0/0}$:$Bax^{-/-}$ and $NP^{0/0}$-*Hu-bcl-2* double mutants have more PCs than $NP^{0/0}$ mutants at 12 months (Heitz et al., 2007).

The double transgenic mice $NP^{0/0}$-*Hu-bcl-2* contain many more PCs than the single $NP^{0/0}$ mutants during the period studied (10–21 months). Whereas the number of PCs in the *Hu-bcl-2* mutant declines significantly from 6 to 21 months (Zanjani et al., 2004 and present data), the number of PCs in the $NP^{0/0}$-*Hu-bcl-2* mutant is stable from 12 to 24 months. Thus, the long-lasting effect of *Hu-bcl-2* overexpression on the $NP^{0/0}$ PC population cannot be explained by the rescue of PCs from developmental cell death by overexpressing *Hu-bcl-2*. Our previous data showed that BAX contributes to Dpl-mediated cell death (Heitz et al., 2007) and that increased levels of BCL-2 enable some PCs to resist Dpl neurotoxicity. This suggests that the $NP^{0/0}$ PCs rescued by *Hu-bcl-2* overexpression are likely to be the same PCs rescued by deletion of the *Bax* gene (Heitz et al., 2007), providing further evidence that Dpl activates a BCL-2 family-mediated cell death pathway. Indeed, the number of rescued PCs in the $NP^{0/0}$-*Hu-bcl-2* and in the $NP^{0/0}$:$Bax^{-/-}$ double mutants was not significantly different between 10 and 21 months. An $NP^{0/0}$-specific upregulation of *Hu-bcl-2* expression remains to be explored as a possible reason for increased PC survival in the $NP^{0/0}$-*Hu-bcl-2* double mutant since it could sustain PC rescue from developmental cell death longer than in the *Hu-bcl-2* single mutant. However, this seems unlikely because PC survival has similar kinetics in both $NP^{0/0}$:$Bax^{-/-}$ and $NP^{0/0}$-*Hu-bcl-2* double mutants. In addition, the intensity of *Hu-bcl-2* immunoperoxidase staining was not increased in the $NP^{0/0}$-*Hu-bcl-2* PCs compared to the *Hu-bcl-2* PCs at 12 months when *Hu-bcl-2* expression levels are known to be decreased (Zanjani et al., 2004), indicating that *Hu-bcl-2* expression is not modified by the $NP^{0/0}$ condition.

Neither *Bax* deficiency with normal *Bcl-2* expression (Heitz et al., 2007) nor *Hu-bcl-2* overexpression with normal *Bax* and *Bcl-2* expression (Zanjani et al., 2004 and present results) is able to sustain supernumerary PCs survival during adulthood. Thus, mechanisms independent of the BAX/BCL-2 couple are likely to be responsible for supernumerary PC death in both $Bax^{-/-}$ and *Hu-bcl-2* mice. Furthermore, the gradual decline in the $NP^{0/0}$-*Hu-bcl-2* PC population during this 20-month-long study indicated that overexpression of *Hu-bcl-2* alone is not sufficient to counteract Dpl-mediated apoptosis of all PCs. As early as 10 months, the number of PCs in $NP^{0/0}$-*Hu-bcl-2* mice was significantly less than in wild-type mice. This suggests that BCL-2-insensitive death mechanisms can be specifically activated by Dpl in the prion protein-deficient Ngsk PCs. Anyway, the PC survival in Zürich-1 (ZH-I) (Büeler et al., 1993) and Edbr (Manson et al., 1994) *Prnp*-knock-out mice that do not overexpress Dpl rules out PrP-deficiency as a BCL-2-insensitive cause of PC death in the $NP^{0/0}$-*Hu-bcl-2* mice. Thus the BCL-2-like neuroprotective properties of PrP^{c} (Bouhnar et al., 2001; Li and Harris, 2005; Bounhar et al., 2006) are probably not responsible for its anti-Dpl activity (Nishida et al., 1999; Yamaguchi et al., 2004).

Whereas PC survival was the same in $NP^{0/0}$ and wild-type mice at 4 months, PC numbers were reduced in the $NP^{0/0}$-*Hu-bcl-2* double mutants compared with the *Hu-bcl-2* mutants. This suggested that PCs are more sensitive to Dpl neurotoxicity in *Hu-bcl-2* than the wild-type mice. The loss of $NP^{0/0}$-*Hu-bcl-2* PCs at 4 months is probably provoked by PC fragility due to excessive number of PCs overexpressing *Hu-bcl-2*. This decline in supernumerary PC numbers during adulthood in the $Bax^{-/-}$ and *Hu-bcl-2* overexpressing mice suggests that the PCs in $NP^{0/0}$-*Hu-bcl-2* mice which overexpress *Hu-bcl-2* and have a $Bcl\text{-}2^{+/+}$ background that is highly neuroprotective, are likely to die by a mechanism independent of the BCL-2 family of pro-apoptotic factors.

According to our present and previous (Heitz et al., 2007) results, the ectopic expression of Dpl in the $NP^{0/0}$ mice may induce BAX/BCL-2-dependent and BAX/BCL-2-independent mechanisms in the same PCs. Alternatively, the two pathways could be mutually exclusive such that Dpl may selectively stimulate one pathway or the other in different PCs. Against this hypothesis, neither Dpl-induced PC loss nor PC rescue induced by either *Bax* deletion or *Hu-bcl-2* overexpression showed significant variations along the lateral axis of the cerebellum in the $NP^{0/0}$, $NP^{0/0}$:$Bax^{-/-}$, and $NP^{0/0}$-*Hu-bcl-2* mice suggesting that the neurotoxicity of Dpl and in particular its BAX-mediated component, is evenly distributed along the lateral axis of the cerebellum. However, PC loss was significantly different between aldolase C-positive and -negative compartments in the 18-month-old $NP^{0/0}$ cerebellum, suggesting that acuity of Dpl neurotoxicity is modulated by specific properties of PCs in the aldolase C compartments (Gravel et al., 1987; Wassef et al., 1992; Bailly et al., 1995; Voogd and

Ruigrok, 2004; Sugihara and Quy, 2007). Alternatively, the $NP^{0/0}$ condition may have a differential effect on *Hu-bcl-2* expression level as a function of aldolase C expression. In other words, the transgene *Hu-bcl-2* is selectively upregulated in the aldolase C-positive PCs which display the strongest resistance to Dpl neurotoxicity. However, the similar intensity of *Hu-bcl-2* immunostaining of aldolase C-positive and -negative PCs does not support this possibility. As early as 6 months, PC-death-induced reactive astrogliosis was detected exclusively in the molecular layer of the aldolase C-negative compartments where the most of PCs were lost. Such a causal relationship between PC loss and astrogliosis has previously been suggested by the topographical coincidence of PC death and astrogliosis in the $NP^{0/0}$ cerebellar cortex (Heitz et al., 2007).

Favoring the existence of cell-specific differential sensitivity of PCs to Dpl neurotoxicity, PC loss was increased in the anterior cerebellum (Heitz et al., 2007). This suggests that Dpl neurotoxicity varies along the rostro-caudal axis of the cerebellum and could be related to the antero-posterior compartmentalization of the PC population (Duchala et al., 2004). However, since PC survival was similar in the anterior and posterior cerebellum of the $NP^{0/0}$: $Bax^{-/-}$ and $NP^{0/0}$-*Hu-bcl-2* as well, the rescue effect of *Bax* knock-out and of *Hu-bcl-2* overexpression did not change between anterior and posterior PCs suggesting that the BAX/BCL-2-mediated effect of Dpl is not related to the rostro-caudal compartmentalization of PC population. Rather, since aldolase-C negative PCs are more sensitive to Dpl neurotoxicity, the increased PC loss in the anterior cerebellum is likely to be related to the aldolase-C negative/aldolase-C positive ratio of PC population in the anterior cerebellum.

Aside from signal transduction and antioxidant activities, PrP^c is neuroprotective because of its BCL-2-like activity and acts as a potent BAX inhibitor. In favour of an antagonistic function of PrP^c on mitochondrial apoptotic pathways, PrP^c protects against cell death by preventing the conformational change of BAX that occurs during BAX activation (Roucou et al., 2005). Although not exactly identical to BCL-2, PrP^c may functionally replace BCL-2 when it decreases in the aging brain (see review in Roucou et al., 2005; Bounhar et al., 2006). On the other hand, BAX-induced apoptosis cannot be counteracted by PrP^c devoid of its N-terminal octapeptide repeats suggesting that this domain, partially homologous to the BH2 domain of the BCL-2 family of proteins (Yin et al., 1994; Roucou et al., 2004), is crucial for the neuroprotective functions of PrP^c. Interestingly, an important function of BCL-2 is to antagonize the pro-apoptotic effect of BAX through direct interaction at this BH2 domain (Oltvai et al., 1993; Gross et al., 1999; Cheng et al., 2001), which is missing in both Dpl and mutated neurotoxic forms of PrP: ΔPrP (Shmerling et al., 1998; Flechsig et al., 2003; Li et al., 2007) and Tg(PG14)PrP (Chiesa et al., 1998). Indeed, fusion of Dpl to a BH2-containing octapeptide repeat and the N-terminal half of hydrophobic region of PrP^c confer resistance to serum deprivation (Lee et al., 2006). Interestingly, N-terminally deleted forms of PrP^c have been recently shown to activate both *Bax*-dependent and *Bax*-independent apoptotic pathways (Li et al., 2007). A direct effect of Hu-BCL-2 on BAX is the most likely mechanism involved in the $NP^{0/0}$ PC rescue reported in the present study. Although PrP^c is mainly present at the cell surface (Fournier et al., 2000; Bailly et al., 2004), it has recently been localized in the cytoplasm where it could directly interfere with BAX-mediated cell death (Ma and Lindquist, 2001; Yedidia et al., 2001; Roucou et al., 2003).

Hu-bcl-2 Overexpression Rescues $NP^{0/0}$ Astrocytes from Activation

Increased immunolabeling for GFAP is displayed by astrocytes in the cerebellar cortex of the 4 month-old $NP^{0/0}$ mutants indicating astroglial activation (Atarashi et al., 2001; Heitz et al., 2007). At this age, astrogliosis occurred in patches reminiscent of parasagittal compartments delineated by PC clusters in the cerebellar cortex (Bailly et al., 1995; Sugihara and Quy, 2007). From 10 months on, astrogliosis propagated throughout the cerebellar cortex following a time course parallel with PC loss.

Since activation of astrocytes *in vivo* does not induce neuronal death (Mallucci et al., 2003), gliosis is likely to be a consequence of PC damage in the cerebellum of the $NP^{0/0}$ mice. In the present study, *Hu-bcl-2* is under control of the NSE promoter and therefore specifically expressed in neurons. Thus, the only explanation is that PC rescue by *Hu-bcl-2* expression leads to decreased gliosis in the cerebellar cortex of $NP^{0/0}$-*Hu-bcl-2* mice. This is also supported by the topographic coincidence of astrogliosis and PC loss demonstrated in our previous study (Heitz et al., 2007). In all cases, regions with gliosis overlapped PC-free areas, whereas regions with normal GFAP fluorescence of glial cells contained surviving PCs, suggesting that activation of astrocytes could result from degeneration signals from PCs. The activation of astrocytes was greatly moderated by *Bax* deletion in the cerebellar cortex of the $NP^{0/0}$: $Bax^{-/-}$

mice (Heitz et al., 2007). Although a direct antagonistic effect of *Bax* knock-out in activated astrocytes cannot be ruled out since ischemia has been shown to upregulate *Bax* in astrocytes (Imura and Shimohama, 2000; Giffard and Swanson, 2005), consistent glial expression of BAX could not be detected in mouse and human brain (Hara et al., 1996; Shin et al., 2000) suggesting that *Bax* deletion indirectly represses astrocyte activation by directly counteracting Dpl neurotoxicity in PCs. In agreement with this hypothesis, our present observations in the $NP^{0/0}$-*Hu-bcl-2* show that BCL-2, a direct BAX antagonist sustaining $NP^{0/0}$ PC survival, has a similar repressor effect on glial activation. Thus, our data suggest that *Bax*-dependent PC death is an astrocyte-activating cell death mechanism. Gliosis is almost completely rescued in the cerebellum of the $NP^{0/0}$-*Hu-bcl-2* double mutant in spite of the loss of a great number of PCs by a *Bax*-independent mechanism, suggesting that this latter mechanism does not activate gliosis. According to our data, astrogliosis is triggered by *Bax*-induced PC death starting in the aldolase C-negative compartments.

We thank Laure Rondi-Reig for help with footprint tests, Shigeru Katamine for $NP^{0/0}$ mice, and Nancy Grant for critical review of the manuscript.

REFERENCES

Anderson L, Rossi D, Linehan J, Brandner S, Weissmann C. 2004. Transgene-driven expression of the doppel protein in purkinje cells causes purkinje cell degeneration and motor impairment. Proc Natl Acad Sci USA 101:3644–3649.

Atarashi R, Sakaguchi S, Shigematsu K, Arima K, Okimura N, Yamaguchi N, Li A, et al. 2001. Abnormal activation of glial cells in the brains of prion protein-deficient mice ectopically expressing prion protein-like protein, PrPLP/Dpl. Mol Med 7:803–809.

Bailly Y, Haeberle AM, Blanquet-Grossard F, Chasserot-Golaz S, Grant N, Schulze T, Bombarde G, et al. 2004. Prion protein (PrPc) immunocytochemistry and expression of the green fluorescent protein reporter gene under control of the bovine PrP gene promoter in the mouse brain. J Comp Neurol 473:244–269.

Bailly Y, Schoen SW, Delhaye-Bouchaud N, Kreutzberg GW, Mariani J. 1995. 5′-Nucleotidase activity as a synaptic marker of parasagittal compartmentation in the mouse cerebellum. J Neurocytol 24:879–890.

Bounhar Y, Mann KK, Roucou X, LeBlanc AC. 2006. Prion protein prevents Bax-mediated cell death in the absence of other Bcl-2 family members in *Saccharomyces cerevisiae*. FEMS Yeast Res 6:1204–1212.

Bounhar Y, Zhang Y, Goodyer CG, LeBlanc A. 2001. Prion protein protects human neurons against Bax-mediated apoptosis. J Biol Chem 276:39145–39149

Büeler H, Aguzzi A, Sailer A, Greiner RA, Autenried P, Aguet M, Weissmann C. 1993. Mice devoid of PrP are resistant to scrapie. Cell 73:1339–1347.

Cheng EH, Wei MC, Weiler S, Flavell RA, Mak TW, Lindsten T, Korsmeyer SJ. 2001. BCL-2, BCL-X(L) sequester BH3 domain-only molecules preventing BAX- and BAK-mediated mitochondrial apoptosis. Mol Cell 8:705–7011.

Chiesa R, Piccardo P, Ghetti B, Harris DA. 1998. Neurological illness in transgenic mice expressing a prion protein with an insertional mutation. Neuron 21:1339–1351.

Cui T, Holme A, Sassoon J, Brown DR. 2003. Analysis of doppel protein toxicity. Mol Cell Neurosci 23:144–155.

Duchala CS, Shick HE, Garcia J, Deweese DM, Sun X, Stewart VJ, Macklin WB. 2004. The toppler mouse: A novel mutant exhibiting loss of Purkinje cells. J Comp Neurol 476:113–129.

Eisenman L, Hawkes R. 1993. Antigenic compartmentation in the mouse cerebellar cortex: Zebrin and HNK-1 reveal a complex, overlapping molecular topography. J Comp Neurol 335:586–605.

Flechsig E, Hegyi I, Leimeroth R, Zuniga A, Rossi D, Cozzio A, Schwarz P, et al. 2003. Expression of truncated PrP targeted to Purkinje cells of PrP knockout mice causes Purkinje cell death and ataxia. EMBO J 22:3095–3101.

Fournier JG, Escaig-Haye F, Grigoriev V. 2000. Ultrastructural localization of prion proteins: Physiological and pathological implications. Microsc Res Tech 50:76–88.

Giffard RG, Swanson RA. 2005. Ischemia-induced programmed cell death in astrocytes. Glia 50:299–306.

Gravel C, Eisenman L, Sasseville R, Hawkes R. 1987. Parasagittal organization of the rat cerebellar cortex: Direct correlation between antigenic Purkinje cell bands revealed by mabQ113 and the organization of the olivocerebellar projection. J Comp Neurol 265:294–310.

Gross A, McDonnell JM, Korsmeyer SJ. 1999. BCL-2 family members and the mitochondria in apoptosis. Genes Dev 13:1899–1911.

Hara A, Hirose Y, Wang A, Yoshimi N, Tanaka T, Mori H. 1996. Localization of Bax and Bcl-2 proteins, regulators of programmed cell death, in the human central nervous system. Virchows Arch 429:249–253.

Hawkes R, Leclerc N. 1987. Antigenic map of the rat cerebellar cortex: The distribution of parasagittal bands as revealed by monoclonal anti-Purkinje cell antibody mabQ113. J Comp Neurol 256:29–41.

Heitz S, Lutz Y, Rodeau J-L, Zanjani H, Gautheron V, Bombarde G, Richard F, et al. 2007. BAX contributes to doppel-induced apoptosis of prion protein-deficient Purkinje cells. Dev Neurobiol 67:670–686.

Hendry IA. 1976. A method to correct adequately for the change in neuronal size when estimating neuronal numbers after nerve growth factor treatment. J Neurocytol 5:337–349.

Herrup K, Sunter K. 1986. Cell lineage dependent and independent control of Purkinje cell number in the mammalian CNS: Further quantitative studies of lurcher chimeric mice. Dev Biol 117:417–427.

Hsu SM, Raine L, Fanger H. 1981. Use of avidin-biotin-peroxidase complex (ABC) in immunoperoxidase technics. J Histochem Cytochem 29:577–580.

Imura T, Shimohama S. 2000. Opposing effects of adenosine on the survival of glial cells exposed to chemical ischemia. J Neurosci Res 62:539–546.

Kurschner C, Morgan JI. 1995. The cellular prion protein (PrP) selectively binds to Bcl-2 in the yeast two-hybrid system. Brain Res Mol Brain Res 30:165–168.

Kuwahara C, Takeuchi A, Nishimura T, Haraguchi K, Kubosaki A, Matsumoto Y, Saeki K, et al. 1999. Prions prevent neuronal cell-line death. Nature 400:225–226.

Lee DC, Sakudo A, Kim CK, Nishimura T, Saeki K, Matsumoto Y, Yokoyama T, et al. 2006. Fusion of doppel to octapeptide repeat and N-terminal half of hydrophobic region of prion protein confers resistance to serum deprivation. Microbiol Immunol 50:203–209.

Li A, Barmada S, Roth K, Harris D. 2007. N-terminally deleted forms of the prion protein activate botch Bax-dependent and Bax-independent neurotoxic pathways. J Neurosci 27:852–859

Li A, Harris DA. 2005. Mammalian prion protein suppresses BAX-induced cell death in yeast. J Biol Chem 280:17430–17434.

Li A, Sakaguchi S, Ryuichiro A, Bhabesh CR, Ryota N, Kazuhiko A, Nobuhiko O, et al. 2000. Identification of a novel gene encoding a PrP-like protein expressed as chimeric transcripts fused to PrP exon 1/2 in ataxic mouse line with a disrupted PrP gene. Cell Mol Biol 20:553–567.

Ma J, Lindquist S. 2001. Wild-type PrP and a mutant associated with prion disease are subject to retrograde transport and proteasome degradation. Proc Natl Acad Sci USA 98:14955–14960.

Mallucci G, Dickinson A, Linehan J, Klöhn P-C, Brandner S, Collinge J. 2003. Depleting neuronal PrP in prion infection prevents disease and reverses spongiosis. Science 302:871–874.

Manson JC, Clarke AR, Hooper ML, Aitchison L, McConnell I, Hope J. 1994. 129/Ola mice carrying a null mutation in PrP that abolishes mRNA production are developmentally normal. Mol Neurobiol 8:121–127.

Martinou JC, Dubois-Dauphin M, Staple JK, Rodriguez I, Frankowski H, Missotten M, Albertini P, et al. 1994. Overexpression of BCL-2 in transgenic mice protects neurons from naturally occurring cell death and experimental ischemia. Neuron 13:1017–1030.

Massimino ML, Ballarin C, Bertoli A, Casonato S, Genovesi S, Negro A, Sorgato MC. 2004. Human doppel and prion protein share common membrane microdomains and internalization pathways. Int J Biochem Cell Biol 36:2016–2031.

Moore RC, Lee IT, Bouzamondo E, Silverman GL, Harisson PM, Strome R, Heinrich C, et al. 1999. Ataxia in prion protein (PrP)-deficient mice is associated with upregulation of the novel PrP-like protein doppel. J Mol Biol 292:797–817.

Moore RC, Mastrangelo P, Bouzamondo E, Heinrich C, Legname G, Prusiner SB, Hood L, et al. 2001. Doppel-induced cerebellar degeneration in transgenic mice. Proc Natl Acad Sci USA. 98:15288–15293.

Moore RC, Redhead NJ, Selfridge J, Hope J, Manson JC, Melton DW. 1995. Double replacement gene targeting for the production of a series of mouse strains with different prion protein gene alterations. Biotechnology (NY) 13:999–1004.

Nishida N, Tremblay P, Sugimoto T, Shigematsu K, Shirabe S, Petromilli C, Erpel SP, et al. 1999. A mouse prion protein transgene rescues mice deficient for the prion protein gene from Purkinje cell degeneration and demyelination. Lab Invest 79:689–697.

Oltvai ZN, Milliman CL, Korsmeyer SJ. 1993. Bcl-2 heterodimerizes in vivo with a conserved homolog, Bax, that accelerates programmed cell death. Cell 74:609–619.

Prusiner SB. 1998. Prions. Proc Natl Acad Sci USA 95: 13363–13383.

Qin K, Coomaraswamy J, Mastrangelo P, Yang Y, Lugowski S, Petromilli C, Prusiner SB, et al. 2003. The PrP-like protein Doppel binds copper. J Biol Chem 278: 8888–8896.

Rossi D, Cozzio A, Flechsig E, Klein MA, Rulicke T, Aguzzi A, Weissmann C. 2001. Onset of ataxia and Purkinje cell loss in PrP null mice inversely correlated with Dpl level in brain. EMBO J 20:694–702.

Roucou X, Gains M, LeBlanc AC. 2004. Neuroprotective functions of prion protein. J Neurosci Res 75:153–161.

Roucou X, Giannopoulos PN, Zhang Y, Jodoin J, Goodyer CG, LeBlanc A. 2005. Cellular prion protein inhibits proapoptotic Bax conformational change in human neurons and in breast carcinoma MCF-7 cells. Cell Death Differ 12:783–795.

Roucou X, Guo Q, Zhang Y, Goodyer CG, LeBlanc AC. 2003. Cytosolic prion protein is not toxic and protects against Bax-mediated cell death in human primary neurons. J Biol Chem 278:40877–40881.

Sakaguchi S, Katamine S, Nishida N, Moriuchi R, Shigematsu K, Sugimoto T, Nakatani A, et al. 1996. Loss of cerebellar purkinje cells in aged mice homozygous for a disrupted PrP gene. Nature 380:528–531.

Sakaguchi S, Katamine S, Shigematsu K, Nakatani A, Moriuchi R, Nishida N, Kurokawa K, et al. 1995. Accumulation of proteinase K-resistant prion protein (PrP) is restricted by the expression level of normal PrP in mice inoculated with a mouse-adapted strain of the Creutzfeldt-Jakob disease agent. J Virol 69:7586–75892.

Sakudo A, Lee DC, Nakamura I, Taniuchi Y, Saeki K, Matsumoto Y, Itohara S, et al. 2005. Cell-autonomous PrP-Doppel interaction regulates apoptosis in PrP gene-deficient neuronal cells. Biochem Biophys Res Commun 333:448–454.

Shin C-M, Chung YH, Kim MJ, Shin DH, Kim YS, Gurney ME, Lee KW, et al. 2000. Immunohistochemical study on the distribution of Bcl-2 and Bax in the central nervous system of the transgenic mice expressing a human Cu/Zn SOD mutation. Brain Res 887:309–315.

Shmerling D, Hegyi I, Fischer M, Blattler T, Brandner S, Gotz J, Rulicke T, et al. 1998. Expression of amino-terminally truncated PrP in the mouse leading to ataxia and specific cerebellar lesions. Cell 93:203–214.

Silverman GL, Qin K, Moore RC, Yang Y, Mastrangelo P, Tremblay P, Prusiner SB, et al. 2000. Doppel is an N-glycosylated, glycosylphosphatidylinositol-anchored protein. Expression in testis and ectopic production in the brains of Prnp(0/0) mice predisposed to purkinje cell loss. J Biol Chem 275:26834–26841.

Sugihara I, Quy PN. 2007. Identification of aldolase C compartments in the mouse cerebellar cortex by olivocerebellar labelling. J Comp Neurol 500:1076–1092.

Sugihara I, Shinoda Y. 2004. Molecular, topographic, and functional organization of the cerebellar cortex: A study with combined aldolase C and olivocerebellar labeling. J Neurosci 24:8771–8785.

Tsujimoto Y, Croce CM. 1986. Analysis of the structure, transcripts, and protein products of bcl-2, the gene involved in human follicular lymphoma. Proc Natl Acad Sci USA 83:5214–5218.

Voogd J, Ruigrok TJ. 2004. The organization of the corticonuclear and olivocerebellar climbing fiber projections to the rat cerebellar vermis: The congruence of projection zones and the zebrin pattern. J Neurocytol 33:5–21.

Wassef M, Cholley B, Heizmann CW, Sotelo C. 1992. Development of the olivocerebellar projection in the rat. II. Matching of the developmental compartmentations of the cerebellum and inferior olive through the projection map. J Comp Neurol 323:537–550.

Weissmann C, Aguzzi A. 1999. PrP double causes trouble. Science 286:914–915.

Wetts R, Herrup K. 1982. Cerebellar Purkinje cells are descended from a small number of progenitors committed during early development: Quantitative analysis of lurcher chimeric mice. J Neurosci 2:1494–1498.

Wong BS, Liu T, Paisley D, Li R, Pan T, Chen SG, Perry G, et al. 2001. Induction of HO-1 and NOS in doppel-expressing mice devoid of PrP: Implications for doppel function. Mol Cell Neurosci 17:768–775.

Yamaguchi N, Sakaguchi S, Shigematsu K, Okimura N, Katamine S. 2004. Doppel-induced Purkinje cell death is stoichiometrically abrogated by prion protein. Biochem Biophys Res Commun 319:1247–1252.

Yedidia Y, Horontchik L, Tzaban S, Yanai A, Taraboulos A. 2001. Proteasomes and ubiquitin are involved in the turnover of the wild-type prion protein. EMBO J 20: 5383–5391.

Yin XM, Oltvai ZN, Korsmeyer SJ. 1994. BH1 and BH2 domains of Bcl-2 are required for inhibition of apoptosis and heterodimerization with Bax. Nature 369:321–323.

Yokoyama T, Kimura KM, Ushiki Y, Yamada S, Morooka A, Nakashiba T, Sassa T, et al. 2001. In vivo conversion of cellular prion protein to pathogenic isoforms, as monitored by conformation-specific antibodies. J Biol Chem 276:11265–11271.

Zanjani H, Lemaigre-Dubreuil Y, Tillakaratne NJ, Blokhin A, McMahon RP, Tobin AJ, Vogel MW, et al. 2004. Cerebellar Purkinje cell loss in aging *Hu-bcl-2* transgenic mice. J Comp Neurol 475:481–492.

Zanjani HS, Vogel MW, Delhaye-Bouchaud N, Martinou JC, Mariani J. 1996. Increased cerebellar Purkinje cell numbers in mice overexpressing a human bcl-2 transgene. J Comp Neurol 374:332–341.

BRAIN PATHOLOGY

Autophagy and cell death of Purkinje cells overexpressing Doppel in Ngsk Prnp-deficient mice.

Journal:	*Brain Pathology*
Manuscript ID:	BPA-08-06-RA-081.R1
Article Type:	Research Article
Date Submitted by the Author:	09-Oct-2008
Complete List of Authors:	Heitz, Stéphane; INCI/ CNRS UMR7168, Neurotransmission et Sécrétion Neuroendocrine Grant, Nancy; INCI/ CNRS UMR7168, Neurotransmission et Sécrétion Neuroendocrine Leschiera, Raphael; INCI/ CNRS UMR7168, Neurotransmission et Sécrétion Neuroendocrine Haeberlé, Anne-Marie; INCI/ CNRS UMR7168, Neurotransmission et Sécrétion Neuroendocrine Demais, Valérie; IFR37, Plateforme d'Imagerie in-vitro Bombarde, Guy; INCI/ CNRS UMR7168, Neurotransmission et Sécrétion Neuroendocrine Bailly, Yannick; INCI/ CNRS UMR7168, Neurotransmission et Sécrétion Neuroendocrine
Keywords:	Purkinje cell, Doppel, prion protein, autophagy, neuronal death

Dear Editor,

We are pleased to submit our revised article "Autophagy and cell death of Purkinje cells overexpressing Doppel in Ngsk *Prnp*-deficient mice" by Heitz S., Grant N. J, Leschiera R., Haeberlé A.-M., Demais V., Bombarde G., Bailly Y. for publication as a research article in Brain Pathology.

All concerns of reviewer 1 and reviewer 2 have been taken into account and modifications of the manuscript appear in red in the revised text. In addition, you will find our specific responses to the reviewer's comments in the space provided in the electronic submission form.

Briefly, an extensive semi-quantitative analysis of autophagic nerve profiles has been achieved at the ultrastructural level in both cerebellar cortex and deep cerebellar nuclei to demonstrate a major autophagic stress at axon terminal level. In addition, double immunohistofluorescence labelling of autophagy and lysosomes is presented to show that autophagy-associated lysosomal recruitment occurs in the $NP^{0/0}$ PCs. Finally, RT-PCR analysis of LC3B and p62 mRNAs confirms unchanged synthesis but rather decreased protein degradation of autophagic products in these PCs.

These new data indicate that autophagic flux is impaired in $NP^{0/0}$ PCs which could contribute to neuronal loss.

We thank you for considering our revised manuscript for publication in Brain Pathology and remain

Yours sincerely

The authors

Autophagy and cell death of Purkinje cells overexpressing Doppel in Ngsk *Prnp*-deficient mice.

Heitz S.[1], Grant N. J[1], Leschiera R.[1], Haeberlé A.-M.[1], Demais V.[2], Bombarde G.[1], Bailly Y.[1,2]

[1] Institut des Neurosciences Cellulaires et Intégratives, Département Neurotransmission et Sécrétion Neuroendocrine, UMR7168-LC2 CNRS and Université Louis Pasteur, IFR 37 des Neurosciences de Strasbourg, 5 rue Blaise Pascal 67084 Strasbourg France.

[2] Plateforme d'Imagerie *in vitro*, IFR 37 de Neurosciences, 5 rue Blaise Pascal 67084 Strasbourg France.

Corresponding author: YB[1] UMR7168 CNRS, 5 rue Blaise Pascal 67084 Strasbourg France Tel. 33.3.88.45.66.36, Fax. 33.3.88.60.16.64, Email: byan@neurochem.u-strasbg.fr

Keywords: Purkinje cell, Doppel, prion protein, autophagy, neuronal death

Running title: Autophagy in Doppel-induced Purkinje cell death.

ABSTRACT

In Ngsk prion protein (PrP)-deficient mice ($NP^{0/0}$), ectopic expression of PrP-like protein Doppel (Dpl) in central neurons induces significant Purkinje cell (PC) death resulting in late-onset ataxia. $NP^{0/0}$ PC death is partly prevented by either knocking-out the apoptotic factor BAX or overexpressing the anti-apoptotic factor BCL-2 suggesting that apoptosis is involved in Dpl-induced death. In this study, Western blotting and immunohistofluorescence show that both before and during significant PC loss, the scrapie responsive gene 1 (Scrg1), potentially associated with autophagy, and the autophagic markers LC3B and p62 increased in the $NP^{0/0}$ PCs while RT-PCR shows stable mRNA expression, suggesting that degradation of autophagic products is impaired in $NP^{0/0}$ PCs. At the ultrastructural level, autophagic-like profiles accumulated in somato-dendritic and axonal compartments of $NP^{0/0}$, but not wild-type PCs. The most robust autophagy was observed in $NP^{0/0}$ PC axon compartments in the deep cerebellar nuclei suggesting that it is initiated in these axons. Our previous and present data indicate that Dpl triggers autophagy and apoptosis in $NP^{0/0}$ PCs. As observed in amyloid neurodegenerative diseases, upregulation of autophagic markers as well as extensive accumulation of autophagosomes in $NP^{0/0}$ PCs are likely to reflect a progressive dysfunction of autophagy which could trigger apoptotic cascades.

INTRODUCTION

Doppel (Dpl) was the first identified homologue of the cellular prion protein PrP^c which is implicated in the pathogenesis of transmissible spongiform encephalopathies (TSE) (48). Large deletions in the PrP^c gene *Prnp*, for example in the Ngsk $Prnp^{0/0}$ ($NP^{0/0}$) mouse line, result in the ectopic expression of Dpl in brain neurons (51) that induces significant levels of cerebellar Purkinje cell (PC) death as early as 6 months after birth (26). PrP-deficient cells have been shown to undergo Dpl-induced apoptosis in a dose-dependent, cell autonomous manner (40, 51, 54). Expression of the N-terminal truncated form of PrP (ΔPrP) in *Prnp*-ablated mouse lines (21) has neurodegenerative effects in PCs, similar to those observed when Dpl is over-expressed (1, 64). Moreover, the neurotoxic effects of Dpl and ΔPrP are both antagonized by PrP^c (1, 11, 21, 64) suggesting that Dpl and ΔPrP may cause cell death by similar mechanisms, perhaps by interfering with a cellular signalling pathway essential for cell survival and normally controlled by full-length PrP^c (1, 56, 61). To date, only a few studies have investigated the mechanism by which Dpl kills neurons. Oxidative stress linked with glial activation may play a role in the death of neurons because NOS activity is induced by Dpl both *in vitro* and *in vivo* (2, 11, 62).

In a recent study which investigated the involvement of the mitochondrial pro-apoptotic factor BAX in the Dpl-induced apoptosis of PCs, we have shown that deletion of Bax expression rescues many PCs from Dpl-induced cell death in $NP^{0/0}$:$Bax^{-/-}$ double knockout mutant mice (26). Since PrP^c has the ability to counteract Dpl neurotoxicity and has BCL-2-like properties which promote neuronal survival, we also examined the capacity of the anti-apoptotic factor BCL-2 to prevent Dpl neurotoxicity *in-vivo*. *Hu-bcl-2* overexpression in $NP^{0/0}$-*Hu-bcl-2* double mutants was found to rescue PCs in similar proportions to that observed when *Bax* was deleted in $NP^{0/0}$:$Bax^{-/-}$ double knock-out mutants (27). The capacity of BCL-2 to compensate PrP^c deficiency and rescue PCs from Dpl-induced death suggests that this BCL-2-like

property of PrP^c impairs Dpl-like neurotoxic pathways in wild-type neurons. These studies indicate that the pro-apoptotic factor BAX contributes to the neurotoxic mechanisms triggered by Dpl in the $NP^{0/0}$ PCs and that the anti-apoptotic factor BCL-2 can counteract this neurotoxic mechanism. However, $NP^{0/0}$ PC numbers are not fully restored to wild type levels suggesting that the ectopic expression of Dpl induces both BAX-dependent and BAX-independent cell death pathways.

A Dpl-activated, BAX-independent cell death mechanism may involve neuronal autophagy since $NP^{0/0}$ PCs have been recently shown to express Scrg1, a novel protein having a potential link with autophagy (18). Indeed, neuronal Scrg1 mRNA and protein levels are increased in prion-diseased brains (12, 13, 17). At the ultrastructural level, Scrg1 is associated with dictyosomes of the Golgi apparatus and autophagic vacuoles in degenerating neurons of scrapie-infected Scrg1-overexpressing transgenic and wild-type mice (18). Indeed, autophagy was first reported in experimentally-induced scrapie a long time ago (6), and recently has been implicated in an alternative cell death program in prion diseases (35).

For this reason, we investigated the expression of Scrg1 and two characteristic markers of autophagy, LC3B and p62, (5, 4, 37, 63) prior to significant PC loss in the 3-4 month-old $NP^{0/0}$ cerebellum and, when PC degeneration peaks in the 6-8 month-old $NP^{0/0}$ cerebellum (26). We also looked for ultrastructural signs of autophagy in the dendrites, axons and somata of PCs in the cerebellar cortex and deep cerebellar nuclei of $NP^{0/0}$ mice.

MATERIALS AND METHODS

Animals and genotyping

As previously reported, $NP^{0/0}$ mice were generated by deleting the entire open reading frame (ORF) of the *Prnp* gene, located in exon 3, as well as 5' and 3' non-coding flanking regions (48). The deleted sequences were replaced by a Neo cassette. The *Prnp* ORF was identified using the following primers: forward 5'CCGCTACCCTAACCAAGTGT3' and reverse 5'CCTAGACCACGAGAATGCGA3', both located within *Prnp* ORF. The following primers were used to identify the $NP^{0/0}$ mutants: forward 5'TGCCGCACTTCTTTGTGAAT3' and reverse 5'CGGTGGATGTGGAATGTGT3' (within Neo domain).

For this study, founding mice ($NP^{0/0}$ gift from S. Katamine) were first backcrossed with C57BL/6 mice for at least 10 generations. These mice were then intercrossed and $NP^{0/0}$, and wild-type (WT) pups were selected and bred at the animal facility of the Neurosciences IFR37 in Strasbourg, according to the NIH guidelines (NIH Publication 80-23, revised 1996) and the European Communities Council Directive of November 24, 1986 (86/609/EEC).

Western Blot analysis of LC3B, p62 and Lamp1

3-4 and 6-8 month-old wild-type (n = 3/age) and $NP^{0/0}$ (n = 3/age) littermates were anaesthetized with a mixture of ketamine 5% and xylazine 2% (0.1 mL of the mix per 30 g by i.p.) and then killed by decapitation. Cerebella were dissected and first homogenized in cold extraction TX-DOC buffer (50mM Tris-HCl pH 7.4, 150mM NaCl, 2mM EDTA (ethylene-diamine-tetra-acetic acid), 0.5% sodium deoxycholate, 0.5% Triton X-100, 1/500 Sigma Protease Inhibitor Cocktail). After centrifugation, the cleared extracts were taken up in Laemmli sample buffer (10mM Tris pH 7.0, 1mM EDTA, 3% SDS (sodium dodecyl sulfate), 10% Glycerol, 20mM DTT (dithiotreithol), 10% bromophenol blue) before heat denaturation.

The remaining protein pellets were washed with phosphate-buffered saline (PBS) before extraction with 2% SDS-containing sample buffer (insoluble fraction). An equivalent of 100 µg of brain tissue per well was run on 4-20% (LC3B and p62) and 4-12% (p62 and Lamp1) Nupage gels (Invitrogen). Proteins were transferred onto nitrocellulose membrane following the manufacturer's recommendations and routinely monitored with Ponceau S staining. Blots were pre-incubated for 1h in blocking solution (5% milk powder (Sigma), 0.1% Tween-20 in 0.1 M phosphate buffer saline pH 7.3 PBS). Antibodies were diluted in blocking solution and blots were incubated overnight with anti-actin mouse monoclonal antibody (1/10000, Sigma-Aldrich), anti-Lamp1 rabbit polyclonal antibody (1/1000, Abcam), anti-LC3B mouse monoclonal antibody (1/200, Nanotools) and anti-p62 mouse monoclonal antibody (1/1000, BD Transduction Labs). The anti-LC3B antibody was directed against the N-terminal end of the LC3B molecule and reacts with both LC3B-I and LC3B-II proteins. The anti-p62 antibody was directed against amino acids 257- 437 sequence of the human p62 molecule. The anti-Lamp1 antibodies were directed against a synthetic peptide within residues 350 to the C-terminus of human Lamp1 (100% identity with mouse Lamp1). Immunoreactivity was revealed using the SuperSignal West Dura Extended Duration Substrate reagent kit (Pierce) and images were obtained with a Chemi-Smart 5000 camera using the Chemi-capt software (Vilber-Lourmat). Quantification of protein bands was done using the Bio1D software (Vilber-Lourmat). Values have been corrected for variation in actin values and are expressed as a percentage of the values obtained for control animals.

RT-PCR analysis of LC3B and p62

Total RNA was extracted from isolated cerebellum from 3 and 6 month-old control wild-type mice and age-matched *NP*$^{0/0}$ mice with the GenElute Kit (Sigma-Aldrich), and mRNA was transcribed into cDNA using oligo(dT) and Superscript RNase H- Moloney murine leukemia

virus reverse transcriptase (Invitrogen). PCR amplification was performed using specific primers for p62: forward: 5'GATGTGGAACATGGAGGGAAGAG3' and reverse: 5'AGTCATCGTCTCCTCCTGAGCA3'; PCR product 246 bp (GI: 118130186), for LC3: forward: 5'ATGCCGTCCGAGAAGACCTTC3' and reverse: 5'TTACACAGCCATTGCTGTC3'; PCR product 377 bp (GI: 141601716) and for actin: forward: 5'GTGGGCCGCTCTAGGCACCAA3' and reverse: 5'CTCTTTGATGTCACGCACGATTTC3'; PCR product 540 bp (GI: 141601716). PCR cycles consisting of 94°C for 45sec, 55°C, (except for actin 60°C) for 30sec and 70°C for 30sec were varied between 18 and 27 cycles for β-actin and 21 and 33 cycles for p62 and LC3. Aliquots of PCR products were then migrated on 2% agarose gels and stained with ethidium bromide. The relative expression of the autophagic markers produced in the exponential phase of the PCR amplifications was calculated by a semi quantitative analysis using the Image J program. Similar measurements on the endogenous reference gene β-actin served as a control for the quantity of RNA input.

Immunohistofluorescence

Wild-type (n = 2) and $NP^{0/0}$ (n = 3) mice aged of 6-8 months were anaesthetized as described above and transcardiacally perfused with 4% paraformaldehyde (PAF) in 0.1M phosphate buffer, pH 7.3 (PB). The cerebellum was dissected and immersed in the same fixative at 4°C. After immersion in isobutanol for 4 days, the cerebella were embedded in paraffin and sagittal sections (10 µm-thick) were cut with a microtome (Leica). The sections were deparaffinized in toluene and rehydrated in ethanol. After rinsing in PBS, the sections were pre-incubated for 45 min in blocking solution (3% normal goat serum (NGS) in 0.5% Triton X-100 PBS; PBST). The sections were incubated overnight at 4°C in PBST containing 0.3% NGS and mouse monoclonal antibodies against LC3B (Nanotools) diluted 1/10 and rabbit polyclonal

antibodies against 28 kDa calcium binding protein (CaBP; gift from Dr Thomasset) diluted 1/1000 or rabbit polyclonal antibodies against Lamp1 (Abcam) diluted 1/100 for double immunohistofluorescence or with mouse monoclonal antibodies against p62 (BD Transduction Labs) diluted 1/100. The sections were then rinsed in PBS and incubated with Alexa 488-coupled goat anti-mouse and Alexa 546-coupled goat anti-rabbit immunoglobulins (Molecular Probes) diluted 1/1000 in PBS containing 0.3% NGS. After rinsing in PBS, the sections were mounted in Mowiol and examined by epifluorescence (Axioskop-II, Zeiss, Jena, Germany).

Scrg1 immunocytochemistry

Tissue preparation and sampling

Wild-type (8 month, n = 2) and $NP^{0/0}$ (3, 6, 8 months, n = 2/age) mice were anaesthetized as described above and transcardiacally perfused with PAF 1% in PB. The cerebellum was dissected and immersed in the same fixative at 4°C for 4 h.

Immunohistofluorescence

The cerebellum was cryoprotected in sucrose 0.44 M in PB overnight at 4°C before freezing in liquid nitrogen. Sagittal sections (10 µm-thick) were cut with a cryostat (Leica), rinsed in PBS and pre-incubated for 45 min in blocking solution (3% NGS in PBST). After overnight incubation at 4°C in PBST containing 0.3% NGS and rabbit polyclonal antibody against Scrg1 diluted 1/60 (gift from M. Dron) (28), the sections were rinsed in PBS and incubated with goat anti-rabbit immunoglobulins coupled to Alexa 488 (Molecular Probes) diluted 1/500 in PBS containing 0.3% NGS. The sections were then rinsed in PBS and processed for fluorescence microscopy as described above.

Control sections processed either without the anti-LC3 and anti-Scrg-1 primary antibodies or the fluorescent secondary antibodies were devoid of any specific fluorescent signal.

Quantitative analysis of Scrg1-immunofluorescent PCs in the $NP^{0/0}$ cerebellum

Scrg1 immunofluorescent PCs were counted in 7 sagittal sections separated from each other by 400 µm (total sampling distance = 2470 µm) in the cerebellar vermis of the 8 month-old wild-type (n = 2) and *$NP^{0/0}$* mice (n = 3). Data are given as mean ± standard deviation (SD).

Pre-embedding immunogold for electron microscopy

Transversal vibratome sections (60 µm-thick) of 1% PAF-fixed cerebellum were cut and processed, as previously described (16). Briefly, sections were pre-incubated in a blocking solution (0.5% bovine serum albumin, BSA, 0.1% cold water fish skin gelatine and 0.5% NGS in PB) before being rinsed in PBS containing 0.15% acetylated BSA (BSAc, Aurion, the Netherlands) and incubated overnight at 4°C with anti-Scrg1 antibodies (1/50 in PBS-BSAc). After washing in PBS-BSAc, the sections were incubated in Ultra small nanogold F(ab') fragments of goat anti-rabbit IgG (H and L chains, Aurion) diluted 1/100 in PBS-BSAc. After several rinses in PBS-BSAc and in PB, sections were post-fixed in glutaraldehyde 2% in PB before washing in PB and distilled water. Gold particles were then silver enhanced using the R-Gent SE-EM kit (Aurion) before being washed in distilled water and PB. Finally, the sections were postfixed in 0.5% OsO_4 in PB before classical processing for Araldite embedding and ultramicrotomy. The ultrathin sections were counterstained with uranyl acetate and observed with a Hitachi 7500 transmission electron microscope equipped with an AMT Hamamatsu digital camera. In control sections processed without anti-Scrg-1 primary antibodies or gold-labelled secondary antibodies no gold particles were observed.

Postembedding immunogold for detection of GABA

Deep cerebellar nuclei (DCN) were sampled from transverse cerebellar vibratome sections of 10 month-old $NP^{0/0}$ mice (n=2) perfused with a mixture of 2% PAF and 2% glutaraldehyde in 0.1 M PB. After embedding in Araldite, ultrathin sections were submitted to a standard postembedding immunogold protocol for the detection of GABA (15). The sections were immersed in 1% sodium borohydride and after rinsing in distilled water and Tris-buffered saline (TBS) they were incubated with 10% normal goat serum (NGS) in TBS and then with the GABA-specific primary antiserum (0.5 mg/ml; overnight at 4°C) in TBS containing 1% NGS. The sections were rinsed in TBS and incubated in goat anti-rabbit IgG coupled to 15 nm gold particles (Aurion,) diluted 1/200 in TBS containing 1% NGS. After rinsing in TBS and distilled water, sections were counterstained with 1% uranyl acetate. Substitution of the primary antiserum with pre-immune serum or TBS abolished labelling, as did omission of the gold conjugated secondary antibodies. Axonal varicosities establishing asymmetric synapses were always devoid of labelling. Non-specific or background labelling was very low in these preparations.

Semi-quantitative ultrastructural analysis of PC autophagy

Tissue preparation and sampling

Cerebellar cortex and DCN were sampled from transverse vibratome sections of 3 and 6 month-old $NP^{0/0}$ and wild-type mice (n=2/genotype and age) perfused with a mixture of 2% PAF and 2% glutaraldehyde in 0.1 M PB. Regions of cerebellar cortex were randomly sampled in the cerebellar lobules either in the vermis or in the right or left hemispheres in one section of the anterior cerebellum (1 block) and in one section of the posterior cerebellum (1 block). Regions in the fastigial, interposed and dentate nuclei was randomly sampled in sections from the anterior, median and posterior levels (1 block/level) of each right or left

nucleus. After embedding in Araldite, ultrathin sections were obtained from each block. In the cerebellar cortex, 100 PCs in the anterior cerebellum and 100 PCs in the posterior cerebellum were examined. In the deep cerebellar nuclei, 7,000 µm² were examined in the synaptic neuropile between the deep cerebellar neurons and an equivalent area in the synaptic neuropile close to the DCN. This was done at the anterior, median and posterior levels of the three DCN. The deep cerebellar neurons were identified by their large size (mean maximum diameter: 23.07 ± 0.36 µm) and by absence of GABA immunogold labelling. Autophagy was considered to be activated in the neuronal profiles which displayed recognizable structural features of the macroautophagic process. These included isolation membranes or phagophores surrounding neuroplasm with or without organelles and autophagic vacuoles such as complete double membraned autophagosomes and autolysosomes or autophagolysosomes (47).

Semi quantitative analysis of autophagic profiles in the $NP^{0/0}$ *cerebella*

In the cerebellar cortex, activation of autophagy was estimated by the number of PC soma exhibiting abnormal numbers of autophagic features (at least 3 autophagic vacuoles per soma) as a percentage of the total number of PCs examined in each animal. In the DCN, activation of autophagy was estimated by the number of PC presynaptic and pre-terminal axonal profiles exhibiting abnormal numbers of autophagic features (at least 2 autophagic vacuoles per profile) as a percentage of the total number of PC axonal profiles examined in each nucleus.

RESULTS

Scrg1, LC3B, p62 and Lamp1 are upregulated in $NP^{0/0}$ PCs

Since expression of Scrg1 has been previously reported to be a potential marker of autophagy and to increase in central neurons of scrapie-infected mice and in PCs of 12 month-old $NP^{0/0}$ mice (18), we first investigated the immunohistochemical distribution of Scrg1 in the

cerebellar cortex of young, 6-8 month-old $NP^{0/0}$ mice. In these mutants, intense Scrg1 immunofluorescence accumulated in large dots in the apical pole of the soma of a few PCs, reminiscent of Golgi apparatus staining (Fig. 1A). No or very weak labeling was seen in the PC dendrites. Scrg1 labeling was observed in less than 10 PCs per sagittal cerebellar section and was absent in PCs from wild-type age-matched littermates (Fig. 1B, C).

To further substantiate the occurrence of autophagy in the $NP^{0/0}$ PCs, the cerebellar expression of LC3B, a newly discovered autophagy-related variant of LC3, the classical marker of autophagy (63), and in parallel, the expression of p62, a functional autophagic ligand of LC3 (5, 45) were analyzed (Fig. 2). Firstly, RT-PCR analysis of mRNA levels did not reveal any differences in the expression of either LC3B or p62 in the cerebellum of 3 and 6 month-old $NP^{0/0}$ mice compared with wild-type mice (Fig. 2A). Next, changes in the LC3 and p62 protein levels were analyzed by Western blot. The results indicated an increase in the levels of both the autophagy-specific LC3B-II fragment (4.6 fold) and its ligand p62 (3 fold) in the Triton X-soluble fraction (Fig. 2B) but not in the insoluble fraction (data not shown) of the cerebellar extracts from the 3-4 and 6-8 month-old $NP^{0/0}$ mice compared to age-matched wild-type littermates. This increased expression of LC3B-II in the cerebellar cortex of the $NP^{0/0}$ mutants was confirmed in histological sections (Figs. 3, 4). LC3B (Fig. 3D-I) and p62 (Fig. 4B) staining was observed in the soma of $NP^{0/0}$ PCs, but was barely detected in wild-type PCs (Figs. 3A-C, 4A). In addition, CaBP-positive axon terminals of PCs displayed LC3B (Fig. 3M-O) and p62 (Fig. 4D) immunohistofluorescence in the DCN of the $NP^{0/0}$ mice whereas LC3B (Fig. 3J-L) and p62 (Fig. 4C) could not be immuno-detected in wild-type DCN. In agreement, the level of expression of the lysosomal marker Lamp1 was increased (4.1 fold) in the cerebellar extract of all $NP^{0/0}$ mice (Fig. 2B) implicating an upregulation of lysosome recruitment. This was confirmed using Lamp1 and LC3B double immunohistofluorescence which showed colocalization of LC3B- and Lamp1-positive

granules in $NP^{0/0}$ PCs somata in the cerebellar cortex (Fig. 5C) and, in $NP^{0/0}$ PC axonal profiles in the DCN (Fig. 5L).

Scrg1 immunogold labels autophagic $NP^{0/0}$ PC somata but not axon terminals.

Ultrastructural immunogold labelling of PCs from 6-8 month-old $NP^{0/0}$ mice revealed the association of Scrg1 with vesicles and saccules of dictyosomes in the somatic Golgi apparatus. The labelled dictyosomes sometimes had a normal ultrastructural appearance (Fig. 6A), but in most cases, double membrane saccules and intertwined membrane shapes were evident (Fig. 6B-F). Unlabelled autophagic vacuoles, membrane whorls and concentric arrays of membranes (phagophores) also seemed to be derived from other organelles, such as multivesicular bodies, ergastoplasmic saccules (Fig. 7G) and mitochondria (Fig. 6H). Profiles of neurodegeneration were rarely observed in the molecular layer, although autophagosomes and autophagolysosomes were found in some PC dendrites (Fig. 6I). At the nuclear level, no ultrastructural features of apoptotic cell death, such as chromatin condensation and nuclear fragmentation were observed. Presumptive PC myelinated axons exhibiting GABA immunogold labelling and dystrophic shapes contained phagophores, autophagosomes and autophagolysosomes in the deep molecular layer (Fig. 6J), as well as in the granule cell layer and the cerebellar white matter (Fig. 7C-E). None of these dendritic and axonal autophagic profiles displayed Scrg1 immunogold. Although most PCs containing autophagic profiles did not display any other ultrastructural signs of neurodegeneration, some soma clearly displayed features of advanced neurodegeneration, including shrunken soma and a condensed neuroplasm filled with unlabelled phagophores, autophagosomes and autophagolysosomes (Fig. 7A-B).

In all of the DCN, PC axon terminals make inhibitory synapses on the dendrites and soma of the deep cerebellar neurons. Many of these PC pre-synaptic varicosities displayed GABA

immunogold labelling (Fig. 8C) and contained autophagic vacuoles at all ages studied (3-8 months, Fig. 8A-E), but other terminals displayed normal ultrastructural characteristics (Fig. 8D, F), similar to those of PC terminals in the DCN of wild-type animals (Fig. 8G). Scrg1 immunogold did not label autophagic vacuoles in $NP^{0/0}$ PC axon terminals.

Presynaptic autophagy in $NP^{0/0}$ PCs

Semi-quantitative estimation of the percentage of autophagic PCs somata and axon terminals clearly indicated that autophagy was more prevalent in axons and terminal varicosities (14%, Fig. 9A) than in soma and dendrites (2%, Fig. 9A) of the $NP^{0/0}$ PCs at both ages studied (3 and 6 months). No autophagic PC soma and axons were observed in the wild-type cerebella. These results indicate that autophagy is already activated in 3 month-old $NP^{0/0}$ PCs prior to significant PC loss (Fig. 9B) (26). Furthermore, the semi-quantitative data suggest that autophagy is largely restricted to the axonal compartment of the 3-6 month-old $NP^{0/0}$ PCs, whereas the somato-dendritic compartment displays a quasi normal ultrastructure with only discrete alterations including Golgi-derived autophagic-like shapes.

DISCUSSION

The mechanisms by which the prion protein-like Dpl provokes premature PC death in the PrP-deficient $NP^{0/0}$ mice are still poorly understood. Neither *Prnd* knock-out mice nor *Prnp* and *Prnd* double knock-out mice exhibit overt neurological phenotypes indicating that PCs survive in these mutants and that Dpl is responsible for PC death in $NP^{0/0}$ mice (23, 44). Here, we investigated whether neuronal autophagy is activated during Dpl-induced PC death in $NP^{0/0}$ mice.

Using immunochemistry at the biochemical, histological and ultrastructural levels to evaluate this possibility, we demonstrate that $NP^{0/0}$ PCs undergo autophagy as indicated by the

upregulation of Scrg1, a presumed autophagy-associated protein, and two mediators of autophagic degradation LC3B-II and p62, as well as the presence of ultrastructural autophagic profiles in all PC compartments.

Upregulation of Scrg1 and p62/LC3 reflects different phases of autophagy in degenerating *NP*$^{0/0}$ PCs.

The microtubule-associated light chain 3 (LC3) is an essential component of autophagy (29) which acts as an adaptor protein between microtubules and autophagosomes through its N-terminal domain (33). Three isoforms LC3, LC3A and LC3B, have been shown to be associated with autophagic membranes (63) and thus can be used as autophagosomal markers. The punctuate LC3B immunoreactivity observed in the soma of *NP*$^{0/0}$ but not wild-type PCs is likely to indicate the formation of autophagic organelles resulting from the activation of the autophagic machinery in the mutant PCs. In agreement with immunohistochemical data, the Western blot analysis clearly showed that the autophagic membrane-bound marker LC3B-II was increased in the *NP*$^{0/0}$ cerebellum. Furthermore, the increased expression of p62 whose interaction with LC3 is instrumental in mediating autophagic degradation (5, 45) confirms that autophagy is abnormally activated in the *NP*$^{0/0}$ cerebellum (see below). The very early increase of these two markers at 3-4 months when PC loss is not yet significant (26) suggests that autophagy precedes apoptosis. In agreement, PCs with clear ultrastructural signs of advanced autophagy can be found in the cerebellar cortex of the 3 month-old *NP*$^{0/0}$ mice. In the *NP*$^{0/0}$ cerebellum, the increases of p62 and LC3B-II protein levels observed with age are likely to reflect both an increased number of autophagic PCs as indicated by increased PC loss at this age (26), and a decreased cerebellar mass as previously shown by the reduced size of the *NP*$^{0/0}$ cerebellum (26). In many *NP*$^{0/0}$ PCs, this increase may correspond to enhanced cleavage of LC3B-I to form LC3B-II. This would take place only in those PCs which have

entered a stage of advanced neurodegeneration as indicated at the ultrastructural level by robust formation and accumulation of autophagic structures in a fraction of PC population at this time. However, LC3 has been shown to be incorporated into intracellular inclusion bodies induced in a number of pathological conditions indicating that LC3-labeled dots do not necessarily represent autophagic structures (34). In the *NP*$^{0/0}$ PCs, this possibility is unlikely because inclusion bodies were not particularly abundant at the ultrastructural level in these neurons and the quantity of p62 protein in the soluble *NP*$^{0/0}$ cerebellar fraction increases in parallel. The high levels of p62 and LC3B-II in *NP*$^{0/0}$ cerebellum may not only reflect an augmentation in the density of autophagic PCs, but may also be due to an impairment in the autophagic flux (10) (see below). In agreement with this latter possibility, the absence of any detectable changes in the mRNA levels of LC3B and p62 in the *NP*$^{0/0}$ cerebellum compared to wild-type cerebellum strongly argues for a deficient autophagic degradation.

Scrg1, a gene primarily expressed in brain neurons, has been recently shown to be upregulated in several conditions of brain injury, following prion infection of human and animal brains, as well as in the cerebellum of the *NP*$^{0/0}$ mutant mouse (18). In scrapie-infected central neurons of both wild-type and Scrg1-overexpressing transgenic mice, Scrg1 was associated with dictyosomes of the Golgi apparatus and autophagic vacuoles (12) which are hallmarks of prion-induced degeneration (6, 28, 36). In the cerebellum of the 8-12 month-old *NP*$^{0/0}$ mice (18), upregulation of Scrg1 protein was immunodetected in fewer PCs than p62/LC3B-II, but not in any PCs of the wild-type cerebellum. Scrg1-labelling and p62/LC3B-II production was detected only in a few *NP*$^{0/0}$ PCs at any given time, indicating that the proteins may be involved in restricted phases of Dpl-induced stress. These two events may represent distinct steps in the neurodegenerative process because the ultrastructural data indicate that immunogold labelling for Scrg1 was mostly associated with Golgi complexes in *NP*$^{0/0}$ PC somata which display aberrant structures suggesting inaugural signs of autophagy.

Interestingly, the Golgi apparatus of both *NP*$^{0/0}$ and prion-infected PCs displayed similar ultrastructural alterations suggesting that Scrg1 labels Golgi apparatus of PCs that are likely to later undergo autophagy. In *NP*$^{0/0}$ PCs, upregulation of Scrg1 at the dictyosomes may be an early sign of Golgian autophagy which precedes p62/LC3B-II production since very little, if any, Scrg1 labelling of phagophores (25, 42, 37), autophagosomes and autophagolysosomes was observed in these neurons. Nevertheless, the chronology of the two events could not be more accurately determined because simultaneous immunohistochemical staining of Scrg1 and LC3B markers is not possible due to the incompatibility of the fixation protocols required to reveal Scrg1 (light 1% PAF tissue fixation) and LC3B (strong 4% PAF tissue fixation).

The specific Golgian localization confirms the spatial restriction of Scrg1 in the degenerative process of *NP*$^{0/0}$ PCs and is distinct from the more generalized association of LC3 with autophagosomal membranes (29). Thus, upregulation of Scrg1 and LC3 are not only chronologically, but also spatially distinct events. To date, the relationship of Scrg1 with autophagy remains circumstantial and the functional significance to the autophagic process is unknown. Although a potential role in the autophagic machinery was not confirmed by Scrg1 overexpression in transgenic mice further investigations in knock-out mice are merited.

Autophagic stress is a hallmark of *NP*$^{0/0}$ PC death

In addition to its known induction during starvation, differentiation and normal growth control (9, 30, 59), autophagy has been demonstrated in various neurodegenerative disorders including Alzheimer's disease and prion disease (31, 35, 37, 41). Here, autophagic vacuoles were revealed by electron microscopy in both somato-dendritic and axonal compartments of GABA immunogold-labeled *NP*$^{0/0}$ PCs suggesting that autophagy is concomitant to Dpl-induced cell death mechanisms. Nevertheless, the increased concentration of autophagic vacuoles is not necessarily correlated with increased autophagic activity. Instead the striking

accumulation of autophagic profiles in degenerating neurons often reflects an imbalance between the rates of autophagic sequestration and completion of the lysosomal degradation process (31). Increased or continued requirements for autophagy coupled with an impairment of the late phases of autophagic flux may lead to autophagic stress (10). This is likely to occur in known neurodegenerative conditions such as Alzheimer's disease (66) and in the $NP^{0/0}$ cerebellum where the accumulation of cytoplasmic autophagic profiles in PCs and increased p62 protein levels without apparent changes in mRNA expression are likely to reflect a deficit in autophagic flux (67). Robust autophagy may be detrimental, particularly when successful recycling of cellular components is impaired leading to the accumulation of cytoplasmic autophagic vacuoles and contributing to neuronal death (10). The electron dense content of many autophagic vacuoles and phagophores found in the $NP^{0/0}$ PCs are features of autolysosomal stages which suggest that autophagolysosome formation occurs in $NP^{0/0}$ PCs (16). Indeed, an increased lysosomal recruitment is signalled by the upregulation of Lamp1 in $NP^{0/0}$ PCs. Furthermore, double immunohistofluorescence for LC3B and Lamp1 shows a colocalization of both molecules in the same granules within $NP^{0/0}$ PCs suggesting that formation of autophagolysosomes does occur. Thus, the upregulation of autophagic and lysosomal markers as well as the extensive accumulation of autophagosomes and autophagolysosomes in the $NP^{0/0}$ PCs probably reflect a subsequent blockade of autophagic proteolysis. As observed in amyloid neurodegenerative diseases and in other neurological disorders such as ceroid lipofuscinosis (7), leakage of hydrolases induced by membrane destabilization of autophagolysosomes and lysosomes could trigger apoptotic cascades in the $NP^{0/0}$ PCs. Along this line, a genetic deficiency of the glycogen-degrading lysosomal enzyme acid-alpha glucosidase in Pompe-diseased mice induces severe skeletal and cardiac myopathy involving a massive autophagic buildup in myofibers (22, 49). In this case, autophagy is induced, but the muscle pathology manifests as a functional autophagic deficit due to

impaired autophagosomal-lysosomal fusion which leads to an accumulation of autophagic substrates (50).

In the cerebellum of the $NP^{0/0}$ mutants, there are both intact PCs, as well as PCs exhibiting different degrees of macroautophagy. This ranges from PCs with Scrg1-labelled Golgi dictyosomes and moderate amounts of all types of unlabelled autophagic profiles to PCs filled with phagophores, autophagosomes and autophagolysosomes, probably in a late step of cell death. This differential autophagic status of PCs suggests that PC death is asynchronous in $NP^{0/0}$ cerebellum. Also autophagic $NP^{0/0}$ PCs displayed differential intracellular distribution of autophagic profiles which were semi-quantitatively estimated to be more frequent in the axonal compartment (i.e. PC axons and terminals in the deep cerebellar white matter and nuclei) than in the somato-dendritic compartment. In $NP^{0/0}$ PC, the higher frequency of autophagic presynaptic terminals forming synapses on the deep cerebellar neurons compared with relatively few autophagic PCs found in the cerebellar cortex suggests that at least some of the axon terminals displaying autophagic profiles have an intact somato-dendritic compartment. This may indicate that in $NP^{0/0}$ PCs, axonal autophagy precedes somato-dendritic autophagy. Indeed, axonal autophagy has been previously reported in other cases of degenerating central neurons (31, 68), including the PCs of the *Lurcher* mutant mouse where autophagosomes form in axons before being transported to the soma (60, 67). Since Scrg1 labelling was restricted to somatic dictyosomes in $NP^{0/0}$ PCs, the chronology of axonal autophagy and somatic Scrg1 upregulation could not be determined (see above). With our current state of knowledge, we cannot tell if autophagy in the axon terminals of the $NP^{0/0}$ PCs is an initial step of a Dpl-induced autophagic cell death mechanism or a protective reaction of neurons to maintain axonal homeostasis (32) in response to Dpl-induced stress. Nevertheless, the early autophagic destruction of axons observed in the white matter and deep cerebellar nuclei of the 3 month-old $NP^{0/0}$ mice, well before significant PC loss, argues for a

contribution of an autophagy-dependent mechanism (see above) for Dpl-induced PC death rather than for autophagy as an epiphenomenon. To date, the precise subcellular localization of Dpl is unknown although its close structural homology with PrP^c (38, 58) suggests that both proteins should have a similar subcellular expression pattern at the plasma membrane of axons and terminals (3). At these sites, Dpl may induce rapid physiological alterations within axons that locally trigger the autophagic machinery.

Dpl-induced PC death: apoptosis and/or autophagy?

To date, little is known about how Dpl kills neurons. Our recent data show that *Bax* knockout or overexpression of *Bcl-2* partly rescues PCs from Dpl-induced cell death in $NP^{0/0}$:$Bax^{-/-}$ (26) and $NP^{0/0}$-*Hu-bcl-2* (27) double mutant mice. This partial recovery suggests that *Bcl-2* family-dependent apoptotic pathways are not the only death mechanism implicated in Dpl neurotoxicity. According to the present results, another possibility may be related to non-apoptotic autophagic cell death. Indeed, Dpl has been shown to induce the production of reactive oxygen species (ROS) (11, 62), which are able to activate both apoptosis (43) and autophagy (55). However, the respective contribution of apoptosis and autophagy to Dpl-induced cell death remains unclear. There are several explanations for the occurrence of both autophagy and Bax-dependent apoptosis of PCs in the cerebellum of the $NP^{0/0}$ mouse. Firstly, intrinsic differences between PCs could make them susceptible to different cell death pathways in response to Dpl-induced stress. Supporting this hypothesis, PCs exhibit different resistance levels to Dpl toxicity related to both their anterior *versus* posterior position and their aldolase C expression in the $NP^{0/0}$ cerebellum (27). This may determine a differential specificity of Dpl-triggered cell death program among PCs. Secondly, a defective autophagic flux in $NP^{0/0}$ PCs may ultimately trigger apoptotic cell death. Indeed, recent findings obtained both in non-neuronal cells (19, 24, 39, 57, 65) and neurons (8), argue against a clear-cut

distinction between autophagy and apoptotic cell death. Recognition of the extensive cross talk between different cell death pathways is beginning to provide insight into the complex patterns of neuronal cell death seen in nervous system diseases (42). Recent data highlight the ability of BCL-2 to not only function as an anti-apoptotic factor, but also as an anti-autophagic factor via its inhibitory interaction with Beclin1 (46). This could contribute to *NP*$^{0/0}$ PC survival in the *NP*$^{0/0}$*-Hu-bcl-2* double mutants (27). In these mutants, the *NP*$^{0/0}$ PCs which die in spite of Bcl-2 overexpression are likely to undergo Bcl-2-independent cell death processes which need further investigations.

To conclude, our results reveal that the autophagic machinery is activated early in the process leading to Dpl-induced neuronal death in *NP*$^{0/0}$ PCs. This shows that autophagy is related to Dpl-induced PC neurodegeneration. In this way, *NP*$^{0/0}$ PCs display many signs of impaired autophagic flux which could convert an initial autophagic defence reaction to Dpl neurotoxicity into a neurodegenerative mechanism. Our present data support emerging concepts in the field of neuronal death such as axonal initiation of neuronal autophagy and crosstalk between autophagic and apoptotic pathways. Designing specific drugs to modulate autophagy are challenging but promising avenues for future therapy of neurodegenerative diseases.

Aknowledgements

The authors are greatly indebted to Dr Patrice Codogno for helpful discussion and critical reading of the manuscript, to Drs. Françoise Dandoy-Dron and Michel Dron for helpful assistance in Scrg1 experiments and to Dr. Sophie Reibel-Foisset and Nicolas Lethenet for excellent assistance in breeding the *NP*$^{0/0}$ mice in the Plateforme d'Expérimentation Animale of the IFR37 des Neurosciences de Strasbourg. This study was supported by the G.I.S.

Maladies à Prions. SH was supported by a 1 year salary provided by the Roche Research Foundation and the Fondation Novartis pour la Recherche.

REFERENCES

1. Anderson L, Rossi D, Linehan J, Brandner S, Weissmann C (2004) Transgene-driven expression of the Doppel protein in Purkinje cells causes Purkinje cell degeneration and motor impairment. *Proc Natl Acad Sci USA* **101**:3644-49.
2. Atarashi R, Sakaguchi S, Shigematsu K, Arima K, Okimura N, Yamaguchi N, Li A, Kopacek J, Katamine S (2001) Abnormal activation of glial cells in the brains of prion protein-deficient mice ectopically expressing prion protein-like protein, PrPLP/Dpl. *Mol Med* **7**:803-9.
3. Bailly Y, Haeberlé AM, Blanquet-Grossard F, Chasserot-Golaz S, Grant N, Schulze T, Bombarde G, Grassi J, Cesbron JY, Lemaire-Vieille C (2004) Prion protein (PrPc) immunocytochemistry and expression of the green fluorescent protein reporter gene under control of the bovine PrP gene promoter in the mouse brain. *J Comp Neurol* **473**:244-69.
4. Bjørkøy G, Lamark T, Brech A, Outzen H, Perander M, Overvatn A, Stenmark H, Johansen T (2005) p62/SQSTM1 forms protein aggregates degraded by autophagy and has a protective effect on huntingtin-induced cell death. *J Cell Biol* **171**:603-14.
5. Bjørkøy G, Lamark T, Johansen T (2006) p62/SQSTM1: a missing link between protein aggregates and the autophagy machinery. *Autophagy* **2**:138-9.
6. Boellaard JW, Kao M, Schlote W, Diringer H (1991) Neuronal autophagy in experimental scrapie. *Acta Neuropathol* **82**:225-8.
7. Boland B, Nixon RA (2006) Neuronal macroautophagy: from development to degeneration. *Mol Aspects Med* **27**:503-19.
8. Canu N, Tufi R, Serafino AL, Amadoro G, Ciotti MT, Calissano P (2005) Role of the autophagic-lysosomal system on low potassium-induced apoptosis in cultured cerebellar granule cells. *J Neurochem* **92**:1228-42.

9. Cao Y, Espinola JA, Fossale E, Massey AC, Cuervo AM, MacDonald ME, Cotman SL (2006) Autophagy is disrupted in a knock-in mouse model of juvenile neuronal ceroid lipofuscinosis. *J Biol Chem* **281**:20483-93

10. Chu CT (2006) Autophagic stress in neuronal injury and disease. *J Neuropathol Exp Neurol* **65**:423-32.

11. Cui T, Holme A, Sassoon J, Brown DR (2003) Analysis of doppel protein toxicity. *Mol Cell Neurosci* **23**:144-55.

12. Dandoy-Dron F, Guillo F, Benboudjema L, Deslys J-P, Lasmézas C, Dormont D, Tovey MG, Dron M (1998) Gene Expression in Scrapie. Cloning of a new scrapie-responsive gene and the identification of increased levels of seven other mRNA transcripts. *J Biol Chem* **273**:7691-7.

13. Dandoy-Dron F, Benboudjema L, Guillo F, Jaegly A, Jasmin C, Dormont D, Tovey MG, Dron M (2000) Enhanced levels of scrapie responsive gene mRNA in BSE-infected mouse brain. *Brain Res Mol Brain Res* **76**:173-9.

14. Dandoy-Dron F, Griffond B, Mishal Z, Tovey MG, Dron M (2003) Scrg1, a novel protein of the CNS is targeted to the large dense-core vesicles in neuronal cells. *Eur J Neurosci* **18**:2449-59.

15. De Biasi S, Vitellaro-Zuccarello L, Bernardi P, Valtschanoff JG, Weinberg RJ (1994) Ultrastructural and immunocytochemical characterization of primary afferent terminals in the rat cuneate nucleus. *J Comp Neurol* **347**:275–287.

16. Ding WX, Yin XM (2008) Sorting, recognition and activation of the misfolded protein degradation pathways through macroautophagy and the proteasome. *Autophagy* **4**:141-50.

17. Dron M, Dandoy-Dron F, Guillo F, Benboudjema L, Hauw J-J, Lebon P, Dormont D, Tovey MG (1998) Gene expression in scrapie. Cloning of a new scrapie-responsive

gene and the identification of increased levels of seven other mRNA transcripts. *J Biol Chem* **273**:7691-7.

18. Dron M, Bailly Y, Beringue V, Haeberlé A-M, Griffond B, Risold P-Y, Tovey MG, Laude H, and Dandroy-Dron F (2005) Scrg1 is induced in TSE and brain injuries, and associated with autophagy. *Eur J Neurosci* **22**:133-46.
19. Espert L, Denizot M, Grimaldi M, Robert-Hebmann V, Gay B, Varbanov M, Codogno P, Biard-Piechaczyk M (2006) Autophagy is involved in T cell death after binding of HIV-1 envelope proteins to CXCR4. *J Clin Invest* **116**:2161-72.
20. Filimonenko M, Stuffers S, Raiborg C, Yamamoto A, Malerød L, Fisher EM, Isaacs A, Brech A, Stenmark H, Simonsen A (2007) Functional multivesicular bodies are required for autophagic clearance of protein aggregates associated with neurodegenerative disease. *J Cell Biol* **179**:485-500.
21. Flechsig E, Hegyi I, Leimeroth R, Zuniga A, Rossi D, Cozzio A, Schwarz P, Rulicke T, Gotz J, Aguzzi A, Weissmann C (2003) Expression of truncated PrP targeted to Purkinje cells of PrP knockout mice causes Purkinje cell death and ataxia. *EMBO J* **22**:3095-3101.
22. Fukuda T, Roberts A, Ahearn M, Zaal K, Ralston E, Plotz PH, Raben, N (2006) Autophagy and lysosomes in Pompe disease. *Autophagy* **2**:318-320.
23. Genoud N, Behrens A, Miele G, Robay D, Heppner FL, Freigang S, Aguzzi A (2004) Disruption of Doppel prevents neurodegeneration in mice with extensive Prnp deletions. *Proc Natl Acad Sci U S A* **101**:4198-203.
24. Gonzalez-Polo RA, Boya P, Pauleau AL, Jalil A, Larochette N, Souquère S, Eskelinen EL, Pierron G, Saftig P, Kroemer G (2005) The apoptosis/autophagy paradox: autophagic vacuolization before apoptotic death. *J Cell Sci* **118**:3091-102.

25. Hariri M, Millane G, Guimond MP, Guay G, Dennis JW, Nabi IR (2000) Biogenesis of multilamellar bodies via autophagy. *Mol Biol Cell* **11**:255-68.

26. Heitz S, Lutz Y, Rodeau J-L, Zanjani H, Gautheron V, Bombarde G, Richard F, Fuchs J-P, Vogel M, Mariani J, Bailly Y (2007) BAX contributes to Doppel-induced apoptosis of prion protein-deficient Purkinje cells. *Dev Neurobiol* **67**:670-86.

27. Heitz S, Gautheron V, Lutz Y, Rodeau J-L, Zanjani H, Sugihara I, Bombarde G, Richard F, Fuchs J-P, Vogel MW, Mariani J, Bailly Y (2008) BCL-2 opposes Dpl-induced apoptosis of prion protein-deficient Purkinje cells in the Ngsk *Prnp*$^{0/0}$ mouse. *Dev Neurobiol* **68**:332-48.

28. Jeffrey M, Goodsir CM, Bruce ME, McBride PA, Scott JR, Halliday WG (1992) Infection specific prion protein (PrP) accumulates on neuronal plasmalemma in scrapie infected mice. *Neurosci Lett* **147**:106-9.

29. Kabeya Y, Mizushima N, Ueno T, Yamamoto A, Kirisako T, Noda T, Kominami E, Ohsumi Y, Yoshimori T (2000) LC3, a mammalian homologue of yeast Apg8p, is localized in autophagosome membranes after processing. *EMBO J* **19**:5720-8.

30. Klionsky DJ (2007) Autophagy: from phenomenology to molecular understanding in less than a decade. *Nat Rev Mol Cel Biol* **8**:931-7.

31. Koike M, Shibata M, Waguri S, Yoshimura K, Tanida I, Kominami E, Gotow T, Peters C, von Figura K, Mizushima N, Saftig P, Uchiyama Y (2005) Participation of autophagy in storage of lysosomes in neurons from mouse models of neuronal ceroid-lipofuscinoses (Batten disease). *Am J Pathol* **167**:1713-28.

32. Komatsu M, Wang QJ, Holstein GR, Friedrich VL Jr, Iwata J, Kominami E, Chait BT, Tanaka K, Yue Z (2007) Essential role for autophagy protein Atg7 in the maintenance of axonal homeostasis and the prevention of axonal degeneration. *Proc Natl Acad Sci U S A* **104**:14489-94.

33. Kouno T, Mizuguchi M, Tanida I, Ueno T, Kanematsu T, Mori Y, Shinoda H, Hirata M, Kominami E, Kawano K (2005) Solution structure of microtubule-associated protein light chain 3 and identification of its functional subdomains. *J Biol Chem* **280**:24610-7.

34. Kuma A, Matsui M, Mizushima N (2007) LC3, an autophagosome marker, can be incorporated into protein aggregates independent of autophagy: caution in the interpretation of LC3 localization. *Autophagy* **3**:323-8.

35. Larsen KE, Sulzer D (2002) Autophagy in neurons: a review. *Histol Histopathol* **17**:897-908.

36. Liberski PP, Sikorska B, Bratosiewicz-Wasik J, Gajdusek DC, Brown P (2004) Neuronal cell death in transmissible spongiform encephalopathies (prion diseases) revisited: from apoptosis to autophagy. *Int J Biochem Cell Biol* **36**:2473-90.

37. Liberski PP, Brown DR, Sikorska B, Caughey B, Brown P (2008) Cell death and autophagy in prion diseases (transmissible spongiform encephalopathies). *Folia Neuropathol*; **46**:1-25.

38. Lu K, Wang W, Xie Z, Wong BS, Li R, Petersen RB, Sy MS, Chen SG (2000) Expression and structural characterization of the recombinant human doppel protein. *Biochemistry* **39**:13575-83.

39. Martin DN, Baehrecke EH (2004) Caspases function in autophagic programmed cell death in Drosophila. *Development* **131**:275-84.

40. Nishida N, Tremblay P, Sugimoto T, Shigematsu K, Shirabe S, Petromilli C, Erpel SP, Nakaoke R, Atarashi R, Houtani T, Torchia M, Sakaguchi S, DeArmond SJ, Prusiner SB, Katamine S (1999) A mouse prion protein transgene rescues mice deficient for the prion protein gene from Purkinje cell degeneration and demyelination. *Lab Invest* **79**:689-97.

41. Nixon RA, Wegiel J, Kumar A, Yu WH, Peterhoff C, Cataldo A, Cuervo AM (2005) Extensive involvement of autophagy in Alzheimer disease: an immuno-electron microscopy study. *J Neuropathol Exp Neurol* **64**:113-22.

42. Nixon RA (2006) Autophagy in neurodegenerative disease: friend, foe or turncoat? *Trends Neurosci* **29**:528-35.

43. Orrenius S. (2007) Reactive oxygen species in mitochondria-mediated cell death. *Drug Metab Rev* **39**:443-55.

44. Paisley D, Banks S, Selfridge J, McLennan NF, Ritchie AM, McEwan C, Irvine DS, Saunders PT, Manson JC, Melton DW (2004) Male infertility and DNA damage in Doppel knockout and prion protein/Doppel double-knockout mice. *Am J Pathol* **164**:2279-88.

45. Pankiv S, Clausen TH, Lamark T, Brech A, Bruun JA, Outzen H, Øvervatn A, Bjørkøy G, Johansen T (2007) p62/SQSTM1 binds directly to Atg8/LC3 to facilitate degradation of ubiquitinated protein aggregates by autophagy. *J Biol Chem* 282:24131-45.

46. Pattingre S, Tassa A, Qu X, Garuti R, Liang XH, Mizushima N, Packer M, Schneider MD, Levine B (2005) Bcl-2 antiapoptotic proteins inhibit Beclin 1-dependent autophagy. *Cell* **122**:927-39.

47. Pattingre S, Espert L, Biard-Piechaczyk M, Codogno P (2008) Regulation of macroautophagy by mTOR and Beclin 1 complexes. *Biochimie*. **90**:313-23.

48. Prusiner SB (1998) Prions. *Proc Natl Acad Sci USA* **95**:13363-83.

49. Raben, N., Takikita, S., Pittis, M.G., Bembi, B., Marie, S.K.N., Roberts, A., Page, L., Kishnani, P.S., Schoser, B.G.H., Chien, Y.H. *et al.*(2007) Deconstructing Pompe disease by analyzing single muscle fibers. *Autophagy*, **3**, 546-552.

50. Raben N, Hill V, Shea L, Takikita S, Baum R, Mizushima N, Ralston E, Plotz P (2008) Suppression of autophagy in skeletal muscle uncovers the accumulation of ubiquitinated proteins and their potential role in muscle damage in Pompe disease. *Hum Mol Genet*. Ahead of print.

51. Rossi D, Cozzio A, Flechsig E, Klein MA, Rülicke T, Aguzzi A, Weissmann C (2001) Onset of ataxia and Purkinje cell loss in PrP null mice inversely correlated with Dpl level in brain. *EMBO J* **20**:694-702.

52. Sakaguchi S, Katamine S, Shigematsu K, Nakatani A, Moriuchi R, Nishida N, Kurokawa K, Nakaoke R, Sato H, Jishage K (1995) Accumulation of proteinase K-resistant prion protein (PrP) is restricted by the expression level of normal PrP in mice inoculated with a mouse-adapted strain of the Creutzfeldt-Jakob disease agent. *J Virol* **69**:7586-92.

53. Sakaguchi S, Katamine S, Nishida N, Moriuchi R, Shigematsu K, Sugimoto T, Nakatani A, Kataoka Y, Houtani T, Shirabe S, Okada H, Hasegawa S, Miyamoto T, Noda T (1996) Loss of cerebellar Purkinje cells in aged mice homozygous for a disrupted PrP gene. *Nature* **380**:528-31.

54. Sakudo A, Lee DC, Nakamura I, Taniuchi Y, Saeki K, Matsumoto Y, Itohara S, Ikuta K, Onodera T (2005) Cell-autonomous PrP-Doppel interaction regulates apoptosis in PrP gene-deficient neuronal cells. *Biochem Biophys Res Commun* **333**:448-54.

55. Scherz-Shouval R, Shvets E, Fass E, Shorer H, Gil L, Elazar Z (2007) Reactive oxygen species are essential for autophagy and specifically regulate the activity of Atg4. *EMBO J* **26**:1749-60.

56. Shmerling D, Hegyi I, Fischer M, Blattler T, Brandner S, Gotz J, Rulicke T, Flechsig E, Cozzio A, von Mering C, Hangartner C, Aguzzi A, Weissmann C (1998)

Expression of amino-terminally truncated PrP in the mouse leading to ataxia and specific cerebellar lesions. *Cell* **93**:203-14.

57. Shimizu S, Kanaseki T, Mizushima N, Mizuta T, Arakawa-Kobayashi S, Thompson CB, Tsujimoto Y (2004) Role of Bcl-2 family proteins in a non-apoptotic programmed cell death dependent on autophagy genes. *Nat Cell Biol* **6**:1221-8.
58. Silverman GL, Qin K, Moore RC, Yang Y, Mastrangelo P, Tremblay P, Prusiner SB, Cohen FE, Westaway D(2000) Doppel is an N-glycosylated, glycosylphosphatidylinositol-anchored protein. Expression in testis and ectopic production in the brains of Prnp(0/0) mice predisposed to Purkinje cell loss. *J Biol Chem* **275**:26834-41.
59. Vittorini S, Paradiso C, Donati A, Cavallini G, Masini M, Gori Z, Pollera M, Bergamini E (1999) The age-related accumulation of protein carbonyl in rat liver correlates with the age-related decline in liver proteolytic activities. *J Gerontol A Biol Sci Med Sci* **54**:B318-23.
60. Wang QJ, Ding Y, Kohtz DS, Mizushima N, Cristea IM, Rout MP, Chait BT, Zhong Y, Heintz N, Yue Z. (2006) Induction of autophagy in axonal dystrophy and degeneration. *J Neurosci* **26**:8057-68.
61. Watts JC, Westaway D (2007) The prion protein family: diversity, rivalry, and dysfunction. *Biochim Biophys Acta* **1772**:654-72.
62. Wong BS, Liu T, Paisley D, Li R, Pan T, Chen SG, Perry G, Petersen RB, Smith MA, Melton DW, Gambetti P, Brown DR, Sy MS (2001) Induction of HO-1 and NOS in doppel-expressing mice devoid of PrP: implications for doppel function. *Mol Cell Neurosci* **17**:768-75.

63. Wu J, Dang Y, Su W, Liu C, Ma H, Shan Y, Pei Y, Wan B, Guo J and Yu L (2006) Molecular cloning and characterization of rat *LC3A* and *LC3B*—Two novel markers of autophagosome. *Biochem Biophys Res Commun* **339**:437-42

64. Yamaguchi N, Sakaguchi S, Shigematsu K, Okimura N, Katamine S (2004) Doppel-induced Purkinje cell death is stoichiometrically abrogated by prion protein. *Biochem Biophys Res Commun* **319**:1247-52.

65. Yousefi S, Perozzo R, Schmid I, Ziemiecki A, Schaffner T, Scapozza L, Brunner T, Simon HU (2006) Calpain-mediated cleavage of Atg5 switches autophagy to apoptosis. *Nat Cell Biol* **8**:1124-32.

66. Yu WH, Cuervo AM, Kumar A, Peterhoff CM, Schmidt SD, Lee JH, Mohan PS, Mercken M, Farmery MR, Tjernberg LO, Jiang Y, Duff K, Uchiyama Y, Näslund J, Mathews PM, Cataldo AM, Nixon RA (2005) Macroautophagy--a novel Beta-amyloid peptide-generating pathway activated in Alzheimer's disease. *J Cell Biol* **171**:87-98.

67. Yue Z, Wang QJ, Komatsu M (2007) Neuronal autophagy: Going the distance to the axon. *Autophagy* **4**:94-6.

68. Zanjani SH, Selimi F, Vogel MW, Haeberlé AM, Boeuf J, Mariani J, Bailly YJ (2006) Survival of interneurons and parallel fiber synapses in a cerebellar cortex deprived of Purkinje cells: studies in the double mutant mouse Grid2Lc/+;Bax(-/-). *J Comp Neurol* **497**:622-35.

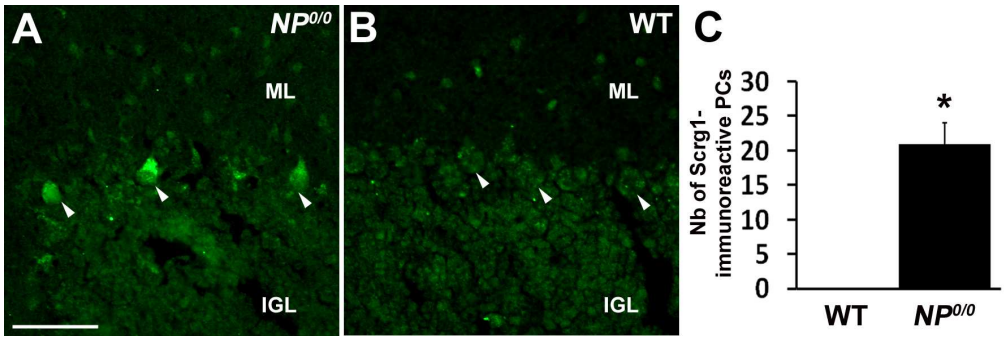

Figure 1. Immunohistofluorescence of Scrg1 in the 8 month-old cerebellar cortex of NP0/0 and wild-type mice. A. A few PCs (arrowheads) display Scrg1 fluorescence in the cerebellar cortex of a NP0/0 mouse. B. PCs remain devoid of Scrg1 fluorescence in the cerebellar cortex of the wild-type mouse. A and B, bar = 50µm. C. Quantitative analysis of Scrg1-immunofluorescent PCs. The number of Scrg1-immunoreactive PCs per 7 sagittal cerebellar sections sampled in each of 3 wild-type (WT) and 3 NP0/0 mice is plotted on a y axis.
300x99mm (150 x 150 DPI)

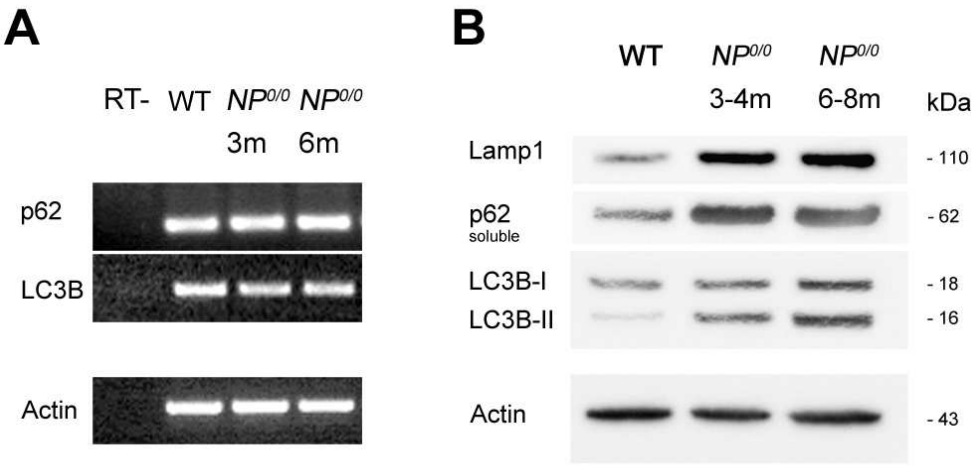

Figure 2. A. RT-PCR analysis of mRNA expression of p62 and LC3 in the NP0/0 cerebellum. mRNA levels of LC3B and p62 in both 3 month-old (lane 3) and 6 month-old mice (lane 4) are equivalent to the wild-type (lane 2). The expression of β-actin was analyzed as an internal control. Negative control samples which were not reverse transcribed (RT-) are shown (lane 1). B. Western blot analysis of the LC3B, p62 and Lamp1 proteins in the NP0/0 cerebellum. The 16-kDa LC3B-II protein, the 62 kDa p62 protein and the 110 kDa Lamp1 protein are increased in both 3-4 month-old (lane 2) and 6-8 month-old (lane 3) extracts of cerebellum from NP0/0 mice compared with adult WT (lane 1). As a control for equivalent protein loading, 42-kDa actin was revealed.
85x43mm (300 x 300 DPI)

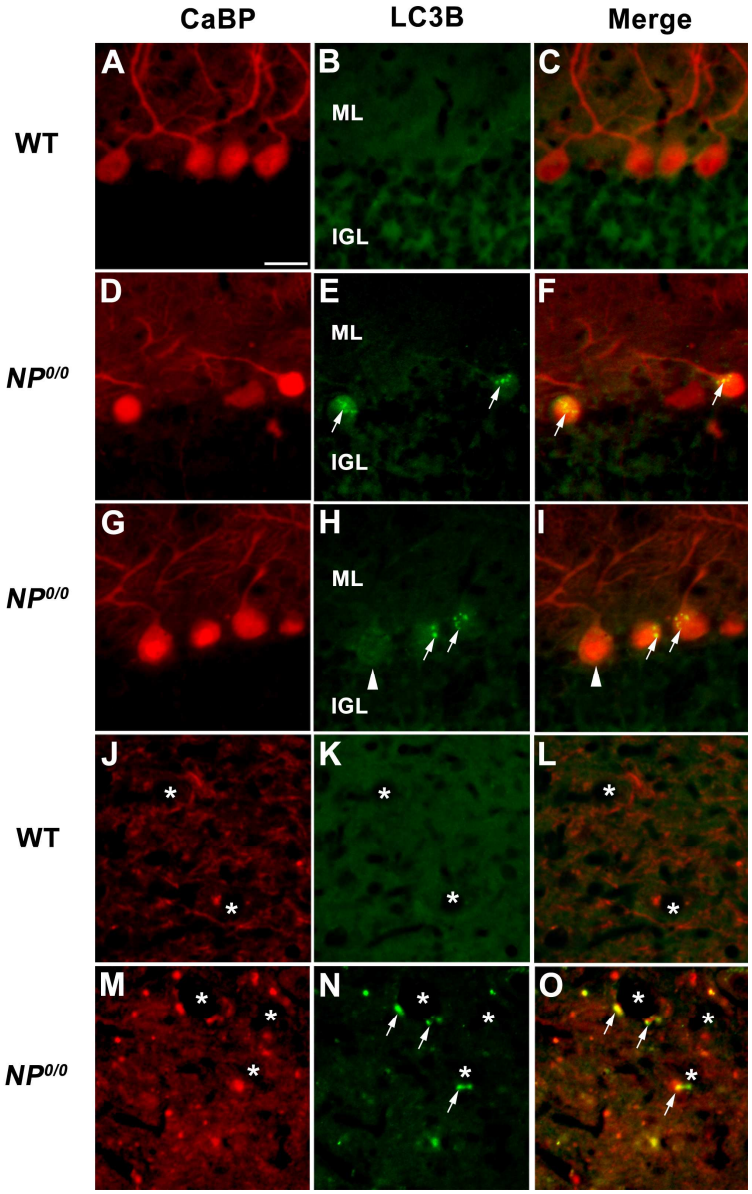

Figure 3. Immunohistofluorescence for LC3B and CaBP in the cerebellum of the 6-8 month-old NP0/0 and wild-type mice. In the cerebellar cortex, double immunohistofluorescence for CaBP (A, D, G, J, M, red) and LC3B (B, E, H, K, N, green) shows that the NP0/0 PC somata contain a punctuate LC3B staining (arrows in E, F, H, I). Some NP0/0 PCs do not display LC3B fluorescence (arrowheads) like wild-type PCs (B, C). In a deep cerebellar nucleus, some NP0/0 PC axon terminals close to deep cerebellar neurons (asterisks) display red CaBP (M, O) and green LC3B (N, O) immunohistofluorescence. Some other CaBP-positive PC terminals do not display LC3B labeling in the merged image (O). All CaBP-labelled PC axon terminals (J, L) are LC3B-negative (K, L) in the wild-type. Bar = 20μm in A to O.
352x549mm (150 x 150 DPI)

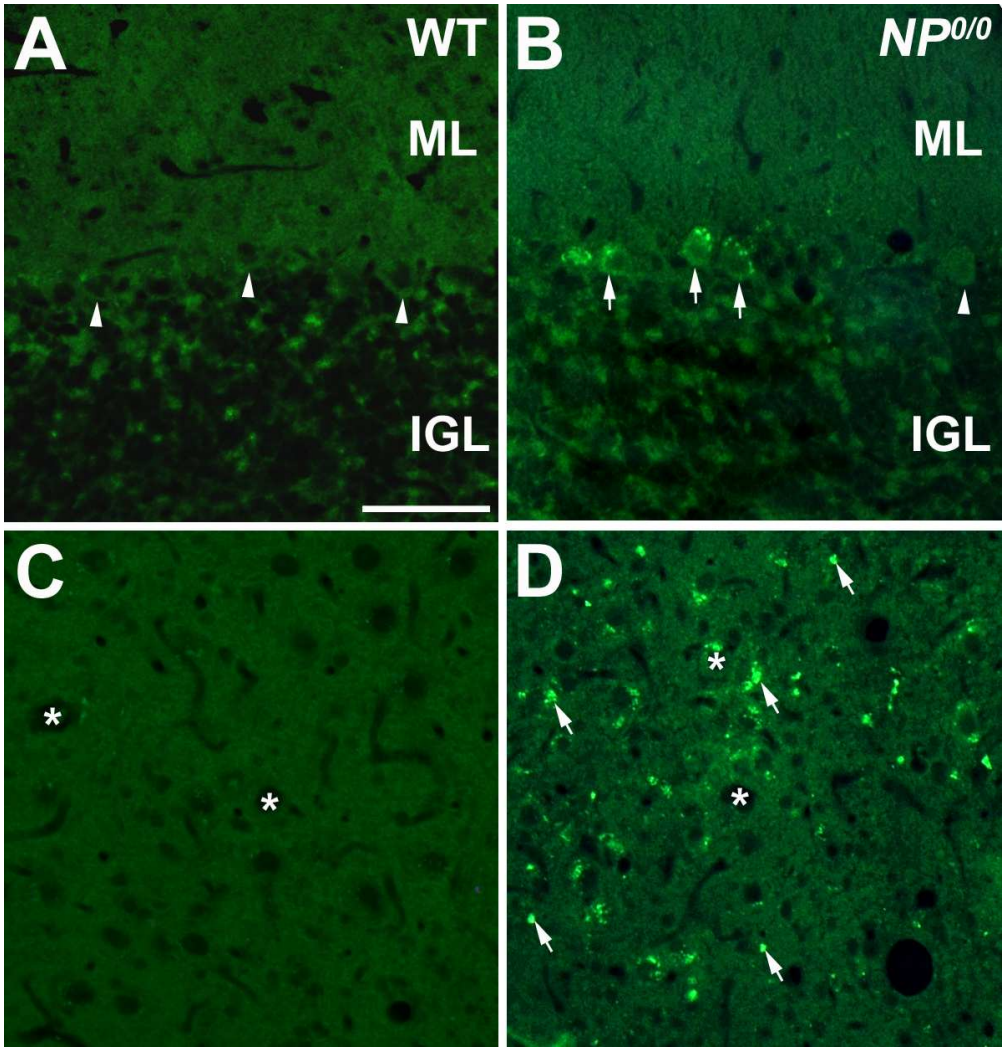

Figure 4. Immunohistofluorescence for p62 in the cerebellum of 6-8 month-old NP0/0 and wild-type mice. A, B. In the cerebellar cortex, p62 appears as cytoplasmic dots in the soma of NP0/0 PCs (arrows) displays. Some NP0/0 PCs as well as wild-type PCs (A) do not display p62 fluorescence (arrowheads). C, D. P62 immunofluorescence of presumptive PC axon terminals is observed in the deep cerebellar nucleus of NP0/0 mouse (arrows, D) but not wild-type mouse (C). Asterisks indicate deep cerebellar neurons soma. Bar = 20μm in A to D.
202x210mm (150 x 150 DPI)

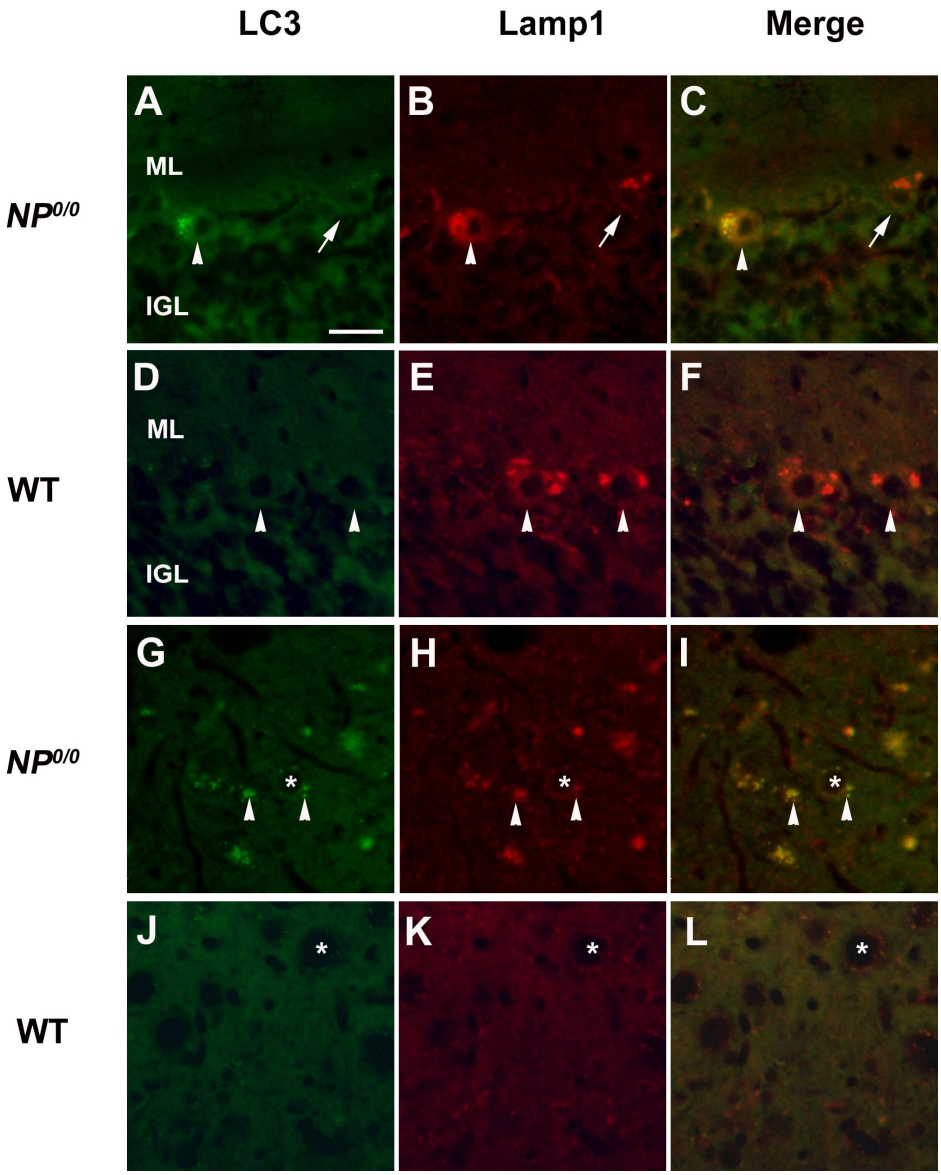

Figure 5. Immunohistofluorescence for Lamp1 and LC3B in the cerebellum of 6 month-old NP0/0 and wild-type mice. Double immunohistofluorescence for LC3B (A, D, G, J, green) and Lamp1 (B, E, H, K, green) shows colocalization of Lamp1 and LC3B staining in a NP0/0 PC soma (arrowhead in C). Some NP0/0 PCs do not display LC3B fluorescence (arrows in A, C) like wild-type PCs (D, F). In a deep cerebellar nucleus, some NP0/0 PC axon terminals close to deep cerebellar neurons (asterisks) display red Lamp1 (arrowheads in H, I) and green LC3B (arrowheads in G, I) immunohistofluorescence. All PC axon terminals in wild-type mice are LC3B- (J, L) and Lamp1-negative (K, L). Bar = 20μm in A to L.
354x450mm (150 x 150 DPI)

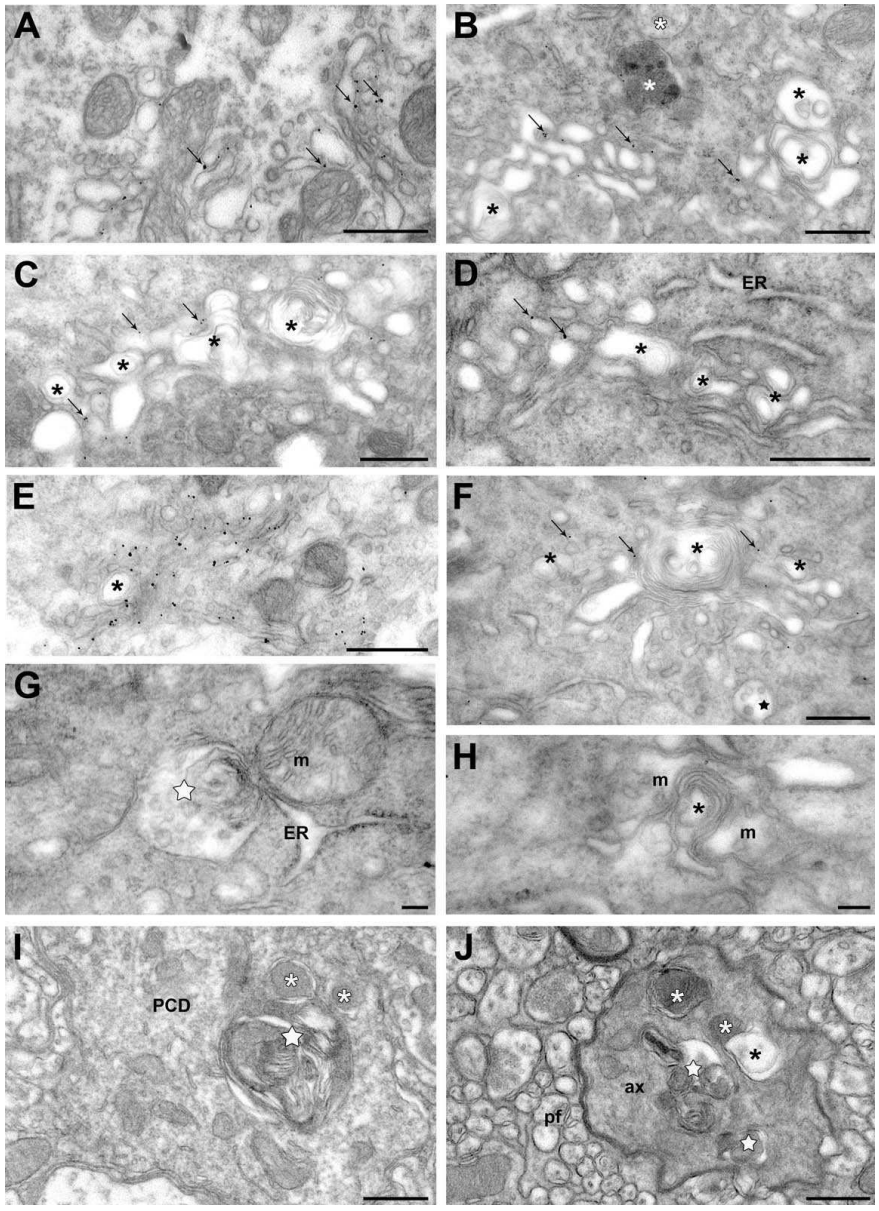

Figure 6. Autophagy in the somato-dendritic and axonal compartments of Scrg1-immunogold labelled Purkinje cells of the NP0/0 mouse. A-H. Purkinje cell soma. A. Immunogold particles (arrows) label saccules and vesicles of an apparently intact dictyosome of the Golgi apparatus. B-F. Golgi apparatus dictyosomes with Scrg1-immunogold labelling (arrows) and autophagic-like double membrane vacuoles and membrane whorls (asterisks). White asterisks in B, lysosomes. ER in D, rough endoplasmic reticulum. Star in F, multivesicular body. G. A multivesicular body (white star) is engaged in autophagic-like membrane wrapping with a rough ER saccule. m, mitochondria. H. Mitochondria (m) around autophagic-like membrane whorls (asterisk). None of the organelles in G and H are labelled with Scrg1 immunogold. I, J. Molecular layer. I. Fusion of an autophagosome (white star) with lysosomes (white asterisks) in a Scrg1-negative Purkinje cell primary dendrite (PCD). J. Autophagosomes (white stars) and autophagolysosomes (white asterisks) and in a Scrg1-negative myelinated presumptive Purkinje cell recurrent axon collateral (ax). Note the fusion of a

lysosome with a double membrane autophagosome (black asterisk). pf, parallel fibres. Bars: 500 nm in A-F, I, J; 100 nm in G, H.
195x269mm (150 x 150 DPI)

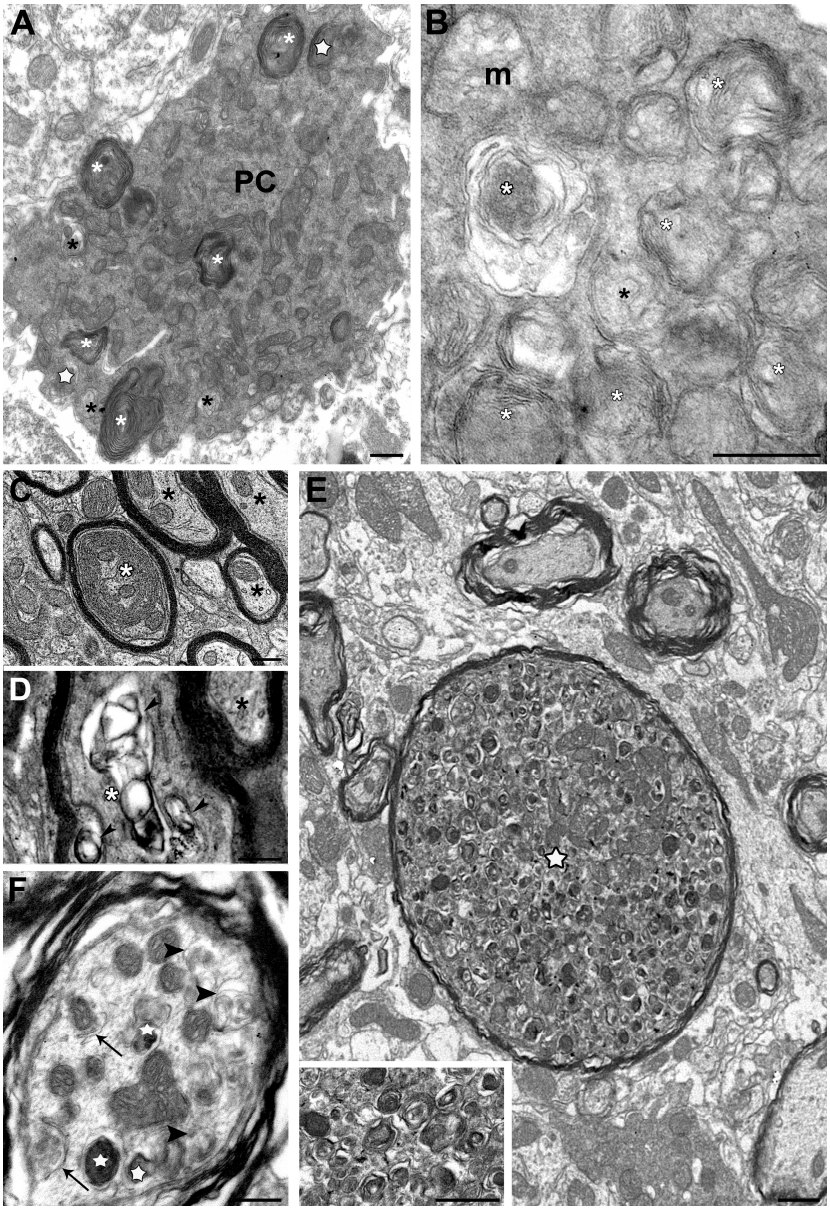

Figure 7. Autophagy in the soma and axons of NP0/0 Purkinje cells. Immunogold electron microscopy did not reveal Scrg1 in any of the areas shown. A. A degenerating autophagic Purkinje cell (PC) filled with autophagosomes, autophagolysosomes (white asterisks) and lysosomes (white stars) and has a shrunken shape. B. High magnification of neuroplasmic content of an autophagic Purkinje cell soma. m, mitochondria; white asterisks, autophagic vacuoles; asterisk, phagophore. C-D. Degenerating myelinated Purkinje cell axons in the white mater surrounding the fastigial deep cerebellar nucleus. C. A phagophore made of concentric wrapping of membrane around a core of axoplasm (white asterisk) fills a myelinated axon profile. D. Collapsed autophagic-like vacuoles (arrowheads) in a myelinated axon (asterisk). Black asterisks show intact myelinated axons in C and D. E. A dystrophic axon (star) with features of acute autophagy: thinned myelin sheath, swollen shape and numerous autophagic vacuoles at different stages of maturation and electron-dense lysosomes (see higher magnification in inset). Compare with surrounding intact myelinated axons.

F. Numerous reticular phagophores (white arrowhead) encircling axoplasmic material, autophagosomes (black arrowheads) and autophagolysosomes (white stars) reflect advanced stages of axonal autophagy. Bars: 500 nm in A-D, inset E and F; 2 µm in E.
195x284mm (400 x 400 DPI)

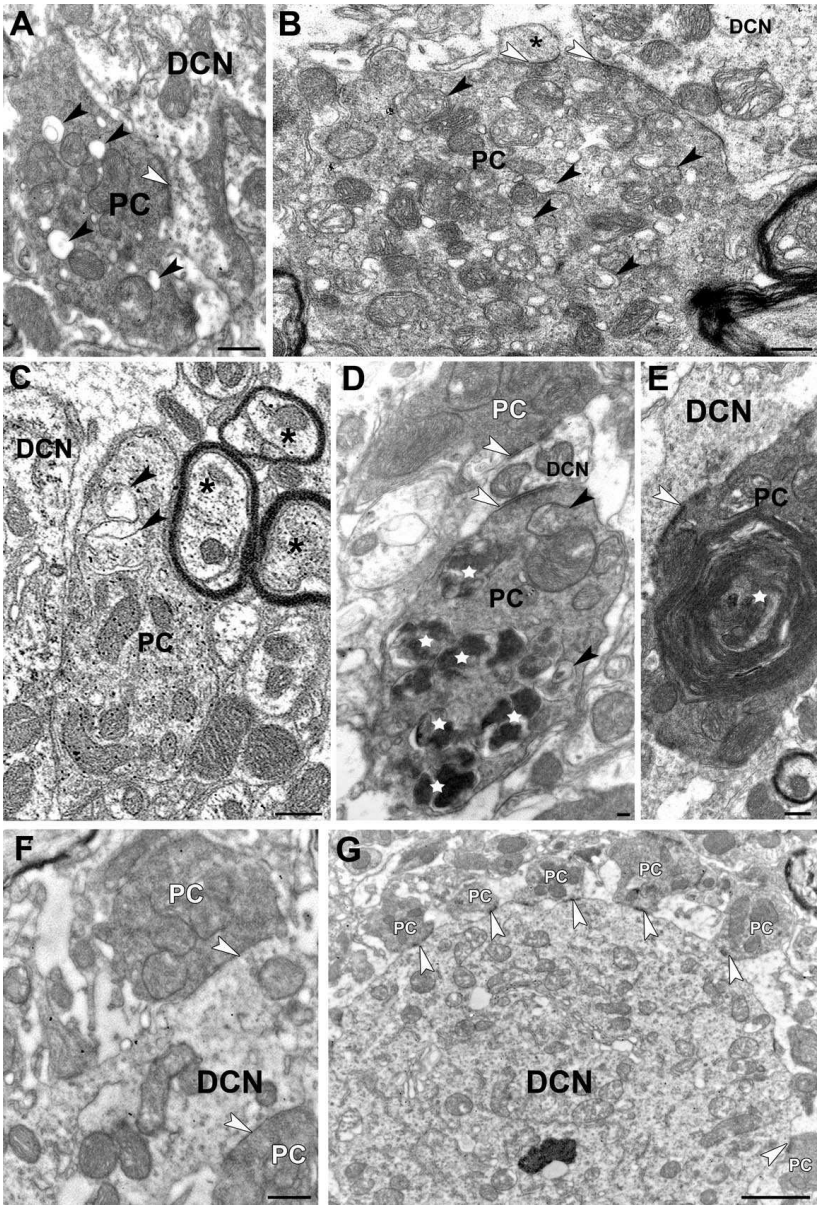

Figure 8. Purkinje cell axon terminals in the fastigial deep cerebellar nucleus of NP0/0 (A-F) and wild-type (G) mice. A-F. NP0/0 mouse. Immunogold electron microscopy does not reveal Scrg1 in any of these areas. A-B. Early stages of autophagy in presynaptic PC terminals making symmetric axo-somatic (A) and axo-dendritic (B) synapses (white arrowheads) on fastigial neurons (DCN). Black arrowheads point to autophagic double-membrane and small vacuoles within the PC terminals. Asterisk indicates a postsynaptic fastigial dendritic spine. C. Immunogold labelling for GABA. In a GABA-immunolabelled preterminal PC axon terminal close to a DCN, cytoplasmic material is isolated by an endoplasmic saccule (arrowhead) in an autophagic-like manner featuring an early stage of autophagy. See the surrounding double membrane autophagic-like vacuole (arrowhead). Asterisks show intact myelinated axons. D. An autophagic PC axon terminal containing autophagosomes (arrowheads) and many autophagolysosomes (white stars). This PC terminal makes an symmetric synapse (white arrowhead) on a postsynaptic fastigial dendrite (DCN) similar

to that made by an intact PC terminal (white PC) on the opposite side of the dendrite. E. Huge autophagosome featured by multiple membrane wrapping around cytoplasmic material (white star) in a PC terminal making a symmetric synapse (white arrowhead) on a fastigial dendrite (DCN). F. Two intact presynaptic PC axon terminals make symmetric synapses (white arrowheads) on a fastigial dendrite (DCN). G. Six intact presynaptic PC axon terminals make symmetric synapses (white arrowheads) on a large fastigial dendrite (DCN). Bars: 500 nm.
195x287mm (150 x 150 DPI)

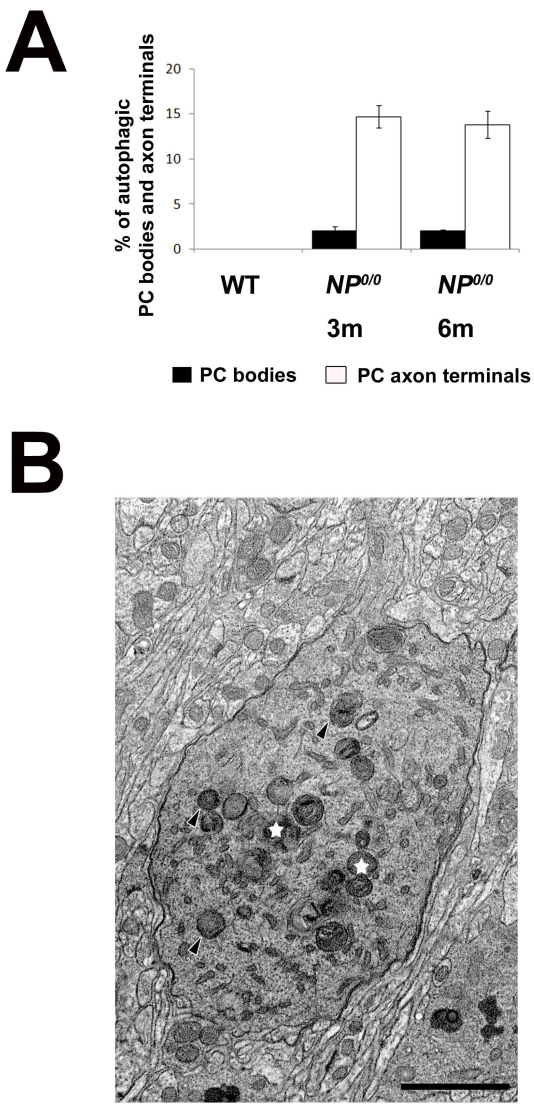

Figure 9. A Semi-quantitative analysis of autophagic PC somata and axon terminals in the cerebellar cortex and deep cerebellar nuclei of the 3 and 6 month-old wild-type and NP0/0 mice. The percentage of autophagic somata (black) and axon terminals (white) in the wild-type and NP0/0 mice is plotted on y axis. B. Autophagosomes (black arrowheads) and autophagolysosomes (white stars) in the somatic neuroplasm of a PC in the cerebellar cortex of a 3 month-old mouse. Bar = 2 µm.
135x298mm (300 x 300 DPI)

Résumé

Les neuropathologies mettent en jeu l'apoptose et l'autophagie, deux mécanismes de mort cellulaire programmée qui requièrent l'activation de voies signalétiques spécifiques. L'identification au niveau moléculaire des voies spécifiques de mort cellulaire déclenchées par des situations pathologiques variées dans les différents types neuronaux sensibles est d'une importance critique dans l'élaboration de stratégies destinées à prévenir la perte des neurones centraux.

Mes recherches s'intéressent aux cellules de Purkinje du cervelet dans des modèles murins de mutations affectant spécifiquement ces neurones. La mort des cellules de Purkinje a été étudiée chez des souris *Lurcher* et *hotfoot* présentant des mutations du gène *Grid2* codant pour le récepteur glutamatergique GluRδ2 et dans la souris mutante Nagasaki $Prnp^{0/0}$ ($NP^{0/0}$) déficiente en protéine prion et sur-exprimant son paralogue neurotoxique Doppel.

Le récepteur muté GluRδ2^{Lc} induit l'autophagie avant la mort excitotoxique des cellules de Purkinje chez la souris mutante hétéroallélique GluRδ2$^{Lc/ho}$. Mes études en culture organotypique de cervelet révèlent un lien entre l'autophagie et l'excitotoxicité dans les cellules de Purkinje GluRδ2$^{Lc/+}$ qui sont protégées de la mort cellulaire excitotoxique et ne présente plus d'autophagie après traitement avec l'agent bloquant de canaux cationiques NASP. La synaptogenèse excitatrice des cellules de Purkinje avec les fibres parallèles et grimpantes implique GluRδ2. En effet, mes résultats indiquent que la translocation somato-dendritique des fibres grimpantes au cours du développement postnatal des cellules de Purkinje pourrait être soumise au contrôle de la croissance dendritique des cellules de Purkinje par GluRδ2.

En l'absence de protéine prion chez la souris mutante Nagasaki, son paralogue Doppel induit une perte progressive des cellules de Purkinje qui implique BAX, un membre de la famille de Bcl-2, dans la voie apoptotique intrinsèque. La survie d'une partie des cellules de Purkinje chez les double mutants $NP^{0/0}$*:Bax*$^{-/-}$ et $NP^{0/0}$*-Hu-bcl-2* révèle la contribution d'une voie de mort cellulaire indépendante de BAX. Ce processus pourrait mettre en jeu soit l'autophagie qui est détectée très tôt dans les axones au niveau ultrastructural et par l'augmentation de l'expression de marqueurs autophagiques soit un mécanisme apoptotique extrinsèque encore non identifié.

Mes résultats suggèrent que des stimuli pathogènes différents déclenchent des modalités de mort cellulaire différentes qui mettent en jeu l'apoptose et l'autophagie dans un même neurone. L'interaction entre ces voies multiples de mort cellulaire programmée demande à âtre étudiée plus avant dans des modèles animaux de maladies neurodégénératives afin d'ouvrir de nouvelles voies thérapeutiques.

Abstract

Neuropathologies often involve apoptosis and autophagy, two mechanisms of programmed cell death which require activation of specific signaling pathways. Determining the specific death pathways operating in different types of neurons in various pathological situations is important to gain insight into the strategies for preventing loss of central neurons.

My investigations were focused on cerebellar Purkinje cells in mouse models of mutations specifically affecting these neurons. Purkinje cell death was investigated in *Lurcher* and *hotfoot* mice with mutations in the *Grid2* gene coding for the glutamatergic receptor GluRδ2, and in the Nagasaki $Prnp^{0/0}$ ($NP^{0/0}$) mutant mouse deficient for the prion protein and overexpressing its neurotoxic paralogue Doppel.

The mutated glutamatergic receptor GluRδ2^{Lc} was shown to induce autophagy preceding excitotoxic cell death in the Purkinje cells of the heteroallelic GluRδ2$^{Lc/ho}$ mutant mouse. The present studies in organotypic cerebellar cultures elucidate a link between autophagy and excitotoxicity in the GluRδ2$^{Lc/+}$ Purkinje cells which are rescued from excitotoxic cell death and do not display autophagy anymore after treatment with the channel blocker NASP. Excitatory synaptogenesis of Purkinje cells with parallel and climbing fibers is known to involve GluRδ2. Indeed, my present data indicate that somato-dendritic translocation of climbing fibers during postnatal development of Purkinje cells could be regulated by a GluRδ2-dependent control of Purkinje cell dendritic growth.

In the absence of prion protein in the Nagasaki mutant mouse, its paralogue Doppel induces progressive Purkinje cell loss that involves Bcl-2 family members of the intrinsic apoptotic pathway such as BAX. The partial rescue of Purkinje cells in $NP^{0/0}$*:Bax*$^{-/-}$ and $NP^{0/0}$-*Hu-bcl-2* double mutants indicate the contribution of a BAX-independent cell death pathway. This process may occur either by autophagy which is detected early at the axonal level as evidenced by increased expression of autophagic markers and electron microscopy or by an unidentified extrinsic apoptotic mechanism.

These data suggest that different pathogenic stimuli trigger different cell death modalities involving apoptosis and autophagy in the same neuron. The interplay between these multiple pathways of programmed cell death needs to be further investigated in animal models of neurodegenerative diseases to provide new therapeutic approaches.

Stéphane HEITZ
9, rue Charles Gerhardt
F – 67000 STRASBOURG
(33) 6.37.08.14.36
st.heitz@yahoo.fr

Born on 06/01/1979
Married, 1child

NEUROSCIENCES PHD

Fundamental research experiences

2004-2008	Neurosciences Thesis, Anatomisches Institut (Prof Kapfhammer), Universität Basel, Switzerland and Team "Cytologie et Cytopathologie Neuronales" (Dr Yannick Bailly) CNRS UPR 2356 Centre de Neurochimie Strasbourg, France. **"Neuronal death mechanisms in cerebellar Purkinje cells."**
2003-2004	DEA training course, Team "Cytologie et Cytopathologie Neuronales" (Dr Yannick Bailly) CNRS UPR 2356 Centre de Neurochimie Strasbourg, France (1 year). "**Bcl-2, Bax and Purkinje cell death induced by Doppel in the Prion Protein deprived mouse line *Ngsk*." Histology, immuno-histochemistry, management of transgenic mice.**

Studies

2005	Formation for the experimental procedures on living animals authorization.
2003-2004	DEA de Neurosciences Université Louis Pasteur France.
2002-2003	Maîtrise de Neurosciences Université Louis Pasteur France.
2001-2002	Licence de Biologie cellulaire et Physiologie Université Louis Pasteur France.
1999-2001	DEUG Biologie Université Louis Pasteur France.
1997-1999	1ère année du premier cycle d'études médicales Université Louis Pasteur France.
1997	Baccalauréat Série Scientifique option Sciences de la Vie.

Communication

English	fluent level, read, written and spoken.
German	school level.
Informatic	MSWord, MSPowerpoint, MSExcel (notions), Internet, Adobe Photoshop

Grants:

10/2007-09/2008	Financial support from the Fondation Novartis pour la Recherche. CHF 44500.
01/2007-09/2007	Financial support from the Roche research foundation. CHF 34200.
08/2004-12/2006	Financial support from the Neurex/Eltem organization. 34800€.

Memberships

2006- present	Member of the Society for Neurosciences (USA)
2005- present	Member of the Société des Neurocience (France)